



Provided by the author(s) and University of Galway in accordance with publisher policies. Please cite the published version when available.

Title	Bioethanol and biobutanol production from CO and CO ₂ using solventogenic acetogens
Author(s)	He, Yaxue
Publication Date	2022-01-27
Publisher	NUI Galway
Item record	http://hdl.handle.net/10379/17017

Downloaded 2024-04-28T21:44:04Z

Some rights reserved. For more information, please see the item record link above.





Bioethanol and Biobutanol Production from CO and CO₂ using Solventogenic Acetogens

Yaxue He

Supervisor: Prof. Piet N. L. Lens

Co-supervisor: Prof. Christian Kennes

A thesis submitted to the National University of Ireland as fulfilment of the
requirements for the degree of Doctor of Philosophy

School of Natural Sciences

November 2021

Declaration

I, Yaxue He, declare that this thesis or any part thereof has not been, or not currently being, submitted for any degree at the National University of Ireland, or any other University. I further declare that the work embodied is my own.

Yaxue He

Summary

This research aimed at enhancing ethanol and butanol production from H₂/CO₂ and CO by anaerobic sludge from wastewater treatment plants via investigating the environmental parameters in a semi-gas fed bioreactor and enrichment of CO-converting solventogenic *Clostridium* bacteria.

In the first part of the study, a fermentation process that converts CO₂ to ethanol using H₂ as electron donor and anaerobic granular sludge as inoculum was studied at different temperatures. Besides, the effects of pH, carbon source (HCO₃⁻ and glucose supplementation) and trace metals on ethanol production were also investigated. Results from the experiments showed that fermentation at 25°C and initial pH of 6 achieved the highest ethanol production (17.1 mM). Ethanol production occurred when both the pH decreased to 4.7 and acetic acid accumulated to 15 mM at 25°C by granular sludge using H₂/CO₂ as the substrate. with *Clostridium* being the functional microorganism at genus level at both 25 and 37°C. However, methane was produced from H₂/CO₂ at 55°C. The use of glucose and CO₂ as co-substrate enhanced butyric acid production (3.3 mM), while ethanol production occurred at a pH as low as 4. The presence of 10 μM W and 2 μM Mo enhanced the ethanol production by 7.0 and 5.4-fold, respectively. A continuous fermentation further showed the change of H₂/CO₂ to 100% H₂ in the gaseous substrate enhanced butyric acid and hexanoic acid production at pH 4.5.

The second part of this study investigated ethanol and butanol production using CO as the sole carbon source with anaerobic sludge as inoculum in an intermittent gas-fed bioreactor. CO and syngas metabolizing solventogenic acetogens were enriched from anaerobic sludge at pH 5.7-6.5 and produced up to 6.8 g/L butanol in an intermittent gas-fed bioreactor. Additional tests under controlled pH demonstrated that the lowest pH of 5.7 stimulated ethanol and butanol production in the enriched culture. The applied enrichment procedure efficiently selected for a range of *Clostridium* species. Thereafter, successive enrichment obtained a high (74%) amount of unidentified *Clostridium* species, which produced 11.7 g/L ethanol with low accumulation of acetic acid over a wide pH range of 6.45-4.95. Besides, the enriched *Clostridium* bacteria in the present study produced 2.7 g/L butanol from exogenous butyric acid with a 100% conversion efficiency using CO as reducing power. The highest butanol concentration was produced (3.4 g/L) with 14 g/L butyric acid addition using CO as gaseous substrate by the *Clostridium* bacteria. Butanol was significantly enhanced up to 2.4 fold when adding CO after endogenous butyric acid production from glucose compared to when adding CO initially with glucose (co-fermentation)

Acknowledgement

This PhD thesis is the output of the effort and support of several people to whom I am extremely grateful. First and foremost, I thank my supervisors Professor Piet Lens and co-supervisor Professor Christian Kennes for their supervision and enabling me to finish the entire work. Thanks Dr. Florence and Prof. Luisa for each of your suggestions on this thesis.

Prof. Piet, thank you so much for each comments on every manuscripts and presentations by a lot of patience. My PhD started with the 2 am interview at a day seems nothing special, but I did not realize how my career had been changed after that interview. It has been a privilege to work with you.

Prof. Christian, I count myself very blessed when I consider the mobility to Spain and work to with you. Every discussion on the data, I gained a lot about research. Thanks for the chance to move to A Coruna, Spain, a such beautiful city near sea, this experience teach me that PhD is not just mean a degree, it means completely different living culture, different people with different culture. Thanks for Prof. María C. Veiga for your support on research and every nice talk.

I would like to thank Dr. Chiara Cassarini. Chiara, I remember each discussion and each suggestions you gave me. Thank you let me know how to tackle difficulties, relationships, and different cultures. Thanks Prof. Xinmin, Dr. Gavin and Dr. Pau, thank you for the annual GRC meeting and all suggestions and without your help, I would be not so confident to finish my PhD thesis and defense.

Anna, Thanks so much for all your helps in lab, DNA extraction teaching, and every nice talk, which becomes a treasure during my PhD. Lea, thanks for your helps in lab and in life and every nice talk with you. It is a lucky to meet so many nice people. Borja, thank you for the technical support in the lab always with patient. Tania, thank you for all the kind helps in lab and share the apartment finding experience when I move to Spain. Paolo, thank you for every suggestions on my research and helps in lab and every nice talk with you. Rachel, thanks for all your helps in lab and every nice chatting. Postdoc. Collette J. Mulkeen, thanks for your helps on my research for the reactor set-up although I could not make it at the end. I remember every nice talk and encourage from you. I would also like to thank for the nice helps from Dr. Harish, Joyabrata, Arindam, Priyanka, Qidong.

I am lucky that I also met so nice colleagues, Juan, thank you so much for every talk and dinner, and also thank you for Monica and Alihanta, which will be one of the most beautiful memories during the journey. Carlos, thank you so much for every talk and R language teaching. Peyman, thank you for each talk and encouragement, which was a nice experience. Thanks Farzenh for

every talk and encouragement. Thanks to my colleagues and friends: Federica, Simone, Armando, Jewel, Sudeshna, Mohan. Thanks for the PhDs that help me and in the same office Neyaz, Laura, Nick, Jasemine, Simon, Victor, Daniel and Theo.

Thanks for Muara, my Ireland mom also my friend for her take care when I first in Galway, and together with her entire family, Bill and Kevin. Yuchen and Jialun, you are the best friends I met in Ireland and we will keep in touch.

2020 is another journey to move to Spain, unfortunately, COVID-19 pandemic started. The most important lesson is to keep your mind peaceful, focus and insist, which are important to be success. I met nice people, Kubra, Carla, Rual, Busra, Haris, Anna, Marta, Noria, Ruth, it is a pity that we could not together much time due to the pandemic but thanks so much for all of your kind helps in lab and help me solve the visa problem.

Thanks Miaoqing's company me back to Tianjin from Madrid. Thanks the people who worked on the defense of Covid and the nice and humous people from Tianjin I met in the bus from Tianjing airport to the quarantine hotel.

Finally, I would like to thank my parents for their supporting on my every decisions. My boyfriend Zhengwei, I could not go this far without your support and encouragement.

I will always remember the time spent in NUIG and Ireland, this green island with lovely views, windy weathers, falling rains, as a sweet dream in my life.

Table of Contents

Declaration.....	ii
Summary.....	iii
Acknowledgement.....	iv
Table of figures.....	xii
Table of tables.....	xx
List of publications and chapter contributions.....	xxii
Funding.....	xxiii
Nomenclature.....	xxiv
Chapter 1 General introduction.....	1
1.1 CO/CO ₂ bioconversion: simultaneous biofuel production and carbon neutrality.....	2
1.1.1 Renewable fuels for achieving carbon neutrality.....	2
1.1.2 Biological production of ethanol/butanol from CO/CO ₂	3
1.2 Objectives and scope of this PhD study.....	4
1.3 Thesis outline.....	5
1.4 References.....	7
Chapter 2 Enhanced solventogenesis using syngas bioconversion.....	9
Abstract.....	10
2.1 Ethanol and butanol production from CO/syngas.....	10
2.2 Solventogenesis in syngas fermentation.....	13
2.3 Microorganisms.....	14
2.4 Process parameters for enhanced ethanol production.....	17
2.4.1 Gas phase.....	17
2.4.2 Fermentation conditions.....	19
2.4.3 Medium composition.....	21
2.5 Thermodynamic calculation of Gibbs free energy.....	23
2.5.1 Gibbs free energy calculation.....	23
2.5.2 CO conversion to acetic acid and ethanol under different CO pressures and pH, at 25, 33 and 55°C.....	24
2.5.3 CO to butyric acid and butanol under different CO pressures and pH, at 25, 33 and 55°C.....	26
2.6 Conclusion.....	30
References.....	30

Chapter 3 Homoacetogenesis and solventogenesis from H ₂ /CO ₂ by granular sludge at 25, 37 and 55°C	39
Abstract.....	40
3.1 Introduction	40
3.2 Materials and methods.....	42
3.2.1 Biomass and medium composition	42
3.2.2 Batch experimental set-up.....	42
3.2.3 Analytical methods.....	43
3.2.4 Thermodynamic calculations	44
3.2.5 Carbon balance and electron balance calculation	44
3.2.6 Undissociated acids calculation	45
3.2.7 Thermodynamic and electron calculation process	45
3.3 Results and discussion.....	47
3.3.1 Acetic acid and ethanol production at 25, 37 and 55°C from H ₂ /CO ₂ by granular sludge	47
3.3.2 Threshold pH and acetic acid concentration for ethanol production	50
3.3.3 Methane production at 55°C from H ₂ /CO ₂ by granular sludge	53
3.3.4 Gas consumption and production rates	55
3.3.5 Carbon and electron balance	57
3.3.6 HCO ₃ ⁻ enhanced acetic acid production and inhibited ethanol production.....	59
3.3.7 Microbial community analysis.....	60
3.4 Conclusions	61
3.5 References	62
Chapter 4 Bioethanol production from H ₂ /CO ₂ by solventogenesis using anaerobic granular sludge: effect of process parameters	68
Abstract.....	69
4.1 Introduction	69
4.2 Materials and methods.....	71
4.2.1 Biomass.....	71
4.2.2 Medium composition	71
4.2.3 Experimental set-up	71
4.2.4 Experimental design.....	72
4.2.5 Analytical methods.....	72
4.3 Results	73

4.3.1 Effect of initial pH on H ₂ /CO ₂ bioconversion at 25°C.....	73
4.3.2 Effect of temperature on H ₂ /CO ₂ fermentation by granular sludge	73
4.3.3 Effect of glucose on H ₂ /CO ₂ bioconversion at 25°C	76
4.3.4 Effect of trace metals (W, Mo, Zn, Ni) on H ₂ /CO ₂ fermentation at 25°C	80
4.4 Discussion.....	83
4.4.1 Effect of temperature and pH on solventogenesis.....	83
4.4.2 Effect of organic and inorganic carbon source on solventogenesis	85
4.4.3 Enhanced ethanol production by trace metal addition	86
4.5 Conclusion.....	87
4.6 References	88
Chapter 5 Enrichment of homoacetogens converting H ₂ /CO ₂ into acids and ethanol and simultaneous methane production.....	93
Abstract.....	94
5.1 Introduction	94
5.2 Materials and methods.....	95
5.2.1 Biomass and medium composition	95
5.2.2 Experimental design.....	96
5.2.3 Analysis.....	97
5.3 Results	98
5.3.1 Enrichment of acetogenic sludge and production of acids and ethanol in gas fed reactor	98
5.3.2 Effect of exogenous acetate and tungsten addition on H ₂ /CO ₂ conversion by enriched sludge	101
5.3.3 Effect of exogenous acetate on with H ₂ /CO ₂ conversion by enriched sludge	102
5.3.4 Acetate and ethanol conversion in the presence of H ₂ /CO ₂ by enriched sludge.....	104
5.3.5 Microbial analysis	105
5.4 Discussion.....	108
5.4.1 VFAs and ethanol production by anaerobic granular sludge in the gas fed reactor	108
5.4.2 Methane production in batch tests by enriched sludge in batch tests	109
5.4.3 Effect of exogenous acetate on acetogenesis and methanogenesis by enriched sludge	109
5.5 Conclusion.....	110
5.6 References	110

Chapter 6 Selective butanol production from carbon monoxide by an enriched anaerobic culture	113
Abstract.....	114
6.1 Introduction	114
6.2 Materials and methods.....	116
6.2.1 Biomass	116
6.2.2 Medium composition	116
6.2.3 Experimental set-up	117
6.2.4 Experimental design.....	120
6.2.5 Carbon balance calculation	121
6.2.6 Microbial analysis	122
6.2.7 Analytical methods.....	123
6.3 Results	124
6.3.1 Enrichment and selective butanol production by anaerobic granular sludge in FB1	124
6.3.2 Conversion pathways for selective butanol production by enriched sludge	128
6.3.3 Ethanol and butanol production by the enriched culture at pH 6.2 and 5.7 in FB2.	132
6.3.5 Microbial community analysis	133
6.4 Discussion.....	135
6.4.1 Selective butanol production by CO fed anaerobic sludge	135
6.4.2 Ethanol and butanol oxidation in the presence of CO ₂	138
6.4.3 H ₂ production during start-up period	140
6.5 Conclusions	142
6.6 References	143
Chapter 7 Enhanced ethanol production from carbon monoxide by enriched <i>Clostridium</i> bacteria.....	149
Abstract.....	150
7.1 Introduction	150
7.2 Materials and methods.....	152
7.2.1 Source of inoculum	152
7.2.2 Medium composition	152
7.2.3 Experimental set-up	152
7.2.4 Analytical methods.....	154
7.2.5 Microbial analysis	154

7.3 Results	157
7.3.1 Enrichment of CO-converting acetogens	157
7.3.2 Enhanced ethanol production with minor acetic acid accumulation.....	163
7.3.3 Butanol production from exogenous butyric acid using CO as reducing power	169
7.3.4 Glucose and CO co-fermentation.....	172
7.3.5 CO conversion with pH controlled at 5.7 and 6.2.....	174
7.4 Discussion.....	176
7.4.1 Enhanced ethanol production with minor accumulation of acetic acid by highly enriched <i>Clostridium</i> sludge	176
7.4.2 Enrichment of CO-converting microorganisms for enhanced ethanol production ..	178
7.4.3 Enhanced butanol production from exogenous butyric acid by enriched <i>Clostridium</i> populations.....	180
7.4.4 Bioconversion of glucose or glucose and CO co-fermentation by the enriched culture	181
7.5 Conclusions	182
7.6 References	182
Chapter 8 Effect of endogenous and exogenous butyric acid on butanol production with CO by enriched <i>Clostridia</i>	187
Abstract.....	188
8.1 Introduction	188
8.2 Materials and methods.....	190
8.2.1 Source of inoculum	190
8.2.2 Medium composition	190
8.2.3 CO fed batch reactor set-up.....	191
8.2.4 Experimental design.....	191
8.2.5 Analytical methods.....	194
8.2.6 Calculations.....	194
8.2.7 Microbial analysis	195
8.3 Results	195
8.3.1 Ethanol and butanol production with exogenous acetic acid, ethanol and butyric acid using CO as the carbon source.....	195
8.3.2 Effect of exogenous butyric acid supply on butanol production.....	199
8.3.3 Fermentation with endogenous butyric acid from glucose	201
8.3.4 Microbial analysis	204

8.4 Discussion.....	210
8.4.1 Exogenous butyric acid enhanced butanol production using CO as reducing power	210
8.4.2 The presence of acetate and ethanol favored butanol production from butyric acid using CO as reducing power	212
8.4.3 CO triggered butanol production from endogenous butyric acid produced from glucose with no significant microbial community change.....	213
8.4.4 Glucose and CO co-fermentation enhanced butyric acid but not butanol production	214
8.5 Conclusions	215
8.6 References	215
Chapter 9 General Discussion and Future Perspectives	220
9.1 General discussion.....	221
9.1.1 Ethanol production from H ₂ /CO ₂ by mixed cultures	225
9.1.2 Enhancement and selective butanol production from CO by anaerobic sludge.....	226
9.1.3 Enrichment of solventogenic acetogens from CO	226
9.1.4 Enhancement strategies for butanol production by exogenous butyric acid.....	226
9.2 Future perspectives	227
9.2.1 Microbial resource management	227
9.2.2 Reactor design.....	228
9.2.3 Mass transfer	229
9.2.4 Longer chain solvents and other valuable chemicals from CO/CO ₂	230
9.2.5 Scale-up of syngas fermentation	231
9.3 Conclusions	232
9.4 References	233
Author information	238
Biography	238
Publications	238
Conferences	239
Courses and modules	239

Table of figures

Fig. 1.1 Diagram of the chapters this PhD thesis	5
Fig. 2.1 Biofuel production from a variety of resources using direct fermentation of the organic feedstock, eventually after a pretreatment or indirect fermentation of CO upon incomplete combustion of the feedstock to syngas (CO, H ₂ , CO ₂).	11
Fig. 2.2 Wood–Ljungdahl pathway and metabolites formation from acetyl-CoA, with the corresponding metalloenzymes. The corresponding microorganisms under Acetyl-CoA, Butyryl-CoA and Hexanoyl-CoA represent their ethanol, butanol and hexanol production ability. The corresponding ethanol, butanol and hexanol microorganisms and the potential mixotrophy strains (Maru et al., 2018). The pathway was adapted from previous publications (Fast et al., 2015; Norman et al. 2018; Kennes et al. 2016).....	12
Fig. 2.3 Process parameters influencing syngas fermentation by microorganism.	13
Fig. 2.4 Diagram of the <i>C. acetobutylicum</i> and <i>C. ljungdahlia</i> co-culture. <i>C. acetobutylicum</i> consumes glucose to produce solvents, while releasing CO ₂ and H ₂ . <i>C. ljungdahlia</i> consumes H ₂ and CO ₂ for survival and growth producing acetate and ethanol through WLP.	16
Fig. 2.5 Diagram of the co-culture of <i>C. autoethanogenum</i> and <i>C. kluyveri</i> using CO as the substrate.	16
Fig. 2.6 The theoretical Gibbs free energy of CO to acetic acid when the pH varies from 1 to 12, corresponding to the different CO gas pressure (0.01-10 bar) at 25, 33 and 55°C....	28
Fig. 2.7 The theoretical Gibbs free energy of CO to ethanol conversion under the different CO gas pressure (0.01-10 bar) at 25, 33 and 55°C.	28
Fig. 2.8 The theoretical Gibbs free energy of CO to ethanol, butyric acid and butanol conversion under the different CO gas pressure (0.01-10 bar) at 25, 33 and 55°C. (Calculated by 1 mol butyric acid production and without considering pH)	29
Fig. 3.1 Acetic acid and ethanol yield a) at 25°C, b) at 37°C, c) at 55 °C, d) pH, e) CO ₂ uptake and f) H ₂ uptake for the incubations with heat-treated granular sludge at 25, 37, 55 °C. Every point shows the average of three independent batch cultures, error bars of acetic acid and ethanol production at 25 and 37 °C indicate the standard deviation of the triplicates. H ₂ /CO ₂ was injected at every time point.....	49
Fig. 3.2 Undissociated acetic acid concentrations and the linear fit at 25°C and 37°C using H ₂ /CO ₂ as substrate by heat-treated granular sludge (0.104 h ⁻¹ at 25°C, R ² = 0.97; 0.145 h ⁻¹ at 37°C, R ² = 0.98).	50

Fig. 3.3 Ethanol production at 25°C using H ₂ /CO ₂ as the substrate by granular sludge as a function of a) the molar ethanol (x-axis) and acetic acid concentration (y-axis) and b) the molar ethanol.....	51
Fig. 3.4 Relative taxonomic abundance of <i>Clostridium sp.</i> with heated treated granular sludge as inoculum at the end of incubation at a) 25, b) 37 and c) 55 °C using H ₂ /CO ₂ as substrate and d) raw granular sludge ; e) 25 °C using H ₂ /CO ₂ + HCO ₃ ⁻ as the substrate.....	52
Fig. 3.5 Gibbs free energy change of a) acetic acid production as a function of pH at different CO ₂ /H ₂ partial pressures and b) ethanol production as function of pH at different H ₂ partial pressures and 1 M acetic acid.	53
Fig. 3.6 Relative abundance of thermoanaerobic bacteria species with heated treated granular sludge as inoculum at the end of incubation at 55 °C using H ₂ /CO ₂ as the substrate.	55
Fig. 3.7 a) Ethanol to acetic acid ratio using H ₂ /CO ₂ or H ₂ /CO ₂ + HCO ₃ ⁻ as the substrate at 25 and 37 °C by granular sludge; b) Consumed H ₂ to CO ₂ ratio using H ₂ /CO ₂ as the substrate at 25, 37 and 55°C by granular sludge.	55
Fig. 3.8 H ₂ and CO ₂ consumption rate, CH ₄ , acetic acid and ethanol production rate at a) 25°C, b) 37°C and c) 55 °C by heat treated granular sludge using H ₂ /CO ₂ as substrate.....	57
Fig. 3.9 Carbon distribution at the end of each batch culture (each time injecting gas means a batch culture at a) 25°C, b) 37°C and c) 55°C. The columns refer to the mmol of carbon found in the different metabolites at the end of every batch culture and the black dots represent their sum. The green dots with dash line represent the mmol carbon of consumed CO ₂ . Every column or point shown in the graphs is calculated as the average of three independent batch cultures, error bars indicate the standard deviation of the triplicates.	58
Fig. 3.10 Acetic acid, ethanol and CH ₄ yield at a) 25°C, b) 37°C, c) 55 °C and d) pH in incubations with the heat-treated granular sludge at 25, 37, 55 °C in the presence of HCO ₃ ⁻ . Every point shown in the graphs is calculated as the average of three independent batch cultures, error bars indicate the standard deviation of the triplicates.	59
Fig. 3.11 Relative taxonomic abundance of the batch cultures at genus level with heated treated granular sludge as inoculum at the end of incubation at a) 25, b) 37 and c) 55 °C using H ₂ /CO ₂ as substrate and d) untreated granular sludge ; e) 25 °C using H ₂ /CO ₂ + HCO ₃ ⁻ as substrate.	61
Fig. 4.1 Acetic acid and ethanol production from H ₂ /CO ₂ by heat-treated granular sludge at 25°C at (A) pH 7, (B) pH 6, (C) pH 5 and (D) change of pH over time.....	74

Fig. 4.2 Acetic acid and ethanol yield and pH change using (A) and (B) H_2/CO_2 ; (C) and (D) $H_2/CO_2 + HCO_3^-$ by heat-treated granular sludge at 18, 25, 30 °C. Every point shown in the graphs is calculated as the average of three independent batch cultures, error bars indicate the standard deviation of the triplicates.75

Fig. 4.3 Gas pressure using (A) H_2/CO_2 , (B) H_2/CO_2 with HCO_3^- by heat-treated granular sludge at 18, 25, 30 °C. Every point shown in the graphs is calculated as the average of three independent batch cultures, error bars indicate the standard deviation of the triplicates.76

Fig. 4.4 Acetic acid, ethanol and butyric acid production by heated-treated granular sludge at 25°C using (A) glucose+ H_2/CO_2 , (B) H_2/CO_2 and (C) glucose as the substrate and (D) change of pH. The dashed vertical lines represent the different phases in the fermentation process; I: 0-120 h, II: 120-192 h, III: 192-264 h, IV: 264-552 h.77

Fig. 4.5 Acetic acid and ethanol production by heat-treated granular sludge using H_2/CO_2 as the substrate at 25°C with the addition of (A) 2 μ M, 10 μ M W, (B) 2 μ M, 10 μ M Mo, (C) 10 μ M Ni, 50 μ M Zn, (D) No trace metals and (E) and (F) change of pH.81

Fig. 4.6 The mole ratio of ethanol to acetic acid by heat-treated granular sludge using H_2/CO_2 as the substrate at 25°C with the standard medium, control and addition of 2 μ M, 10 μ M W, 2 μ M, 10 μ M Mo, 10 μ M Ni and 50 μ M Zn82

Fig. 4.7 H_2 and CO_2 uptake with the addition of (A) 2 μ M, 10 μ M Mo, (B) 2 μ M, 10 μ M W, (C) 10 μ M Ni, 50 μ M Zn and (D) H_2/CO_2 uptake ratio by heat-treated granular sludge using H_2/CO_2 as the substrate at 25°C with initial pH 6.83

Fig. 5.1 Diagram of the up-flow gas reactor with pH control96

Fig. 5.2 H_2/CO_2 fermentation in a semi-continuous gas fed reactor by anaerobic granular sludge. a) acids and ethanol production, b) change of pH and c) H_2 , CO_2 concentration from H_2/CO_2 or H_2 by granular sludge. The substrate of stage I, II and III are, respectively, H_2/CO_2 , H_2 and $H_2 + 10 \mu$ M tungsten..... 100

Fig. 5.3 H_2 and CO_2 consumption and CH_4 , acetate and ethanol production by enriched sludge sampled on day 70 from the bioreactor using a) H_2/CO_2 , b) $H_2/CO_2 + 15$ mM acetate and c) $H_2/CO_2 + 10 \mu$ M tungsten as the substrate and d) change of pH in these incubations. 101

Fig. 5.4 Effect of 10, 15, 30 and 45 mM exogenous acetate on production profiles by enriched sludge (day 70 of bioreactor operation) using H_2/CO_2 as the substrate a) acetate concentration, b) CH_4 , c) CO_2 and d) H_2 production, e) change of pH and f) gas pressure. . 103

Fig. 5.5 H ₂ and CO ₂ consumption and CH ₄ , acetate and ethanol production in the presence of a) 15 mM acetate + 5 mM Ethanol and b) 30 mM Acetate + 15 mM Ethanol, c) pH and d) gas pressure change by enriched sludge sampled on day 70 using H ₂ /CO ₂ as the substrate.	104
Fig. 5.6 Effect of glucose (0.5 g/L) on H ₂ /CO ₂ bioconversion by enriched sludge.	105
Fig. 5.7 Relative abundance of microorganism from suspended sludge at 10 d, and the end of stage I, II, III (III-a, b and c are triplicates) and the granular sludge inoculum (G-a, G-b) at genus level. The two batch bottles used the sludge taken from the bioreactor as inoculum (stage I, day 26) (I-a, I-b). a) Microbial analysis of all bacteria; b) Genus level in the <i>Clostridiales</i> order, the relative abundance is relative to all the bacteria, and c) Genus level in the <i>Clostridiales</i> order, the relative abundance is relative to the <i>Clostridiales</i> order.....	106
Fig. 5.8 Acetic acid and ethanol production of the two enriched bottles using sludge from the bioreactor (day 26, stage I) as inoculum.	107
Fig. 6.1 Schematic diagram of the CO fed batch reactor set-up.....	118
Fig. 6.2 CO bioconversion for ethanol and butanol production by heat-treated granular sludge in an intermittent gas-fed bioreactor (FB1) with initial CO gas pressure of 1.8 bar. a) Production of acetic acid (HAc), propionic acid (HPr), butyric acid (HBu), ethanol (EtOH) and butanol (BtOH), b) gas pressure, c) pH, d) CO ₂ and H ₂ production and CO consumption and e) CO ₂ and H ₂ production and CO consumption (mmol L ⁻¹ d ⁻¹) at each CO feeding. The orange dots inside the dash box in panel represent 1.8 bar CO feeding. The red cross mark in panel c) represents pH adjustment to 5.7 each time CO was added.	126
Fig. 6.3 Carbon balance for ethanol and butanol production using CO as the sole carbon source by heat-treated granular sludge in an intermittent gas-fed bioreactor (FB1). The input mmol carbon of CO consumption and distributed as CO ₂ and acids and alcohols production, produced carbon as sum of CO ₂ , acids and alcohols.	127
Fig. 6.4 Studies of CO (a, b) and syngas (c, d) bioconversion by enriched sludge sampled day 127 at initial pH 6.2 in batch experiments. a) and c) products profiles; b) and d) change of pH and gas pressure by enriched sludge in batch tests with initial CO/syngas gas pressure 1.8 bar. Red cross marks in panel b) and d) represent pH adjustment to 5.7 each time CO was added.	128
Fig. 6.5 Effect of exogenous acetic acid and ethanol addition on the production of acetic acid, propionic acid, butyric acid, ethanol and butanol, change of pH and OD ₆₀₀ by enriched sludge (sampled day 127 from FB1) in batch tests. a) N ₂ + initial pH 6.5, b) N ₂ + initial pH 5.7, c) CO ₂ + initial pH 6.5 and d) CO ₂ + initial pH 5.7 as well as e) Net production of acetic acid	

and ethanol and molar ratio of consumed ethanol and produced acetic acid. Red cross marks in panel c) and d) represent manual pH adjustment..... 130

Fig. 6.6 Production of acetic acid, propionic acid, butyric acid, ethanol, and butanol from exogenous butanol + CO₂ by the enriched sludge sampled at day 127 from FB1. Initial pH of a) 6.5 and b) 5.7 and corresponding changes in pH and OD₆₀₀ of c) and d). Red cross mark represents manual pH adjustment. 131

Fig. 6.7 a) Acetic acid, propionic acid, ethanol, butyric acid, butanol and cell concentrations (OD₆₀₀) and b) change of pH and gas pressure using CO as the sole substrate by the enriched sludge (sampled day 127) with intermittent CO gas feeding (FB2) on days 0, 14, 16, 17, 18, 19, 21, 22, 24, 26 and 28 d. Dash line in panel b represent CO feeding..... 132

Fig. 6.8 Relative taxonomic abundance at a) genus and b) *Clostridium* species level of the enriched sludge from FB1 at day 127. 134

Fig. 6.9 Relative taxonomic abundance at family (a) and genus (b) level of the inoculum granular sludge..... 134

Fig. 6.10 a) Net production rates of acetic acid, propionic acid, butyric acid, ethanol and butanol in the intermitted fed reactor in mmol C L⁻¹ d⁻¹ and b) CO consumption and production of CO₂ and H₂. The blue triangle inside the dash square means CO feeding. 141

Fig. 7.1 Distribution of scaftig length (>=500bp) 156

Fig. 7.2 Enrichment of CO converting solventogenic bacteria among the five transfers using CO as the carbon source by enriched sludge with initial CO gas pressure of 1.8 bar. (A), (C), (E), (G) and (I) represent the changes of gas pressure and pH of the 1st, 2nd, 3rd, 4th and 5th transfer, respectively. (B), (D), (F), (H) and (J) represent cell concentration (OD₆₀₀) acetic acid (HAc), propionic acid (HPr), butyric acid (HBu), ethanol (EtOH), isovaleric acid (i-Hval) and butanol (BtOH) production of the 1st, 2nd, 3rd, 4th and 5th transfer, respectively. The dash lines in Figure (A), (C), (E), (G) and (I) represent 1.8 bar CO addition and pH adjustment. 159

Fig. 7.3 Changes of pH and gas pressure (A) and cell concentration (OD₆₀₀), acetic acid, propionic acid, butyric acid, ethanol, butanol and molar ratio of ethanol to acetic acid (B) using CO as the carbon source with initial CO gas pressure of 1.8 bar in the 6th transfer by enriched sludge. The dash lines in Fig. 7.2A represent 1.8 bar CO addition and pH adjustment. 164

Fig. 7.4 Comparison of the maximum ethanol and butanol concentration (A) and acetic acid, butyric acid and cell concentration (OD₆₀₀) (B) of the 1st, 2nd, 3rd, 4th and 5th transfer using CO as the carbon source by enriched sludge. 165

Fig. 7.5 Relative abundance at genus level of (A) the initial inoculum, (B) 2nd, (C) 4th, (D) 5th and (E) 6th transfers for enriched acetogens using CO as the carbon source. 166

Fig. 7.6 Production of acetic acid (Hac), propionic acid (HPr), butyric acid (Hbu), ethanol (EtOH), isovaleric acid (i-Hval) and butanol (BtOH) of different transfer times and change of gas pressure and pH at 7 th using CO as the carbon source by enriched sludge with initial CO.	167
Fig. 7.7 Relative abundance at genus level of the a) 7 th and b) 8 th transfer to enrich CO converting acetogens.....	167
Fig. 7.8 Clustering tree based on Bray-Curtis distance of the inoculum, 2 nd , 4 th , 5 th , 6 th , 7 th , 8 th and exogenous butyric acid addition.	168
Fig. 7.9 Venn diagrams of (A) the whole genes and (B) genes in <i>Clostridium</i> genus level present in the inoculum, 2 nd , 4 th , 5 th , 6 th , 7 th , 8 th and exogenous butyric acid addition of enrichment study; (C) the whole genes and (D) genes in <i>Clostridium</i> genus level pH 5.7, pH 6.2 and 6 th transfer enriched sludge for ethanol production under pH control. The overlapping parts represent the number of common genes among samples (groups); the other parts represent the number of special genes present in a particular sample.	169
Fig. 7.10 Effect of exogenous 3.2 g/L butyric acid on acetic acid, propionic acid, isovaleric acid, butyric acid, ethanol, butanol production and cell concentration (OD ₆₀₀) (A), change of pH and gas pressure (B) and molar ratio of butyric acid consumption/butanol production and butyric acid consumption percentage (C) using CO as the carbon source with initial CO gas pressure of 1.8 bar by enriched sludge.	170
Fig. 7.11 Microbial community analysis of (A) exogenous 3.2 g/L butyric acid addition inoculated with the 5 th transfer enriched sludge, (B) exogenous 5 g/L glucose addition inoculated with 6 th transfer enriched sludge; (C) pH 6.2 and (D) pH 5.7 inoculated with 7 th enriched sludge.	172
Fig. 7.12 Glucose consumption and acetic acid, propionic acid, butyric acid, ethanol, butanol production in mmol·L ⁻¹ C using (A) 5 g/L glucose + N ₂ and (B) 5 g/L glucose + CO as the substrate by the enriched sludge (6 th transfer) and (C) cell concentration (OD ₆₀₀).....	173
Fig. 7.13 Acetic acid, propionic acid, butyric acid, ethanol and butanol production and change of gas pressure and pH, respectively, under pH control of 5.7 (A) and (B), 6.2 (C) and (D) and manually pH adjustment (E) and (F) using CO as the carbon source with initial CO gas pressure 1.8 bar by the enriched sludge from the 7 th transfer.	176
Fig. 8.1 Schematic diagram of a) influence of exogenous acetate, butyrate and ethanol on butanol production using CO as gaseous substrate, b) endogenous butyric acid from glucose (Glucose +N ₂) and c) co-fermentation of CO and glucose (Glucose+CO).	192

Fig. 8.2 Production of acids and alcohols, cells concentration and change of gas pressure in semi-gas feeding reactors by enriched sludge from 6th transfer using CO as the carbon source. a) and b) exogenous acetic acid and ethanol; c) and d) exogenous acetic acid, ethanol and butyric acid; e) and f) exogenous butyric acid; g) and h) control without exogenous acids or ethanol. The dashed lines represent CO addition and pH regulation..... 197

Fig. 8.3 Production of acids and alcohols, cells concentration and change of gas pressure in semi-gas feeding reactors by enriched sludge from 6th transfer (He et al. 2021b) using CO as the carbon source. a) and b) exogenous 7 g/L butyric acid; c) and d) exogenous 14 g/L butyric acid. The dashed lines represent CO addition and pH regulation.....200

Fig. 8.4 a) Production of acids and alcohols and b) cell concentration and pH by enriched sludge using 5 g/L glucose as the substrate in batch tests. Down arrows in a) represent 1.1 bar CO addition at 120, 216 and 264 h. pH was adjusted to 5.9 on a daily basis.....202

Fig. 8.5 a) Production of acids and alcohols and b) cell concentration and pH by enriched sludge using 5 g/L glucose as the substrate in a gas fed reactor (Glucose+N₂). Down arrows represent 1.1 bar CO addition at 180, 252, 360 and 432 h. pH was controlled at 5.5 – 6.2. .203

Fig. 8.6 a) Production of acids and alcohols and b) cell concentration and pH by enriched sludge from 6th transfer using 5 g/L glucose and CO as substrate in a gas fed reactor with intermittent CO gas feeding (Glucose+CO). Down arrows in a) represent 1.1 bar CO addition at 0, 180, 276 and 432 h, respectively. pH was controlled at 5.5 – 6.2.206

Fig. 8.7 The microbial community analysis of the initial inoculum, after glucose fermentation and CO and glucose co-fermentation from 6th transfer.207

Fig. 8.8 Clustering tree based on Bray-Curtis distance of the microbial community after G+N and G+C fermentation by enriched sludge from 6th transfer. ‘(G+N)₁’ represent when glucose totally consumed using glucose as substrate and ‘(G+N)₂’ represent at the end of the incubation after CO was added. ‘(G+C)₁’ represent when glucose totally consumed and ‘(G+C)₂’ represent at the end of the incubation in glucose and CO co-fermentation.....208

Fig. 8.9 Venn diagrams of gene number of a) the total genes and b) the genes in *Clostridium* genus level. The overlap parts represent the number of common genes between/among samples (groups); the other parts represent the number of special genes of samples (groups).210

Fig. 9.1 Integrated process parameters for bioethanol production from H₂/CO₂ using anaerobic granular sludge of a) chapter 3, chapter 4 and c) chapter 5.....222

Fig. 9.2 Overview of CO fermentation for ethanol and butanol production and enrichment of CO converting <i>Clostridium</i> bacteria present in anaerobic granular sludge in a) chapter 6, b) chapter 7 and c) chapter 8.	223
Fig. 9.3 Summary of the major findings of this PhD research	224
Fig. 9.4 Integrated syngas and CO ₂ /H ₂ bioconversion for ethanol, butanol and hexanol production. CSTR: continuous stirred tank reactor; BTF: Bio-trickling filter; HFM: hollow fiber membrane.	232

Table of tables

Table 2.1 Alcohol and organic acid concentrations, yields and productivities during syngas fermentation using various bio-catalysts.	15
Table 2.2 Theoretical reactions of syngas fermentation to ethanol and butanol.	18
Table 3.1 Ethanol fermentation using H ₂ /CO ₂ or H ₂ /CO ₂ /CO as the substrate by mixed and pure cultures in batch experiments.	47
Table 3.2 The average relative abundance (%) at genus level at the end of assay using H ₂ /CO ₂ as substrate at 25, 37 and 55 °C and H ₂ /CO ₂ + HCO ₃ ⁻ as the substrate at 25°C by heat-treated granular sludge.	51
Table 3.3 Shift pH from acetic acid to ethanol of <i>Clostridium sp.</i> or anaerobic sludge at various temperatures using H ₂ or syngas as the substrate.	53
Table 3.4 Molar concentration changes of products with H ₂ /CO ₂ as the carbon source at the end of the incubation.	56
Table 4.1 Effect of pH, carbon supplements and trace metals on the maximum acetic acid and ethanol concentrations and H ₂ and CO ₂ consumption from H ₂ /CO ₂ by heat-treated anaerobic granular sludge (at the end of incubation).	78
Table 4.2 Effect of HCO ₃ ⁻ on the maximum acetic acid and ethanol concentration from H ₂ /CO ₂ by heat-treated anaerobic granular sludge at initial pH 6.	79
Table 5.1 The operational taxonomic units (OTUs) sequence table per sample statistics for microbial community analysis. Samples taken from suspended sludge at 10 d, and the end of stage I, II, III (III-a, b and c are triplicates) and the granular sludge inoculum (G-a, G-b) at genus level. The two batch bottles used the sludge taken from the bioreactor as inoculum (stage I, day 26) (I-a, I-b).	98
Table 5.2 The highest production of acetic acid and ethanol, CH ₄ accumulation, H ₂ and CO ₂ consumption at the end of incubation by enriched sludge in batch tests.	101
Table 6.1 The operational conditions and production profile, highest alcohol to acids ratio and highest concentration of acids and alcohols in period I (0- 99 d) and II (100-127 d) in FB1 using CO as the sole substrate by the heat treated enriched anaerobic culture.	119
Table 6.2 Maximum ethanol and butanol concentrations achieved during syngas and CO fermentation by pure and mixed cultures in batch and continuous bioreactor systems.	139
Table 6.3 Environmental conditions of H ₂ production using CO as substrate by pure cultures and enrichments.	142
Table 7.1 The Statistic of gene catalogues.	154

Table 7.2 Relative abundance of <i>Clostridium</i> spp. at genus level in the initial inoculum sludge and the 2 nd , 4 th , 5 th , 6 th , 7 th and 8 th transfer as well as in the incubation with exogenous butyric acid (HBu) and glucose addition (Glucose), controlled pH 6.2 and pH 5.7.....	161
Table 7.3 Highest ethanol and butanol concentrations during syngas/CO fermentation using various biocatalysts.	162
Table 8.1 The highest net acids and alcohol production, mole ratio of ethanol to acetic acid and butanol to butyric acid, butyric acid conversion and butanol yield of experiments on the influence of acetate, butyrate and ethanol on butanol production using CO as gaseous substrate.	193
Table 8.2 The highest net production of acids and alcohol, mole ratio of butanol to butyric acid and butanol yield.	202
Table 8.3 Relative abundance of <i>Clostridium</i> spp. at species level in Glucose+CO and Glucose +N ₂ by enriched sludge from 6 th transfer.....	209

List of publications and chapter contributions

The work contained in this thesis consists of the following publications in international peer-reviewed journals:

Publication	Author contributions
Chapter 3 He, Y., Cassarini, C., Marciano, F. and Lens, P. N. L. 2020. Homoacetogenesis and solventogenesis from H ₂ /CO ₂ by granular sludge at 25, 37 and 55°C. <i>Chemosphere</i> , 128649.	He, Y.: Conceptualization, Methodology, Formal analysis, Investigation, Writing - original draft, Visualization. Cassarini, C.: Conceptualization, Software, Data curation, Writing – review & editing Flora Marciano, Investigation. Lens, P. N. L.: Project administration, Resources, Supervision, Funding acquisition, Writing - review & editing.
Chapter 4 He, Y., Cassarini, C., Marciano, F. and Lens, P. N. L. 2021. Bioethanol production from H ₂ /CO ₂ by solventogenesis using anaerobic granular sludge: effect of process parameters. <i>Frontiers in Microbiology</i> 12, 647370.	He, Y. carried out all experimental incubations, data analysis and drafted the manuscript. Cassarini, C. conceived the study, participated in its design and coordination and reviewed the manuscript. Lens, P. N. L. conducted the project supervision and the manuscript revision.
Chapter 6 He Y., Lens, P. N. L., Veiga, M. C. and Kennes, C. 2022. Enhanced ethanol production from carbon monoxide by enriched <i>Clostridium</i> bacteria. <i>Frontiers in Microbiology</i> 12, 754713.	He, Y. carried out all experimental incubations and data analysis and drafted the manuscript. Lens, P. N. L. conducted the project supervision and the manuscript revision. Veiga, M. C. provided the research resources. Kennes, C. conceived the study, participated in its design and coordination, and reviewed the manuscript.
Chapter 7 He Y., Lens, P. N. L., Veiga, M. C. and Kennes, C. 2022. Selective butanol production from carbon monoxide by an enriched anaerobic culture. <i>Science of the Total Environment</i> , 806, 150579.	He, Y. carried out all experimental incubations and data analysis and drafted the manuscript. Lens, P. N. L. conducted the project supervision and the manuscript revision. Veiga, M. C. provided the research resources. Kennes, C. conceived the study, participated in its design and coordination, and reviewed the manuscript.
Chapter 8 He Y., Lens, P. N. L., Veiga, M. C. and Kennes, C. 2022. Effect of endogenous and exogenous butyric acid on butanol production from CO by enriched <i>Clostridia</i> . <i>Frontiers in Bioengineering and Biotechnology</i> . Accepted.	He, Y. carried out all experimental incubations, data analysis, and drafted the manuscript. Lens, P. N. L. conducted the project supervision and the manuscript revision. Veiga, M. C. provided the research resources. Kennes, C. conceived the study, participated in its design and coordination, and reviewed the manuscript.

Funding

This PhD thesis was supported by the Science Foundation Ireland (SFI) through the SFI Research Professorship Program entitled *Innovative Energy Technologies for Biofuels, Bioenergy and a Sustainable Irish Bioeconomy* (IETS BIO3; Grant Number 15/RP/2763) and *the Research Infrastructure research grant Platform for Biofuel Analysis* (Grant Number 16/RI/3401).

Nomenclature

ABE: acetone-butanol-ethanol
ADH: alcohol dehydrogenase
AOR: aldehyde:ferredoxin oxidoreductase
BTF: bio-trickling filter
BtOH: butanol
CSTR: continuous stirred tank reactor
CO: carbon monoxide
CO₂: carbon dioxide
CODH: carbon monoxide dehydrogenase
EPA: Environmental Protection Agency
EtOH: ethanol
FDH: formate dehydrogenase
Fe: iron
H₂: hydrogen
HAc: acetic acid
HBu: butyric acid
HFM: hollow fiber membrane
HPr: propionic acid
H₂S: hydrogen sulfide
Mo: molybdenum
NH₃: ammonia
Ni: Nickel
non-ETS: non-Emissions Trading Scheme
NO_x: nitrogen oxides
UASB: upflow anaerobic sludge bed
W: tungsten
WLP: Wood-Ljungdahl pathway
Zn: Zinc

Chapter 1 General introduction

1.1 CO/CO₂ bioconversion: simultaneous biofuel production and carbon neutrality

1.1.1 Renewable fuels for achieving carbon neutrality

The ever-increasing emissions worldwide of the greenhouse gas carbon dioxide (CO₂) cause global warming and climate change. Ireland's target for the year 2020 is to achieve a 20% reduction in emissions of the non-Emissions Trading Scheme (non-ETS) sector from the 2005 levels, with annual binding limits set for each year over the period 2013- 2020 (EPA, Ireland, 2019). However, the latest projections indicate that Ireland will exceed the carbon budget over the period 2021-2030 by 52-67 Mt CO₂ (EPA, Ireland, 2019). It is imperative to adopt a sustainable way to achieve the reduced carbon emission goals. On the other hand, the increasing demand for fuels and rapidly depleting fossil fuel reserves necessitate the development of new technologies for alternative fuel production, such as biofuels. Renewable energy sources such as wind and solar power are facing the challenges of balancing power production and demand (Pereira et al., 2013). One promising approach is to convert the excess power to H₂ gas and merge it with CO₂ for biofuel production using microbial fermentation.

On the other hand, a huge amount of organic solid waste is generated annually from agricultural farms in Ireland with an estimated abatement potential of more than 18 Mt CO₂eq emission between 2021 and 2030 (EPA, Ireland, 2019). A significant portion of biomass sources like straw and wood is poorly degradable, thus making it difficult substrates for conversion to biofuels by microorganisms. Gasification of such recalcitrant biomass and other solid wastes like sludge from wastewater treatment plants produces a mixture of gases, including CO, CO₂ and H₂, referred to as syngas. This syngas could offer a solution to reduce carbon emission, as some microorganisms can convert it to biofuels and other valuable products. CO is a toxic gas and has also been found in several industrial gas emissions such as in steel plants (Yu et al, 2015).

Biofuels such as ethanol and butanol can be produced from carbon dioxide using microorganisms, either directly or indirectly, thereby simultaneously mitigating climate change and generating valuable bioenergy products. Ethanol and butanol are both valuable chemicals that can amended into fuels (Kennes et al., 2016). For instance, ethanol can be mixed up to 10% in gasoline. Butanol (C₄H₉OH, 1-butanol) is an alternative liquid fuel due to its sufficiently similar characteristics to gasoline and can be used directly in any gasoline engine without modification and/or substitution (Yu et al., 2015). Butanol thus gains more value than ethanol as biofuel (Lee et al. 2008; Knoshaug and Zhang, 2009).

1.1.2 Biological production of ethanol/butanol from CO/CO₂

Syngas conversion to biofuels such as ethanol and butanol via the water-gas shift reaction by microorganisms has gained increased attention recently (Fernández-Naveira et al., 2017). Only a low number of solventogenic carboxydrotrophic acetogens have been isolated so far, from a variety of environments such as soil, sediments, anaerobic sludge and animal manure, including *Clostridium ljungdahlii* (Tanner et al., 1993), *Clostridium autoethanogenum* (Abrini et al., 1994), *Clostridium carboxidivorans* (Liou et al., 2005) and *Butyribacterium methylotrophicum* (Lynd et al., 1982). Except the limited numbers of strains, to date, research seldom reported selective butanol production from CO or syngas and usually butanol was produced along with acetic acid, ethanol and butyric acid (Fernández-Naveira et al., 2017). The selective production of butanol in pure or mixed cultures is far less understood. Besides, the known *Clostridium* strains hardly produced butanol at concentrations higher than 2.7 g/L from syngas or CO (Fernández-Naveira et al., 2016).

Different than pure cultures, anaerobic sludge from Upflow Anaerobic Sludge Bed (UASB) wastewater treatment plants can be used as inoculum since it consists of mixed microbial communities. Mixed culture fermentations may be easier to implement at large scale compared to pure cultures, as they may be more resistant and do not require sterile conditions, among others (Charubin et al., 2019).

Despite the increasing attention paid to solventogenic syngas bioconversion, syngas fermentation still has many challenges. Some pure strains of *Clostridium* spp. have been widely studied in solventogenic conversions from syngas. However, pure culture strains face the problem of contamination, while mixed cultures can overcome the disadvantages of non-sterile conditions and are thus suitable for large application scale. Moreover, metabolic products can be obtained that are theoretically not possible in pure culture. The first challenge is the lack of understanding on the environmental conditions, especially temperature and the C/H ratio, on the ethanol production by mixed cultures. The report of sub-mesophilic (25°C) or thermophilic (55°C) conditions are rare while most studies focused on mesophilic (33-37°C) temperatures, the optimum growth temperatures of *Clostridium* spp. The fermentation process parameters, such as pH, carbon source (HCO₃⁻ and glucose supplementation) and trace metals remain unclear in autotrophic ethanol production by anaerobic sludge. The second challenge is the low ethanol and butanol concentration, especially butanol production, due to the limited energy gain of autotrophic metabolism. One strategy as described before, is the enrichment of CO/syngas conversion by mixed cultures for enhanced ethanol and butanol production; the second one is that the addition of exogenous acids of the corresponding solvents from acetic

acid and butyric acid would be generated using CO as reducing power, or the mixotrophy with sugar fermentation such as glucose during which endogenous butyric acid and more ATP is generated.

1.2 Objectives and scope of this PhD study

This research investigated new strategies for enhanced and selective ethanol and butanol production from H₂/CO₂ or CO. The specific objectives of this research are to:

1. Investigate ethanol production using CO₂ as the sole carbon source and H₂ as the sole electron donor by mixed cultures at submesophilic (25°C), mesophilic (37°C) and thermophilic (55°C) conditions and different C/H ratio by adding HCO₃⁻ and the enrichment of autotrophic CO₂ converting solventogenic acetogens.

2. Investigate homoacetogenesis and solventogenesis under submesophilic conditions, i.e., 18, 25 and 30 °C using CO₂ as the carbon source and H₂ as sole electron donor by anaerobic sludge. Besides, the effects of pH, also the effects of the carbon source (HCO₃⁻ and glucose) and trace metals (supplementation) on ethanol production were investigated.

3. Bioreactor study of H₂/CO₂ conversion for ethanol production by anaerobic sludge.

4. Obtain higher and selective ethanol and butanol production using CO as the sole carbon source with anaerobic sludge as the inoculum in an intermittent gas-fed bioreactor, enriching and identifying efficient CO converting solventogenic acetogens from anaerobic sludge.

5. Enrich CO metabolizing, solvent producing acetogens using 100% CO as the sole carbon source and enhance ethanol and butanol production by the enriched acetogenic bacteria and identify the functional acetogens via microbial community analysis.

6. Outline the different strategies for the addition of butyric acid, i.e. via exogenous acetic acid and ethanol, exogenous and endogenous butyric acid to enhance the selectivity of butanol by enriched sludge with high *Clostridium* spp. using CO as reducing power. To understand the change in microbial community structure upon glucose and CO co-fermentation or solely CO conversion and identify the dominant microorganisms during glycolysis with glucose as the substrate and WLP with CO as electron donor.

1.3 Thesis outline

The PhD thesis was divided into 9 chapters (Fig. 1.1).

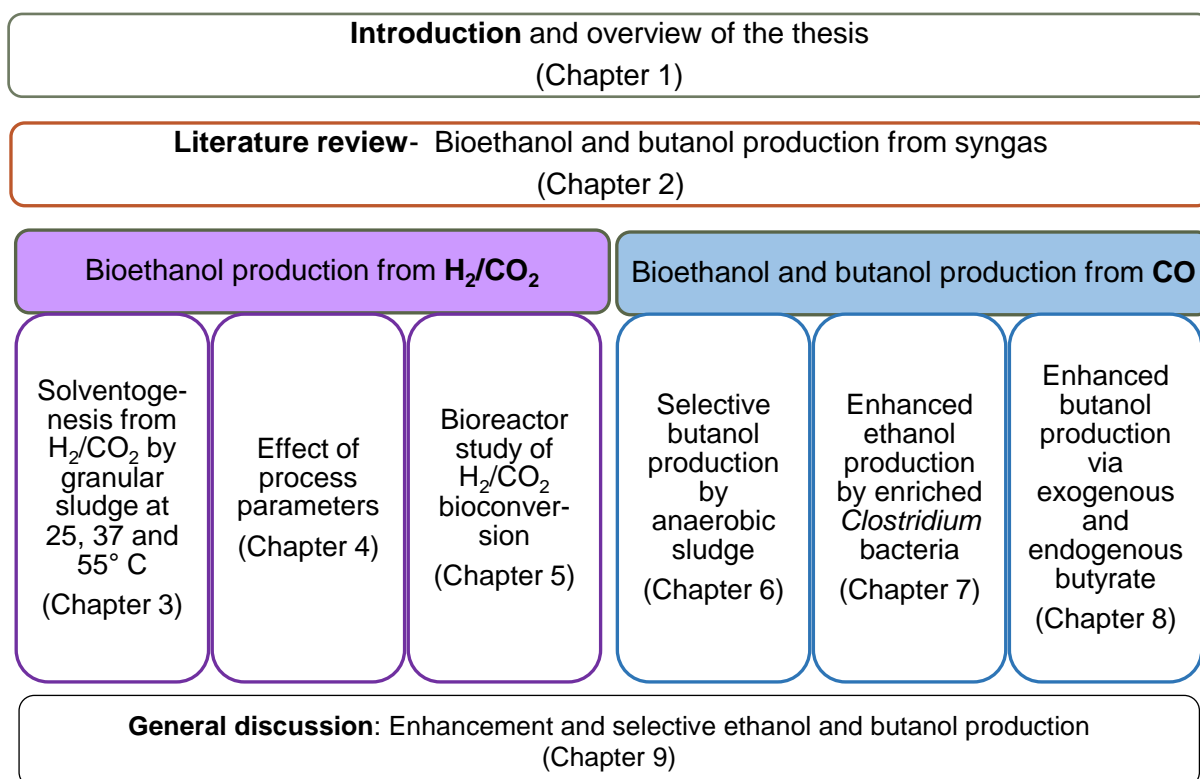


Fig. 1.1 Diagram of the chapters this PhD thesis

Chapter 1 presents an overview of this research, including background, problem description, research objectives and thesis outline. Chapter 3, 4 and 5 investigated bioethanol production from H₂/CO₂ and Chapter 6, 7 and 8 focused on bioethanol and butanol production from CO.

Chapter 2 provides a literature review on bioethanol and butanol production from syngas and comprehensively elucidates the process factors in four aspects: gaseous substrate, fermentation medium, inoculum and environmental conditions, which can influence solventogenesis. The review also discussed future trends for enhanced ethanol and butanol production via different ways, such as mixotrophy and electron transfer favored by added materials.

In chapter 3, a fermentation process that converts CO₂ to ethanol using H₂ as electron donor and anaerobic granular sludge as inoculum was studied at submesophilic (25°C), mesophilic (37°C) and thermophilic (55°C) conditions. Furthermore, the effect of bicarbonate on fermentation processes has been investigated for acetic acid and ethanol production. The

enriched and functional microbial community for solventogenesis at these submesophilic, mesophilic and thermophilic conditions has been investigated.

Chapter 4 further investigated homoacetogenesis and solventogenesis under submesophilic conditions, i.e., 18, 25 and 30 °C using CO₂ as carbon source and H₂ as sole electron donor by the same anaerobic granular sludge as used in chapter 3. Besides, the effects of pH, carbon source (HCO₃⁻ and glucose supplementation) and trace metals on ethanol production were also investigated.

Chapter 5 investigated H₂ and CO₂ bioconversion by heat-treated granular sludge in a bioreactor with both gas and medium circulation at 25°C. It is hypothesized that ethanol production could be enhanced by feeding 100% H₂ or tungsten from exogenous acetic acid conversion. Exogenous acetate with H₂/CO₂ or pure H₂ as the gaseous substrate and ethanol degradation were further investigated in batch tests by the enriched sludge taken from the reactor, from which the homoacetogenic, methanogenic and solventogenic potential has been quantified.

Chapter 6 studied selective ethanol and butanol production using CO as the sole carbon source with an anaerobic granular sludge as inoculum in an intermittent gas-fed incubation. The conversion pathway for selective butanol production by the enriched sludge in a CO fed batch reactor was elucidated. In addition, a pH shift from 6.2 to 5.7 was applied for inducing solventogenesis from CO.

Based on the CO converting solventogenic enriched sludge in chapter 6, chapter 7 first conducted the enrichment of CO metabolizing, solvent producing bacteria via six successive transfers using 100% CO as the carbon and energy source. The enriched bacteria were then determined and the functional acetogens were identified via microbial community analysis. Secondly, this study further explored the effect of exogenous butyric acid and glucose on enhanced butanol production as well as the effect of pH regulation on enhanced ethanol and butanol production by the enriched acetogenic bacteria.

Chapter 8 explored different strategies for enhanced butanol production via exogenous and endogenous acetic acid, ethanol and butyric acid by the enriched bacteria. The microbial community and identified dominated strains responsible for the butanol production via endogenous butyric acid under solely glucose fermentation followed by CO addition (Glucose + N₂) and co-fermentation of glucose and CO (Glucose + CO) by the enriched sludge were characterized.

Chapter 9 provides a general discussion based on the specific research objectives of this thesis and explores strategies for enhanced and selective ethanol and butanol production in future trends.

1.4 References

Charubin, K. and Eleftherios, T. P. 2019. Direct cell-to-cell exchange of matter in a synthetic *Clostridium syntrophy* enables CO₂ fixation, superior metabolite yields, and an expanded metabolic space. *Metabolic Engineering*, 52: 9–19.

EPA 2019 GHG Emissions Projections Report. Ireland's Greenhouse Gas Emissions Projections. 2018-2040. Environment Protection Agency, Ireland.

Fernández-Naveira, Á., Veiga, M.C. and Kennes, C. 2017. H-B-E (hexanol-butanol-ethanol) fermentation for the production of higher alcohols from syngas/waste gas. *Journal of Chemical Technology & Biotechnology*, 92 (4): 712-731.

Fernández-Naveira, Á., Abubackar, H. N., Veiga, M.C. and Kennes, C. 2016. Carbon monoxide bioconversion to butanol-ethanol by *Clostridium carboxidivorans*: kinetics and toxicity of alcohols. *Applied Microbiology and Biotechnology*, 100 (9): 4231-4240.

Kennes, D., Abubackar, H.N., Diaz, M., Veiga, M.C. and Kennes, C. 2016. Bioethanol production from biomass: carbohydrate vs syngas fermentation. *Journal of Chemical Technology and Biotechnology*, 91: 304-317.

Knoshaug, E. P. and Zhang, M. 2009. Butanol tolerance in a selection of microorganisms. *Applied Biochemistry & Biotechnology*, 153: 13-20.

Lee, S. Y., Park, J. H., Jang, S. H., Nielsen, L. K., Kim, J. and Jung, K. S. 2010. Fermentative butanol production by clostridia. *Biotechnology & Bioengineering*, 101 (2): 209-228.

Liou, J. S.-C., Balkwill, D. L., Drake G. R. and Tanner, R. S. 2005. *Clostridium carboxidivorans* sp. nov., a solvent-producing *Clostridium* isolated from an agricultural settling Lagoon, and reclassification of the acetogen *Clostridium scatologenes* strain SL1 as *Clostridium drakei* sp. nov. *International Journal of Systematic and Evolutionary Microbiology*, 55 (5): 2085–91.

Lynd, L. H., Kerby, R. and Zeikus, J. G. 1982. Carbon monoxide metabolism of the methylotrophic acidogen *Butyribacterium methylotrophicum*. *Journal of Bacteriology*, 149 (1): 255-263.

Pereira, I. A., 2013. An enzymatic route to H₂ storage. *Science*, 342 (6164): 1329-1330.

Tanner, R. S., Miller, L. M. and Yang, D., 1993. *Clostridium ljungdahlii* sp. nov., an acetogenic species in *Clostridial* rRNA homology group I. *International Journal of Systematic and Evolutionary Microbiology* 43 (2): 232–36.

Yu, J., Liu, J., Jiang, W., Yang, Y. and Sheng, Y., 2015. Current status and prospects of industrial bio-production of n-butanol in China. *Biotechnology Advances*, 33 (7):1943-15.

Chapter 2 Enhanced solventogenesis using syngas bioconversion

Abstract

Biofuels, such as ethanol and butanol, from carbon monoxide rich gas or syngas bioconversion (solventogenesis) is an attractive alternative to traditional fermentation with merits of non-food consuming and sustainability. However, there is a lack of comprehensive understanding on the process parameters and mechanisms for solventogenesis during the fermentation process. This chapter provides an overview of the current state of the art of the influencing factors during the syngas fermentation process by *Clostridium* and undefined mixed cultures. The role of syngas pressure, syngas components, fermentation pH, temperature, trace metals, organic compounds and additional materials is overviewed. Thermodynamic calculations of the Gibbs free energy of CO conversion to acetic acid, ethanol, butyric acid and butanol under varied CO pressure and pH at 25, 33 and 55°C have also been investigated.

2.1 Ethanol and butanol production from CO/syngas

Traditional fossil fuel utilization induces increased carbon emissions, further resulting in environmental problems such as climate change and global warming (Latif et al., 2014). On the other hand, the increasing demand of energy and the gradual depletion of fossil fuel renders the development of renewable energy necessary and emergent (Devarapalli and Atiyeh 2015). Compared to the traditional heterotrophic ABE (acetone-butanol-ethanol) fermentation from sugars, syngas fermentation (as an alternative to carbohydrates) for biofuel production became a promising technology for valuable chemical production such as ethanol and butanol (Bajón et al. 2017; Sathukhan et al. 2016; Fernández-Naveira et al. 2017). Syngas is generated by thermal gasification of biomass like organic wastes from agriculture, cellulose, semi-cellulose and coal (Fig. 2.1). Syngas is not only meaningful for biofuels, but also for reduction of the carbon emission, e.g. CO₂ can be converted to CO by electrolysis, yielding a mixture of CO and H₂ and unreacted CO that can be further used in syngas fermentation (Stoll et al., 2020). Ethanol and butanol are both valuable fuels, for instance, ethanol can be mixed with 10% in gasoline for energy while butanol has a similar energy content as gasoline and a higher commercial value than ethanol and can potentially replace and reduce fossil fuel consumption.

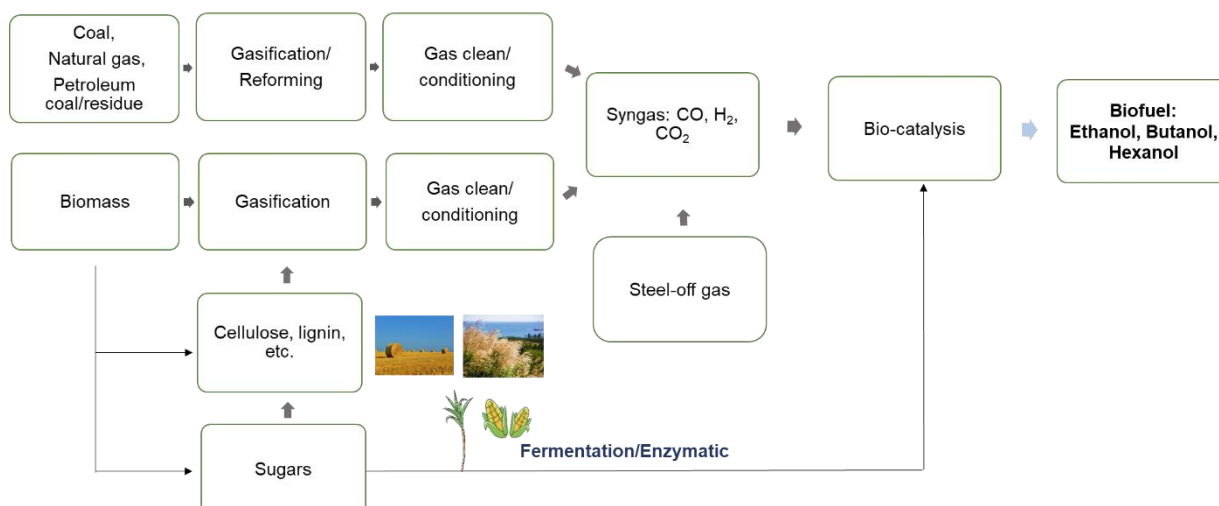


Fig. 2.1 Biofuel production from a variety of resources using direct fermentation of the organic feedstock, eventually after a pretreatment or indirect fermentation of CO upon incomplete combustion of the feedstock to syngas (CO, H₂, CO₂).

Bioconversion of syngas offers several advantages, such as higher product selectivity, greater product titers and lower energy costs (Klasson et al. 1992; Munasinghe and Khanal 2010). A handful of acetogens have been isolated which are able to use syngas as the substrate to grow. Among them, *Clostridium spp.* are the main functional species due to a special enzyme, carbon monoxide dehydrogenase (CODH), which allows them to overcome the toxicity of carbon monoxide. *Clostridium spp.* convert carbon dioxide and carbon monoxide via the Wood-Ljungdahl pathway (WLP) (Fig. 2.2), leading to the production of acetic acid, butyric acid, ethanol and butanol (Bengelsdorf et al., 2013). WLP is the most effective, non-photosynthetic carbon fixation pathway (Jones et al., 2016). In the WLP, CO is first converted to CO₂, then two moles of CO₂ are reduced, using H₂ as the electron donor, to form one mole of acetyl-CoA (Ragsdale 1997) (Fig.2.2). Two essential enzymes are included in the pathway: carbon monoxide dehydrogenase (CODH) and acetyl coenzyme A (acetyl-CoA) synthase (ACS). CODH catalyzes the reversible oxidation of CO to CO₂, and ACS combines with CODH to form a CODH/ACS complex for acetyl-CoA fixation (Liew et al. 2016).

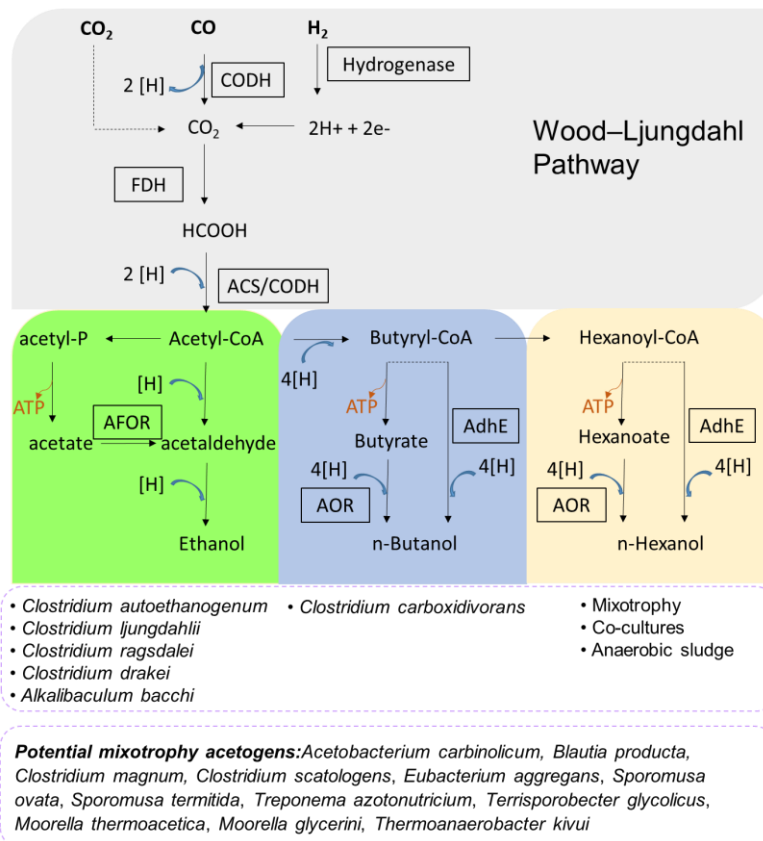


Fig. 2.2 Wood-Ljungdahl pathway and metabolites formation from acetyl-CoA, with the corresponding metalloenzymes. The corresponding microorganisms under Acetyl-CoA, Butyryl-CoA and Hexanoyl-CoA represent their ethanol, butanol and hexanol production ability. The corresponding ethanol, butanol and hexanol microorganisms and the potential mixotrophy strains (Maru et al., 2018). The pathway was adapted from previous publications (Fast et al., 2015; Norman et al. 2018; Kennes et al. 2016).

Biofuel production from syngas has received increasing attention only since the last decade and this process is far less understood than sugar fermentation. The recent reviews on biofuel production studied syngas fermentation, however, the thermodynamic view of CO conversion was seldom reported (Sun et al. 2019). Mixed cultures of *Clostridium spp.* have been investigated but excluded mixed undefined cultures such as anaerobic sludge (Cui et al., 2020) and the product was limited to one alcohol production such as butanol (Pinto et al., 2021). Considering its huge potential for sustainable biofuel production and promising applications, this review discussed the mechanism of biofuel production, identified process parameters for solventogenesis and explored future strategies for enhanced ethanol production. As shown in Fig. 2.3, four main aspects have been integrated, i.e., i) gas phase, including gas pressure and components, ii) medium composition including yeast extract and trace metals, iii) environmental conditions including pH and temperature and iv) microorganisms including pure cultures, co-cultures and anaerobic sludge (Fig. 2.3). This review also looked at the recent

approaches using i) additional materials such as biochar, granular activated carbon, nanoparticles and electron shuttles and ii) mixotrophy to enhance solventogenesis.

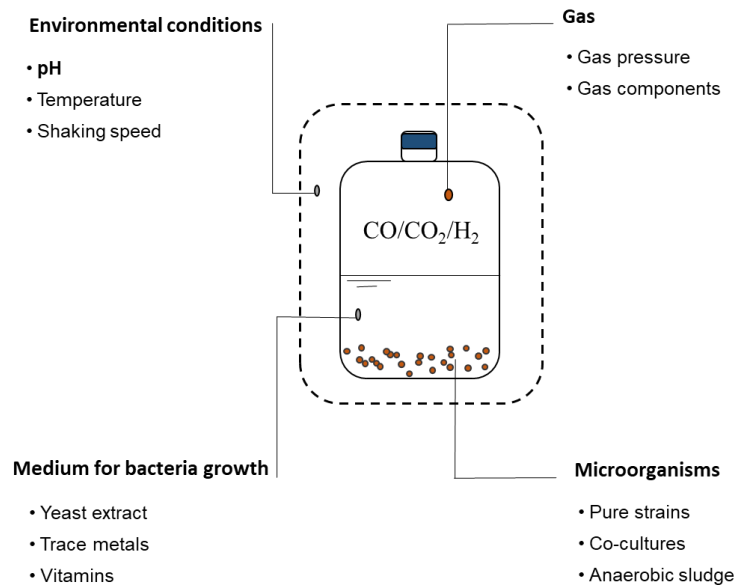


Fig. 2.3 Process parameters influencing syngas fermentation by microorganism.

2.2 Solventogenesis in syngas fermentation

Syngas fermentation for biofuel production is considered to comprise of two stages: acetic acid accumulation (acetogenesis) and ethanol conversion (solventogenesis) (Fernández-Naveira et al., 2017). Acidogenesis releases ATP for cell growth and metabolism (Yang et al. 2018), however, solventogenesis generates less ATP than acetogenesis and is thus deemed as a passive choice by acetogens (Richter et al. 2016a).

The mechanism of solventogenesis remains not fully understood although solventogenesis has been shown to be triggered by stressful conditions such as low pH or nutrient limitations (Fernández-Naveira et al., 2017). There are several hypothesis and explanations of the mechanism in the literature. One is the pH decrease view (Ganigué et al., 2016): when the pH decreases along with the accumulation of acids, undissociated acids are able to cross the cytoplasmic membrane by diffusion. To avoid cell damage or death due to the protons released by dissociated acetic and butyric acids, the microorganisms will convert the acids to neutral charged solvents (Fernández-Naveira et al. 2017). Therefore, solventogenesis is a strategy for preventing a further pH drop at the expense of a lower ATP yield and risk of toxicity from the solvents. Another explanation was from the energetic view (Liu et al., 2020): ethanol production is the preferred NADH sink and can relief energy and sustain cell survival via ethanol oxidation during the stationary phase. NADH acts as an electron carrier in large quantities accompanied by ATP synthesis.

In the acetogenesis process, the high undissociated acid accumulation rate or concentration (37-54 mM or above) under uncontrolled pH conditions might cause an 'acid crash' (Mohammadi et al. 2014), which makes the cultures lose their alcohol conversion ability and further induces failed alcohol production (Wang et al. 2011; Mohammadi et al. 2014). Therefore, in uncontrolled pH conditions, the slow-down of the acid concentration and accumulation rate could improve solventogenesis, which could be achieved by slowing down the metabolism/growth of bacteria, such as fermentation under low temperatures and nutrient limitations.

Ethanol production is considered as a by-product produced by the resting non-growth stage cells (Cotter et al., 2009). However, recent research revealed ethanol production at the exponential growth stage. In fact, solventogenesis at non-growth or exponential stage varied with different fermentation conditions, such as the partial pressure of CO. Growth-associated ethanol production was shown when the CO partial pressure increased to 2 atm by *C. carboxidivorans* P7^T (Hurst and Lewis, 2010). Recent research on *Clostridium ljungdahlii* revealed that ethanol production is a process of NADH/NAD⁺ related to autotrophic growth and ethanol was formed during the exponential phase, closely accompanied by biomass production using CO:CO₂ (vol/vol, 80/20) supply (Liu et al., 2020).

2.3 Microorganisms

Three types of inocula have been studied in the literature (Table 2.1): i) pure cultures representing *Clostridium spp.*, ii) co-cultures, either a combination of autotrophic and heterotrophic acetogens (Fig. 2.4), *C. autoethanogenum* can convert CO or syngas to ethanol and acetate, but when co-cultured with *Clostridium kluyveri*, the co-culture ends up producing butanol or hexanol with CO as reducing power, not found in any of those individual strains (Diender et al., 2016), and iii) mixed undefined cultures such as anaerobic sludge, sediments and animal manure (Chakraborty et al., 2019). The latter were also the source of enrichment and isolation for novel autotrophic species, e.g., *Clostridium aceticum* (Arslan et al. 2019), *Acetobacterium wieringae* Strain JM grown at 1.70 bar CO (Arantes et al., 2020) and *Clostridium sp.* AWRP grown on syngas (Lee et al., 2019). *Clostridium butyricum*, an organic carbon utilizing *Clostridium sp.* has been recently shown to produce ethanol using syngas (CO/CO₂/H₂/CH₄/N₂, 22.92/7.90/13.05/1.13/45.58) (Monir et al., 2020). Limited studies have reported mixed culture C₁-gas fermentation for the production of solvents, except some pure culture species as shown in Table 2.1.

Table 2.1 Alcohol and organic acid concentrations, yields and productivities during syngas fermentation using various bio-catalysts.

Microorganism	Reactor	Gas	volume (L)	Temperature (°C)	Agitation (rpm)	Gas flow (ml/min)	Time/d	pH	Highest alcohols (g/L)		Reference	
									Ethanol	Butanol		
Pure strains	<i>Alkalibaculum bacchi</i> CP15	CSTR	CO/CO ₂ /H ₂ /N ₂ (20/15/5/60)	3.3/7	37	150	NA	51	8.0	6.0	1.1	Liu et al. 2014
		CSTR	100% CO	1.2/2	33	250	10	21	5.75, 4.75	5.55	2.66	Fernández et al. 2016a
	<i>C. carboxidivorans</i> P7	Batch	CO/CO ₂ /H ₂ /Ar (56/20/9/15)	0.03/0.125	37-25	100	NA	5	NA	3.64	1.35	Shen et al. 2020
		CSTR	CO/CO ₂ (60/40)	^{1st} 1/2 ^{2nd} 1.5/2.4	37	NA	5 L h ⁻¹	6	6.0, 5.0	6.1	0.7	Doll et al. 2018
	<i>C. autoethanogenum</i>	CSTR	100% CO	1.2/2	30	250	10	7	6.0, 4.75	0.9	NA	Abubackar et al., 2015
	<i>C. ljungdahlii</i>	Batch	CO/CO ₂ /H ₂ (20/20/5)	200/250	37	200	NA	24 h	6.7 with nanoparticles	0.3	NA	Kim et al. 2014
		Batch	CO/CO ₂ /H ₂ (20/20/5)	200/250	37	200	NA	60 h	10.9 with CoFe ₂ O ₄	0.5	NA	Kim and Lee, 2016
	<i>C. aceticum</i>	CSTR	CO/CO ₂ /H ₂ /N ₂ (30/5/15/50)	1.2/2	30	150	10	52	6.98	5.6	NA	Arslan et al. 2019
<i>C. ragsdalei</i>	Tricking bed reactor	CO/CO ₂ /H ₂ /N ₂ (38/28.5/28.5/5)	1	37	NA	5	70	5.8-4.6	5.7	NA	Devarapalli et al. 2016	
Co-culture	<i>C. autoethanogenum</i> & <i>C. kluyveri</i>	Fed batch	CO	0.07/0.25	37	NA	NA	NA	NA	NA	NA	Diender et al. 2016
Mixed undefined cultures	Anaerobic sludge from industry wastewater treatment	CSTR	100% CO	1.2/2	33	120	10	42	6.2, 4.9	11.1	1.8	Chakraborty et al. 2019
	CO adapted enriched sludge	Fed batch	100% CO	0.1/0.5	33	150	NA	29	5.0-6.3	11.8	1.0	He et al. 2021
	<i>C. ljungdahlii</i> and <i>C. kluyveri</i>	CSTR	CO/CO ₂ /H ₂ /N ₂ (60/35/5)	1/2	37	--	30-80	93	5.7-6.4	144.7 mmol C·L ⁻¹ ·d ⁻¹	39.2 mmol C·L ⁻¹ ·d ⁻¹	Richter et al. 2016b

*NA-not applied.

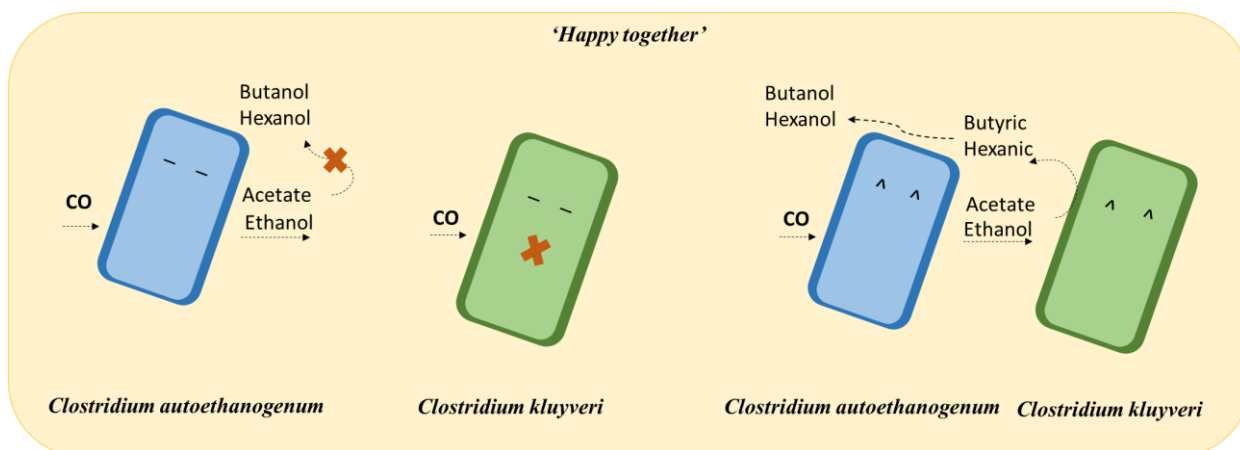


Fig. 2.4 Diagram of the *C. acetobutylicum* and *C. ljungdahlii* co-culture. *C. acetobutylicum* consumes glucose to produce solvents, while releasing CO₂ and H₂. *C. ljungdahlii* consumes H₂ and CO₂ for survival and growth producing acetate and ethanol through WLP.

Pure cultures of solventogens have a slow growth rate, low cell density and their metabolites produced in large quantities contain no more than two carbons (Liu et al. 2014). For instance, *C. carboxidivorans* is the only reported butanol producer from syngas bioconversion (Fig. 2.2). Instead, co-cultures provide a promising solution for enhancing ethanol and longer carbon chain solvent production (Fig. 2.5). For example, in co-cultures of the CO-utilizing *C. autoethanogenum* and the non-CO utilizing *C. kluyveri*, *C. autoethanogenum* facilitates the growth of *C. kluyveri* using CO as carbon source and both butanol and hexanol were obtained in the co-culture (Diender et al. 2016).

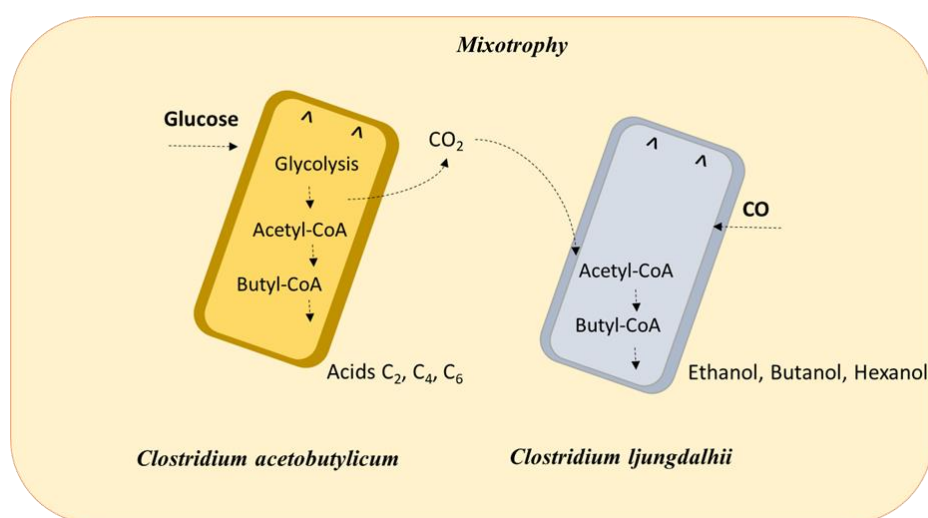


Fig. 2.5 Diagram of the co-culture of *C. autoethanogenum* and *C. kluyveri* using CO as the substrate.

Anaerobic sludges from wastewater treatment plants are a source of microbial species such as methanogens, hydrogenogens and acetogens, capable of syngas to solvents conversion (Arantes et al., 2020; Li et al., 2020). From a practical point of view, mixed culture

fermentations were easy to implement at large scale due to the non-sterile bioreactor conditions (Charubin et al., 2019). On the other hand, the presence of a broad range of acetogenic organisms in mixed cultures can resist unfavorable environmental conditions, such as wide pH range for alcohol production (Liu et al., 2014).

2.4 Process parameters for enhanced ethanol production

2.4.1 Gas phase

2.4.1.1 Gas pressure

Different from the traditional fermentation with sugar substrates in the liquid medium, syngas fermentation processes can be considered as a two step fermentation: first mass transfer from gaseous substrates to the liquid phase followed by the utilization of the dissolved gas by the microbial cells. Thus, the fermentation is partly limited by the mass transfer rate from the gas to the liquid phase, which is further related to the thermodynamic properties of the gaseous substrate. H₂ and CO both act as electron donor but from the Gibbs free energy, CO delivers electrons at a much lower half cell potential and releases about 80 kJ/mol more Gibbs free energy to produce ethanol than H₂ (Table 2.2, Eq. 4, 5). However, H₂ will provide the reducing equivalents for only one third of the carbon in CO (Table 2.2, Eq. 2). CO has a much greater Henry's law constant ($K_H = 7.4 \text{ mM/atm}$) than H₂ ($K_H = 0.78 \text{ mM/atm}$) and is thus more difficult to dissolve into the liquid, so the presence of both CO₂ and H₂ affect the fermentation products (Jack et al. 2019).

Pressurization of the CO partial pressure (P_{CO}) from 0.35 to 2 atm increased the cell growth with 440% and the ethanol production was not observed when the P_{CO} was above 0.35 atm and the ethanol production was growth-associated while the P_{CO} increased to 2 atm by *C. carboxidivorans* P7^T (Hurst and Lewis, 2010). The increase initial pressure enhanced the ethanol production by *C. autoethanogenum* when the CO pressure varied between 0.8–1.6 bar (Abubackar et al., 2012). Cultivation with CO pressure maintained above 50 kPa of co-culture of *C. autoethanogenum* and *C. kluyveri* resulted in less oxidation of ethanol back to acetate (Diender et al. 2016).

2.4.1.2 Gas composition

Gas composition, mainly the different ratios among CO, CO₂ and H₂, is another factor influencing solventogenic processes, for instance, a H₂/CO ratio of 0.36 reached a maximum ethanol to acetate ratio of 16, while increasing the H₂/CO ratio to 1.2 induced a lower ethanol to acetate ratio of 2.5 in *C. ljungdahlii* (Mohammadi et al. 2011).

Table 2.2 Theoretical reactions of syngas fermentation to ethanol and butanol.

Products	Reactions	Gibbs free energy	
Acetic acid	$4\text{CO}(g) + 2\text{H}_2\text{O}(l) \rightarrow \text{CH}_3\text{COOH}(l) + 2\text{CO}_2(g)$	$\Delta G_r^0 = -154.6 \text{ kJ/mol}$	(1)
	$\text{CO}(g) + \text{H}_2(g) \rightarrow \text{CH}_3\text{COOH}$	$\Delta G_r^0 = -114.5 \text{ kJ/mol}$	(2)
	$2\text{CO}_2(g) + 4\text{H}_2(g) \rightarrow \text{CH}_3\text{COOH}(l) + 2\text{H}_2\text{O}(l)$	$\Delta G_r^0 = -75.4 \text{ kJ/mol}$	(3)
Ethanol	$6\text{CO}(g) + 3\text{H}_2\text{O}(l) \rightarrow \text{CH}_3\text{CH}_2\text{OH}(l) + 4\text{CO}_2(g)$	$\Delta G_r^0 = -217.4 \text{ kJ/mol}$	(4)
	$2\text{CO}(g) + 4\text{H}_2(g) \rightarrow \text{CH}_3\text{CH}_2\text{OH}(l) + \text{H}_2\text{O}(l)$	$\Delta G_r^0 = -137.1 \text{ kJ/mol}$	(5)
	$2\text{CO}_2(g) + 6\text{H}_2(g) \rightarrow \text{CH}_3\text{CH}_2\text{OH}(l) + 3\text{H}_2\text{O}(l)$	$\Delta G_r^0 = -96.5 \text{ kJ/mol}$	(6)
	$\text{CH}_3\text{COOH}(l) + 2\text{H}_2(g) \rightarrow \text{CH}_3\text{CH}_2\text{OH}(l) + \text{H}_2\text{O}(l)$	$\Delta G_r^0 = -21.6 \text{ kJ/mol}$	(7)
Butyric acid	$10\text{CO}(g) + 4\text{H}_2\text{O}(l) \rightarrow \text{CH}_3\text{CH}_2\text{CH}_2\text{COOH}(l) + 6\text{CO}_2(g)$	$\Delta G_r^0 = -420.8 \text{ kJ/mol}$	(8)
Butanol	$12\text{CO}(g) + 5\text{H}_2\text{O}(l) \rightarrow \text{CH}_3\text{CH}_2\text{CH}_2\text{CH}_2\text{OH}(l) + 8\text{CO}_2(g)$	$\Delta G_r^0 = -486.4 \text{ kJ/mol}$	(9)
Ethanol oxidation	$2\text{CH}_3\text{CH}_2\text{OH}(l) + 2\text{CO}_2(g) \rightarrow 3\text{CH}_3\text{COOH}(l)$	$\Delta G_r^0 = -32.2 \text{ kJ/mol}$	(10)
Butanol oxidation	$2 \text{CH}_3\text{CH}_2\text{CH}_2\text{CH}_2\text{OH} + 2 \text{CO}_2 \rightarrow 2 \text{CH}_3\text{CH}_2\text{CH}_2\text{COOH} + \text{CH}_3\text{COOH}$		(11)

When grown on H₂/CO₂, *C. autoethanogenum* cell extracts had an enzyme concentration higher than in those of CO grown cells (Mock et al., 2015). This was attributed to the fact that during growth on H₂/CO₂ the function of the enzyme is to catalyze the endergonic reduction of CO₂ to CO with reduced ferredoxin, whereas during growth on CO the function of the enzyme is to catalyze the exergonic oxidation of CO to CO₂ with ferredoxin (Mock et al., 2015).

CO₂ may also influence the process of ethanol degradation (Table 2.2, Eq. 10). However, only few studies reported ethanol degradation during the process of syngas bioconversion. Tan et al. (2014) investigated the butanol dehydrogenases in butanol degradation in the presence of 0.25% butanol by *C. ljungdahlii* and found 0.05% butyrate at the end of growth under the effect of two butanol-dehydrogenase-encoding genes (CLJU_c24880 and CLJU_c39950). Supplementing media with carbon dioxide can be essential or greatly stimulatory to acetogenesis. The presence of carbon dioxide (CO/CO₂, v/v, 70/30) enhanced both the acetic acid concentration and production compared to incubations with pure CO.

Acetate production enhanced by the increased H₂/CO ratio from 22.6 at a ratio of 0.5 increased to 35.2 mM at a ratio of 2, conversely, ethanol production increased correspondingly from 5.4 to 7.4 mM when the H₂/CO ratio increased from 0.5 to 2.0 by *Clostridium ljungdahlii*. Therefore, the more reduced metabolite product (such as ethanol) was favored by the increased CO concentration in the headspace. The higher Gibbs free energy released from the direct CO conversion while CO₂ had to be reduced to CO consuming additional electrons (from H₂) when CO is absent, yielding less free energy and electron-dense by-products (Jack et al., 2019).

2.4.2 Fermentation conditions

2.4.2.1 pH

pH can significantly affect both the growth rate and product formation of microorganisms. Solventogenesis pH varied depending on different strains, 4.75 for *Clostridium autoethanogenum* (Abubackar et al. 2015a) and 5.3-5.8 for *C. carboxidivorans* P⁷ (Fernández-Naveira et al. 2016a).

Due to the acid accumulation, the external pH begins to drop. To prevent a further drop in pH, an organism may begin to produce neutral charged solvents (Padan et al., 1981; Cotter et al., 2009). Note that the intercellular pH is higher than the external pH due to a proton translocation process catalyzed by a membrane-bound ATPase (Gottwald and Gottschalk 1985). Haris et al. (2012) investigated the effect of the initial pH (4.75–5.75) on biological solvent production by *C. autoethanogenum* DSM 10061 and also used the Minitab analysis at a two level four factor (2⁴) and found that lowering the pH resulted in the production of more

reduced compounds such as ethanol. Therefore, lowering the pH is facilitated to produce highly reduced products such as ethanol. However, lowering pH causes a decrease in electron and carbon flow from the substrate toward the cell mass and reduces the overall productivity of the process (Worden et al. 1989; Phillips et al. 1993).

2.4.2.2 Temperature

The growth temperature of solventogenic *Clostridium spp.* ranges from 20 to 42 °C, with the optimum temperature of 37°C (Naik et al. 2010). This is also the most common temperature applied in the literature (Munasinghe and Khanal 2010). A limited number of studies reported on the less optimal temperature, i.e., sub-mesophilic and psychrophilic conditions for solvents production from syngas (Kundiya et al. 2011).

A higher ethanol and butanol production was obtained at 25°C for syngas (CO/H₂/CO₂/N₂, 32/32/8/28, v/v) fermentation by *C. carboxidivorans* compared to 37°C by avoiding the ‘acid crash’ and the pH dropped below 4.8 at 25°C (Ramió-Pujol et al., 2015). Although higher temperatures have a negative impact on the solubility of CO and H₂, which also decreases the mass transfer rate of these gases to cells, this negative part can be neglected compared to the positive role of the non-acid phenomenon at lower temperatures (Henstra et al. 2007). To achieve both high cell growth and alcohol production, two-step temperature (TST) cultures were developed, for instance, 37–25°C and 37–29°C fermentation could overcome cellular agglomeration at 37°C and low biomass growth at 25°C and achieve a higher alcohol production and yield. Gene expression revealed the carbon-fixation pathway at 37°C and product biosynthetic pathway at 25°C (Shen et al., 2020).

The exploration of solventogenesis under thermophilic conditions via syngas fermentation is seldom reported. This is partly due to the mesophilic *Clostridium spp.* since their growth temperature is up to 42°C. Shen et al. (2018) reported acetate, butyrate and caproate production by *Clostridium* under mesophilic conditions, while acetate was the main product with *Thermoanaerobacterium* as the main microorganism under thermophilic conditions from syngas (CO/H₂, v/v, 40/60) fermentation in hollow-fiber membrane biofilm reactors by anaerobic sludge.

Acetate productivity was enhanced at thermophilic (55°C) conditions with anaerobic sludge using syngas (H₂/CO₂, v/v, 60/40) as the substrate with 10 mmol/L bromoethane sulfonate (BES) to inhibit methanogenesis (Wang et al., 2017).

Alves et al. (2013) studied the enrichment of anaerobic syngas-converting bacteria for more than one year using municipal solid waste seeded sludge as the inoculum under thermophilic conditions (55°C) and reported *Desulfotomaculum*, *Thermincola*,

Caloribacterium and *Thermoanaerobacter* are associated with syngas and/or CO conversion in thermophilic enrichment cultures. Similarly, formate accumulation was obtained from H₂/CO₂ (80/20, v/v) and 300 mM KHCO₃ at 66°C by *Thermoanaerobacter kivui* LKT-1 (Schwarz and Müller, 2020).

2.4.3 Medium composition

2.4.3.1 Trace metals

Trace metals influence solventogenesis by influencing enzyme synthesis and activity. In WLP (Fig. 2.1), formate dehydrogenase (FDH) is one of the key enzymes, transferring CO₂ to formate and can be stimulated by tungsten (W), selenium (Se) and molybdenum (Mo) addition (Yamamoto et al. 1983). The other key metalloenzyme related to Mo and W is alcohol dehydrogenase (ADH) catalyzing the reduction of acetyl CoA to ethanol (Chen, 1995; Andreesen and Makdessi, 2008).

At the same time these trace metals might exhibit different effects in different CO-metabolizing strains. The 0.75 µM W addition reached the highest ethanol to acetic acid ratio of 0.19 by *Clostridium autoethanogenum*, 173% higher than the ratio obtained in the experiment with 1.44 µM Se (Abubackar et al., 2015b).

Comparing the 35 mM ethanol production at the standard metal concentrations, the concentrations of ethanol production are enhanced to 180, 200, 60, and 90 mM, corresponding with the optimal concentrations of 8.5, 35, 5 and 7 µM of Ni²⁺, Zn²⁺, SeO₄²⁻, and WO₄²⁻, respectively by boosting *Clostridium ragsdalei* cell growth (Saxena and Tanner 2011).

The presence of both W (0.68 µM) and Se (1.15 µM) allowed to accumulate high amounts of alcohols (8.0 g/L total alcohols and 3.0 g/L total acids) at pH 5.0 from syngas (CO/CO₂/H₂/N₂, 30/10/20/40, v/v) by *Clostridium carboxidivorans* P7. Instead, the absence of W and Se induced organic acids (9.6 g/L) accumulation and almost no alcohol production (0.7 g/L). When omitting W but not Se, as high as 11.3 g/L acids were accumulated with poor alcohol production. Therefore, tungsten has been shown to play the major role for solventogenesis, while selenium seems to be less significant (Fernández-Naveira et al., 2019a).

Ni and Fe were found to be two vital metals for the growth of *C. carboxidivorans* P7 during syngas (CO/CO₂/H₂, v/v/v, 50/35/15) fermentation (Han et al., 2020). Decreasing the molybdenum concentration from 55 to 23 µg/L dramatically promotes cell growth and alcohol synthesis, particularly for ethanol and butanol production (Han et al., 2020). The high molybdate concentration of 55 µg/L inhibited the butanol synthesis pathways and the acid re-assimilation pathway (Han et al., 2020). The expression levels of the acetate synthesis genes

ack (Ccar_00695) and *pta* (Ccar_00690) were significantly downregulated in the 23 µg/L Mo incubation. The regulation of trace metals not only stimulated production of alcohol, but was also a trigger of acid reuse or re-assimilation leading to the transition from acidogenesis to solventogenesis in *C. carboxidivorans* strain P7 (Li et al., 2018).

Despite the essential investigation of W and Mo, zinc also enhanced ethanol production from syngas (CO/CO₂/H₂, v/v/v, 50/35/15) by *Clostridium carboxidivorans* P7 via upregulation of the expression of *fdhII* and *bdh*: ethanol 3.02-fold, butanol 7.60-fold (0.4 g/L) and hexanol 44-fold (0.1 g/L) with 280 µM Zn²⁺ compared with those in the control medium (7 µM Zn²⁺). Although a considerable enhancement of the alcohol production was reached, the obtained concentration of ethanol, butanol and hexanol were not much higher compared to other studies, which ethanol concentrations of around 2 g/L, butanol 0.4 g/L and hexanol 0.1 g/L, respectively, upon addition of 280 µM Zn²⁺ in the fermentation medium (Li et al., 2018).

2.4.3.2 Yeast extract

To ensure a certain amount of acid production, an easy consumable sugar such as glucose and yeast extract are usually added as nitrogen source to enhance cell growth during ethanol fermentation from C₁ gas (Chakraborty et al. 2019).

Yeast extract is an important nitrogen source required for microorganisms. Strong negative effects on the production rates, and a significant increase of the lag phase were found when the yeast extract concentration is lower than 0.5 g/L by a synthetic co-culture of *Clostridium autoethanogenum* and *Clostridium kluyveri* grown on carbon monoxide (Diender et al. 2016). In a bioreactor with continuous CO supply and with 1 g/L yeast extract at pH 5.75, the maximum biomass concentration obtained was 302.4 mg/L, which is comparable to the maximum cell mass concentration obtained at pH 6.0 (Abubackar et al., 2015a).

However, eliminating YE is found to enhance the ethanol production using *C. ljungdahlii* (Barik et al. 1988). But for this organism to provide structural integrity, a minimum concentration of 0.01% is necessary (Abubackar et al., 2011). Abubackar et al. (2012) investigated the effect of the yeast extract concentration (0.6–1.6 g/L) on biological solvent production by *C. autoethanogenum* DSM 10061 and also used the Minitab analysis at a two level four factor (2⁴) and found that lowering the YE concentration results in the production of more reduced compounds such as ethanol.

Other cheap nutrient sources such as cotton seed extract (CSE) and corn steep liquor (CSL) can also replace yeast extract to enhance the ethanol production (Silveira et al. 2001). CSE with a cost of \$ 0.91/kg is considerable cheaper than yeast extract \$ 183/kg. CSL, as a major by-product of the corn wet milling industry, comprises of a rich source of important nutrients (Hull

et al. 1996). Kundiyana et al. (2010) examined the ethanol and acetic acid production using cotton seed extract (CSE) as the fermentation medium for *Clostridium* strain P11 and reported 2.66 g/l ethanol in the batch medium containing 0.5 g/l of CSE after 15 days fermentation. The standard fermentation medium of *Clostridium* strain P11 could be replaced with CSE, since CSE contains minerals and vitamins which are very similar to the standard fermentation medium.

Benevenuti et al. (2020) rendered a medium TPYGarg (12 g/L of tryptone, 12 g/L of peptone from gelatin, 7 g/L of yeast extract, 1.2 g/L of l-arginine, and 1 g/L of glucose), using 1.22 atm syngas (CO/CO₂/H₂/CH₄/N₂, 25/10.02/43.9/11.01/10.05). They produced 5-fold higher ethanol and 2 fold higher butanol concentrations at a 31% reduced cost compared to the standard medium ATCC 2713.

Gunay et al. (2020) investigated corn syrup and whey powder as cheap substitutes for expensive basal-medium components. They demonstrated enhanced ethanol production with CO co-fermentation by *Clostridium ljungdahlii*. Whey powder has been shown to be cheaper and a better substrate so that *C. ljungdahlii* can grow without yeast extract and ethanol production was enhanced 3 fold with 2.5 g/L than the basal medium. However, yeast extract is critical to support cell growth when using corn syrup by *C. ljungdahlii*.

2.5 Thermodynamic calculation of Gibbs free energy

2.5.1 Gibbs free energy calculation

The thermodynamics of syngas bioconversion processes are rarely studied or reviewed due to its complexity in processes involving biomass (Gildemyn et al. 2017). To simplify, the following Gibbs free energy calculations do not involve biomass. Gibbs free energy of formation is zero for the elements in their most stable state, e.g., CO (g), H₂ (g), CO₂ (g), acetic acid (l), under standard conditions (1 bar, 298.15 K, 1 mol·L⁻¹, pH 0) (Franses, 2014). Gibbs free energies ($\Delta_r G_m$) for the production of acetic acid, ethanol, butyric acid and butanol from CO were calculated from the respective standard Gibbs free energies ($\Delta_r G_m^\theta$) and the actual concentrations of reactants and products using Van't Hoff equation (Eq. 1) (Thauer et al. 1977). If $\Delta_r G_m$ is negative then the system loses energy and does work. In this case, the lower $\Delta_r G_m$ means that the reactions are more favourable to proceed. Conversely, if $\Delta_r G_m$ is positive, then the system has to gain energy from the work that has been done by the surroundings (Kenneth, 2017). Thus, $\Delta_r G_m$ provides a valuable criterion for determining whether a reaction can occur spontaneously or not (Oubrahim and Chock, 2016).

It should be noted that for a thermodynamically unfavorable reaction ($\Delta_r G_m > 0$), if biological systems are involved, the overall $\Delta_r G_m$ of the pathway can become negative since biological systems can formulate their metabolic pathways by coupling enzyme-catalyzed reactions (Oubrahim and Chock, 2016). But this is out of the scope of this study. The Gibbs free energy calculated in this study can be applied to compare the extent of the reaction system and if it is favorable with same substrate (e.g., CO) and microorganism.

For the reaction: $cC + dD = yY + zZ$

$$\Delta_r G_m = \Delta_r G_m^\theta + RT \ln J \quad (1)$$

Where, $\Delta_r G_m^\theta$ is the standard reaction Gibbs energy, under standard conditions (T=298.15 K, P = 100 kPa, concentration of 1 molar).

Constant R = 8.314 J/(mol·K), T = (273.15 + °C) K, J is the reaction quotient,

$$\text{For gases: } J = \frac{\{P(Y)/P^\theta\}^y \{P(Z)/P^\theta\}^z}{\{P(C)/P^\theta\}^c \{P(D)/P^\theta\}^d}$$

$$\text{For liquid: } J = \frac{\{c(Y)/c^\theta\}^y \{c(Z)/c^\theta\}^z}{\{c(C)/c^\theta\}^c \{c(D)/c^\theta\}^d}$$

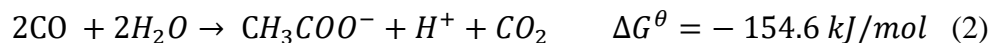
$$P^\theta = 100 \text{ kPa}, c^\theta = 1 \text{ mol} \cdot \text{L}^{-1}$$

2.5.2 CO conversion to acetic acid and ethanol under different CO pressures and pH, at 25, 33 and 55°C

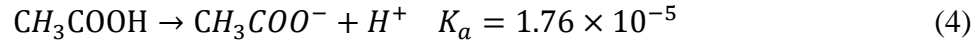
2.5.2.1 Acetic acid production

Gibbs free energy for the production of acetic acid from CO ($\Delta_r G_m(HAc)$) can be calculated according to Eq. 2 and Eq. 3. One mole acetic acid and accordingly 1 mole CO₂ are assumed to be produced (Eq. 2). Considering acetic acid as a weak acid and the ionization constant (pKa) (Eq. 4, 5, 6 and 7), $\Delta_r G_m(HAc)$ is a function of CO gas pressure, CO₂ gas pressure and pH ($-\lg[H^+]$) (Eq. 8). CO₂ is a product along with acetic acid with a molar ratio of 1 and hence its concentration is 1 mol·L⁻¹. Therefore, the CO₂ gas pressure can be calculated according to the Ideal-Gas Equation (Eq. 9). The final $\Delta_r G_m(HAc)$ is a function of CO gas pressure and pH (Eq. 10).

Fig. 2.6 shows the Gibbs free energy of production of acetic acid from different CO gas pressures (0.01-10 bar) and pH varying from 1 to 12, at 25, 33 and 55°C. To conclude, acetic acid production is enhanced with increased CO gas pressures and pH. At the same pH and CO gas pressure, acetic acid production is thermodynamically enhanced at 25°C compared to 33 and 55°C (Fig. 2.6).



$$\Delta_r G_m(HAc) = \Delta G_r^0 + RT \ln \frac{[CH_3COO^-][H^+][p_{CO_2}]}{[p_{CO}]} \quad (3)$$



$$K_a = \frac{[CH_3COO^-][H^+]}{[CH_3COOH]} \quad (5)$$

The total concentration of acetic acid is:

$$[Acid] = [CH_3COO^-] + [CH_3COOH] \quad (6)$$

From Eq. 5 and 6,

$$[CH_3COO^-] = \frac{[Acid]K_a}{K_a + [H^+]} \quad (7)$$

Thus,

$$\Delta_r G_m(HAc) = \Delta G_r^0 + RT \ln \frac{[Acid][p_{CO_2}]}{[p_{CO}]^2} + RT \ln \frac{K_a[H^+]}{K_a + [H^+]} \quad (8)$$

There is production of 1 mole acetic acid and 1 mole CO₂,

The Ideal-Gas Equation is $pV=nRT$ (9)

With $22.4 \text{ L} \cdot \text{mol}^{-1}$, $p=nRT/V=[8.314*(273.15+33)/(22.4*0.001)] \text{ Pa}=113.6 \text{ kPa}=1.136$

bar

p -Pa, V -m³, n -mole, $R=8.314$, T -K

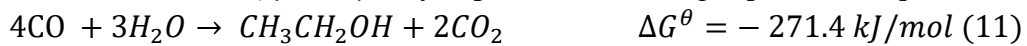
$$\Delta G_r' = \Delta G_r^0 + RT \ln \frac{1*1.136}{[p_{CO}]^2} + RT \ln \frac{K_a[H^+]}{K_a + [H^+]} \quad (10)$$

2.5.2.2 Ethanol production

Theoretically, ethanol can be produced from CO or acetic acid and CO (WLP). Therefore, the Gibbs free energy of production of ethanol from CO ($\Delta_r G_m(EtOH)$) can be calculated in two different ways, according to Eq. 11 and Eq. 13.

1) $\Delta_r G_m(EtOH)$ from CO (Eq. 11)

According to Eq. 11, it is considered that CO is directly converted to ethanol and does not involve acetic acid. Thus, 1 mole ethanol and accordingly 2 mole CO₂ are assumed to be produced. Therefore, $\Delta_r G_m(EtOH)$ only depends on the CO gas pressure (Eq. 12).



There is production of 1 mole ethanol and 2 mole CO₂,

The Ideal-Gas Equation, with $22.4 \text{ L} \cdot \text{mol}^{-1}$, is $pV=nRT$,

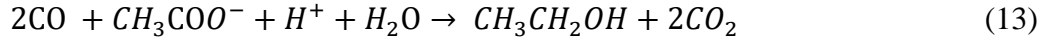
$p=nRT/V=[2*8.314*(273.15+33)/(22.4*0.001)] \text{ Pa}=227.3 \text{ kPa}=2.273 \text{ bar}$

p -Pa, V -m³, n -mole, $R=8.314$, T -K

$$\Delta_r G_m(EtOH) = -271.4 + RT \ln \frac{1*2.273^2}{[p_{CO}]^4} \quad (12)$$

2) $\Delta_r G_m(EtOH)$ from CO and acetic acid

Considering the According to Eq. 13, it is considered that CO and acetic acid are converted to ethanol. Gibbs free energy of ethanol production is shown in Eq. 14. 1 mole ethanol and accordingly 2 mole CO₂ are assumed to be produced. Referring to section 6.2.1, $\Delta_r G_m(EtOH)$ is a function of CO gas pressure and pH (Eq. 15).



$$\Delta_r G_m(EtOH) = \Delta G_r^0 + RT \ln \frac{[CH_3CH_2OH][p_{CO_2}]^2}{[Acid][p_{CO}]^2} + RT \ln \frac{K_a + [H^+]}{K_a [H^+]} \quad (14)$$

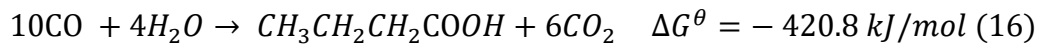
$$\Delta_r G_m(EtOH) = \Delta G_r^0 + RT \ln \frac{1 \cdot 2.273^2}{[Acid][p_{CO}]^2} + RT \ln \frac{K_a + [H^+]}{K_a [H^+]} \quad (15)$$

Fig. 2.7 shows the Gibbs free energy of production of ethanol from different CO gas pressures (0.01-10 bar) and pH values varying from 1 to 12, at 25, 33 and 55°C. To conclude, increased CO gas pressures and lower temperatures, among 25, 33 and 55°C, enhance thermodynamically ethanol production (Fig. 2.7). Besides, the decrease of pH enhances ethanol production (Fig. 2.7), which is in accordance with the experimental discussion highlighting that a low pH enhanced ethanol production (section 4.2.1).

2.5.3 CO to butyric acid and butanol under different CO pressures and pH, at 25, 33 and 55°C

2.5.3.1 Butyric acid production

The Gibbs free energy for the production of butyric acid from CO ($\Delta_r G_m(HBu)$) can be calculated according to Eq. 16. One mole butyric acid and accordingly 6 moles CO₂ are assumed to be produced. $\Delta_r G_m(HBu)$ is a function of CO gas pressure (Eq. 17). Then, butanol production is thermodynamically enhanced along with CO pressure increases and slightly enhanced at 25°C compared to 33 and 55°C (Fig. 2.8).



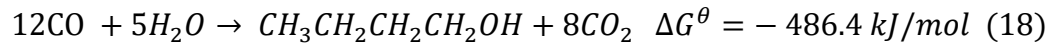
There is production of 1 mole butyric acid and 6 moles CO₂,

The Ideal-Gas Equation, with 22.4 L· mol⁻¹, is pV=nRT,
 $p = nRT/V = [6 \cdot 8.314 \cdot (273.15 + 33)] / (22.4 \cdot 0.001) \text{ Pa} = 6.819 \text{ kPa} = 6.819 \text{ bar}$

$$\Delta_r G_m(HBu) = -420.8 + RT \ln \frac{1 \cdot 6.819^6}{[p_{CO}]^4} \quad (17)$$

2.5.3.2 Butanol production

The Gibbs free energy of production of butanol from CO ($\Delta_r G_m(BtOH)$) can be calculated according to Eq. 18. 1 mole butanol and accordingly 8 mole CO₂ are assumed to be produced. $\Delta_r G_m(BtOH)$ is a function of CO gas pressure (Eq. 19). Then, butanol production is thermodynamically enhanced along with CO pressure increases and slightly enhanced at 25°C compared to 33 and 55°C (Fig. 2.8).



There is production of 1 mole butanol and 8 mole CO₂,

The Ideal-Gas Equation, with 22.4 L· mol⁻¹, is pV=nRT,

$$p=nRT/V=[8*8.314*(273.15+33)/(22.4*0.001)] \text{ Pa}=9.092 \text{ kPa}=9.092 \text{ bar}$$

$$\Delta_r G_m(BtOH) = -486.4 + RT \ln \frac{1*9.902^8}{[p_{CO}]^{12}} \quad (19)$$

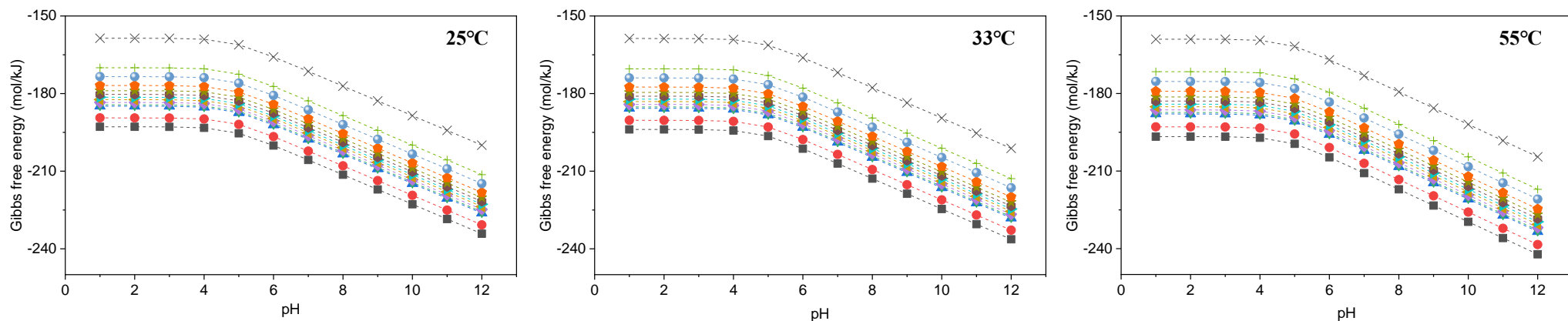


Fig. 2.6 The theoretical Gibbs free energy of CO to acetic acid when the pH varies from 1 to 12, corresponding to the different CO gas pressure (0.01-10 bar) at 25, 33 and 55°C.

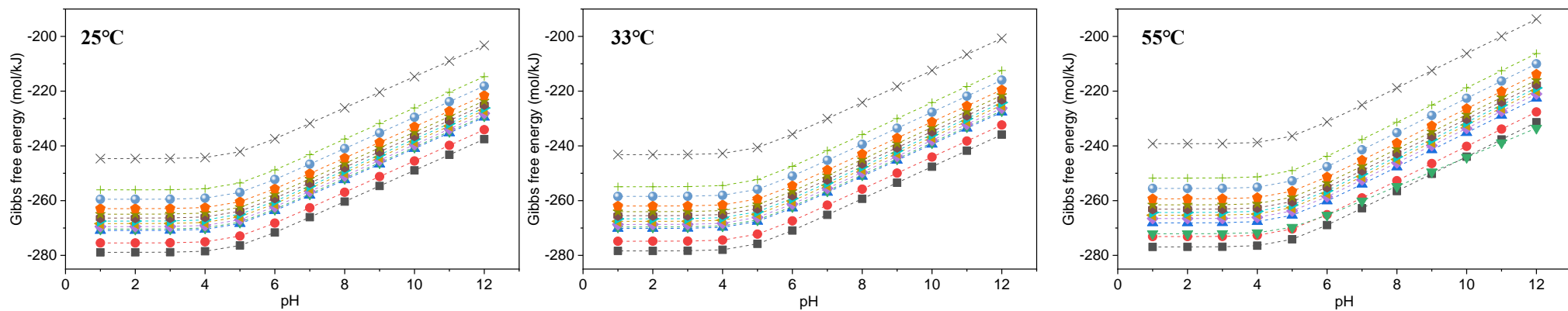
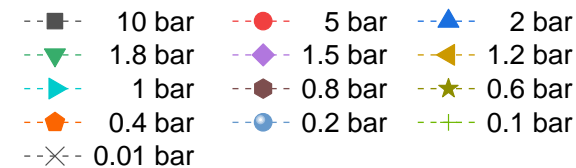


Fig. 2.7 The theoretical Gibbs free energy of CO to ethanol conversion under the different CO gas pressure (0.01-10 bar) at 25, 33 and 55°C.

(Calculated by 1 mol ethanol produced and without considering pH)



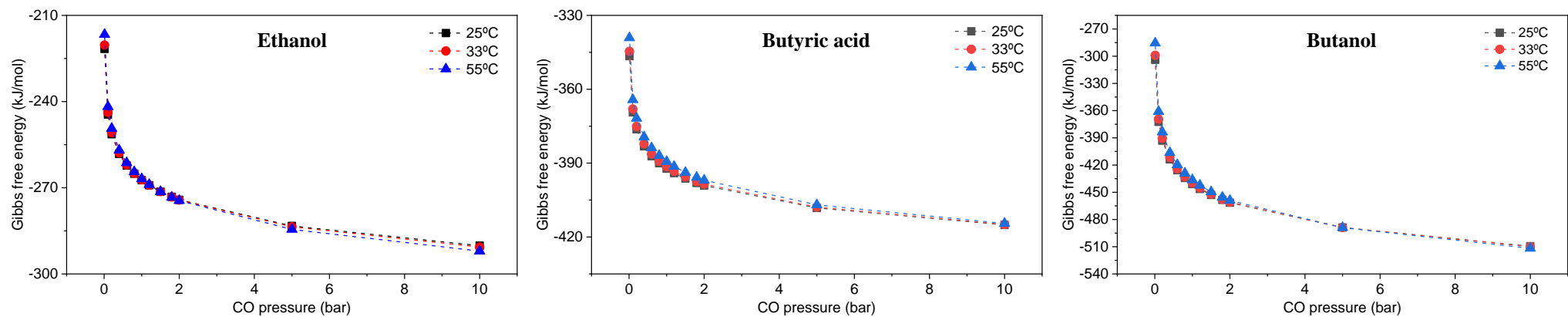


Fig. 2.8 The theoretical Gibbs free energy of CO to ethanol, butyric acid and butanol conversion under the different CO gas pressure (0.01-10 bar) at 25, 33 and 55°C. (Calculated by 1 mol butyric acid production and without considering pH)

2.6 Conclusion

This chapter reviewed the process parameters of solventogenic syngas bioconversion, the potential functional microorganisms and thermodynamic calculations of acid and alcohol production. pH acted as one of the key factors influencing solvent production, some hypotheses have been discussed. However, the mechanism of pH upon solventogenesis and metabolic processes of microorganisms remain to be studied. Mixed cultures will act as the potential inocula for longer carbon chain solvents production. Thermodynamic calculations revealed that acetic acid was enhanced along with the increasing CO₂/H₂ or CO pressure and pH, while ethanol was enhanced as the gas pressure or pH decrease.

References

Abrini, J., Naveau, H. and Nyns, E. J., 1994. *Clostridium autoethanogenum*, sp. nov., an anaerobic bacterium that produces ethanol from carbon monoxide. Archives of Microbiology 161 (4): 345–51.

Abubackar, H. N., Veiga, M. C. and Kennes, C., 2011. Biological conversion of carbon monoxide: rich syngas or waste gases to bioethanol. Biofuels, Bioproducts and Biorefining 5 (1): 93–114.

Abubackar, H. N., Veiga, M. C. and Kennes, C., 2015a. Carbon monoxide fermentation to ethanol by *Clostridium autoethanogenum* in a bioreactor with no accumulation of acetic acid. Bioresource technology, 186, pp.122-127.

Abubackar, H. N., Veiga, M. C. and Kennes, C., 2015b. Ethanol and acetic acid production from carbon monoxide in a *Clostridium* strain in batch and continuous gas-fed bioreactors. International Journal of Environmental Research and Public Health 12 (1): 1029–43.

Alves, J. I., Stams, A. J., Plugge, C. M., Alves, M. and Sousa, D. Z., 2013. Enrichment of anaerobic syngas-converting bacteria from thermophilic bioreactor sludge. FEMS Microbiology Ecology 86 (3): 590–97.

Andreesen, J. R. and Makdessi, K., 2008. Tungsten, the surprisingly positively acting heavy metal element for prokaryotes. Annals of the New York Academy of Sciences 1125 (1): 215–29.

Arantes, A. L., Moreira, J. P., Diender, M., Parshina, S. N., Stams, A. J., Alves, M. M., Alves, J. I. and Sousa, D. Z., 2020. Enrichment of anaerobic syngas-converting communities and isolation of a novel carboxydophilic *Acetobacterium wieringae* Strain JM. Frontiers in Microbiology, 11: 58.

Arslan, K., Bayar, B., Abubackar, H. N., Veiga, M. C. and Kennes, C., 2019. Solventogenesis in *Clostridium aceticum* producing high concentrations of ethanol from syngas. *Bioresource Technology*, 292: 121941.

Bajón Fernández, Y., Soares, A., Koch, K., Vale, P. and Cartmell, E., 2017. Bioconversion of carbon dioxide in anaerobic digesters for on-site carbon capture and biogas enhancement—A review. *Critical Reviews in Environmental Science and Technology*, 47 (17): 1555-1580.

Barik, S., Prieto, S., Harrison, S. B., Clausen, E. C. and Gaddy, J. L., 1988. Biological Production of Solvents from Coal through Indirect Liquefaction. *Applied Biochemistry and Biotechnology* 18 (1): 363–78.

Bengelsdorf, F. R., Straub, M. and Dürre, P., 2013. Bacterial Synthesis Gas (Syngas) Fermentation. *Environmental Technology* 34 (13–14): 1639 – 51.

Benevenuti, C., Botelho, A., Ribeiro, R., Branco, M., Pereira, A., Vieira, A. C., Ferreira, T. and Amaral, P., 2020. Experimental design to improve cell growth and ethanol production in syngas fermentation by *Clostridium carboxidivorans*. *Catalysts* 10 (1): 59.

Braun, M., Mayer, F. and Gottschalk, G. 1981. *Clostridium aceticum* (wieringa), a microorganism producing acetic acid from molecular hydrogen and carbon dioxide. *Archives of Microbiology*, 128(3), 288-293.

Braun, M. and Gottschalk, G. 1982. *Acetobacterium wieringae* sp. nov. a new species producing acetic acid from molecular hydrogen and carbon dioxide. *Zentralblatt für Bakteriologie Mikrobiologie und Hygiene: I. Abt. Originale C: Allgemeine, angewandte und ökologische Mikrobiologie*, 3(3), 368-376.

Chakraborty, S., Rene, E. R., Lens, P. N., Veiga, M. C. and Kennes, C., 2019. Enrichment of a solventogenic anaerobic sludge converting carbon monoxide and syngas into acids and alcohols. *Bioresource Technology*, 272: 130-136.

Charubin, K. and Papoutsakis, E. T., 2019. Direct cell-to-cell exchange of matter in a synthetic *Clostridium* syntrophy enables CO₂ fixation, superior metabolite yields, and an expanded metabolic space. *Metabolic engineering*, 52: 9-19.

Chen, J. S., 1995. Alcohol dehydrogenase: multiplicity and relatedness in the solvent-producing clostridia. *FEMS Microbiology Reviews* 17 (3): 263–73.

Cotter, J. L., Chinn, M. S. and Grunden, A. M., 2009. Ethanol and acetate production by *Clostridium ljungdahlii* and *Clostridium autoethanogenum* using resting cells. *Bioprocess and biosystems engineering*, 32 (3): 369-380.

Cui, Y., Yang, K. and Zhou, K., 2020. Using co-culture to functionalize *Clostridium* fermentation. *Trends in Biotechnology*.

Devarapalli, M. and Atiyeh, H. K., 2015. A review of conversion processes for bioethanol production with a focus on syngas fermentation. *Biofuel Research Journal*, 2 (3): 268-280.

Devarapalli, M., Atiyeh, H. K., Phillips, J. R., Lewis, R. S. and Huhnke, R. L., 2016. Ethanol production during semi-continuous syngas fermentation in a trickle bed reactor using *Clostridium ragsdalei*. *Bioresource Technology*, 209: 56-65.

Diender, M., Stams, A. J. and Sousa, D. Z., 2016. Production of medium-chain fatty acids and higher alcohols by a synthetic co-culture grown on carbon monoxide or syngas. *Biotechnology for Biofuels*, 9 (1): 82.

Doll, K., Rückel, A., Kämpf, P., Wende, M. and Weuster-Botz, D., 2018. Two stirred-tank bioreactors in series enable continuous production of alcohols from carbon monoxide with *Clostridium carboxidivorans*. *Bioprocess and Biosystems Engineering* 41 (10): 1403-416.

Fast, A. G., Schmidt, E. D., Jones, S. W. and Tracy, B. P., 2015. Acetogenic mixotrophy: novel options for yield improvement in biofuels and biochemicals production. *Current Opinion in Biotechnology*, 33: 60-72.

Fernández-Naveira, Á., Abubackar, H.N., Veiga, M.C. and Kennes, C., 2016a. Efficient Butanol-Ethanol (BE) Production from Carbon Monoxide Fermentation by *Clostridium carboxidivorans*. *Applied Microbiology and Biotechnology* 100 (7): 3361–70.

Fernández-Naveira, Á., Veiga, M. C. and Kennes, C. 2017. H-B-E (Hexanol-butanol-ethanol) fermentation for the production of higher solvents from syngas/waste gas. *Journal of Chemical Technology & Biotechnology* 92 (4): 712–31.

Fernández-Naveira, Á., Veiga, M. C. and Kennes, C., 2019a. Selective anaerobic fermentation of syngas into either C₂-C₆ organic acids or ethanol and higher alcohols. *Bioresource Technology*, 280: 387-395.

Fernández-Naveira, Á., Veiga, M. C. and Kennes, C. 2019b. Effect of salinity on C1-gas fermentation by *Clostridium carboxidivorans* producing acids and alcohols. *ABM Express*, 9: 110.

Franses, Elias I. 2014. Further Implications of the Second Law. Introduction of the Helmholtz free energy, Gibbs free energy, chemical potential, and applications to phase equilibria, heat transfer, and mass transfer. *Thermodynamics with Chemical Engineering Applications*. 213-242.

Ganigué, R., Sánchez-Paredes, P., Bañeras, L. and Colprim, J. 2016. Low fermentation pH is a trigger to alcohol production, but a killer to chain elongation. *Frontiers in Microbiology*, 7, 702.

Gildemyn S., Rozendal, R. A., Rabaey K. 2017. A Gibbs free energy-based assessment of microbial electrocatalysis. *Trends in Biotechnology*, 35 (5): 393-406.

Gottwald, M. and Gottschalk G., 1985. The Internal pH of *Clostridium acetobutylicum* and its effect on the shift from acid to solvent formation. *Archives of Microbiology*, 143 (1): 42–46.

Gunay, B., Azbar, N. and Keskin, T., 2020. The effect of corn syrup and whey on the conversion process of CO to ethanol using *Clostridium ljungdahlii*. *Chemosphere*, 261: 127734.

Han, Y. F., Xie, B. T., Wu, G. X., Guo, Y. Q., Li, D. M. and Huang, Z. Y., 2020. Combination of trace metal to improve solventogenesis of *Clostridium carboxidivorans P7* in syngas fermentation. *Frontiers in Microbiology*, 11:2376.

Henstra, A. M., Sipma, J., Rinzema, A. and Stams, A. J., 2007. Microbiology of synthesis gas fermentation for biofuel production. *Current Opinion in Biotechnology*, 18 (3): 200-206.

Hull, S. R., Yang, B. Y., Venzke, D., Kulhavy, K. and Montgomery, R., 1996. composition of corn steep water during steeping. *Journal of Agricultural and Food Chemistry* 44 (7): 1857–63.

Hurst, K. M. and Lewis, R. S., 2010. Carbon monoxide partial pressure effects on the metabolic process of syngas fermentation. *Biochemical Engineering Journal*, 48 (2): 159-165.

Jack, J., Lo, J., Maness, P. C. and Ren, Z. J., 2019. Directing *Clostridium ljungdahlii* fermentation products via hydrogen to carbon monoxide ratio in syngas. *Biomass and Bioenergy*, 124: 95-101.

Jones, S. W., Fast, A. G., Carlson, E. D., Wiedel, C. A., Au, J., Antoniewicz, M. R., Papoutsakis, E. T. and Tracy, B. P., 2016. CO₂ fixation by anaerobic non-photosynthetic mixotrophy for improved carbon conversion. *Nature communications*, 7 (1): 1-9.

Kennes, D., Abubackar, H. N., Diaz, M., Veiga, M. C. and Kennes, C., 2016. Bioethanol production from biomass: carbohydrate vs syngas fermentation. *Journal of Chemical Technology & Biotechnology*, 91 (2): 304-317.

Kim, Y. K. and Lee, H., 2016. Use of magnetic nanoparticles to enhance bioethanol production in syngas fermentation. *Bioresource technology*, 204: 139-144.

Kim, Y. K., Park, S. E., Lee, H. and Yun, J. Y., 2014. Enhancement of bioethanol production in syngas fermentation with *Clostridium ljungdahlii* using nanoparticles. *Bioresource technology*, 159: 446-450.

Klasson, K. T., Ackerson, M. D., Clausen, E. C. and Gaddy, J. L., 1992. Bioconversion of synthesis gas into liquid or gaseous fuels. *Enzyme and Microbial Technology*, 14 (8): 602-608.

Kundiyaana, D. K., Huhnke, R. L., Maddipati, P., Atiyeh, H. K. and Wilkins, M. R., 2010. Feasibility of incorporating cotton seed extract in *Clostridium strain* P11 fermentation medium during synthesis gas fermentation. *Bioresource Technology*, 101 (24): 9673-9680.

Kundiyaana, D. K., Wilkins, M. R., Maddipati, P. and Huhnke, R. L., 2011. Effect of temperature, pH and buffer presence on ethanol production from synthesis gas by “*Clostridium ragsdalei*”. *Bioresource Technology*, 102 (10): 5794-5799.

Latif, H., Zeidan, A. A., Nielsen, A. T. and Zengler, K., 2014. Trash to treasure: production of biofuels and commodity chemicals via syngas fermenting microorganisms. *Current Opinion in Biotechnology* 27: 79-87.

Lee, J., Lee, J. W., Chae, C. G., Kwon, S. J., Kim, Y. J., Lee, J. H. and Lee, H. S., 2019. Domestication of the novel alcohologenic acetogen *Clostridium sp.* AWRP: from isolation to characterization for syngas fermentation. *Biotechnology for biofuels*, 12 (1): 1-14.

Li, D., Meng, C., Wu, G., Xie, B., Han, Y., Guo, Y., Song, C., Gao, Z. and Huang, Z., 2018. Effects of zinc on the production of alcohol by *Clostridium carboxidivorans* P⁷ using model syngas. *Journal of Industrial Microbiology & Biotechnology* 45 (1): 61-69.

Liew, F., Henstra, A. M., Winzer, K., Köpke, M., Simpson, S. D. and Minton, N. P., 2016. Insights into CO₂ fixation pathway of *Clostridium autoethanogenum* by targeted mutagenesis. *MBio* 7 (3): e00427-16.

Liou, J. S. C., Balkwill, D. L., Drake, G. R. and Tanner, R. S., 2005. *Clostridium carboxidivorans* sp. nov., a solvent-producing clostridium isolated from an agricultural settling lagoon, and reclassification of the acetogen *Clostridium scatologenes* strain SL1 as *Clostridium drakei* sp. nov. *International Journal of Systematic and Evolutionary Microbiology*, 55 (5): 2085-2091.

Liu, C., Shi, Y., Liu, H., Ma, M., Liu, G., Zhang, R. and Wang, W., 2020a. Insight of co-fermentation of carbon monoxide with carbohydrate-rich wastewater for enhanced hydrogen production: homoacetogenic inhibition and the role of pH. *Journal of Cleaner Production* 267: 122027.

Liu, C., Wang, W., Sompong, O., Yang, Z., Zhang, S., Liu, G. and Luo, G., 2020b. Microbial insights of enhanced anaerobic conversion of syngas into volatile fatty acids by co-fermentation with carbohydrate-rich synthetic wastewater. *Biotechnology for Biofuels* 13 (1): 53.

Liu, K., Atiyeh, H. K., Stevenson, B. S., Tanner, R. S., Wilkins, M. R. and Huhnke, R. L., 2014. Mixed culture syngas fermentation and conversion of carboxylic acids into alcohols. *Bioresource Technology*, 152: 337-346.

Liu, Z. Y., Jia, D. C., Zhang, K. D., Zhu, H. F., Zhang, Q., Jiang, W. H., Gu, Y. and Li, F. L., 2020. Ethanol metabolism dynamics in *Clostridium ljungdahlii* grown on carbon monoxide. *Applied and Environmental Microbiology*, 86, 14: e00730-20

Lynd, L., Kerby, R. and Zeikus, J. G., 1982. Carbon monoxide metabolism of the methylotrophic acidogen *Butyribacterium methylotrophicum*. *Journal of Bacteriology*, 149 (1): 255-263.

Maru, B. T., Munasinghe, P. C., Gilary, H., Jones, S. W. and Tracy, B. P., 2018. Fixation of CO₂ and CO on a diverse range of carbohydrates using anaerobic, non-photosynthetic mixotrophy. *FEMS Microbiology Letters*, 365 (8): fny039.

Mock, J., Zheng, Y., Mueller, A. P., Ly, S., Tran, L., Segovia, S., Nagaraju S., Köpke M., Dürre P. and Thauer, R. K., 2015. Energy conservation associated with ethanol formation from H₂ and CO₂ in *Clostridium autoethanogenum* involving electron bifurcation. *Journal of Bacteriology*, 197 (18): 2965-2980.

Mohammadi, M. and Mohamed, A. R., 2014. Effect of organic substrate on promoting solventogenesis in ethanologenic acetogene *Clostridium ljungdahlii* ATCC5538. *International Journal of Engineering*, 27 (2): 185-194.

Mohammadi, M., Najafpour, G. D., Younesi, H., Lahijani, P., Uzir, M. H. and Mohamed, A. R., 2011. Bioconversion of synthesis gas to second generation biofuels: A review. *Renewable and Sustainable Energy Reviews*, 15 (9): 4255-4273.

Monir, M. U., Abd Aziz, A., Khatun, F. and Yousuf, A., 2020. Bioethanol production through syngas fermentation in a tar free bioreactor using *Clostridium butyricum*. *Renewable Energy* 157: 1116-123.

Munasinghe, P. C. and Khanal, S. K., 2010. Biomass-derived syngas fermentation into biofuels: opportunities and challenges. *Bioresource Technology*, 101 (13): 5013-5022.

Naik, S. N., Goud, V. V., Rout, P. K. and Dalai, A. K., 2010. Production of first and second generation biofuels: a comprehensive review. *Renewable and sustainable energy reviews*, 14 (2):578-597.

Norman, R. O., Millat, T., Winzer, K., Minton, N. P. and Hodgman, C., 2018. Progress towards platform chemical production using *Clostridium autoethanogenum*. *Biochemical Society Transactions*, 46 (3): 523-535.

Oubrahim, H., and Chock, P. B. 2016. Chemical and Physical Principles. *Encyclopedia of Cell Biology*. Elsevier, 5-13.

Padan, E., Zilberstein, D. and Schuldiner, S., 1981. pH homeostasis in bacteria. *Biochimica et Biophysica Acta (BBA)-Reviews on Biomembranes*, 650 (2-3): 151-166.

Phillips, J. R., Klasson, K. T., Clausen, E. C. and Gaddy, J. L., 1993. Biological production of ethanol from coal synthesis gas. *Applied Biochemistry and Biotechnology*, 39 (1): 559-571.

Pinto, T, Flores-Alsina, X, Gernaey, K.V, and Junicke, H., 2021. Alone or together? A review on pure and mixed microbial cultures for butanol production. *Renewable and Sustainable Energy Reviews*, 147:111244.

Ragsdale, S. W., 1997. The eastern and western branches of the Wood/Ljungdahl pathway: how the east and west were won. *Biofactors*, 6 (1): 3-11.

Ramió-Pujol, S., Ganigué, R., Bañeras, L. and Colprim, J., 2015. Incubation at 25°C prevents acid crash and enhances alcohol production in *Clostridium carboxidivorans* P7. *Bioresource Technology*, 192: 296-303.

Richter, H., Molitor, B., Wei, H., Chen, W., Aristilde, L. and Angenent, L. T., 2016a. Ethanol production in syngas-fermenting *Clostridium ljungdahlii* is controlled by thermodynamics rather than by enzyme expression. *Energy & Environmental Science*, 9 (7): 2392-2399.

Richter, H., Molitor, B., Diender, M., Sousa, D. Z. and Angenent, L. T., 2016b. A narrow pH range supports butanol, hexanol, and octanol production from syngas in a continuous co-culture of *Clostridium ljungdahlii* and *Clostridium kluyveri* with in-line product extraction. *Frontiers in Microbiology*, 7: 1773.

Sadhukhan, J., Lloyd, J. R., Scott, K., Premier, G. C., Eileen, H. Y., Curtis, T. and Head, I. M., 2016. A critical review of integration analysis of microbial electrosynthesis (MES) systems with waste biorefineries for the production of biofuel and chemical from reuse of CO₂. *Renewable and Sustainable Energy Reviews*, 56: 116-132.

Saxena, J. and Tanner, R. S., 2011. Effect of trace metals on ethanol production from synthesis gas by the ethanologenic acetogen, *Clostridium ragsdalei*. *Journal of Industrial Microbiology and Biotechnology*, 38 (4): 513-521.

Schwarz, F. M. and Müller, V., 2020. Whole-cell biocatalysis for hydrogen storage and syngas conversion to formate using a thermophilic acetogen. *Biotechnology for Biofuels*, 13 (1): 1-11.

Shen, N., Dai, K., Xia, X. Y., Zeng, R. J. and Zhang, F., 2018. Conversion of syngas (CO and H₂) to biochemicals by mixed culture fermentation in mesophilic and thermophilic hollow-fiber membrane biofilm reactors. *Journal of Cleaner Production* 202: 536-542.

Shen, S., Wang, G., Zhang, M., Tang, Y., Gu, Y., Jiang, W., Wang, Y. and Zhuang, Y., 2020. Effect of temperature and surfactant on biomass growth and higher-alcohol production

during syngas fermentation by *Clostridium carboxidivorans* P⁷. *Bioresources and Bioprocessing* 7 (1): 1-13.

Silveira, M., Wisbeck, E., Hoch, I. and Jonas, R., 2001. Production of glucose–fructose oxidoreductase and ethanol by *Zymomonas mobilis* ATCC 29191 in medium containing corn steep liquor as a source of vitamins. *Applied Microbiology and Biotechnology*, 55(4): 442-445.

Stoll, I. K. , Boukis, N. and Sauer, J. 2020. Syngas fermentation to alcohols: reactor technology and application perspective. *Chemie Ingenieur Technik*, 92 (1-2).

Sun, X., Atiyeh, H. K., Huhnke, R. L. and Tanner, R. S., 2019. Syngas fermentation process development for production of biofuels and chemicals: A review. *Bioresource Technology Reports*, 7: 100279.

Tan, Y., Liu, J., Liu, Z. and Li, F., 2014. Characterization of two novel butanol dehydrogenases involved in butanol degradation in syngas-utilizing bacterium *Clostridium ljungdahlii* DSM 13528. *Journal of Basic Microbiology*, 54 (9): 996-1004.

Tanner, R. S., Miller, L. M. and Yang, D., 1993. *Clostridium ljungdahlii* sp. nov., an acetogenic species in *Clostridial* rRNA homology group I. *International Journal of Systematic and Evolutionary Microbiology*, 43 (2): 232-236.

Thauer, R. K., Jungermann, K. and Decker, K. 1977. Energy conservation in chemotrophic anaerobic bacteria. *Bacteriological Reviews*, 41: 100-180.

Wang, Y. Q., Yu, S. J., Zhang, F., Xia, X. Y. and Zeng, R. J., 2017. Enhancement of acetate productivity in a thermophilic (55°C) hollow-fiber membrane biofilm reactor with mixed culture syngas (H₂/CO₂) fermentation. *Applied Microbiology and Biotechnology*, 101 (6): 2619-2627.

Wang, Y. Q., Zhang, F., Zhang, W., Dai, K., Wang, H. J., Li, X. and Zeng, R. J., 2018. Hydrogen and carbon dioxide mixed culture fermentation in a hollow-fiber membrane biofilm reactor at 25°C. *Bioresource Technology*, 249: 659-665.

Wang, S., Zhang, Y., Dong, H., Mao, S., Zhu, Y., Wang, R., Luan, G. and Li, Y., 2011. Formic acid triggers the “acid crash” of acetone-butanol-ethanol fermentation by *Clostridium acetobutylicum*. *Applied and Environmental Microbiology*, 77 (5): 1674-1680.

Worden, R. M., Grethlein, A. J., Zeikus, J. G. and Datta, R., 1989. Butyrate production from carbon monoxide by *Butyribacterium methylotrophicum*. *Applied Biochemistry and Biotechnology*, 20 (1): 687-698.

Xu, H., Liang, C., Chen, X., Xu, J., Yu, Q., Zhang, Y. and Yuan, Z., 2020. Impact of exogenous acetate on ethanol formation and gene transcription for key enzymes in *Clostridium autoethanogenum* grown on CO. *Biochemical Engineering Journal*, 155: 107470.

Yamamoto, I., Saiki, T., Liu, S. M. and Ljungdahl, L. G., 1983. Purification and properties of NADP-dependent formate dehydrogenase from *Clostridium thermoaceticum*, a tungsten-selenium-iron protein. *Journal of Biological Chemistry*, 258 (3): 1826-1832.

Yu, J., Liu, J., Jiang, W., Yang, Y. and Sheng, Y., 2015. Current status and prospects of industrial bio-production of n-butanol in China. *Biotechnology Advances*, 33 (7): 1493-1501.

Chapter 3 Homoacetogenesis and solventogenesis from H₂/CO₂ by granular sludge at 25, 37 and 55°C

A modified version of this chapter has been published as:

He, Y., Cassarini, C., Marciano, F. and Lens, P. N. L. 2020. Homoacetogenesis and solventogenesis from H₂/CO₂ by granular sludge at 25, 37 and 55°C. *Chemosphere*, 128649.

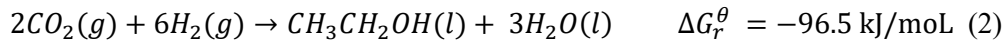
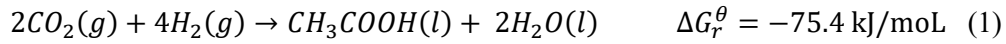
Abstract

CO₂ fermentation is a promising process to produce biofuels like ethanol. It can be integrated in third generation biofuel production processes to substitute traditional sugar fermentation when supplied with cheap electron donors, e.g., hydrogen derived from wind energy or as surplus gas in electrolysis. In this study, granular sludge from an industrial wastewater treatment plant was tested as inoculum for ethanol production from H₂/CO₂ via non-phototropic fermentation at submesophilic (25°C), mesophilic (37°C) and thermophilic (55°C) conditions. The highest ethanol concentration (17.11 mM) was obtained at 25°C and was 5-fold higher than at 37°C (3.36 mM), which was attributed to the fact that the undissociated acid (non-ionized acetic acid) accumulation rate constant (0.145 h⁻¹) was 1.39 fold higher than at 25°C (0.104 h⁻¹). Methane was mainly produced at 55°C, while neither acetic acid nor ethanol were formed. Ethanol production was linked to acetic acid production with the highest ethanol to acetic acid ratio of 0.514 at 25°C. The carbon recovery was 115.7%, 131.2% and 117.1%, while the electron balance was almost closed (97.1%, 110.1% and 109.1%) at 25°C, 37°C and 55°C, respectively. The addition of bicarbonate inhibited ethanol production both at 25°C and 37°C. *Clostridium sp.* were the prevalent species at both 25 and 37°C at the end of the incubation, which possibly contributed to the ethanol production.

3.1 Introduction

Carbon dioxide (CO₂) is the first largest contributor to human-induced global warming. Renewable energy sources such as wind and solar power are facing the challenges of balancing power production and demand. One promising approach is to convert the excess power to H₂ gas, which is a good alternative for fossil fuels. However, the storage and safety of H₂ are big challenges (Pereira 2013). Using H₂ in CO₂ or syngas (mainly containing CO, H₂ and CO₂) fermentation to generate biocommodities (e.g. acetic acid) or biofuel (e.g. ethanol or butanol) is a future trend with economical and sustainable advantages (Burk et al. 2010), such as CO₂ valorization (Bajón Fernández et al. 2017, Sadhukhan et al. 2016), compared to traditional corn (Mohammadi et al. 2011; Eisentraut 2010) or cellulosic biomass (Naik et al. 2010) fermentation. Acetic acid and ethanol production from CO₂ occur via the Wood-Ljungdahl pathway (WLP), which is the most effective non-photosynthetic carbon fixation pathway by acetogens (Charubin et al. 2019). The known acetogens comprise more than 100 bacterial species, with *Clostridium sp.* as an omnipresent species (Fast and Papoutsakis 2012). In the WLP, two moles of CO₂ are reduced, using H₂ as electron donor, to form one mole of acetyl-CoA (Ragsdale 1997). Several species such as *Clostridium autoethanogenum*, *Clostridium ljungdahlii* and

Clostridium carboxidivorans convert syngas to acetate and ethanol in pure culture fermentation via, respectively, homoacetogenesis and solventogenesis (Abubackar et al. 2012; Guo et al. 2010). However, mixed cultures have advantages over pure cultures, such as no contamination problems, higher flexibility and resistance to changes in operation conditions. Homoacetogenesis (Eq. 1), solventogenesis (Eq. 2) and methanogenesis (Eq. 3) from H₂/CO₂ are shown in the following reactions:



Anaerobic sludge from wastewater treatment processes has been studied as inoculum to produce valuable chemicals, such as volatile fatty acids (VFAs) (Dogan et al. 2005), H₂ (Liu and Fang 2003) and ethanol (Steinbusch et al. 2008). Pretreatment methods, including heat (Dessi et al. 2017), acid (Agu et al. 1997) and alkali (Zhu et al. 2006) treatment have been used to eliminate the methanogens and select for spore-performing bacteria, e.g. *Clostridium* sp. Heat treatment has been applied to many inocula, such as sewage sludge (Lay et al. 2012), cow dung sludge (Lin and Hung 2008) and anaerobic sludge.

Temperature is an important factor influencing fermentation, for example, mesophilic conditions (30-37°C) are the optimum temperature range for homoacidogenic *Clostridium* sp. and has been extensively applied in syngas bioconversion (Stoll et al. 2018; Sun et al. 2019). The CO₂ to H₂ ratio influences the conversion of acetic acid and ethanol (Eq. 1, 2). Bicarbonate addition will thus increase the carbon concentration and act as buffer to avoid sharp pH drops. Furthermore, the effect of bicarbonate on fermentation processes has been reported for hydrogen production, while seldom for acetic acid or ethanol production (Panacha et al. 2015). The biological reduction of gaseous inorganic carbon compounds like CO₂ and CO to alcohols has been described for the synthesis of valuable chemicals, such as ethanol and butanol (Kundiya et al. 2011; Richter et al. 2016; Gao et al. 2013; Phillips et al. 2015). Limited studies, however, focused on the comparison of homoacetogenesis and solventogenesis at varied temperatures by mixed cultures (Singla et al. 2014; Liu et al. 2018). Considering the important role of temperature on the microbial community composition during fermentation, the present study investigated ethanol production using CO₂ as the sole carbon source and H₂ as the sole electron donor by mixed cultures at submesophilic (25°C), mesophilic (37°C) and thermophilic (55°C) conditions.

3.2 Materials and methods

3.2.1 Biomass and medium composition

The anaerobic sludge was obtained from a 200 m³ upflow anaerobic sludge bed (UASB) reactor producing methane from dairy industry effluent at 20°C and a hydraulic retention time (HRT) of 9-12 h. The total solid (TS) and volatile solid (VS) content was 42.7 (± 1.0) g/L and 24.8 (± 0.5) g/L, respectively. The granular sludge was first centrifuged at 8000 g for 10 min to remove the supernatant and the solid was heat treated at 90 °C for 15 min as described by Dessì et al. (2017).

1 L medium was prepared according to Stams et al. (1993) and modified as follows: 408 mg/L KH₂PO₄, 534 mg/L Na₂HPO₄·2H₂O, 300 mg/L NH₄Cl, 300 mg/L NaCl, 100 mg/L MgCl₂·6H₂O, 110 mg/L CaCl₂·2H₂O; 1 mL trace metal and 1 mL vitamin stock solution (Stams et al., 1993). 1 L medium (except for CaCl₂·2H₂O and vitamins) was prepared and brought to boiling in order to remove O₂, cooled down to room temperature under an oxygen-free N₂ flow, then CaCl₂·2H₂O and the vitamins were added as well as Na₂S (0.24 g) was added as reducing agent.

3.2.2 Batch experimental set-up

Batch tests were conducted in 125 mL serum bottles with 50 mL medium (gas: liquid ratio of 3:2) and granular sludge with an initial VS concentration of 1.0 g/L. The bottles were sealed with rubber inlets and capped with aluminum crimp caps. A H₂/CO₂ (v/v, 80/20) gas mixture was injected by a gas exchanger system to an initial pressure of 1.8 (± 0.15) bar (P_{H₂}=1.44 bar, P_{CO₂}= 0.36 bar), in which 124.4 mL of the gas mixture was compressed in the 75 mL headspace. Control bottles were set up with H₂/CO₂ (v/v, 80/20) without the granular sludge and N₂ (100%) with the granular sludge with initial VS concentration of 1.0 g/L.

Hydrogen was in excess for acetic acid production (Eq.1), for which a H₂/CO₂ ratio of less than 4/1 is required in the substrate gas. In order to enhance the carbon to hydrogen ratio, 2.1 g/L NaHCO₃ (1.25 mmol of carbon) was added in 50 mL medium, which altered the H₂/CO₂ ratio to 64/36 (v/v). 1 mL of 1M HCl was added in order to correct the pH increase upon the addition of NaHCO₃. At the start of experiments, the gas pressure was measured every 24 h. The headspace was vacuumed and then H₂/CO₂ was injected again by a gas exchange system after 96 h when the gas pressure decreased below 1 bar. Then, the gas was injected every 48 h till the end of the incubation (408 h). All experiments were performed in triplicates.

1 mL of headspace and 1 mL of liquid sample were withdrawn from each bottle every 24 h to analyze the gas and liquid phases. The liquid sample was then centrifuged at 8000×g for 5 min

and the supernatant was used to analyze the ethanol and acetic acid concentrations. The microbial community of the seed granular sludge, enriched sludge samples at 25, 37 and 55°C using H_2/CO_2 and 25°C using $H_2/CO_2 + HCO_3^-$ as the substrate were analyzed.

3.2.3 Analytical methods

3.2.3.1 Gas phase

H_2 and CO_2 concentrations were measured using a HP 6890 gas chromatograph (GC, Agilent Technologies, USA) equipped with a thermal conductivity detector (TCD). The GC was fitted with a 15-m HP-PLOT Molecular Sieve 5A column (ID 0.53 mm, film thickness 50 μm). The oven temperature was kept constant at 60 °C. The temperature of the injection port and the detector were maintained constant at 250 °C. Helium was used as the carrier gas.

3.2.3.2 VFAs and solvent analysis

Ethanol and butanol concentrations were analyzed for each bottle from the liquid phase (1 mL) using high performance liquid chromatography (Agilent Co., USA) equipped with a refractive index detector (RID) and an Agilent Hi-Plex H column (7.7 \times 300 nm, 8 μm). A 5 mM H_2SO_4 solution was used as mobile phase at a flow rate of 0.7 mL/min and with a sample injection volume of 50 μL . The column and refractive index detector (RID) temperatures were, respectively, set at 60°C and 55 °C. TS and VS were measured according to the EPA 2001 methods (Telliard, 2001).

3.2.3.3 Microbial analysis

DNA was extracted using a DNeasy® PowerSoil Kit (QIAGEN, Germany) following the manufacturer's protocol. Approximately 0.5 g of the solids was used for DNA extraction at the end of the incubations at 25°C, 37°C and 55°C. The extracted DNA was quantified and its quality was checked by a Nanodrop 2000c Spectrophotometer (Thermo Scientific, USA). As a first step of the microbiome analysis, all reads with ambiguous bases ("N") were removed. Chimeric reads were identified and removed based on the de-novo algorithm of UCHIME (Edgar et al., 2011) as implemented in the VSEARCH package (Rognes et al., 2016). The remaining set of high-quality reads was processed using minimum entropy decomposition (Eren, 2013 and 2015). Minimum Entropy Decomposition (MED) provides a computationally efficient means to partition marker gene datasets into OTUs (Operational Taxonomic Units). Each OTU represents a distinct cluster with significant sequence divergence to any other cluster. By employing Shannon entropy, MED uses only the information-rich nucleotide positions across reads and iteratively partitions large datasets while omitting stochastic variation. The MED procedure outperforms classical, identity based clustering algorithms. Sequences can

be partitioned based on relevant single nucleotide differences without being susceptible to random sequencing errors. This allows a decomposition of sequence data sets with a single nucleotide resolution. Furthermore, the MED procedure identifies and filters random "noise" in the dataset, i.e. sequences with a very low abundance (less than $\approx 0.02\%$ of the average sample size). To assign taxonomic information to each OTU, DC-MEGABLAST alignments of cluster representative sequences to the sequence database were performed. A most specific taxonomic assignment for each OTU was then transferred from the set of best-matching reference sequences (lowest common taxonomic unit of all best hits). Hereby, a sequence identity of 70%, across at least 80% of the representative sequence was a minimal requirement for considering reference sequences. Further processing of OTUs and taxonomic assignments was performed using the QIIME software package (version 1.9.1, <http://qiime.org/>). Abundances of bacterial taxonomic units were normalized using lineage-specific copy numbers of the relevant marker genes to improve estimates (Angly, 2014). All taxonomic units with less than 0.1% of reads are collapsed in the category "Other". OTU-picking strategy: MED. Reference database: NCBI_nt (Release 2019-08-02). The raw data is available in OneDrive NUIG.

3.2.4 Thermodynamic calculations

The biological reduction of H_2/CO_2 to acetic acid, ethanol or methane and ethanol production from acetic acid and H_2 release energy at standard conditions (Schink 1997; Thauer et al., 1977). The reaction Gibbs free energy for acetic acid production from H_2/CO_2 and for ethanol production from acetic acid was defined by Eq. 5 and Eq. 6, respectively (For derivation see section 3.2.8):

$$\Delta G'_r = \Delta G_r^0 + RT \ln \frac{[Acid]}{[p_{CO_2}]^2 [p_{H_2}]^4} + RT \ln \frac{K_a [H^+]}{K_a + [H^+]} \quad (5)$$

$$\Delta G'_r = \Delta G_r^0 + RT \ln \frac{[CH_3CH_2OH]}{[Acid] [p_{H_2}]^2} + RT \ln \frac{K_a + [H^+]}{K_a [H^+]} \quad (6)$$

3.2.5 Carbon balance and electron balance calculation

The change of the total amount of carbon was defined as the value at time 0 compared to time t. The change of the total amount of carbon of the substrate equals the sum of the total amount of carbon of the products and biomass (Eq. 7), where C_{s_i} is the substrate, C_{p_j} the products and C_b the biomass. Carbon recovery α was calculated by the ratio between the total amount of carbon of the products and the substrates (Eq. 8):

$$\sum_{i=1}^m C_{s_i}(0) - \sum_{i=1}^m C_{s_i}(t) = \sum_{j=1}^m C_{p_j}(t) + C_b(t) \quad (7)$$

$$\alpha = \frac{\sum \Delta C_{p_j}}{\sum \Delta C_{s_i}} \times 100\% \quad (8)$$

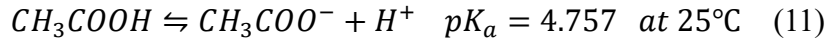
The total amount of electron equivalents (e_{total}) is defined as the sum of the electrons given per reactant (e_{r_i}), per product p_j (e_{p_j}) and per biomass (e_b) (Eq. 9) (Steinbusch, et al. 2008). The electron equivalents of the reactants and products were 12 mol e^- /mol ethanol, 8 mol e^- /mol acetic acid, 0 mol e^- /mol CO_2 , 8 mol e^- /mol CH_4 and 2 mol e^- /mol H_2 (For derivation see Supporting Information). The electron recovery (β) is defined in Eq. 10:

$$e_{total} = \sum_{i=1}^m e_{r_i}(t) + \sum_{j=1}^n e_{p_j}(t) + e_b(t) \quad (9)$$

$$\beta = \frac{\sum_{j=1}^n e_{p_j}(t)}{\sum_{i=1}^m e_{r_i}(t)} \times 100\% \quad (10)$$

3.2.6 Undissociated acids calculation

Considering the ionization of acetic acid (Eq. 11), the free acid concentrations were calculated according to the Henderson-Hasselbalch buffer equation (Maddox et al. 2000) (Eq. 12):



$$[HA] = \frac{10^{-pH} \times C_{Total\ acid}}{10^{-pK_a} + 10^{-pH}} \quad (12)$$

[HA]: concentration of undissociated acid

[A⁻]: concentration of dissociated acid

$C_{total\ acid}$: concentration of total acid

pK_a : negative decadic logarithm of the acid dissociation constant

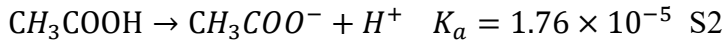
3.2.7 Thermodynamic and electron calculation process

3.2.7.1 Thermodynamic calculation

The reaction for ethanol production from acetic acid and hydrogen could be expressed as:
 $CH_3COO^- + H^+ + 2H_2 \rightarrow CH_3CH_2OH + H_2O \quad \Delta G_r^0 = -9.1\text{kJ/mol} \quad (1)$

The Gibbs free energy change for the reaction calculation:

$$\Delta G'_r = \Delta G_r^0 + RT \ln \frac{[CH_3CH_2OH]}{[CH_3COO^-][H^+][p_{H_2}]^2} \quad S1$$



$$K_a = \frac{[CH_3COO^-][H^+]}{[CH_3COOH]} \quad S3$$

Total concentration of acetic acid is:

$$[Acid] = [CH_3COO^-] + [CH_3COOH] \quad S4$$

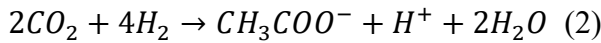
From S3 and S4,

$$[CH_3COO^-] = \frac{[Acid]K_a}{K_a + [H^+]} \quad S5$$

Rewrite S1,

$$\Delta G'_r = \Delta G_r^0 + RT \ln \frac{[CH_3CH_2OH]}{[Acid][p_{H_2}]^2} + RT \ln \frac{K_a + [H^+]}{K_a[H^+]}$$

For the reaction:



$$\Delta G'_r = \Delta G_r^0 + RT \ln \frac{[CH_3COO^-][H^+]}{[p_{CO_2}]^2[p_{H_2}]^4}$$

From S5,

$$\Delta G'_r = \Delta G_r^0 + RT \ln \frac{[Acid]}{[p_{CO_2}]^2[p_{H_2}]^4} + RT \ln \frac{K_a[H^+]}{K_a + [H^+]}$$

3.2.7.2 Electron balance calculation

$$C_2H_5OH = 2 \times (+4) + 5 \times (+1) + (-2) + (-1) = 12 \text{ mole}^-/\text{molEthanol}$$

$$C_2H_4O_2 = 2 \times (+4) + 4 \times (+1) + 2 \times (-2) = 8 \text{ mole}^-/\text{molAcetic}$$

$$CO_2 = (+4) + 2 \times (-2) = 0 \text{ mole}^-/\text{molCO}_2$$

$$CH_4 = (+4) + 4 \times (+1) = 8 \text{ mole}^-/\text{molCH}_4$$

$$H_2 \rightarrow 2H^+ = 2 \text{ mole}^-/\text{mol}$$

3.3 Results and discussion

3.3.1 Acetic acid and ethanol production at 25, 37 and 55°C from H₂/CO₂ by granular sludge

At 25°C and 37°C, the acetic acid concentration constantly increased during the incubation period, reaching a maximum average concentration of 50.06 and 63.25 mM, respectively (Fig. 3.1a, b). Ethanol started to be produced after 88 h at 25°C, while after 64 h at 37°C. Ethanol reached the highest concentration of 17.1 mM after 240 h of incubation at 25°C, corresponding to an acetic acid concentration of 33.3 mM (Fig. 3.1a). After 240 h of incubation, the ethanol concentration did not increase, while the acetic acid concentration kept increasing to 83 mM until the end of the incubation (Fig. 3.1a). The highest average concentration of ethanol reached a maximum of 3.36 mM ethanol at 37°C (Fig. 3.1b). Despite differences in absolute values, the ethanol production and product ratios of each experiment showed a clear trend that more ethanol is produced at lower temperature by granular sludge from H₂/CO₂. The highest ethanol concentration in this batch tests without pH control is comparable with previous work (Table 3.1). The highest ethanol concentration of these studies varied from 3.69 to 13 mM, which is lower than in this study. Besides, the duration of the lag phase in our study (17 d) was shorter than that in other studies using granular sludge (21 d) or manure (30 d) as inoculum (Table 3.1).

Table 3.1 Ethanol fermentation using H₂/CO₂ or H₂/CO₂/CO as the substrate by mixed and pure cultures in batch experiments.

Inoculum	Substrate (v/v)	Batch bottles V Liquid/Total (mL)	T/°C	pH	Time (d)	Gas pressure	Ethanol production (mM)	Reference
Manure samples from cattle farm	CO ₂ /H ₂ (80/20)	100/250	37	7	30 d	1 atm daily flushed	5.49	Xu et al. 2015
<i>Clostridium ljungdahlii</i>	CO ₂ /H ₂ (80/20)	4 L	37	5.9	90 h	1 bar 4 bar 7 bar	13 4 < 2	Stoll et al. 2018
<i>Clostridium ljungdahlii</i>	CO/CO ₂ /H ₂ (20/20/5)	200/250	37	6.8	24 h	NA	2.5 without and 6.7 with nanoparticles	Kim et al. 2014
<i>Clostridium ljungdahlii</i>	CO/CO ₂ /H ₂ (20/20/5)	200/250	37	6.8	60 h	NA	10.9 with CoFe ₂ O ₄	Kim and Lee 2016
Granular sludge	50 mM acetic H ₂ 100%	37.5/120	30	NA	21 d	0.5 bar	3.69	Steinbusch et al. 2008
Granular sludge	CO ₂ /H ₂ (80/20)	50/120	25	4.75	408 h	1.8 bar	17.1	This study

The highest average ethanol concentration at 25°C was 5-fold higher than at 37°C due to the fast acid accumulation at 37°C (Fig. 3.2). The high undissociated acid accumulation

possibly contributed to the premature termination of ethanol production at 37°C. The undissociated acid concentrations increased linearly with time at 25°C and 37°C (Fig. 3.2) and the accumulation rate constant was 0.145 h⁻¹ at 37°C, 1.2-fold higher than at 25°C (0.104 h⁻¹) (Fig. 3.2). Mohammadi et al. (2014) reported that ethanol production was prevented when the undissociated acid concentration was, respectively, 34.5 and 33.16 mM using 9 and 11 g/L fructose as the substrate by *Clostridium ljungdahlii*. Maddox et al. (2000) investigated acetone-butanol-ethanol (ABE) fermentation from glucose by *Clostridium beijerinckii* NRRL at 34°C and found that when the undissociated acid concentration did not exceed 50 mM, the ABE production was high. Ramió et al. (2015) performed batch tests using syngas (CO:H₂:CO₂ [32:32:8]) at 25°C and 37°C by *Clostridium carboxidivorans* P7 and concluded that ethanol and butanol were produced at 25°C, but not at 37°C because of an ‘acid crash’ at pH values below 4.8, where the microbes lose their ability to convert the acids to solvents.

CH₄ production was still observed at 37°C at the end of the incubation (6.7 mM) (Fig. 3.1b), whereas no CH₄ production was observed at 25°C (Fig. 3.1a), which was possibly because the heat-pretreatment did not fully eliminate methanogens and methanogens regrow at mesophilic condition, though the pH of the medium was below 5. Besides, the high H₂ partial pressure in this study (1.44 bar) might be in favor of the hydrogenotrophic mesophilic methanogens. Hydrogenotrophic methanogens in anaerobic sludge have a higher capacity of H₂ consumption than homoacetogens at high H₂ partial pressure, neutral pH and mesophilic temperatures (Liu et al. 2016a; Yasin et al. 2015).

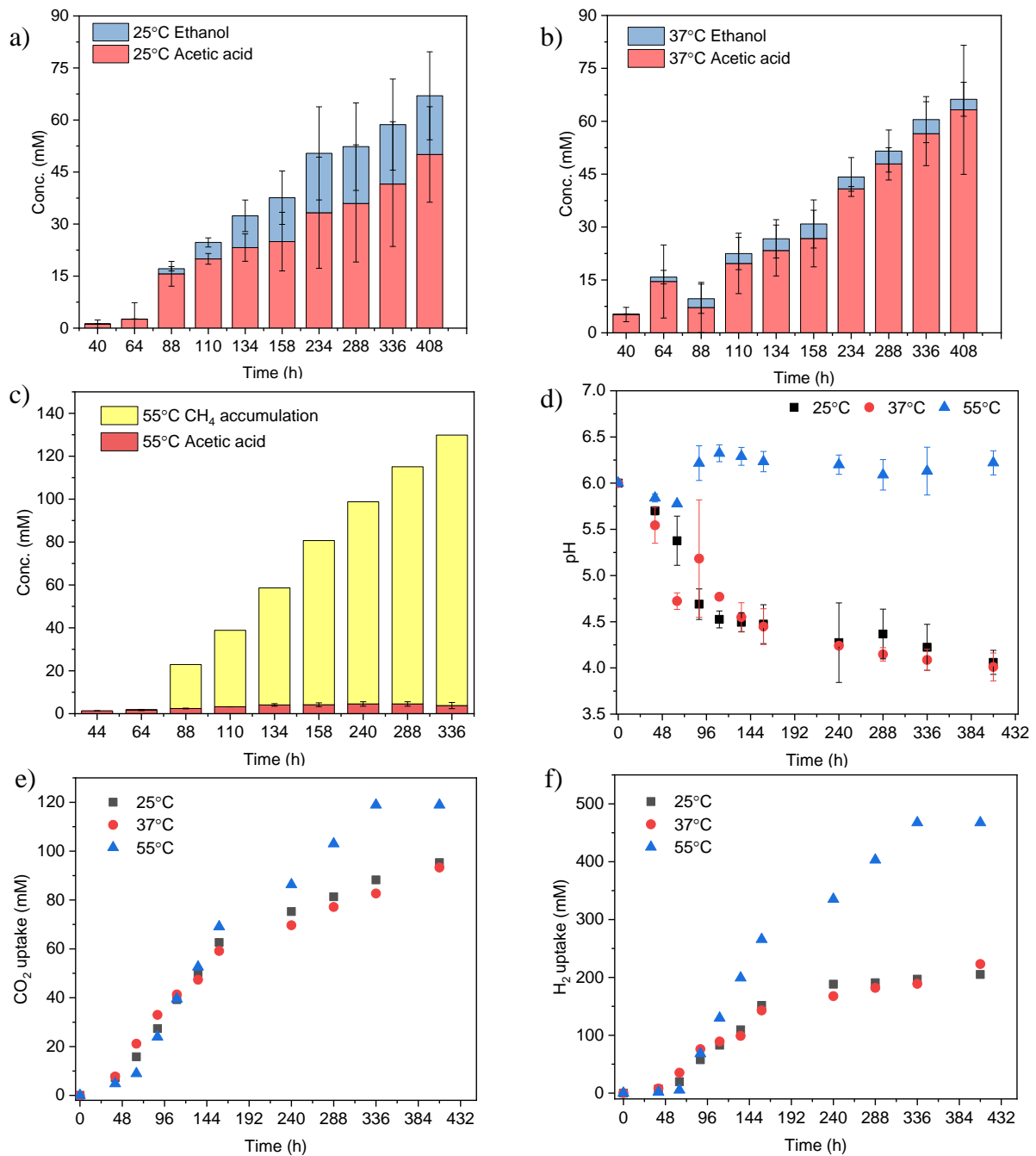


Fig. 3.1 Acetic acid and ethanol yield a) at 25°C, b) at 37°C, c) at 55 °C, d) pH, e) CO₂ uptake and f) H₂ uptake for the incubations with heat-treated granular sludge at 25, 37, 55 °C. Every point shows the average of three independent batch cultures, error bars of acetic acid and ethanol production at 25 and 37 °C indicate the standard deviation of the triplicates.

H₂/CO₂ was injected at every time point.

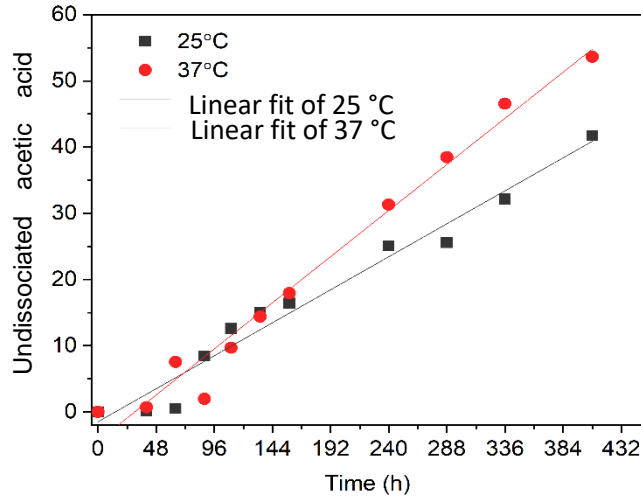


Fig. 3.2 Undissociated acetic acid concentrations and the linear fit at 25°C and 37°C using H₂/CO₂ as substrate by heat-treated granular sludge (0.104 h⁻¹ at 25°C, R² = 0.97; 0.145 h⁻¹ at 37°C, R² = 0.98).

3.3.2 Threshold pH and acetic acid concentration for ethanol production

The fast acetic acid accumulation rate caused a quick decrease in pH from initially 6 to 4.5 after 144 h of incubation at 25°C and 37°C (Fig. 3.1d), while the pH at 37°C decreased faster than at 25°C. After 144 h, the pH at both incubation temperatures (25 and 37°C) decreased slowly to 4.1 until the end of the incubation. A minimum concentration of acidic pH (~ 4.75) and undissociated acid (with an average concentration of 15 mM) seemed to be required for solventogenesis. Increased CO₂ and H₂ pressure and pH could enhance acid production while high H₂ pressure or low pH could enhance ethanol production (Eq. 5 and Eq. 6). Along with the decrease in pH, acetic acid accumulation leveled off, as also in accordance with the thermodynamics (Eq. 5). When ethanol started to be produced (≥ 1 mM), the acetic acid and pH in each bottle were 15.2 mM and 4.68, 19.5 mM and 4.53, 12.5 mM and 4.86, respectively (Fig. 3.3). This is a large difference among the respective triplicates, which is illustrated by the large error bars (standard deviation) (Fig. 3.1). Considering the differences in the triplicates, Fig. 3.3 plotted the acetic acid concentration and pH as a function of the ethanol concentration for each triplicate bottle. The difference in acetic acid and ethanol production among the triplicates at 25°C might be attributed to inhomogeneities among the inocula used. This might have resulted from the heat treatment, which caused differences in the population size of the acetogens in the inoculum at each bottle (Fig. 3.11). Indeed, there was a large difference in the relative abundance of *Clostridium sp.* in the three bottles (Fig. 3.4), which was 1.5%, 30.3% and 59.4% (Table 3.2).

Table 3.2 The average relative abundance (%) at genus level at the end of assay using H₂/CO₂ as substrate at 25, 37 and 55 °C and H₂/CO₂ + HCO₃⁻ as the substrate at 25°C by heat-treated granular sludge.

Taxonomy	H ₂ /CO ₂			H ₂ /CO ₂ +	Original sludge (%)	granular
	25°C (%)	37°C (%)	55°C (%)	HCO ₃ ⁻ 25°C (%)		
<i>k__Bacteria</i>	4.3	0.1	0.7	4.0	0.0	
<i>Atopobium</i>	14.0	0.3	1.0	0.5	0.0	
<i>Olsenella</i>	6.4	1.5	4.1	5.1	7.1	
<i>o_Marinilabiales</i>	6.7	0.3	1.6	5.2	9.6	
<i>Sunxiuqinia</i>	0.7	0.2	0.8	1.6	1.7	
<i>Tangfeifania</i>	3.9	1.7	4.9	5.8	15.9	
<i>Candidatus Cloaci monas</i>	0.1	0.4	1.0	0.6	2.5	
<i>Thermomarinilinea</i>	0.4	0.3	1.0	1.2	1.3	
<i>o_Clostridiales</i>	5.0	2.4	3.2	8.6	0.4	
<i>Caloramator</i>	0.0	4.7	19.8	1.0	0.0	
	30.4					
<i>Clostridium</i>	(1.5, 30.3, 59.4)	56.3	9.3	39.5	0.3	
<i>Caproiciproducens</i>	1.3	1.4	0.5	1.9	0.0	
<i>Moorella</i>	0.0	0.8	6.4	1.1	0.3	
<i>Thermoanaerobact erium</i>	0.0	10.6	6.0	0.0	0.0	
<i>Desulfonatrum</i>	1.6	1.4	3.2	3.0	4.1	
<i>Desulfovibrio</i>	1.8	0.1	0.6	2.3	8.4	
<i>Geobacter</i>	0.5	0.8	1.4	0.8	1.4	
<i>Syntrophus</i>	8.0	1.7	3.9	3.0	9.1	
<i>Desulfovirga</i>	1.8	1.8	0.9	0.9	1.2	
<i>Syntrophorhabdus</i>	3.2	2.8	5.1	2.4	10.7	
<i>Rectinema</i>	0.3	0.4	0.8	0.5	2.3	
Others	9.7	10.0	24.0	11.1	24.0	

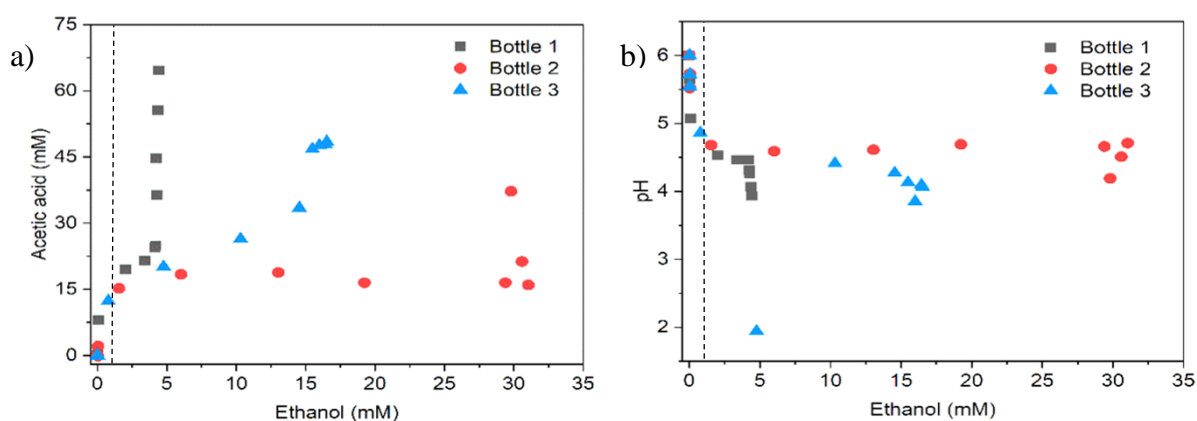


Fig. 3.3 Ethanol production at 25°C using H₂/CO₂ as the substrate by granular sludge as a function of a) the molar ethanol (x-axis) and acetic acid concentration (y-axis) and b) the molar ethanol.

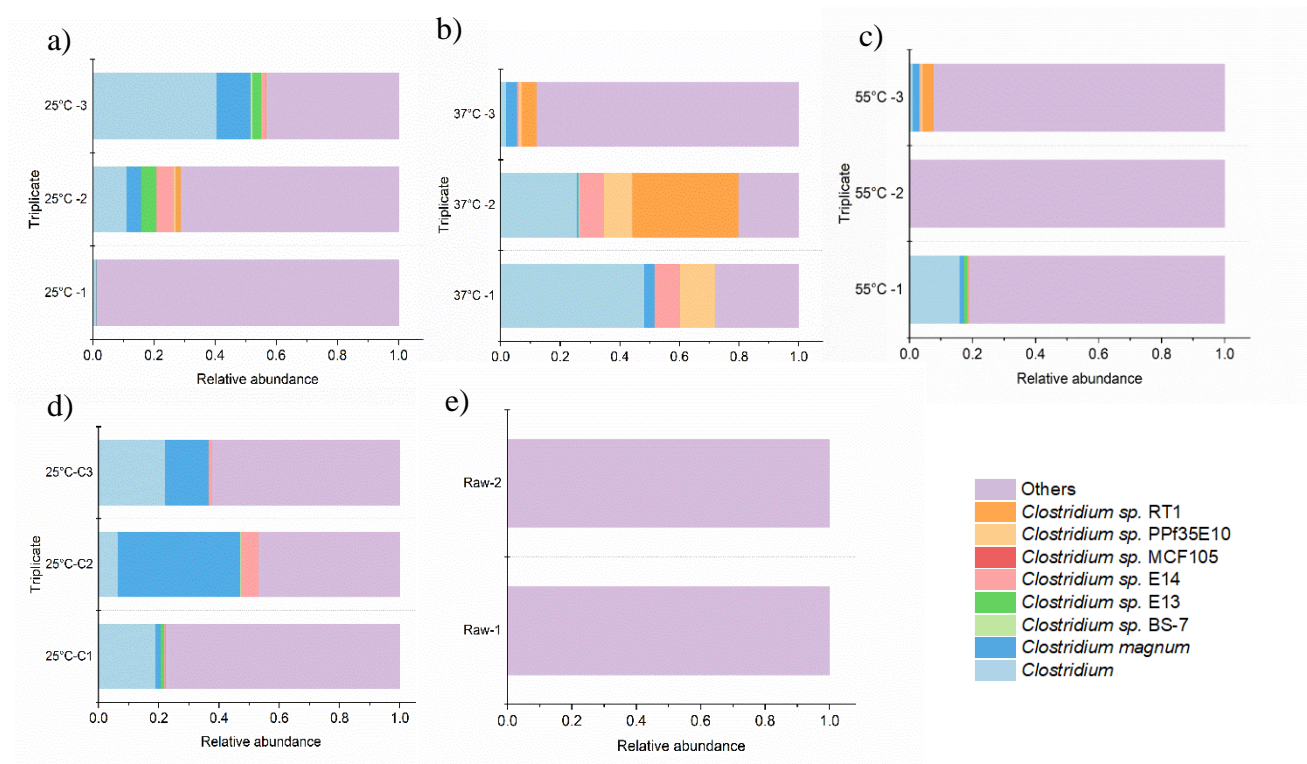


Fig. 3.4 Relative taxonomic abundance of *Clostridium sp.* with heated treated granular sludge as inoculum at the end of incubation at a) 25, b) 37 and c) 55 °C using H_2/CO_2 as substrate and d) raw granular sludge ; e) 25 °C using $H_2/CO_2 + HCO_3^-$ as the substrate.

Solventogenesis occurs at a pH ranging from 4.5 to 5.5, varying according to the different strains (Table 3.3). Acetic acid production is thermodynamically more feasible with an increase in H_2/CO_2 partial pressure and pH (Eq. 5, Fig. 3.5a), whereas ethanol production is thermodynamically more favourable at elevated acetic acid concentrations and high hydrogen partial pressure (higher than 0.1 bar) and low pH at 25 °C (Eq. 5, Fig. 3.5b). Undissociated acetic acid can cross the cytoplasmic membrane by diffusion, reduce the intracellular pH and disrupt the transmembrane proton motive force for ATP formation (Herrero et al. 1985). To avoid inhibition or death of the cells due to the protons released by dissociated acids and prevent a further pH decrease, the cells start to convert acids to neutrally charged alcohols (Liu et al. 2014). Gottwald and Gottschalk (1985) reported that the internal pH needed to stay above 5.5 in cultures of *Clostridium acetobutylicum* for the shift from acid to solvent formation. The *Clostridium sp.* present in the sludge (Fig. 3.11) were unable to keep a constant pH inside the cells when grown in a phosphate-limited synthetic medium.

Table 3.3 Shift pH from acetic acid to ethanol of *Clostridium sp.* or anaerobic sludge at various temperatures using H₂ or syngas as the substrate.

Strain	Substrate (v/v)	Shift pH	T (°C)	Ethanol (mM)	Reference
<i>Clostridium autoethanogenum</i>	CO/CO ₂ (95/5)	4.74	37	5.65	Guo et al. 2010
	CO	4.75	30	19.57	Abubackar et al. 2015
	H ₂ /CO ₂ /N ₂ (65/23/9)	5	37	136.96	Mock et al. 2015
<i>Clostridium carboxidivorans</i>	CO/ H ₂ /CO ₂ /N ₂ (20/5/15/60)	4.5-5.5	37	152.17	Shen et al. 2017
	CO	4.75	30	103.26	Abubackar et al. 2012
	CO	4.75	33	120.65	Fernández-Naveira et al. 2016
<i>Clostridium ljungdahlii</i>	H ₂ /CO ₂ /N ₂ (53.3/26.7/20)	NA	37	13	Stoll et al. 2018
Anaerobic sludge	CO (100%)	4.9	33	241.30	Chakraborty et al. 2019
	CO/ H ₂ /CO ₂ /N ₂ (20/20/15/45)	4.7	37	47.83	Singla et al. 2014
	H ₂ /CO ₂ (80/20)	4.7	25	17.11	This study

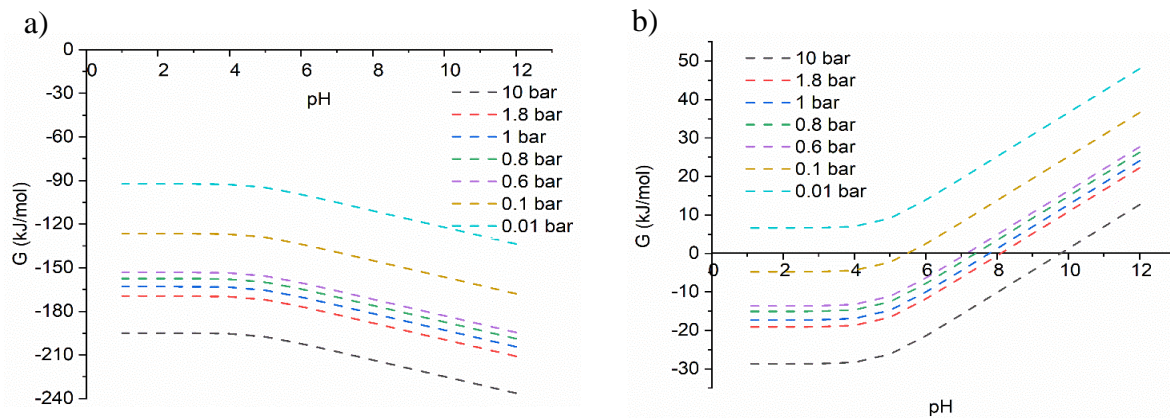


Fig. 3.5 Gibbs free energy change of a) acetic acid production as a function of pH at different CO₂/H₂ partial pressures and b) ethanol production as function of pH at different H₂ partial pressures and 1 M acetic acid.

3.3.3 Methane production at 55°C from H₂/CO₂ by granular sludge

At 55°C, acetic acid increased slowly to 4.07 mM after 134 h of incubation after which it kept stable until the end of the incubation (Fig. 3.1c). Ethanol production was not observed at 55°C. Methane accumulated constantly with a final concentration of 126.05 mM (Fig. 3.1c).

The pH increased to 6.3 and then kept constant at 6.0-6.5 (Fig. 3.1d). The heat pretreatment of the inoculum at 90°C for 15 min did not inhibit methanogenesis and thermoanaerobacteria including *Thermoanaerobacteraceae* and *Theranaerobacterales* were enriched at 55°C (Fig. 3.6). Wang et al. (2017) studied acetate production under thermophilic conditions by acetogens, but required addition of bromoethane sulfonate (BES) to eliminate CH₄ production. Besides, the pH was above 6 (6.0 - 6.5) during the 55°C incubation, which is favorable for methane production since usually methane production is inhibited only at pH values below 6 (Chakraborty et al., 2019). The lack of acetic acid and ethanol production was due to the activity of hydrogen utilizing methanogens in the thermophilic incubation. The ratio of the consumed H₂ and CO₂ in the gas phase was kept at 4 after 96 h at 55°C (Fig. 3.7), which is conform to the theoretical H₂/CO₂ ratio for CH₄ production (Eq. 3). Besides, the low acetic acid concentration during fermentation supports that methane was not produced from acetate via H₂/CO₂ acetogenesis. Indeed, H₂/CO₂ methanogenesis is about 3 times more exergonic than H₂/CO₂ acetogenesis (Breznak and Kane 1990). Moreover, the H₂ utilization threshold for methanogens is 10-100 times lower than that of acetogens. For example, the acetogen *Acetobacterium woodii*, when in a co-culture with a H₂-utilizing methanogen, using fructose as the carbon source transfers fermentatively the generated H₂ to the methanogens, instead of using it for acetogenesis as it would do in pure culture (Lovley and Klug, 1983). Development of solventogenic communities at thermophilic conditions might thus require the deactivation of the methanogens in the inoculum, as also required for dark (Dessi et al., 2017) and syngas (Wang et al., 2017) fermentation.

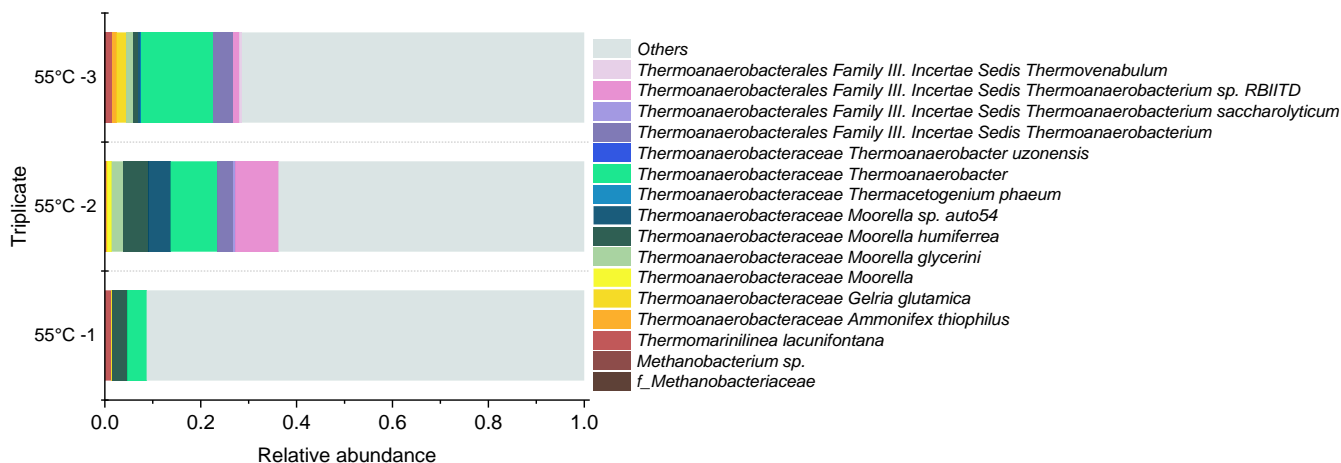


Fig. 3.6 Relative abundance of thermoanaerobic bacteria species with heated treated granular sludge as inoculum at the end of incubation at 55 °C using H₂/CO₂ as the substrate.

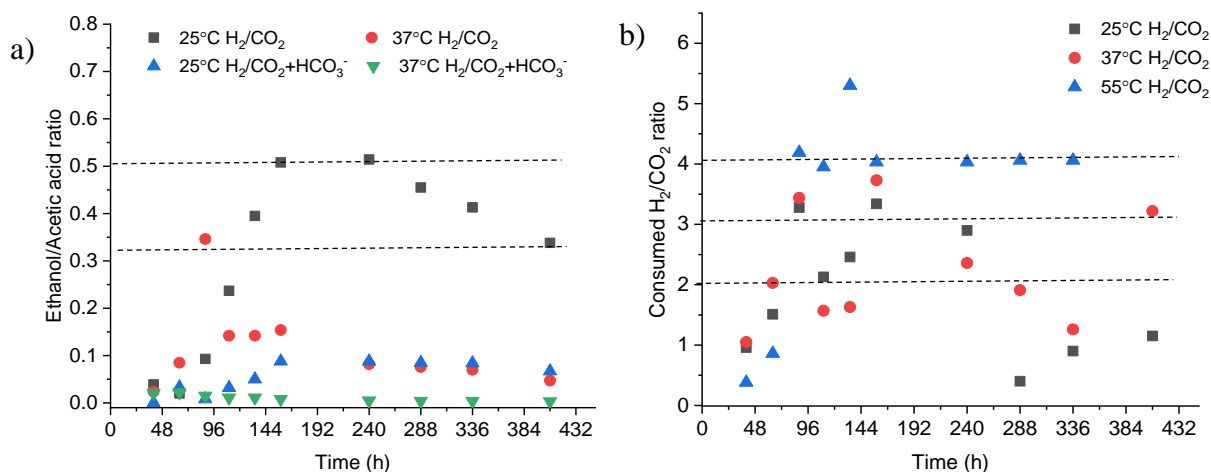


Fig. 3.7 a) Ethanol to acetic acid ratio using H₂/CO₂ or H₂/CO₂ + HCO₃⁻ as the substrate at 25 and 37 °C by granular sludge; b) Consumed H₂ to CO₂ ratio using H₂/CO₂ as the substrate at 25, 37 and 55°C by granular sludge.

3.3.4 Gas consumption and production rates

The amount of CO₂ and H₂ taken up at 25°C was first lower than at 37°C till 110 h and then higher till 336 h (Fig. 3.1 e, f), while H₂ taken up at 37°C was higher than 25 °C at the end of incubation, which might be attributed to the offset of the methane production at 37°C with a higher H₂/CO₂ consuming ratio than acetic acid and ethanol production (Eq. 1, 2 and 3). However, the amount of both CO₂ and H₂ taken up is the highest at 55°C (Fig. 3.1 e, f). The highest CO₂ consumption rate reached at 55°C was 0.779 mmol L⁻¹ h⁻¹, corresponding to the highest H₂ consumption rate of 3.153 mmol L⁻¹ h⁻¹ (Table 3.4). The average CO₂ and H₂ consumption rates in the batches producing methane at 55°C are also higher than in the batches producing acetic acid and ethanol at 25°C and 37°C (Table 3.4).

Table 3.4 Molar concentration changes of products with H₂/CO₂ as the carbon source at the end of the incubation.

Conditions	Substrate					
	H ₂ /CO ₂			H ₂ /CO ₂ +HCO ₃ ⁻		
	25°C	37°C	55°C	25°C	37°C	55°C
Products (mM)						
Acetic acid	41.5 ± 18.0	56.4 ± 9.1	4.3 ± 1.0	118.2 ± 7.7	84.8 ± 33.7	4.5 ± 1.0
Ethanol	17.1 ± 13.4	4.1 ± 6.8	0	8.6 ± 6.4	0.5 ± 0.3	0
Methane	0.2 ± 0.2	1.3 ± 2.3	126.0	0.3	38.4	141.1
CO ₂	-131.1 ^a	-134.1 ^a	-119.5 ^a	-95.9 ^a	-93.26 ^a	-118.9 ^a
H ₂	-524.3 ^a	-536.4 ^a	-478.1 ^a	-205.1 ^a	-223.08 ^a	-467.4 ^a
Highest rates (mmol L⁻¹ h⁻¹)						
H ₂ consumption	1.840	1.909	3.153	2.088	1.155	4.047
CO ₂ consumption	0.593	0.511	0.779	-- ^b	-- ^b	-- ^b
CH ₄	0.005	0.020	0.955	0.002	0.289	0.929
Acetic acid	0.545	1.228	0.185	3.624	2.515	0.167
Ethanol	0.201	0.179	0	0.318	0.023	0
Highest ethanol/acetic ratio	0.514	0.346	0	0.088	0.022	0
H ₂ consumption (%)	39.1	41.6	97.8	49.5	52.3	98.6
CO ₂ consumption (%)	72.7	69.6	99.5	-- ^b	-- ^b	-- ^b
Carbon recovery (%)	115.7	131.2	117.1	-- ^b	-- ^b	-- ^b
Electron recovery (%)	97.1	110.0	109.1	117	121.3	115.9
Recovery in ethanol (%)	31.6	5.9	0	-- ^b	-- ^b	-- ^b

Notes:

^a Negative value indicate an overall consumption of component during the experiment

^b data not known since carbon is excess

Considering both gas consumption (i.e. H₂ and CO₂) and product formation (i.e. acetic acid, ethanol and CH₄), the incubations can be divided in three phases: an adaption (0-88 h), an accumulation (88-240 h) and a stable (240-408 h) phase. The consumption rate of H₂ and CO₂ and the production rate of CH₄, acetic acid and ethanol also demonstrate this (Fig. 3.8). The highest acetic acid and ethanol production rates at 25°C were 0.545 mmol L⁻¹ h⁻¹ and 0.201 mmol L⁻¹ h⁻¹, respectively (Table 3.4). It should be noted that at 25°C the highest ethanol production rate was reached later (at 134 h) than the one of acetic acid (at 64 h) (Fig. 3.8a). At 25°C, the acetic acid production rate was lower, while the ethanol production rate was higher than at 37°C (Fig. 3.8a, b).

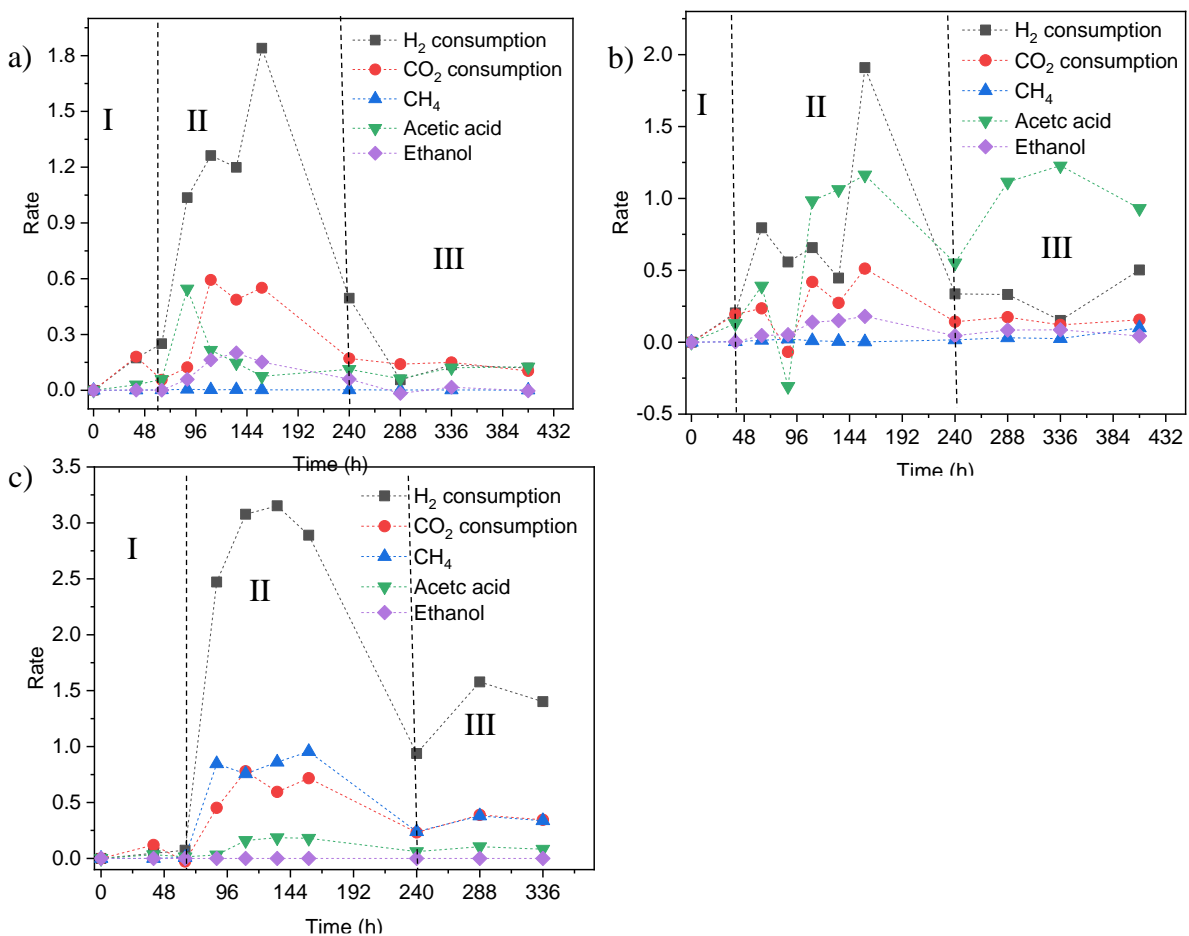


Fig. 3.8 H₂ and CO₂ consumption rate, CH₄, acetic acid and ethanol production rate at a) 25°C, b) 37°C and c) 55 °C by heat treated granular sludge using H₂/CO₂ as substrate.

3.3.5 Carbon and electron balance

Bioconversion of H₂/CO₂ by granular sludge at different temperatures resulted in the production of different amounts of acetic acid, ethanol and CH₄ (Fig. 3.1). Carbon from CO₂ was converted to acetic acid and ethanol at 25°C and 37°C, while CH₄ was the main product at 55°C. The total carbon of acetic acid, ethanol and CH₄ production is higher than the amount

of carbon from CO₂ consumption after 88 h till the end of incubation at 25, 37 and 55°C (Fig. 3.9). The mass balance based on carbon (mmol) was almost closed, while the carbon recovery was higher: 115.7%, 131.2% and 117.1 at 25°C, 37°C and 55°C, respectively (Table 3.4). The carbon released from calcium carbonate precipitates, upon a pH decrease, can cause a positive carbon balance (Liu et al. 2016b). In the control experiment with 100% N₂, acetic acid was still detected at the highest concentration of 1.48, 0.39 and 2.9 mM at, respectively, 25°C, 37°C and 55°C. Along with incubation time and temperature increase, the difference between carbon consumption and production increased (Fig. 3.9). The electron balance was 97.1%, 110.1% and 109.1% at 25°C, 37°C and 55°C, respectively (Table 3.4), which was almost closed and unaffected by carbonate. Ethanol recovery reached 31.6% at 25°C, much higher than at 37°C (5.9%) using H₂/CO₂ as the substrate.

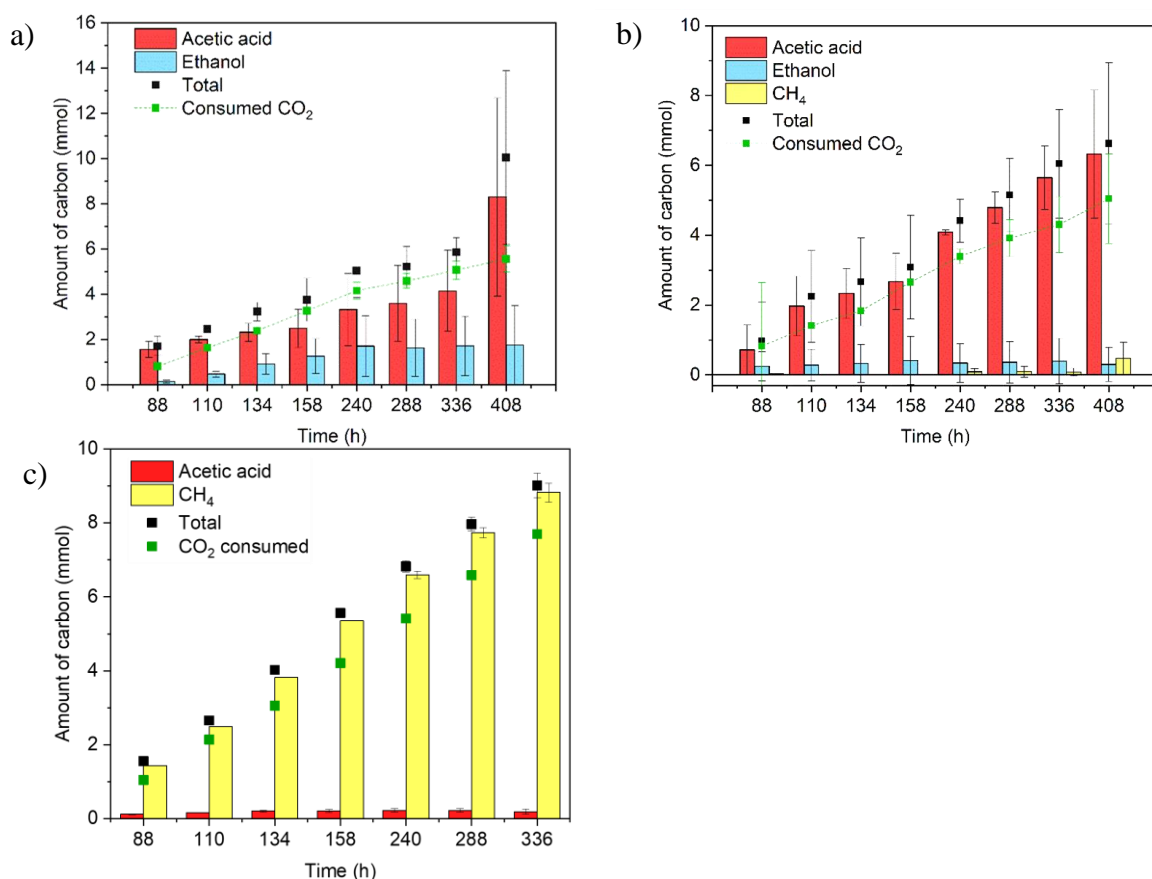


Fig. 3.9 Carbon distribution at the end of each batch culture (each time injecting gas means a batch culture at a) 25°C, b) 37°C and c) 55°C. The columns refer to the mmol of carbon found in the different metabolites at the end of every batch culture and the black dots represent their sum. The green dots with dash line represent the mmol carbon of consumed CO₂. Every column or point shown in the graphs is calculated as the average of three independent batch cultures, error bars indicate the standard deviation of the triplicates.

3.3.6 HCO₃⁻ enhanced acetic acid production and inhibited ethanol production

At 25°C and 37°C, the acetic acid concentration constantly increased during the whole fermentation process, reaching a maximum average concentration of 118.17 and 81.03 mM, respectively (Fig. 3.10a and 4b). The highest average ethanol concentration was 7.31 mM at 25°C and 0.50 mM at 37°C. The highest acetic acid production rate was 3.62 at 25°C, compared to 2.51 at 37°C (Table 3.4). Ethanol production was not observed at 55°C. Acetic acid increased slowly to 5 mM at the end of the incubation. The gas phase methane accumulated constantly till a final concentration of 141.10 mM (Fig. 3.10c). The pH of both incubations at 25°C and 37°C decreased to 4.75 after 144 h of incubation and then varied between 4.5 and 5. At 55°C, the pH increased to 7.0 after 144 h of incubation and subsequently varied between 7.0 and 7.5 until the end of the incubation (Fig. 3.10b).

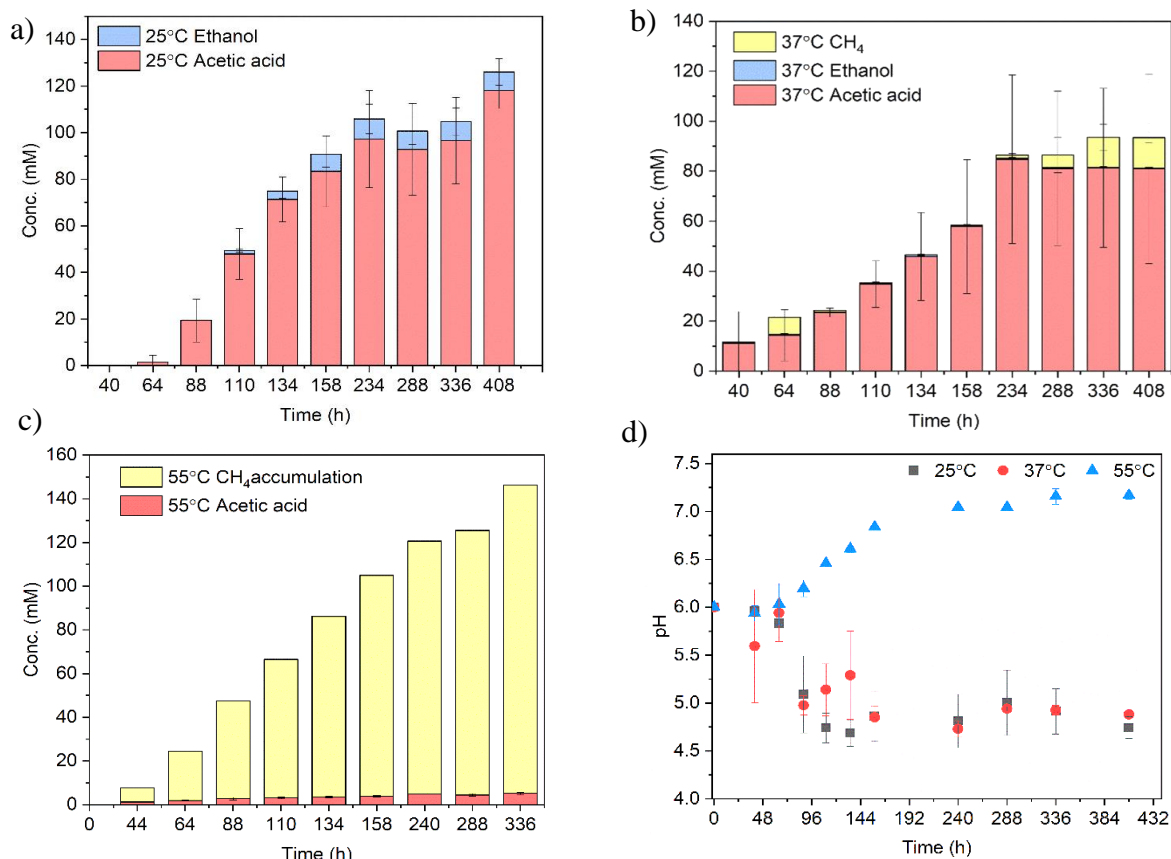


Fig. 3.10 Acetic acid, ethanol and CH₄ yield at a) 25°C, b) 37°C, c) 55 °C and d) pH in incubations with the heat-treated granular sludge at 25, 37, 55 °C in the presence of HCO₃⁻.

Every point shown in the graphs is calculated as the average of three independent batch cultures, error bars indicate the standard deviation of the triplicates.

The ethanol concentration was lower in the presence of HCO₃⁻ than without HCO₃⁻ at both 25°C and 37°C (Fig. 3.10). Bicarbonate is utilized by bacteria as the carbon source, since CO₂

dissolves from the gas phase to the liquid phase as bicarbonate (Zhu et al. 2017). Similarly, the carbon dioxide addition induced an increased growth of acetogenic bacteria during syngas fermentation (Heiskanen et al. 2007). Additionally, the H₂:CO₂ ratio of the 4:1 of feeding gas is stoichiometrically higher than that (3:1) for acetic acid production (Eq. 1). The relative abundance of *Clostridium sp.* was 39.5%, similar to the value obtained for the batch without HCO₃⁻ (30.4%) at 25°C (Table 3.2), which shows that the addition of HCO₃⁻ did not change the bacterial community composition compared to without HCO₃⁻ at the genus level. However, in the presence of HCO₃⁻, the highest acetic acid concentration at 25 and 37°C was, respectively, 2.9 and 1.5-fold higher than without the addition of HCO₃⁻ (Fig. 3.10). The enhanced acetic acid production upon HCO₃⁻ addition might thus cause the accumulation of undissociated acid, thus inhibiting ethanol production (Fig. 3.10a, b). Indeed, the pH of both incubations varied between 4.5 and 5 at both 25°C and 37°C after 144 h of incubation (Fig. 3.10a, b). The strong enhancement of the acetic acid concentration by HCO₃⁻ addition provides a new strategy for enhancing acetic acid production, which can support a high ethanol production yield when using a two stage fermentation process (Richter et al., 2013).

3.3.7 Microbial community analysis

The analysis of the microbial community composition at the end of the batch incubations at genus level revealed significant differences between the inoculum and the different fermentation conditions. The initial granular sludge was dominated by the genera *Tangfeifania* (15.9%), *Desulfonatronum* (8.4%), and *Syntrophus* (9.1%) and the order *Marinilabiliales* (9.6%), whereas other genera like *Clostridium* amounted to less than 1% of the whole microbial community (Fig. 3.11). However, at the end of the incubation the microbial composition had shifted to different dominant genera. *Clostridium sp.* and *Olsenella* were the prevalent species at 25°C at the end of the incubation, with a relative abundance of, respectively, 30.4% and 6.4%. Samples from 37°C incubations exhibited a lower diversity at genus level and represented a high *Clostridium* abundance with an average of 56.3% sequence reads and *Thermoanaerobacterium* with 10.6%. *Caloramator sp.* (19.8%) and *Thermoanaerobacterium sp.* (6.0%) were the dominant bacteria in the 55°C incubation (Fig. 3.11). The average relative abundance of *Thermoanaerobacterium*, including *Thermoanaerobacteraceae* and *Theranaerobacterales*, was 24.5% at 55°C (Fig. 3.4), which may have contributed to the methane production at 55°C.

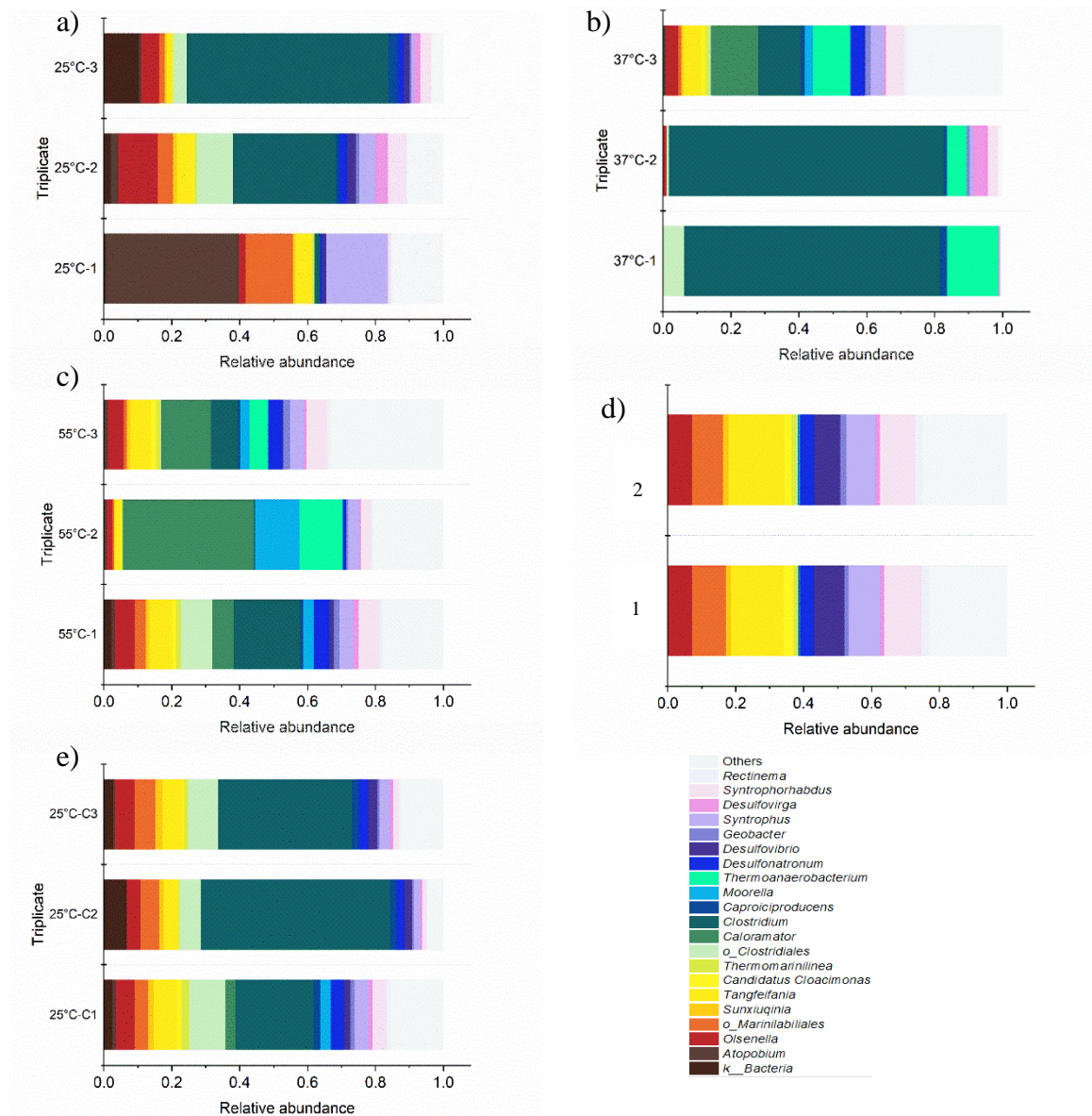


Fig. 3.11 Relative taxonomic abundance of the batch cultures at genus level with heated treated granular sludge as inoculum at the end of incubation at a) 25, b) 37 and c) 55 °C using H_2/CO_2 as substrate and d) untreated granular sludge ; e) 25 °C using $H_2/CO_2 + HCO_3^-$ as substrate.

3.4 Conclusions

A fermentation process that converts CO_2 to ethanol using H_2 as electron donor and anaerobic granular sludge as inoculum was studied at submesophilic (25°C), mesophilic (37°C) and thermophilic (55°C) temperatures. Heat pre-treatment and fermentation at 25°C efficiently inhibited methanogens and achieved the highest ethanol production (17.1 mM). Ethanol production occurred when both the pH decreased to 4.7 and acetic acid accumulated to 15 mM at 25°C by granular sludge using H_2/CO_2 as the substrate. The addition of HCO_3^- promoted

homoacetogenic acetate production both at 25°C and 37°C. Microbial community analysis showed that the addition of H₂/CO₂ and different fermentation temperatures induced changes in the microbial community composition, with *Clostridium* being the functional microorganism at genus level at both 25 and 37°C. Methane was produced from H₂/CO₂ at 55°C.

3.5 References

- Abubackar, H.N., Veiga, M.C. and Kennes, C., 2012. Biological conversion of carbon monoxide to ethanol: effect of pH, gas pressure, reducing agent and yeast extract. *Bioresource technology*, 114, 518-522.
- Abubackar, H.N., Veiga, M.C. and Kennes, C., 2015. Carbon monoxide fermentation to ethanol by *Clostridium autoethanogenum* in a bioreactor with no accumulation of acetic acid. *Bioresource technology*, 186, 122-127.
- Agu, R.C., Amadife, A.E., Ude, C.M., Onyia, A., Ogu, E.O., Okafor, M. and Ezejiofor, E., 1997. Combined heat treatment and acid hydrolysis of cassava grate waste (CGW) biomass for ethanol production. *Waste Management* 17 (1), 91–96.
- Altschul, S.F., Gish, W., Miller, W., Myers, E.W. and Lipman, D.J., 1990. Basic local alignment search tool. *Journal of molecular biology*, 215 (3), 403-410.
- Angly, F.E., Dennis, P.G., Skarszewski, A., Vanwonderghem, I., Hugenholtz, P. and Tyson, G.W., 2014. CopyRighter: a rapid tool for improving the accuracy of microbial community profiles through lineage-specific gene copy number correction. *Microbiome* 2 (1), 11.
- Bajón Fernández, Y., Soares, A., Koch, K., Vale, P. and Cartmell, E., 2017. Bioconversion of carbon dioxide in anaerobic digesters for on-site carbon capture and biogas enhancement – a review. *Critical Reviews in Environmental Science and Technology* 47 (17), 1555–80.
- Breznak, J.A. and Kane, M.D., 1990. Microbial H₂/CO₂ acetogenesis in animal guts: nature and nutritional significance. *FEMS Microbiology Reviews* 7 (3–4), 309–13.
- Burk, M.J., Schilling, C.H., Burgard, A.P. and Trawick, J.D., 2010. Methods and organisms for utilizing synthesis gas or other gaseous carbon sources and methanol, U.S. Patent No.7,803,589.
- Caporaso, J.G., Kuczynski, J., Stombaugh, J., Bittinger, K., Bushman, F.D., Costello, E.K., Fierer, N., Peña, A.G., Goodrich, J.K., Gordon, J.I. and Huttley, G.A., 2010. QIIME allows analysis of high-throughput community sequencing data. *Nature methods*, 7 (5), 335-336.
- Charubin, K. and Papoutsakis, E.T., 2019. Direct cell-to-cell exchange of matter in a synthetic *Clostridium* syntrophy enables CO₂ fixation, superior metabolite yields, and an expanded metabolic space. *Metabolic engineering* 52, 9-19.

- Dessì, P., Lakaniemi, A.M. and Lens, P.N., 2017. Biohydrogen production from xylose by fresh and digested activated sludge at 37, 55 and 70°C. *Water Research* 115, 120–29.
- Dogan, T., Ince, O., Oz, N.A. and Ince, B.K., 2005. Inhibition of volatile fatty acid production in granular sludge from a UASB reactor. *Journal of Environmental Science and Health* 40 (3), 633–44.
- Eisentraut, A., 2010. Sustainable production of second-generation biofuels.
- Edgar, R.C., Haas, B.J., Clemente, J.C., Quince, C. and Knight, R., 2011. UCHIME improves sensitivity and speed of chimera detection. *Bioinformatics*, 27 (16), 2194-2200.
- Eren, A.M., Maignien, L., Sul, W.J., Murphy, L.G., Grim, S.L., Morrison, H.G. and Sogin, M.L., 2013. Oligotyping: differentiating between closely related microbial taxa using 16S rRNA gene data. *Methods in ecology and evolution*, 4 (12), 1111-1119.
- Eren, A.M., Morrison, H.G., Lescault, P.J., Reveillaud, J., Vineis, J.H. and Sogin, M.L., 2015. Minimum entropy decomposition: unsupervised oligotyping for sensitive partitioning of high-throughput marker gene sequences. *The ISME journal*, 9 (4), 968-979.
- Fast, A.G. and Papoutsakis, E.T., 2012. Stoichiometric and energetic analyses of non-photosynthetic CO₂-fixation pathways to support synthetic biology strategies for production of fuels and chemicals. *Current Opinion in Chemical Engineering* 1 (4), 380–95.
- Fernández-Naveira, Á., Abubackar, H.N., Veiga, M.C. and Kennes, C., 2016. Efficient butanol-ethanol (BE) production from carbon monoxide fermentation by *Clostridium carboxidivorans*. *Applied microbiology and biotechnology*, 100(7), 3361-3370.
- Gao, J., Atiyeh, H.K., Phillips, J.R., Wilkins, M.R. and Huhnke, R.L., 2013. Development of low cost medium for ethanol production from syngas by *Clostridium ragsdalei*. *Bioresource Technology* 147, 508–15.
- Gottwald, M. and Gottschalk, G., 1985. The internal pH of *Clostridium acetobutylicum* and its effect on the shift from acid to solvent formation. *Archives of Microbiology*, 143 (1), 42-46.
- Guo, Y., Xu, J., Zhang, Y., Xu, H., Yuan, Z. and Li, D., 2010. Medium optimization for ethanol production with *Clostridium autoethanogenum* with carbon monoxide as sole carbon source. *Bioresource technology*, 101 (22), 8784-8789.
- Heiskanen, H., Virkajärvi, I. and Viikari, L., 2007. The effect of syngas composition on the growth and product formation of *Butyribacterium methylotrophicum*. *Enzyme and Microbial Technology*, 41 (3), 362-367.
- Herrero, A.A., Gomez, R.F., Snedecor, B., Tolman, C.J. and Roberts, M.F., 1985. Growth inhibition of *Clostridium thermocellum* by carboxylic acids: a mechanism based on uncoupling by weak acids. *Applied microbiology and biotechnology*, 22 (1), 53-62.

- Kim, Y.K. and Lee, H., 2016. Use of magnetic nanoparticles to enhance bioethanol production in syngas fermentation. *Bioresource Technology* 204, 139–44.
- Kim, Y.K., Park, S.E., Lee, H. and Yun, J.Y., 2014. Enhancement of bioethanol production in syngas fermentation with *Clostridium ljungdahlii* using nanoparticles. *Bioresource Technology* 159, 446–50.
- Kundiyana, D.K., Wilkins, M.R., Maddipati, P. and Huhnke, R.L., 2011. Effect of temperature, pH and buffer presence on ethanol production from synthesis gas by *Clostridium ragsdalei*. *Bioresource Technology* 102 (10), 5794–99.
- Lay, C.H., Lin, H.C., Sen, B., Chu, C.Y. and Lin, C.Y., 2012. Simultaneous hydrogen and ethanol production from sweet potato via dark fermentation. *Journal of Cleaner Production* 27, 155–64.
- Liu, C., Luo, G., Wang, W., He, Y., Zhang, R. and Liu, G., 2018. The effects of pH and temperature on the acetate production and microbial community compositions by syngas fermentation. *Fuel*, 224, 537-544.
- Liu, H, and HHP Fang. 2003. Hydrogen production from wastewater by acidogenic granular sludge. *Water Science and Technology* 47 (1), 153–58.
- Liu, K., Atiyeh, H. K., Stevenson, B. S., Tanner, R. S., Wilkins, M. R., & Huhnke, R. L. 2014. Mixed culture syngas fermentation and conversion of carboxylic acids into alcohols. *Bioresource technology*, 152, 337-346.
- Liu, R., Hao, X. and Wei, J., 2016a. Function of homoacetogenesis on the heterotrophic methane production with exogenous H₂/CO₂ involved. *Chemical Engineering Journal*, 284, 1196-1203.
- Liu, Y.Q., Lan, G.H. and Zeng, P., 2016b. Size-dependent calcium carbonate precipitation induced microbiologically in aerobic granules. *Chemical Engineering Journal*, 285, 341-348.
- Lovley, D.R. and Klug, M.J., 1983. Methanogenesis from methanol and methylamines and acetogenesis from hydrogen and carbon dioxide in the sediments of a eutrophic lake. *Applied and Environmental Microbiology* 45 (4), 1310–15.
- Maddox, I.S., Steiner, E., Hirsch, S., Wessner, S., Gutierrez, N.A., Gapes, J.R. and Schuster, K.C., 2000. The cause of "acid crash" and "acidogenic fermentations" during the batch acetone-butanol-ethanol (ABE) fermentation process. *Journal of Molecular Microbiology and Biotechnology* 2 (1), 95–100.
- Mock, J., Zheng, Y., Mueller, A.P., Ly, S., Tran, L., Segovia, S., Nagaraju, S., Köpke, M., Dürre, P. and Thauer, R.K., 2015. Energy conservation associated with ethanol formation from

H₂ and CO₂ in *Clostridium autoethanogenum* involving electron bifurcation. *Journal of bacteriology*, 197(18), 2965-2980.

Mohammadi, M., Najafpour, G.D., Younesi, H., Lahijani, P., Uzir, M.H. and Mohamed, A.R., 2011. Bioconversion of synthesis gas to second generation biofuels, a review. *Renewable and Sustainable Energy Reviews* 15 (9), 4255–73.

Naik, S.N., Goud, V.V., Rout, P.K. and Dalai, A.K., 2010. Production of first- and second-generation biofuels, a comprehensive review. *Renewable and Sustainable Energy Reviews* 14 (2), 578–97.

Pancha, I., Chokshi, K., Ghosh, T., Paliwal, C., Maurya, R. and Mishra, S., 2015. Bicarbonate supplementation enhanced biofuel production potential as well as nutritional stress mitigation in the *Microalgae scenedesmus* sp. CCNM 1077. *Bioresource Technology* 193, 315–23.

Pereira, I.A., 2013. An enzymatic route to H₂ storage. *Science* 342 (6164), 1329–30.

Ragsdale, S.W., 1997. The eastern and western branches of the wood/ljungdahl pathway, how the east and west were won. *Biofactors* 6 (1), 3–11.

Ramió-Pujol, S., Ganigué, R., Bañeras, L. and Colprim, J., 2015. Incubation at 25°C prevents acid crash and enhances alcohol production in *Clostridium carboxidivorans* P7. *Bioresource Technology* 192, 296–303.

Phillips, J.R., Atiyeh, H.K., Tanner, R.S., Torres, J.R., Saxena, J., Wilkins, M.R. and Huhnke, R.L., 2015. Butanol and hexanol production in *Clostridium carboxidivorans* syngas fermentation: medium development and culture techniques. *Bioresource Technology*, 190, 114-121.

Rene, E.R., Lens, P.N., Veiga, M.C. and Kennes, C., 2019. Enrichment of a solventogenic anaerobic sludge converting carbon monoxide and syngas into acids and alcohols. *Bioresource technology* 272, 130-136.

Richter, H., Molitor, B., Wei, H., Chen, W., Aristilde, L. and Angenent, L.T., 2016. Ethanol production in syngas-fermenting *Clostridium ljungdahlii* is controlled by thermodynamics rather than by enzyme expression. *Energy & Environmental Science* 9 (7), 2392–99.

Richter, H., Martin, M.E. and Angenent, L.T., 2013. A two-stage continuous fermentation system for conversion of syngas into ethanol. *Energies*, 6 (8), 3987-4000.

Rognes, T., Flouri, T., Nichols, B., Quince, C. and Mahé, F., 2016. VSEARCH: a versatile open source tool for metagenomics. *PeerJ*, 4, e2584.

Sadhukhan, J., Lloyd, J.R., Scott, K., Premier, G.C., Eileen, H.Y., Curtis, T. and Head, I.M., 2016. A critical review of integration analysis of microbial electrosynthesis (mes) systems with

waste biorefineries for the production of biofuel and chemical from reuse of CO₂. *Renewable and Sustainable Energy Reviews* 56, 116–32.

Schink, B., 1997. Energetics of syntrophic cooperation in methanogenic degradation. *Microbiology and Molecular Biology Reviews*. 61 (2), 262–80.

Shen, Y., Brown, R.C. and Wen, Z., 2017. Syngas fermentation by *Clostridium carboxidivorans* P7 in a horizontal rotating packed bed biofilm reactor with enhanced ethanol production. *Applied energy*, 187, 585-594.

Singla, A., Verma, D., Lal, B. and Sarma, P.M., 2014. Enrichment and optimization of anaerobic bacterial mixed culture for conversion of syngas to ethanol. *Bioresource Technology* 172, 41–49.

Stams, A.J., Van Dijk, J.B., Dijkema, C. and Plugge, C.M., 1993. Growth of syntrophic propionate-oxidizing bacteria with fumarate in the absence of methanogenic bacteria. *Applied and Environmental Microbiology* 59 (4), 1114–19.

Steinbusch, K.J., Hamelers, H.V. and Buisman, C.J., 2008. Alcohol production through volatile fatty acids reduction with hydrogen as electron donor by mixed cultures. *Water Research* 42 (15), 4059–66.

Stoll, I.K., Herbig, S., Zwick, M., Boukis, N., Sauer, J., Neumann, A. and Oswald, F., 2018. Fermentation of H₂ and CO₂ with *Clostridium Ljungdahlii* at elevated process pressure—first experimental results. *Chemical Engineering Transactions* 64, 151–56.

Sun, X., Atiyeh, H.K., Zhang, H., Tanner, R.S. and Huhnke, R.L., 2019. Enhanced ethanol production from syngas by *Clostridium ragsdalei* in continuous stirred tank reactor using medium with poultry litter biochar. *Applied Energy* 236, 1269–79.

Telliard, W.A., 2001. Method 1684: Total, fixed, and volatile solids in water, solids, and biosolids. US Environmental Protection Agency, Washington.

Thauer, R.K., Jungermann, K. and Decker, K., 1977. Energy conservation in chemotrophic anaerobic bacteria. *Bacteriological Reviews* 41 (1), 100.

Wang, S., Zhang, Y., Dong, H., Mao, S., Zhu, Y., Wang, R., Luan, G. and Li, Y., 2011. Formic acid triggers the ‘acid crash’ of Acetone-Butanol-Ethanol Fermentation by *Clostridium Acetobutylicum*. *Applied and Environmental Microbiology*. 77 (5), 1674–80.

Wang, Y.Q., Yu, S.J., Zhang, F., Xia, X.Y. and Zeng, R.J., 2017. Enhancement of acetate productivity in a thermophilic (55°C) hollow-fiber membrane biofilm reactor with mixed culture syngas (H₂/CO₂) fermentation. *Applied Microbiology and Biotechnology* 101(6), 2619-2627.

- Xu, S., Fu, B., Zhang, L. and Liu, H., 2015. Bioconversion of H₂/CO₂ by acetogen enriched cultures for acetate and ethanol production: the impact of pH. *World Journal of Microbiology and Biotechnology* 31 (6), 941–50.
- Yasin, N.H.M., Maeda, T., Hu, A., Yu, C.P. and Wood, T.K., 2015. CO₂ sequestration by methanogens in activated sludge for methane production. *Applied Energy*, 142, 426-434.
- Zhu, S., Wu, Y., Yu, Z., Zhang, X., Wang, C., Yu, F. and Jin, S., 2006. Production of ethanol from microwave-assisted alkali pretreated wheat straw. *Process Biochemistry* 41 (4), 869–73.
- Zhu, Z., Luan, G., Tan, X., Zhang, H. and Lu, X., 2017. Rescuing ethanol photosynthetic production of cyanobacteria in non-sterilized outdoor cultivations with a bicarbonate-based pH-rising strategy. *Biotechnology for Biofuels*, 10 (1), 93.

Chapter 4 Bioethanol production from H₂/CO₂ by solventogenesis using anaerobic granular sludge: effect of process parameters

A modified version of this chapter has been published as:

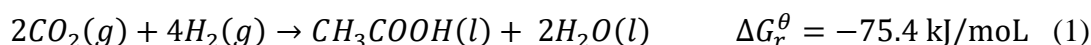
Yaxue He, Chiara Cassarini, and Piet N.L. Lens. 2021. Bioethanol production from H₂/CO₂ by solventogenesis using anaerobic granular sludge: effect of process parameters. **Frontiers in Microbiology**, 12, 647370.

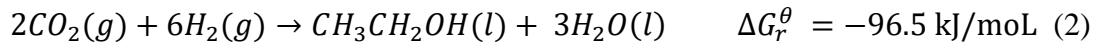
Abstract

CO₂ fermentation by biocatalysis is a promising route for the sustainable production of valuable chemicals and fuels, such as acetic acid and ethanol. Considering the important role of environmental parameters on fermentation processes, granular sludge from an industrial anaerobic wastewater treatment system was tested as inoculum for ethanol production from H₂/CO₂ at psychrophilic (18°C), submesophilic (25°C) and mesophilic (30°C) temperatures. The highest acetic acid and ethanol production was obtained at 25°C with a final concentration of 29.7 and 8.8 mM, respectively. The presence of bicarbonate enhanced acetic acid production 3.0 ~ 4.1-fold, while inhibiting ethanol production. The addition of 0.3 g/L glucose induced butyric acid production (3.7 mM), while 5.7 mM ethanol was produced at the end of the incubation at pH 4 with glucose. The addition of 10 μM W enhanced ethanol production up to 3.8 and 7.0-fold compared to, respectively, 2 μM W addition and the control. The addition of 2 μM Mo enhanced ethanol production up to 8.1-fold and 5.4-fold compared to, respectively, 10 μM Mo and the control. This study showed that ethanol production from H₂/CO₂ conversion using granular sludge as the inoculum can be optimized by selecting the operational temperature and by trace metal addition.

4.1 Introduction

The increasing demand for fuel energy and its gradual depletion renders the development of renewable energy necessary and emergent (Devarapalli and Atiyeh 2015). An innovative solution is to use C₁ gases (i.e., one carbon atom gases) as the substrate to produce valuable chemicals, e.g. volatile fatty acids (VFAs) as well as ethanol and butanol by microbes (Fernández-Naveira et al. 2017a, Sadhukhan et al. 2016). These C₁ compounds include carbon monoxide (CO), carbon dioxide (CO₂), methane (CH₄) and synthesis gas (CO/CO₂ and H₂ mixtures) produced from biomass and domestic/agricultural wastes. Besides, H₂ becomes available from the conversion of excess power produced by renewable energy sources, such as wind and solar power, which face challenges of balancing power production and demand. The generation of valuable chemicals and fuels from H₂/CO₂ and syngas (mainly containing CO, H₂ and CO₂) fermentation is economic and has sustainable advantages (Burk et al. 2014) compared to traditional corn (Mohammadi et al. 2011; Eisentraut 2010) or cellulosic material (Naik et al. 2010) fermentation. Moreover, ethanol has a higher energy density and easier storage and transportability than H₂ (Pereira 2013; Sarkar et al., 2017). Homoacetogenesis and solventogenesis from H₂/CO₂ occur according to reactions 1 and 2:





with ΔG_r^θ is the standard reaction Gibbs energy, $T = 298.15\text{K}$ and $P = 100\text{kPa}$

Granular sludge from Upflow Anaerobic Sludge Bed (UASB) wastewater treatment plants can be used as inoculum for VFAs (Dogan et al. 2005) and ethanol (Steinbusch et al. 2008) production. UASB sludge consists of mixed microbial communities and its full-scale applications have less contamination problems compared to pure cultures. Temperature is an important factor influencing fermentation, for example, mesophilic conditions are optimum for homoacetogen *Clostridium sp.* in syngas fermentation (Shen et al., 2017; Singla et al., 2014). Limited studies focus on psychrophilic or submesophilic conditions for alcohol production from C_1 gas or syngas by mixed cultures (Liu et al., 2018). Instead, substantial studies focused on mesophilic conditions despite submesophilic conditions are with merits of low energy consumption for high temperature control (Ramió-Pujol et al., 2015). Also the pH can significantly affect both biomass growth and the product formation rate. As the external pH begins to drop due to acid accumulation, an organism may begin to produce alcohols to prevent a further drop in pH (Padan et al. 1981; Cotter et al. 2009). Glucose addition to the medium can enhance alcohol production via overexpressing the ferredoxin-dependent aldehyde oxidoreductase (AOR) gene in *Clostridium carboxidivorans* (Cheng et al., 2019). AOR is involved in conversion of carboxylic acids into their corresponding alcohols without ATP consumption in acetogens such as *C. ljungdahlii* and *C. autoethanogenum* (Cheng et al., 2019; Liu et al. 2012). Besides, glucose offers extra carbon source and releases CO_2 during the glycolysis pathway, which can be re-assimilated via the Wood Ljungdahl pathway (WLP) with H_2 as electron donor and thus enhance the carbon conversion efficiency.

Acetic acid and ethanol are produced from CO_2 by acetogens via the Wood-Ljungdahl pathway (WLP) catalyzed by different enzymes (Fast and Papoutsakis 2012). Formate dehydrogenase (FDH) is one of the key enzymes in the WLP, converting CO_2 into acetyl-CoA and leading to the production of acetate. Acetate yields acetaldehyde catalyzed by ferredoxin aldehyde oxidoreductase (AOR). Then, ethanol is produced through the reduction of acetaldehyde by alcohol dehydrogenase (ADH) catalyzing the reduction of acetyl CoA to ethanol (Jiann-Shin 2010; Andreesen and Makdessi 2008). Several studies compared the effect of trace metal addition on ethanol production from syngas in pure cultures of *Clostridium ragsdalei* (Saxena and Ralph, 2011). The presence of W enhances ethanol production compared to the absence of W from carbon monoxide by anaerobic granular sludge (Chakraborty et al., 2020). Molybdate (Mo) is an analog of tungsten (W) and binds in the active

sites of some enzymes, such as AOR and ADH (Fernández-Naveira et al., 2017b). Other trace metals like zinc (Zn) and nickel (Ni) can stimulate alcohol production by enhancing the FDH and ADH synthesis and activity (Yamamoto et al. 1983).

Based on our previous study on the optimization of ethanol production from H₂/CO₂, the highest ethanol production was reached at 25°C compared to 37 and 55 °C by anaerobic granular sludge (He et al., 2020). This study further investigated homoacetogenesis and solventogenesis under submesophilic conditions, i.e., 18, 25 and 30 °C using CO₂ as carbon source and H₂ as sole electron donor by the same anaerobic granular sludge as used by He et al. (2020). Besides, the effects of pH, carbon source (HCO₃⁻ and glucose supplementation) and trace metals on ethanol production were also investigated.

4.2 Materials and methods

4.2.1 Biomass

The anaerobic granular sludge was obtained from a 200 m³ UASB reactor producing methane from dairy industry effluent at 20°C and a hydraulic retention time (HRT) of 9-12 h. The total solid (TS) and volatile solid (VS) content was 42.7 (± 1.0) g/L and 24.8 (± 0.5) g/L, respectively. The granular sludge was first centrifuged at 8000 g for 10 min to remove the supernatant and the pellet was heat-treated at 90 °C for 15 min to select for spore forming acetogens as described by Dessì et al. (2017).

4.2.2 Medium composition

Medium was prepared according to Stams et al. (1993) and modified as follows: 408 mg/L KH₂PO₄, 534 mg/L Na₂HPO₄·2H₂O, 300 mg/L NH₄Cl, 300 mg/L NaCl, 100 mg/L MgCl₂·6H₂O, 110 mg/L CaCl₂·2H₂O; 1 mL trace metal and 1 mL vitamin stock solution (Stams et al., 1993). 1 L medium (except for CaCl₂·2H₂O and vitamins) was prepared and brought to boiling in order to remove O₂, cooled down to room temperature under an oxygen-free N₂ flow, then CaCl₂·2H₂O and the vitamins were added as well as Na₂S (0.24 g/L) as reducing agent.

4.2.3 Experimental set-up

Batch tests were conducted in 125 mL serum bottles with 50 mL medium (gas: liquid ratio of 3:2) and granular sludge with an initial VS concentration of 1.0 g/L. The bottles were sealed with rubber inlets and capped with aluminum crimp caps. A H₂/CO₂ (v/v, 80/20) gas mixture was injected by a gas exchanger system (GW-6400-3111, Germany) to an initial pressure of

1.8 (\pm 0.15) bar (P_{H_2} =1.44 bar, P_{CO_2} = 0.36 bar), in which 124.4 mL of the gas mixture was compressed in the 75 mL headspace. Blank experiments were set up with a H_2/CO_2 (v/v, 80/20) headspace without the granular sludge as well as a N_2 (100%) headspace with the granular sludge (initial VS concentration 1.0 g/L). At the start of the experiments, the gas pressure was measured every 24 h. H_2/CO_2 was injected when the gas pressure was detected below 1 bar. All experiments were performed in triplicates.

4.2.4 Experimental design

In order to enhance the C/H ratio of the substrate and thus enhance the electron donor utilization efficiency considering the substrate C/H ratio is 1/4 lower than the theoretical utilization ratio (Eq. 1), 2.1 g/L $NaHCO_3$ (1.25 mmol carbon) was added in 50 ml medium to increase the CO_2/H_2 ratio to theoretically obtain a H_2/CO_2 ratio of 64/36 (v/v). 1 mL 1M HCl was also added to balance the pH increase by $NaHCO_3$ (He et al., 2020).

The first batch test was set up at different temperatures (18, 25 and 30°C) using H_2/CO_2 or H_2/CO_2 with HCO_3^- . The second batch test was performed at 25°C at different pH 7, 6 and 5 and 0.3 g/L glucose with initial pH of 6. 0.3g/L glucose + H_2/CO_2 , H_2/CO_2 with no glucose and 0.3 g/L glucose with no H_2/CO_2 were supplied again when they were totally consumed. The third batch test was set up with different trace metal concentrations, namely 2 μ M W (20 \times), 2 μ M Mo (20 \times), 10 μ M W (100 \times), 10 μ M Mo (100 \times), 10 μ M Ni (100 \times) and 50 μ M Zn (100 \times) compared with 0.1 μ M W, 0.1 μ M Mo, 0.1 μ M Ni and 0.5 μ M Zn in the control. Incubations with medium with no trace metals were set up as control experiments.

Headspace (1 mL) and liquid (1 mL) samples were withdrawn from each vial every 24 h to analyze the gas and liquid phase. Liquid samples were centrifuged at 8000 \times g for 5 min and the supernatant was filtered with a syringe using a 0.22 μ m PTFE-filter prior to analyzing ethanol and acetic acid concentrations.

4.2.5 Analytical methods

4.2.5.1 Gas-phase analysis

H_2 , CO_2 and CH_4 concentrations were measured using a HP 6890 gas chromatograph (GC, Agilent Technologies, USA) equipped with a thermal conductivity detector (TCD). The GC was fitted with a 15-m HP-PLOT Molecular Sieve 5A column (ID 0.53 mm, film thickness 50 μ m). The oven temperature was kept constant at 60 °C. The temperature of the injection port and the detector were maintained constant at 250 °C. Helium was used as the carrier gas. Standard gas mixtures of CH_4 , H_2 and CO_2 were measured every time along with the sample measurements.

4.2.5.2 VFAs and alcohols analysis

VFA and alcohol concentrations were analyzed for each bottle from the liquid samples (1 mL) using high performance liquid chromatography (Agilent Co., USA) equipped with a refractive index detector (RID) and an Agilent Hi-Plex H column (Internal diameter \times length, 7.7 \times 300 mm, size 8 μ m). A H₂SO₄ solution (5 mM) was used as mobile phase at a flow rate of 0.7 ml/min and with a sample injection volume of 50 μ l. The column temperature was set at 60°C and the RID detector at 55 °C. Total solid (TS) and volatile solid (VS) were measured according to standard methods (EPA, 2001). Calibration curves from 0.5 to 100 mM acetic acid, ethanol and butyric acid were made. The carbon (C) and electron (e⁻) recoveries were calculated according to our previous study (He et al., 2020).

4.3 Results

4.3.1 Effect of initial pH on H₂/CO₂ bioconversion at 25°C

The highest ethanol production was 2.5, 3.6 and 1.7 mM at initial pH of 7, 6 and 5, respectively (Table 4.1). The highest ethanol concentration was reached at an initial pH of 6, while the highest acetic acid concentration at pH 7 (Fig. 4.1A, B, Table 4.1). A neutral initial pH enhanced the acetic acid production, but this may not be the best condition for ethanol production (Fig. 4.1A). The pH decreased along with time: after 168 h of fermentation all pH values had decreased below 5 (Fig. 4.1D). Ethanol production was detected at 120 h for the batches with initial pH of 7 and 6, while for pH 5, ethanol was observed at 360 h (Fig. 4.1). It was noted that at initial pH 5, the acetic acid concentration reached 7.4 mM at 120 h, similar for the batch experiment at pH 6 with an acetic acid concentration of 9.0 mM, but ethanol production was not observed (Fig. 4.1B, C). The C and e⁻ recovery were, respectively, 123.6% and 123.1% at pH 5, 151.8% and 137.1% at pH 6, 112.6% and 116.0% at pH 7 (Table 4.1). A small amount of acetic acid (data not shown) production was detected in the control bottles without H₂/CO₂ (with 100% N₂) (Table 4.1).

4.3.2 Effect of temperature on H₂/CO₂ fermentation by granular sludge

Acetic acid was the main fermentation product with the highest acetic acid concentration of 6.5 (\pm 2.6), 29.7 (\pm 3.3) and 27.0 (\pm 2.4) mM at 18°C, 25°C and 30°C, respectively (Table 4.2). The pH decreased along with the acetic acid accumulation from initially pH 6 to 5.0, 4.4 and 4.4 at 18°C, 25°C and 30°C (Fig. 4.2B), respectively. The highest ethanol concentration of 8.8 mM was obtained at 25°C with the highest average production rate of 0.03 mmol L⁻¹ h⁻¹ (Table 4.2). Ethanol started to be produced when acetic acid was more than 16.3 mM and 21.6

mM and the pH was lower than 4.9 at 25°C and 4.7 at 30°C, respectively (Fig. 4.2A). The highest ethanol production rate was 0.11 mmol·L⁻¹·h⁻¹ after 140 h of incubation at 30°C, while the highest acetic acid production rate was 0.32 mmol·L⁻¹·h⁻¹ after 120 h of incubation at 25°C (Fig. 4.3, Table 4.2).

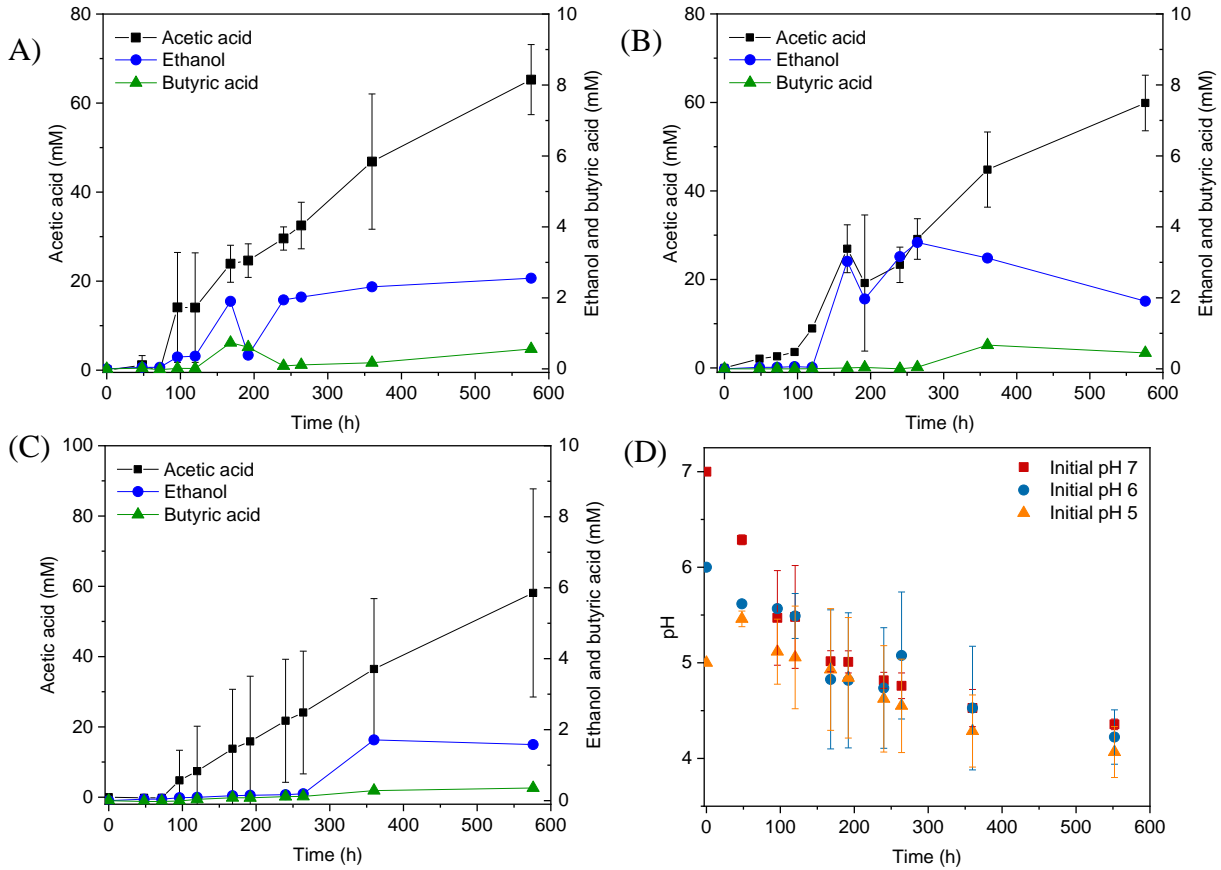


Fig. 4.1 Acetic acid and ethanol production from H₂/CO₂ by heat-treated granular sludge at 25°C at (A) pH 7, (B) pH 6, (C) pH 5 and (D) change of pH over time.

The mesophilic (30°C) or psychrophilic (18°C) temperatures with an initial incubation pH of 6.0 negatively affected the ethanol production. The highest C and e⁻ recovery obtained at 25°C were 120.4 (± 36.9) % and 82.3 (± 31.0) %, respectively (Table 4.2). The acetic acid concentration after 72 h of incubation varied at 0.8, 2.7 and 11.2 mM in the 18, 25 and 30°C incubations, respectively (Fig. 4.2A), which demonstrated that higher temperatures reduced the lag phase of the acetic acid production. The average acetic acid and ethanol production rate were much lower at 18°C than at 25°C or 30°C (Table 4.2). At 30°C, the C and e⁻ recovery were 88.5 (± 20.0) % and 75.5 (± 20.0) %, respectively, which were both lower than at 25°C. The lowest C and e⁻ recovery of 25.5 (± 10.2) % and 20.5 (± 8.2) %, respectively, were observed at 18°C (Table 4.2).

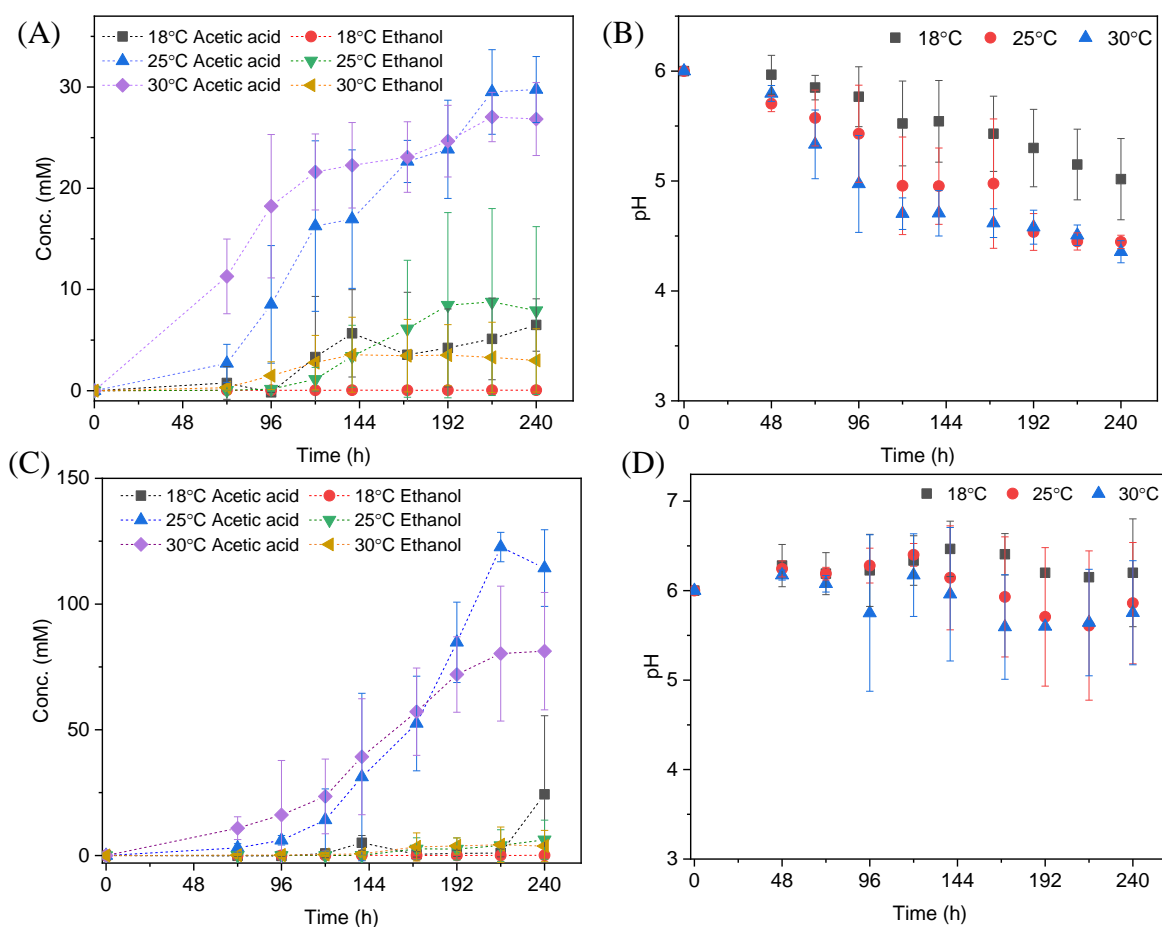


Fig. 4.2 Acetic acid and ethanol yield and pH change using (A) and (B) H_2/CO_2 ; (C) and (D) $H_2/CO_2 + HCO_3^-$ by heat-treated granular sludge at 18, 25, 30 °C. Every point shown in the graphs is calculated as the average of three independent batch cultures, error bars indicate the standard deviation of the triplicates.

Upon the addition of HCO_3^- , the acetic acid production was highly enhanced at 25°C and 30°C, while the ethanol production was below 4 mM (Fig. 4.2C). Up to 122.7 (\pm 5.8) mM acetic acid was obtained, which was 4.1-fold more than the highest acetic acid concentration (29.7 ± 3.3 mM) without HCO_3^- addition at 25°C (Table 4.2). Similarly, the highest acetic acid concentration with HCO_3^- was 3.0-fold higher than without HCO_3^- at 30°C (Table 4.2). The highest acetic acid production rate amounted to 0.97, 0.79 and 1.58 $mmol \cdot L^{-1} \cdot h^{-1}$ at 18°C, 25°C and 30°C, respectively, which are all higher than in the absence of HCO_3^- (Fig. 4.3B, Table 4.2). The pH increased initially from 6 to 6.2 at 120 h at 18, 25 and 30°C. At the end of the incubation, the pH varied between 6.2 to 6.5 at 18°C, decreased to 5.6 at 25°C and 5.3 at 30°C (Fig. 4.2D). Overall, the pH kept stable between 5.2 to 6, although the acetic acid concentration was much higher than in the absence of HCO_3^- (Fig. 4.2D).

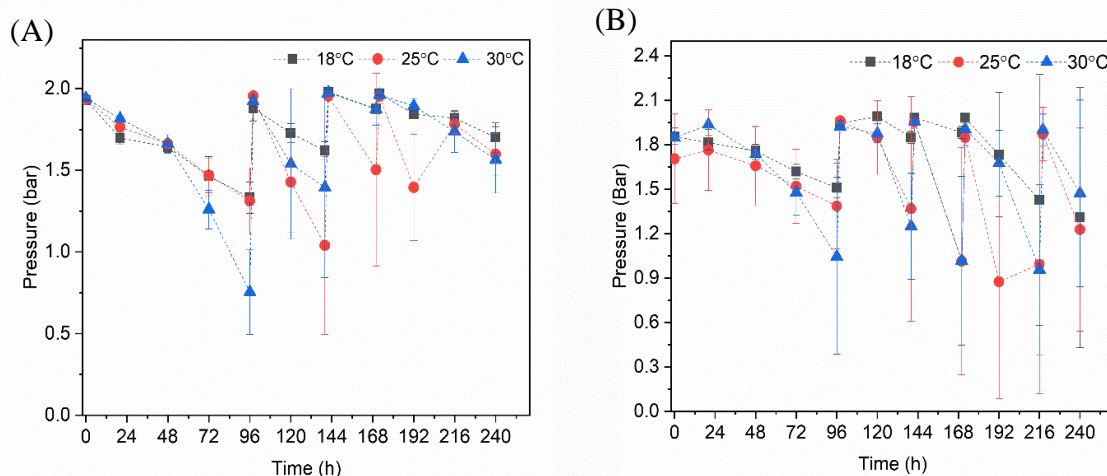


Fig. 4.3 Gas pressure using (A) H_2/CO_2 , (B) H_2/CO_2 with HCO_3^- by heat-treated granular sludge at 18, 25, 30 °C. Every point shown in the graphs is calculated as the average of three independent batch cultures, error bars indicate the standard deviation of the triplicates.

4.3.3 Effect of glucose on H_2/CO_2 bioconversion at 25°C

The fermentation process using solely H_2/CO_2 could be separated in four stages (Fig. 4.4): stage I (0-120 h) is the acetic acid accumulation phase, stage II (120-192 h) and III (192-264 h) represent, respectively, the quick acetic acid production and butyric acid accumulation, whereas ethanol was produced in stage IV (264-552 h). In stage I, when using glucose + H_2/CO_2 as the substrate, acetic acid was not detected after 48 h of incubation, then 16.5 mM acetic acid and 0.45 mM butyric acid were observed at 120 h. Thereafter, acetic acid production rate reached its maximum ($0.32 \text{ mmol} \cdot \text{L}^{-1} \cdot \text{h}^{-1}$) at 168 h in stage II (Fig. 4.4A). The acetic acid concentration kept relatively stable during stage III, during which the butyric acid concentration started to increase (from 0.5 to 3.3 mM) (Fig. 4.4A). Ethanol started to increase during stage IV and reached $5.7 (\pm 2.4)$ mM when the pH decreased below 4 (Fig. 4.4A, D).

When using glucose as the sole substrate, the acetic acid concentration reached 7.9 mM at 48 h. The highest acetic acid concentration reached 14.8 mM after 360 h of incubation. The highest butyric acid (3.3 mM) and ethanol (0.6 mM) concentrations were obtained at 360 h (Fig. 4.1C, Table 4.1). The distinct change when adding glucose was the quick decrease in pH from initially 6 to 4.8 after 48 h of incubation (Fig. 4.4D). During stage II and III, the pH decreased quickly to below 4 for the batches with both glucose and H_2/CO_2 and to 4.5 for the glucose only batches (Fig. 4.4D). Compared to the H_2/CO_2 solely incubation (Fig. 4.4B), the addition of glucose enhanced the butyric acid production. The C and e^- recovery were,

respectively, 89.1% and 99.6% in the batches with glucose, compared to 89.0% and 80.4% for glucose + H₂/CO₂ (Table 4.1).

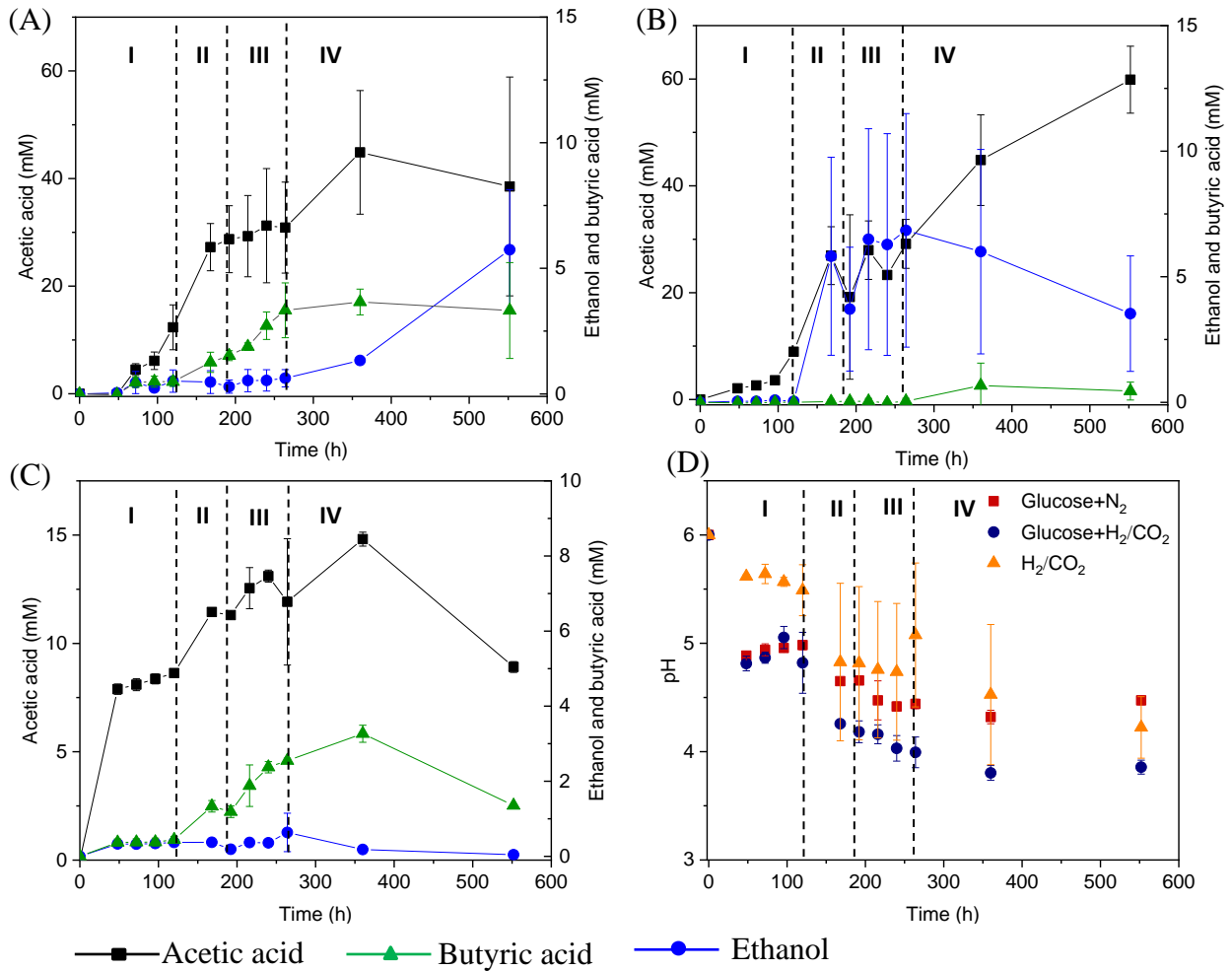


Fig. 4.4 Acetic acid, ethanol and butyric acid production by heated-treated granular sludge at 25°C using (A) glucose+H₂/CO₂, (B) H₂/CO₂ and (C) glucose as the substrate and (D) change of pH. The dashed vertical lines represent the different phases in the fermentation process; I: 0-120 h, II: 120-192 h, III: 192-264 h, IV: 264-552 h.

Table 4.1 Effect of pH, carbon supplements and trace metals on the maximum acetic acid and ethanol concentrations and H₂ and CO₂ consumption from H₂/CO₂ by heat-treated anaerobic granular sludge (at the end of incubation).

Conditions	Products (mM)						H ₂ consumption (%)	CO ₂ consumption (%)	C recovery (%)	e ⁻ recovery (%)
	Acetic acid	Butyric acid	Ethanol	CO ₂	H ₂	CH ₄				
pH 7	65.3 ± 7.9	0.6±0.2	2.6 ± 3.1	-46.9 ^a	-96.7 ^a	0	35.5	69.0	123.6	123.1
pH 6	59.9 ± 6.3	0.7±0.2	8.5 ± 3.1	-38.0 ^a	-86.1 ^a	0	31.5	55.7	151.8	137.1
pH 5	58.1 ± 29.6	0.4±0.3	1.7 ± 2.7	-40.3 ^a	-81.7 ^a	0	29.4	58.0	112.6	116.0
Glucose	14.8 ± 0.3	3.3±0.2	0.6 ± 0.5	-- ^b	-- ^b	0	-- ^b	-- ^b	89.1	99.6
Glucose+H ₂ /CO ₂	44.9 ± 11.5	3.7±0.5	5.7 ± 2.4	-39.3 ^a	-104.9 ^a	0	37.5	56.2	89.0	80.4
Control	38.4 ± 15.8	0	7.6 ± 4.3	-42.7 ^a	-80.8 ^a	0	26.8	56.5	141.2 ± 26.2	176.5 ± 20.2
2 μM W	33.3 ± 13.8	0	3.9 ± 2.6	-36.9 ^a	-81.5 ^a	0	26.6	48.2	130.0 ± 18.7	145.6 ± 52.8
10 μM W	53.0 ± 4.4	0	14.8 ± 10.2	-48.5 ^a	-107.1 ^a	0	34.9	63.3	153.0 ± 20.0	172.7 ± 22.8
2 μM Mo	40.2 ± 16.0	0	11.3 ± 2.1	-47.2 ^a	-91.7 ^a	0	31.5	64.6	141.9 ± 25.1	178.4 ± 32.8
10 μM Mo	66.9 ± 11.0	0	1.4 ± 1.1	-51.0 ^a	-95.5 ^a	0	31.2	66.7	174.9 ± 15.8	204.1 ± 9.8
10 μM Ni	42.7 ± 6.9	0	3.7 ± 2.2	-40.3 ^a	-70.9 ^a	0	23.2	52.8	150.5 ± 13.5	197.1 ± 20.9
50 μM Zn	28.5 ± 7.7	0	3.3 ± 2.3	-34.0 ^a	-47.9 ^a	0	16.6	47.4	122.6 ± 12.0	203.5 ± 30.0

a Negative values indicate an overall consumption of component during the experiment

b data not known since carbon is excess

Table 4.2 Effect of HCO_3^- on the maximum acetic acid and ethanol concentration from H_2/CO_2 by heat-treated anaerobic granular sludge at initial pH 6

System conditions	Substrate					
	H_2/CO_2			$\text{H}_2/\text{CO}_2+\text{HCO}_3^-$		
	18°C	25°C	30°C	18°C	25°C	30°C
Products (mM)						
Acetic acid	6.5±2.6	29.7±3.3	27.0±2.4	24.3±31.2	122.7±5.8	81.3±23.3
Ethanol	0.1	8.7±9.2	3.6±3.7	0.1	6.3±7.8	4.3±7.0
CO ₂	29.3	35.8	38.5	--	--	--
H ₂	73.3	115.6	95.0	--	--	--
Undissociated acid	--	22±0.1	19±3.2	--	36±7.5	16±12.5
H ₂ consumption (%)	26.4	41.7	34.0	--	--	--
CO ₂ consumption (%)	42.3	51.6	55.3	--	--	--
C recovery (%) ^a	25.5±10.2	120.4±36.9	88.5±20.0	--	--	--
e ⁻ recovery (%) ^b	20.5±8.2	82.3±31.0	75.5±20.0	--	--	--
Highest rate (mmol·L⁻¹·h⁻¹)						
H ₂ consumption	0.455	1.160	0.492	--	--	--
CO ₂ consumption	0.188	0.411	0.229	--	--	--
CH ₄	0	0	0	0	0	0
Acetic acid	0.145	0.32	0.289	0.97	0.79	1.58
Ethanol	0.00	0.11	0.05	0.00	0.09	0.10

^a carbon recovery; ^b electron recovery

4.3.4 Effect of trace metals (W, Mo, Zn, Ni) on H₂/CO₂ fermentation at 25°C

Upon the addition of 2 and 10 μM W, acetic acid production constantly increased to the highest concentration of 33.3 (\pm 13.8) and 53.0 (\pm 4.4) mM, respectively (Fig. 4.5A). Ethanol kept increasing after 120 h with the addition of 10 μM W and reached 14.8 (\pm 10.2) mM (Fig. 4.5A). The addition of 10 μM W also reached the highest mole ratio of ethanol to acetic acid of 0.48 at 263 h and 0.28 at the end of the incubation (Fig. 4.6). With the addition of 2 μM W, ethanol increased to 3.2 mM then kept relatively stable till 3.9 (\pm 2.6) mM at the end of the incubation (Fig. 4.5A). The addition of 2 μM W reached the highest mole ratio of ethanol to acetic acid of 0.26 at 131 h and 0.12 at the end of the incubation (Fig. 4.6). The addition of 10 μM W enhanced ethanol production up to 3.8 and 7.0 fold than with, respectively, 2 μM W and the control. Upon the addition of 2 and 10 μM W, H₂ consumption was, respectively, 81.5 (\pm 32.5) and 107.1 (\pm 50.5) mM (Fig. 4.7A), which are both higher than in the absence of trace metals (80.8 \pm 14.0 mM, Fig. 4.7A). The addition of 10 μM W to the medium enhanced the ethanol production with the highest ethanol to acetic acid ratio of 0.48.

Upon addition of 2 and 10 μM Mo, the acetic acid concentration constantly increased to the highest value of 40.2 (\pm 16.0) and 66.9 (\pm 11.4) mM, respectively (Fig. 4.5B). Ethanol kept increasing with the addition of 2 μM Mo and reached 11.3 (\pm 2.1) mM at the end of the incubation (Fig. 4.5B). However, ethanol was not significantly produced, with the maximum concentration of 1.4 (\pm 1.1) mM with 10 μM Mo. The addition of 2 μM Mo enhanced ethanol production up to 8.1 and 5.4-fold, respectively, compared to 10 μM Mo and the control. The acetic acid production with the addition of 2 and 10 μM Mo was, respectively, 6.7 mM and 5.6 mM at 120 h, which was lower than the 11.7 mM produced by the control (Fig. 4.5B). The acetic acid concentration increased quickly to a higher acetic acid concentration with 10 μM Mo compared to with 2 μM Mo and the control after 120 h. The pH decreased along with the accumulation of acetic acid (Fig. 4.5E). The addition of 2 μM Mo reached the highest ethanol to acetic acid ratio of 0.28, while the ratio was 0.02 for 10 μM Mo addition at the end of the incubation (Fig. 4.6).

With the addition of 10 μM Ni, the highest acetic acid and ethanol concentration amounted to, respectively, 42.7 (\pm 6.9) mM and 3.7 (\pm 2.2) mM (Fig. 4.5C). The highest acetic acid and ethanol concentration with the addition of 50 μM Zn were 28.5 (\pm 7.7) mM and 3.3 (\pm 2.3) mM, respectively. Either 10 μM Ni or 50 μM Zn did not significantly enhance the ethanol production.

The presence of 50 μM Zn inhibited the acetic acid production compared to the control (Fig. 4.5C).

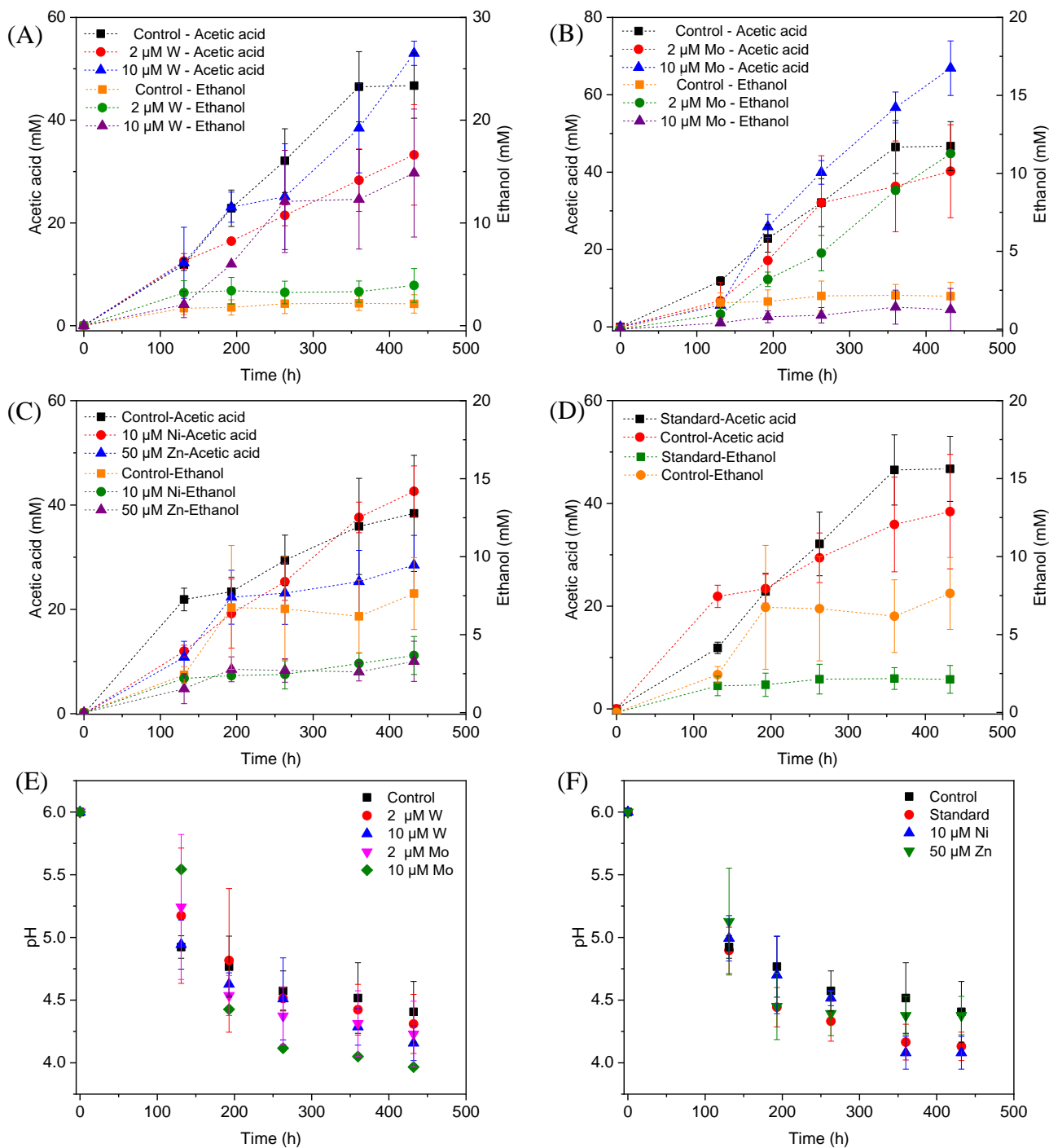


Fig. 4.5 Acetic acid and ethanol production by heat-treated granular sludge using H_2/CO_2 as the substrate at 25°C with the addition of (A) 2 μM , 10 μM W, (B) 2 μM , 10 μM Mo, (C) 10 μM Ni, 50 μM Zn, (D) No trace metals and (E) and (F) change of pH.

Surprisingly, the ethanol concentration in the incubation without trace metal supplementation is higher than with the control (Fig. 4.5D). The highest acetic acid and ethanol

concentration reached $46.7 (\pm 8.3)$ and $2.1 (\pm 1.9)$ mM, respectively, in the control. With no trace metals addition, ethanol started to be produced after 131 h and quickly increased to 6.7 mM, and then slightly increased to 7.6 mM at the end of the incubation. Ethanol production started at 131 h with a concentration of 1.7 mM, and then kept stable till the end of the incubation (2.1 mM) in the control (Fig. 4.5D).

Overall, the acetic acid production was enhanced by the addition of 10 μM Mo, followed by 10 μM W and 2 μM Mo, whereas the presence of 50 μM Zn, 2 μM W, 10 μM Ni or the absence of trace metals inhibited acetic acid production compared to the control (Fig. 4.5). The ethanol production was the highest in the presence of 10 μM W, followed by 2 μM Mo, while the absence of trace metals reached a higher ethanol production than the 10 μM Ni, 10 μM Mo, 2 μM W, 50 μM Zn and control incubation (Fig. 4.5).

The decrease in pH corresponded to the accumulation of acetic acid. In the presence of 10 μM Mo, the pH reached the lowest value at the end of the incubation and the acetic acid concentration reached the highest compared to 2 μM and the control (Fig. 4.5e). Ethanol production started after 120 h; the pH varied from 4.75 to 5.5 (Fig. 4.5E). In the presence of 2 μM Mo and 10 μM W, ethanol production was enhanced even though the pH dropped to 4.2 (Fig. 4.5E). The cumulative H_2 uptake in all media was between 211.7 and 245.3 mM. The cumulative CO_2 uptake with different trace metal concentrations was between 61.4 and 68.7 mM (Fig. 4.7).

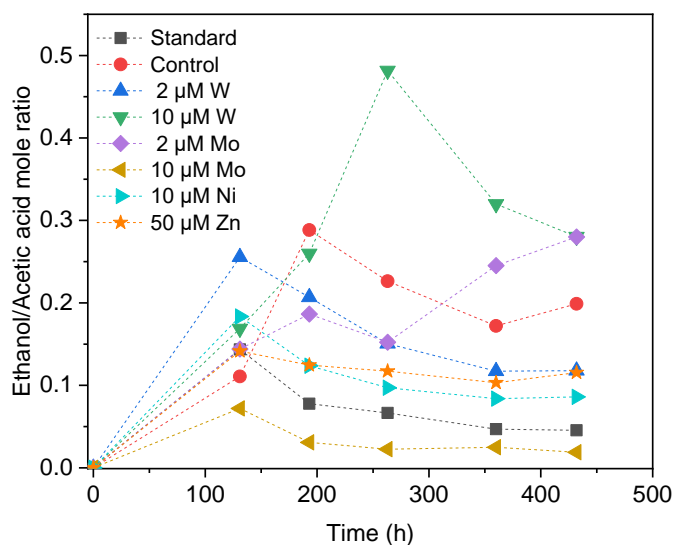


Fig. 4.6 The mole ratio of ethanol to acetic acid by heat-treated granular sludge using H_2/CO_2 as the substrate at 25°C with the standard medium, control and addition of 2 μM , 10 μM W, 2 μM , 10 μM Mo, 10 μM Ni and 50 μM Zn

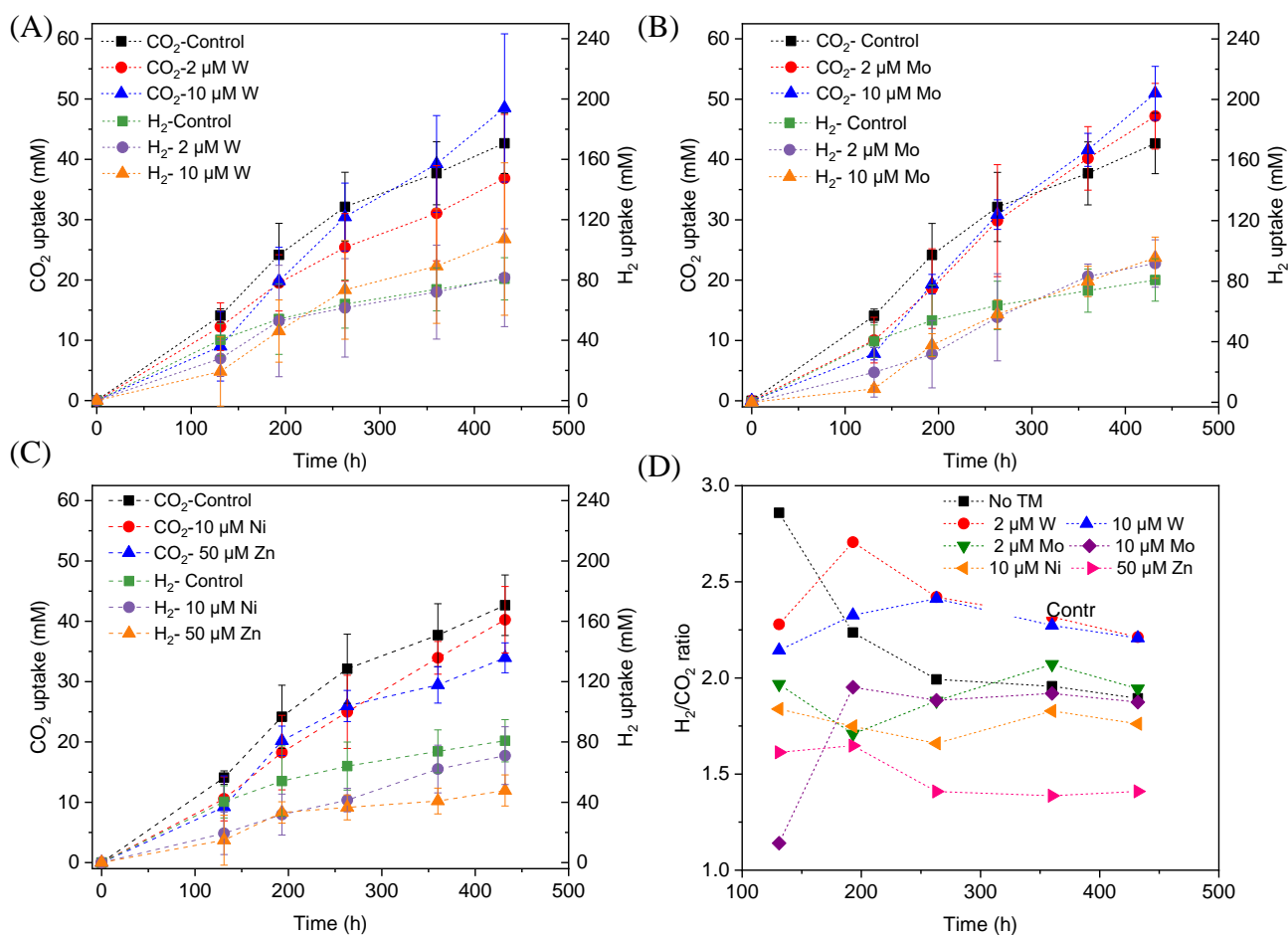


Fig. 4.7 H_2 and CO_2 uptake with the addition of (A) 2 μM , 10 μM Mo, (B) 2 μM , 10 μM W, (C) 10 μM Ni, 50 μM Zn and (D) H_2/CO_2 uptake ratio by heat-treated granular sludge using H_2/CO_2 as the substrate at 25°C with initial pH 6.

4.4 Discussion

4.4.1 Effect of temperature and pH on solventogenesis

This study showed that the highest ethanol concentration was produced at an initial pH of 6 at 25°C in the H_2/CO_2 incubations. An initial pH of 6 favored the ethanol production compared to pH 7 and 5 from H_2/CO_2 by granular sludge (Fig. 4.1). Ethanol production via solventogenesis is linked to the accumulation of undissociated acetic acid and pH (Richter et al. 2016). Solventogenesis occurs when the pH decreases to 4.5 to 5 and the undissociated acetic acid is able to cross the cytoplasmic membrane by diffusion: alcohol formation then avoids cell damage or death by the protons that would be released by dissociated acetic and butyric acids (Baronofsky et al., 1985; Jones and Woods 1986; Richter et al. 2016). It should be noted that a low pH can stimulate ethanol production, however, incubations conducted with initial pH 5 did not reach higher ethanol concentrations than the incubation with initial pH 6.

Table 4.3 H₂, CO₂ and CH₄ concentration at initial pH 5, 6 and 7 by heated-treated granular sludge using H₂/CO₂ as the substrate at 18, 25 and 30°C.

Temperature	Time/h	H ₂ mmol average	H ₂ mM	Stdev	CO ₂ mmol average	CO ₂ mM	Stdev
25°C	96	2.92	41.75	0.00	0.69	9.88	0.00
	140	2.27	32.38	0.00	0.60	8.55	0.00
	170	2.52	35.94	14.98	0.37	5.35	4.20
	240	3.60	51.45	4.95	0.68	9.74	1.73
30°C	96	1.98	28.30	0.00	0.09	1.36	0.00
	140	3.35	47.79	0.00	0.50	7.10	0.00
	170	3.91	55.81	1.14	0.80	11.38	0.26
	240	3.64	52.01	7.72	0.79	11.32	1.94
18°C	96	3.12	44.54	0.00	0.45	6.48	0.00
	140	3.66	52.28	0.00	0.69	9.85	0.00
	170	4.00	57.09	2.77	0.84	12.05	1.03
	240	3.50	49.94	2.10	0.81	11.61	0.75

This could be because pH 6 facilitated cell growth and reached higher acetic acid concentrations than at pH 5 (Fig. 4.1). Considering the acetic acid concentration of pH 5 and 6 were lower than the pH value that induces an ‘acid crash’ (Mohammadi et al., 2011), the higher acetic acid concentration at pH 6 may obtain a higher ethanol production than at pH 5. Besides, fermentation at an initial pH 5 may have provided an unfavorable environment for cell growth, since the growth pH for the known autotrophic *Clostridium sp.* ranges from pH 5 to 7 (Fernández-Naveira et al., 2017a). Kundiya et al. (2011) studied the ethanol production by *C. ragsdalei* from 10 g corn steep liquor purged daily with syngas (5% H₂, 15% CO₂, 20% CO) with initial incubation at pH 7, 6 and 5 at 32, 37 and 42°C. Without a buffer, their experiment at initial pH 5 produced less ethanol than at pH 7 and 6 at 32°C (Kundiya et al., 2011).

With an initial pH of 6, submesophilic temperatures (25°C) enhanced ethanol production from H₂/CO₂ by granular sludge in this study (Fig. 4.2). The growth temperature of most acetogens ranges from 20 to 42°C, with the optimum at 37°C (Naik et al. 2010; Munasinghe and Khanal 2010). Fermentation at 25°C, which is below the optimum temperature, might slow down microbial metabolism and hence avoid the ‘acid crash’ phenomenon. Solventogenesis is negatively affected or even terminated by a sharp increase of undissociated acids, a so called ‘acid crash’ (Ramió-Pujol et al. 2015). Such an acid crash can be mitigated by slowing down the microbial metabolism, e.g., by lowering the temperature, thus reducing the acid accumulation rates. Similarly, 10 g corn steep liquor and syngas (5% H₂, 15% CO₂, 20% CO) were fermented by *C. ragsdalei* at 32°C, 37°C and 42°C and 1.89 g/L of ethanol was obtained at 32°C, which is 2.7 fold higher than at 37°C (0.69 g/L) with an initial incubation pH of 6.0 (Kundiya et al., 2011). The temperature of 18°C is lower than the reported growth temperatures for most of acetogens (Mohammadi et al., 2011), which likely caused the lower

acetic acid production than at 25 and 37°C. Our previous tests demonstrated the *Clostridium* genus was successfully enriched under mesophilic and submesophilic conditions using the same inoculum (He et al., 2020). Chakraborty et al. (2020) demonstrated enhanced ethanol production from C₁ gas by granular sludge and *Clostridium autoethanogenum* was successfully enriched at 33°C. Similarly, Samanides et al. (2020) reported an increased relative abundance of *Clostridium* of 65.9% in anaerobic granular sludge for acetic acid production, when first exposed to heat (95°C for 30 min) and incubated with 100% CO₂ and 100 g/L zero valent iron at 33°C.

The higher C recovery in acetic acid and ethanol production from CO₂ (Table 4.1) can be attributed to the fact that granular sludge used as inoculum contains a certain amount of calcium carbonate precipitates. Calcium carbonate can precipitate both in the core and on the surface of granular sludge and the surface part of the calcium carbonate precipitates contributes to the aggregation of the granules (Yang et al., 2010). UASB sludge can reach a calcium carbonate content of up to 90% of the ash content in anaerobic wastewater treatment systems (Van Langerak et al. 1998). The high C recovery is in accordance with our previous results using the same UASB sludge (He et al., 2020). The carbon released from the calcium carbonate precipitates results in a positive carbon balance.

Methane was not observed during the whole incubation (Table 4.3), which was attributed to the heat-pretreatment and initial pH of 6. Similarly, Modestra et al. (2020) reported that both heat and acid treatment of granular sludge inhibited methane production and enriched for homoacetogenic bacteria when using gaseous substrate H₂/CO₂.

4.4.2 Effect of organic and inorganic carbon source on solventogenesis

Upon HCO₃⁻ addition to increase the C/H ratio, acetic acid production by granular sludge from H₂/CO₂ was enhanced at 18°C, 25°C and 30°C, but not ethanol production. The failure of enhanced ethanol production could be due to the higher pH caused by the HCO₃⁻ buffering capacity. Ethanol production is triggered at low pH, for instance, 4.5-5 (Ganigué et al., 2016). However, the additional HCO₃⁻ acts as a buffer and prevents the pH decreasing sharply. The high acetic acid and lower ethanol production might thus be attributed to the higher pH: 5.2 and 6 for, respectively, without and with HCO₃⁻ addition than without HCO₃⁻ addition (Fig. 4.2D). On the other hand, HCO₃⁻ offered extract carbon and increased the acetic acid production. Maddox et al. (2000) reported undissociated acid formation above 57-60 mM induced an 'acid crash'. However, the highest undissociated acetic acid concentrations obtained in this study were 36 and 16 mM at 25 and 30°C, respectively (Table 4.2), thus lower than the

reported value at which an acid crash occurs. Upon the addition of HCO_3^- , the *Clostridium* genus had a similar relative abundance compared to without HCO_3^- addition at 25°C from the same inoculum (He et al., 2020).

Glucose enhances the growth of *C. autoethanogenum* and *C. carboxidivorans* (Fernández-Naveira 2017a; Cheng et al., 2019). Addition of 0.3 g/L glucose in H_2/CO_2 gaseous substrate mainly increased the acetic and butyric acid concentration, while the ethanol concentration was a bit decreased (Table 4.1). The inhibited ethanol production can be attributed to the different conversion pathway of the organic substrate glucose (such as glycolysis) and the inorganic substrate H_2/CO_2 . Marcellin et al. (2016) investigated the energy metabolism of a model acetogen *C. autoethanogenum* showing that during heterotrophic growth, cells relied mainly on the Embden–Meyerhof–Parnas (EMP) glycolysis pathway, whereas under autotrophic conditions exclusively the WLP pathway is used. The energy yield (ATP and redox state) is, however, unaffected between heterotrophic and autotrophic growth. Fernandez et al. (2017) investigated the glucose (30 g/L) bioconversion profile at constant pH 6.2 and 5.2 by *Clostridium carboxidivorans*. Acetic acid was formed as the first metabolite and butyric acid appeared a few hours later and kept increasing, while ethanol was produced during the acidification stage at pH 6.2. Fernandez et al. (2017) also found that the glucose consumption stopped after 72 h at pH 5.2. In this study, when the pH dropped to below 4 during stage IV (Fig. 4.4D), increasing concentrations of acetic acid, butyric acid and ethanol were observed (Fig. 4.4A). It should be noted that a small amount of ethanol was produced at a pH value as low as 4 by the granular sludge used in this study (Fig. 4.4A), which is seldom reported before. This might be due to the presence of both heterotrophic and autotrophic acetogens that convert glucose and produce ethanol in the enriched sludge.

4.4.3 Enhanced ethanol production by trace metal addition

Ethanol production from H_2/CO_2 by granular sludge was enhanced by the addition of 2 μM Mo or 10 μM W, while the addition of 10 μM Mo, 2 μM W, 10 μM Ni, and 50 μM Zn did not significantly affect the ethanol production. There are only few studies on the effect of trace metals on ethanol production by mixed cultures compared to studies using pure cultures. Saxena and Tanner (2011) increased the SeO_4^{2-} and WO_4^{2-} concentration to 5.3 and 6.8 μM , respectively, which resulted in an increased ethanol production from synthesis gas by *Clostridium ragsdalei* from 35.73 mM under standard metal concentrations to 54.4 and 72.3 mM, respectively, upon SeO_4^{2-} and WO_4^{2-} addition. They also observed that ethanol production decreased to 23.64 mM at higher concentrations of Mo (8.3 μM). The highest mole

ratio of ethanol to acetic acid of 0.48 with 10 μM W is in accordance with the highest ethanol production in this study (Fig. 4.6). Abubackar et al. (2015) investigated the carbon monoxide fermentation by *Clostridium autoethanogenum* and obtained the highest ethanol to acetic acid ratio of 0.19 in experiments with 0.75 μM W.

Saxena and Tanner (2011) found that ethanol production from synthesis gas by *C. ragsdalei* decreased to 22.02 and 1.55 mM when Fe, Co, Mo and W were eliminated from the medium. This study, however, showed that without trace metals, the ethanol production was enhanced compared to the control. Nutrient-stress conditions such as lack of trace elements may also stimulate the shift from acetic acid to ethanol. Richter et al. (2016) performed proteomic and metabolomic analyses on a two-stage syngas fermentation (*Clostridium ljungdahlii*) system and did not find a difference in the abundance of enzymes of the central metabolic pathways, concluding that nutrient limitation and the resulting growth limitation redirect reducing equivalents toward ethanol production. The H_2 to CO_2 consumption ratio varies between 2.1 and 2.5 (Fig. 4.7D) and thus conform the production of a mixture of acetic acid and ethanol (Eq. 1, 2, Table 4.1). The trace metals affected the enzymes such as FDH, AOR and ADH to catalyze acetic acid and ethanol production and thus strengthen the homoacetogens, such as the *Clostridium* genus as reported by He et al. (2020). The W-containing AOR enzyme has been reported in *Clostridium thermoaceticum* (Strobl et al., 1992). Besides, W can serve as a potential acting element for CO_2 reduction FDHs, W even becomes an essential element for nearly all enzymes of the AOR family (Fernández-Naveira et al. 2019). This study reported lower ethanol production with Mo than W, despite the close chemical similarities between Mo and W. However, it has been demonstrated that W, different than Mo, can be selectively transported into some prokaryotic cells by two ABC-type transporters that contain the binding protein TupA or WtpA (Andreesen and Makdessi 2008).

4.5 Conclusion

The optimum conditions for ethanol production by anaerobic granular sludge using H_2/CO_2 as the substrate were 25°C and an initial pH of 6. An initial pH of 7 enhanced acetic acid production, while an initial pH of 5 totally inhibited ethanol production. The use of glucose and CO_2 as co-substrate enhanced butyric acid production (3.3 mM), while ethanol production occurred at a pH as low as 4. The presence of 10 μM W and 2 μM Mo enhanced the ethanol production by 7.0 and 5.4-fold, respectively.

4.6 References

Abubackar H.N., María C. Veiga, Kennes C., (2015). Carbon monoxide fermentation to ethanol by *Clostridium autoethanogenum* in a bioreactor with no accumulation of acetic acid. *Bioresource Technology*, 186:122-127.

Andreesen, J. R., and Makdessi, K., (2008). Tungsten, the surprisingly positively acting heavy metal element for prokaryotes. *Annals of the New York Academy of Sciences* 1125 (1): 215–29.

Bajón Fernández, Y, Soares, A., Koch, K., Vale, P., and Cartmell, E., (2017). bioconversion of carbon dioxide in anaerobic digesters for on-site carbon capture and biogas enhancement—a review. *Critical Reviews in Environmental Science and Technology* 47 (17): 1555–80.

Baronofsky, J. J., Schreurs, W. J. A., and Kashket, E. R., (1985). Uncoupling by acetic acid limits growth of and acetogenesis by *Clostridium thermoaceticum*. *Applied and Environmental Microbiology* 48 (6): 1134–39.

Burk, M. J., Schilling, C. H., Burgard, A. P., and Trawick, J. D., (2014). Methods and organisms for utilizing synthesis gas or other gaseous carbon sources and methanol, September.

Chakraborty, S., Rene, E. R., Lens, P. N. L., Rintala, J., and Kennes, C., (2020). Effect of tungsten and selenium on C1 gas bioconversion by enriched anaerobic sludge and microbial community analysis. *Chemosphere*, 250, 126105.

Jiann-Shin, C., (2010). Alcohol Dehydrogenase: Multiplicity and relatedness in the solvent-producing clostridia. *FEMS Microbiology Reviews* 17 (3): 263–73.

Cheng, C., Li, W., Lin, M., and Yang, S. T., (2019). Metabolic engineering of *Clostridium carboxidivorans* for enhanced ethanol and butanol production from syngas and glucose. *Bioresource technology*, 284: 415-423.

Cotter, J. L., Chinn, M. S., and Grunden, A. M., (2009). Ethanol and acetate production by *Clostridium ljungdahlii* and *Clostridium autoethanogenum* using resting cells. *Bioprocess and Biosystems Engineering* 32 (3): 369–80.

Dessi Paolo, Lakaniemi, A. M., and Lens P. N. L., (2017). Biohydrogen production from xylose by fresh and digested activated sludge at 37, 55 and 70°C. *Water Research* 115: 120–29.

Devarapalli, M., and Atiyeh, H. K., (2015). A review of conversion processes for bioethanol production with a focus on syngas fermentation. *Biofuel Research Journal* 2 (3): 268–80.

Dogan, T., Ince, O., Oz, N. A., and Ince, B. K., (2005). Inhibition of volatile fatty acid production in granular sludge from a UASB reactor. *Journal of Environmental Science and Health* 40 (3): 633–44.

Eisentraut, Anselm. 2010. Sustainable Production of Second-Generation Biofuels.

Fast, A. G., and Papoutsakis, E. T., (2012). Stoichiometric and energetic analyses of non-photosynthetic CO₂-fixation pathways to support synthetic biology strategies for production of fuels and chemicals. *Current Opinion in Chemical Engineering* 1 (4): 380–95.

Fernández-Naveira, ánxela, Veiga, María C., and Kennes, C., (2017a). Glucose bioconversion profile in the syngas-metabolizing species *Clostridium carboxidivorans*. *Bioresource Technology* 244: 552–59.

Fernández-Naveira, ánxela, Veiga, María C., and Kennes, C., (2017b). H-B-E (hexanol-butanol-ethanol) fermentation for the production of higher alcohols from syngas/waste gas. *Journal of Chemical Technology and Biotechnology* 92 (4): 712–31.

Fernández-Naveira, ánxela, Veiga, María C., and Kennes, C., (2019). Selective anaerobic fermentation of syngas into either C2-C6 organic acids or ethanol and higher alcohols. *Bioresource Technology*, 280: 387-395.

Ganigué, R., Sanchez-Paredes, P., Baneras, L. and Colprim, J., (2016). Low fermentation pH is a trigger to alcohol production, but a killer to chain elongation. *Frontiers in microbiology*, 7, 702.

He, Y., Cassarini C., Marciano F., and Lens P. N. L., (2020). Homoacetogenesis and solventogenesis from H₂/CO₂ by granular sludge at 25, 37 and 55° C. *Chemosphere*: 128649.

Jones, D. T., and David R W., (1986). Acetone-Butanol Fermentation Revisited. *Microbiological Reviews* 50 (4): 484.

Kundiyana, D. K., Wilkins, M. R., Maddipati, P., and Huhnke, R. L., (2011). Effect of temperature, pH and buffer presence on ethanol production from synthesis gas by *Clostridium Ragsdalei*. *Bioresource Technology* 102 (10): 5794–99.

Liu, C., Luo, G., Wang, W., He, Y., Zhang, R., and Liu, G., (2018). The effects of pH and temperature on the acetate production and microbial community compositions by syngas fermentation. *Fuel* 224: 537-544.

Liu, K., Atiyeh, H. K., Tanner, R. S., Wilkins, M. R., and Huhnke, R. L., (2012). Fermentative production of ethanol from syngas using novel moderately alkaliphilic strains of *Alkalibaculum Bacchi*. *Bioresource Technology* 104: 336–41.

Marcellin, E., Behrendorff, J. B., Nagaraju, S., Detissera, S., and Nielsen, L. K., (2016). Low carbon fuels and commodity chemicals from waste gases—systematic approach to understand energy metabolism in a model acetogen. *Green Chemistry* 18 (10): 3020–28.

Maddox, I. S., E. Steiner, S. Hirsch, S. Wessner, N. A. Gutierrez, J. R. Gapes, and K. C. Schuster., (2000). The cause of " acid crash" and " acidogenic fermentations" during the batch acetone-butanol-ethanol (ABE) fermentation process. *Journal of molecular microbiology and biotechnology* 2 (1): 95-100.

Modestra, J.A., Katakajwala, R. and Mohan, S.V., (2020). CO₂ fermentation to short chain fatty acids using selectively enriched chemolithoautotrophic acetogenic bacteria. *Chemical Engineering Journal*, 124759.

Mohammadi, M., Najafpour, G. D., Younesi, H., Lahijani, P., Uzir, M. H., and Mohamed, A. R., (2011). Bioconversion of synthesis gas to second generation biofuels: a review. *Renewable and Sustainable Energy Reviews* 15 (9): 4255–73.

Munasinghe, P. C., and Khanal, S. K., (2010). Biomass-derived syngas fermentation into biofuels: opportunities and challenges. *Bioresource Technology* 101 (13): 5013–22.

Naik, S. N., Goud, V. V., Rout, P. K., and Dalai, A. K., (2010). Production of first and second generation biofuels: a comprehensive review. *Renewable and Sustainable Energy Reviews* 14 (2): 578–97.

Padan, Etana, Dan Zilberstein, and Shimon Schuldiner., (1981). pH Homeostasis in Bacteria. *Biochimica et Biophysica Acta (BBA)-Reviews on Biomembranes* 650 (2–3): 151–66.

Pereira, I.A., (2013). An enzymatic route to H₂ storage. *Science* 342 (6164): 1329–30.

Ramió-Pujol, Sara, Ramon Ganigué, Lluís Bañeras, and Jesús Colprim. (2015). Incubation at 25°C prevents acid crash and enhances alcohol production in *Clostridium carboxidivorans* P7. *Bioresource Technology* 192: 296–303.

Richter, H, B Molitor, H Wei, W Chen, L Aristilde, and LT Angenent., (2016). Ethanol production in syngas-fermenting *Clostridium ljungdahlii* is controlled by thermodynamics rather than by enzyme expression. *Energy & Environmental Science* 9 (7): 2392–99.

Sadhukhan, Jhuma, Jon R Lloyd, Keith Scott, Giuliano C Premier, H Yu Eileen, Tom Curtis, and Ian M Head., (2016). A Critical Review of Integration Analysis of Microbial Electrosynthesis (MES) Systems with Waste Biorefineries for the Production of Biofuel and Chemical from Reuse of CO₂. *Renewable and Sustainable Energy Reviews* 56: 116–32.

Samanides, C.G., Koutsokeras, L., Constantinides, G. and Vyrides, I., (2020). Methanogenesis inhibition in anaerobic granular sludge for the generation of volatile fatty acids from CO₂ and zero valent iron. *Frontiers in Energy Research*, 8: 37.

Sarkar, O., Butti, S.K. and Mohan, S.V., (2017). Acidogenesis driven by hydrogen partial pressure towards bioethanol production through fatty acids reduction. *Energy*, 118: 425-434.

Saxena, Jyotisna, and Ralph S Tanner., (2011). Effect of trace metals on ethanol production from synthesis gas by the ethanologenic acetogen, *Clostridium ragsdalei*. *Journal of Industrial Microbiology & Biotechnology* 38 (4): 513–21.

Schink, Bernhard., (1997). Energetics of syntrophic cooperation in methanogenic degradation. *Microbiology and Molecular Biology Reviews*, 61 (2): 262–80.

Shen, Y., Brown, R.C. and Wen, Z., (2017). Syngas fermentation by *Clostridium carboxidivorans* P7 in a horizontal rotating packed bed biofilm reactor with enhanced ethanol production. *Applied energy*, 187, 585-594.

Singla, A., Verma, D., Lal, B. and Sarma, P.M., (2014). Enrichment and optimization of anaerobic bacterial mixed culture for conversion of syngas to ethanol. *Bioresource Technology* 172, 41–49.

Shen, Y., Brown, R.C. and Wen, Z., (2017). Syngas fermentation by *Clostridium carboxidivorans* P7 in a horizontal rotating packed bed biofilm reactor with enhanced ethanol production. *Applied Energy*, 187, 585-594.

Singla, A., Verma, D., Lal, B. and Sarma, P.M., (2014). Enrichment and optimization of anaerobic bacterial mixed culture for conversion of syngas to ethanol. *Bioresource Technology* 172, 41–49.

Stams, Alfons JM, Johan B Van Dijk, Cor Dijkema, and Caroline M Plugge. (1993). Growth of syntrophic propionate-oxidizing bacteria with fumarate in the absence of methanogenic bacteria. *Applied and Environmental Microbiology*. 59 (4): 1114–19.

Steinbusch, Kirsten JJ, Hubertus VM Hamelers, and Cees JN Buisman., (2008). Alcohol production through volatile fatty acids reduction with hydrogen as electron donor by mixed cultures. *Water Research* 42 (15): 4059–66.

Strobl, G., Feicht, R., White, H., Lottspeich, F., and Simon, H., (1992). The tungsten-containing aldehyde oxidoreductase from *Clostridium thermoaceticum* and its complex with a viologen-accepting nadph oxidoreductase. *Biological Chemistry Hoppe-Seyler*, 373 (1): 123-132.

Van Langerak, EPA, G Gonzalez-Gil, A Van Aelst, JB Van Lier, HVM Hamelers, and G Lettinga., (1998). Effects of high calcium concentrations on the development of methanogenic sludge in upflow anaerobic sludge bed (UASB) reactors. *Water Research* 32 (4): 1255–63.

Yamamoto, Isamu, Takashi Saiki, Shiu-Mei Liu, and Lars G Ljungdahl., (1983). Purification and Properties of NADP-Dependent Formate Dehydrogenase from *Clostridium Thermoaceticum*, a Tungsten-Selenium-Iron Protein. *Journal of Biological Chemistry* 258 (3): 1826–32.

Yang, S., He, Y., Liu, Y., Chou, C., Zhang, P. and Wang, D., (2010). Effect of wastewater composition on the calcium carbonate precipitation in upflow anaerobic sludge blanket reactors. *Frontiers of Environmental Science & Engineering in China*, 4 (2): 142-149.

Chapter 5 Enrichment of homoacetogens converting H₂/CO₂ into acids and ethanol and simultaneous methane production

Abstract

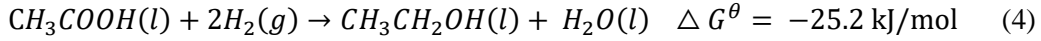
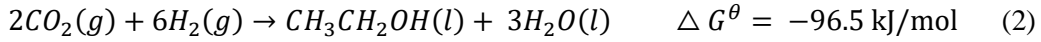
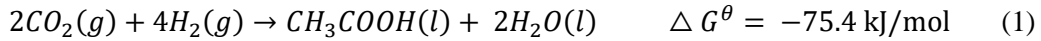
An anaerobic granular sludge was enriched to utilize H₂/CO₂ in a continuous gas-fed up-flow anaerobic sludge reactor by applying operating conditions expected to produce acetic acid, butyric acid and ethanol. Three stages of fermentation were found: Stage I with acetic acid accumulation with the highest concentration of 35 mM along with a pH decrease from initial 6 to 4.5. In Stage II, H₂/CO₂ was replaced by 100% H₂ to induce solventogenesis, whereas butyric acid was produced with the highest concentration of 2.5 mM. At stage III with 10 μM tungsten (W) addition, iso-valeric acid, valeric acid and caproic acid were produced at pH 4.5 -5.0. In the batch tests inoculated with the enriched sludge taken from the bioreactor (day 70), however, methane production occurred at pH 6. Exogenous 15 mM acetate addition enhanced both the H₂ and CO₂ consumption rate compared to exogenous 10, 30 and 45 mM acetate by the enriched sludge. Exogenous acetate was failed to be converted to ethanol using H₂ as electron donor by the enriched acetogens.

5.1 Introduction

CO₂ fermentation to generate bio-commodities (e.g. acetic acid (Karekar et al., 2020)) or biofuels (e.g. ethanol (He et al., 2020) and methane (Liu et al., 2016)) relieves the paradox of fossil fuel utilization and carbon emission reduction. CO₂ fermentation simultaneously mitigates carbon emission and generates valuable bioenergy products and hence becomes a promising economical and sustainable way of biofuel production (Burk et al. 2010; Bhatia et al., 2019; Gunes et al., 2021).

H₂ and CO₂ can be converted to VFAs and alcohols via the Wood-Ljungdahl pathway (WLP) by autotrophic acetogens, mainly containing *Clostridium spp.* According to the two stage fermentation theory for CO₂ bioconversion, the first stage is acetogenesis with accumulation of acetic acid, followed by solventogenesis under stress conditions such as nutrient limitation or low pH (Mohammadi et al. 2012). The mechanism of solventogenesis, however, still remains to be explored. One of the widely recognized mechanisms to induce solventogenesis is a low pH (Ganigué et al., 2016). Low pH (below 5) induces more undissociated acids that can enter the cells, which convert the acids to neutral charged ethanol to avoid their death caused by an intracellular pH drop (Padan et al. 1981; Cotter et al. 2009). On the other hand, microorganisms are one of the key components in CO₂ autotrophic fermentation, e.g. *Clostridium autoethanogenum* (Abrini et al., 1994) and *Clostridium carboxidivorans* (Liou et al., 2005; Fernández-Naveira et al., 2017). Several pure strains have been studied, however, mixed culture fermentations are easier to implement at large scale than

pure cultures with the merits of resistance to non-sterile conditions (Liu et al., 2014). The potential products converted from H₂ and CO₂ include:



Limited studies reported ethanol production from H₂/CO₂ (Modestra et al., 2020; Stoll et al., 2018). The positive role of exogenous acetate on ethanol production by a *Clostridium* strain has been reported using syngas as the gaseous substrate (Xu et al., 2020). However, whether acetic acid with H₂ can be directly converted to ethanol by mixed cultures remains to be explored. Therefore, one possible strategy for enhancing solventogenesis is to supply exogenous acetate with H₂ as the electron donor under low pH by mixed cultures.

Tungsten (W) is an important trace element involved in the formation of enzyme activity such as formate dehydrogenase (FDH), one of key enzymes in the Wood-Ljungdahl pathway, converting CO₂ into formate. It has been reported that FDH synthesis could be stimulated in the presence of W (Yamamoto et al. 1983). The other key metalloenzyme related to W is alcohol dehydrogenase (ADH) catalyzing the reduction of acetyl CoA to ethanol (Andreesen and Makdessi 2008). Tungsten can enhance ethanol production from carbon monoxide by anaerobic granular sludge (Chakraborty et al., 2020).

This study investigated CO₂ and H₂ fermentation by heat-treated granular sludge in a bioreactor with both gas and medium circulation at 25°C. It was assumed that ethanol production could be enhanced by feeding 100% H₂ or tungsten from acetic acid produced by homoacetogens. Acetate produced from H₂/CO₂ or pure H₂ as the gaseous substrate and ethanol degradation were further investigated in batch tests by the enriched sludge taken from the reactor after 70 days of operation, from which the homoacetogenesis, methanogenesis and solventogenesis potential was assessed.

5.2 Materials and methods

5.2.1 Biomass and medium composition

The same inoculum anaerobic granular sludge from a wastewater treatment plant was used as in our previous study on acids and alcohol production from H₂/CO₂ (He et al., 2020). The total solid (TS) and volatile solid (VS) content was 42.7 (± 1.0) g/L and 24.8 (± 0.5) g/L, respectively. The granular sludge was first centrifuged at 8000 g for 10 min to remove the supernatant and the pellet was heat-treated at 90°C for 15 min to select for spore forming

acetogens as described by Dessì et al. (2017). The medium was prepared according to a previous study (He et al., 2020).

5.2.2 Experimental design

5.2.2.1 Semi-continuous gas fed bioreactor

An up-flow semi-continuous gas fed reactor was set-up with a total working volume of 1 L (Fig. 5.1) and liquid flow rate was 60 mL/min by a Verdeflex pump (Utrecht, The Netherlands). A 10 L gas bag filled with H₂/CO₂ (80/20 v/v) was connected on the gas outlet. H₂/CO₂ gas was cycled at a gas flow rate of 10 mL·min⁻¹ controlled by gas tight tubes using a Verdeflex pump (Utrecht, The Netherlands) and a mass flow meter (FMA-1618A, Omega, San Antonio, US). The temperature was controlled at 25°C by a water jacket.

The semi-continuous gas fed bioreactor operation included three stages. In stage I (0-26 d), the reactor was fed with H₂/CO₂ gas (80/20 v/v) with initial pH of 6.0 for acetic acid production without pH control. In stage II (day 27-50), H₂/CO₂ was replaced by 100% H₂ to stimulate ethanol production at a pH controlled at 4.5-5. In stage III (day 50-70), 10 μM tungsten was added to the medium to stimulate solventogenesis according to the report of Chakraborty et al. (2020), while the gas phase was still 100% H₂.

Microbial community analysis was conducted for the anaerobic granular sludge in duplicate (G-a, G-b) on 10 mL bioreactor suspension samples at the end of stage I, II and III (in triplicate, III-a, b and c). At the end of the stage I (day 26, the log phase of the autotrophic acetogens) to sustain and further enrich the sludge, 10 mL liquid sludge from the reactor was inoculated into two 120 mL batch bottles with 50 mL liquid medium (duplicate). H₂/CO₂ (80/20, v/v) was used as the substrate and the initial pH was 6.0. The bottles were incubated at 150 rpm and at 25°C in a water-bath shaker.

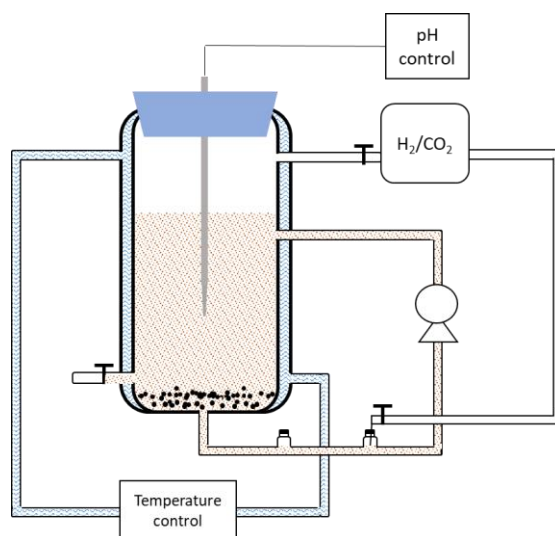


Fig. 5.1 Diagram of the up-flow gas reactor with pH control

5.2.2.2 Batch studies on different H₂/CO₂ ratio utilization by enriched sludge

Batch experiments were conducted in 120 mL serum bottles with 50 mL medium and 5% enriched sludge (day 70). The bottles were sealed with rubber stoppers and capped with aluminum crimp caps. All bottles were pressurized with pure H₂ or H₂/CO₂ (80/20 v/v) at an initial pressure of 1.8 bar and were incubated at 150 rpm and at 25°C.

To elucidate the conversion pathway and failure of solventogenesis in the reactor, batch tests of H₂/CO₂, 15 mmol·L⁻¹ acetate+ H₂/CO₂ and 10 μM tungsten+ H₂/CO₂ were conducted using the bioreactor sludge as the inoculum. The enriched sludge from gas fed reactor after 70 days fermentation was used as the inoculum for the following batch tests. To investigate the effect of exogenous acetate on ethanol production using H₂ as electron donor, the bottles were sparged with 100% H₂ and H₂/CO₂ (v/v, 80/20) and 5% inoculum at an initial pressure 1.8 bar. Acetate was added to make the final concentration of 10, 15, 30 and 40 mmol·L⁻¹, respectively. To test whether acetic acid and ethanol degradation occurred in the reactor, 15 mmol·L⁻¹ acetate + 5 mmol·L⁻¹ ethanol, 30 mmol·L⁻¹ acetate + 15 mmol·L⁻¹ ethanol were added with H₂/CO₂ (v/v, 80/20) in the headspace in batch tests using 5% enriched sludge.

5.2.3 Analysis

5.2.3.1. Gas phase

H₂, CO₂ and CH₄ concentrations were measured using a HP 6890 gas chromatograph (GC, Agilent Technologies, Palo Alto, USA) equipped with a thermal conductivity detector (TCD). The GC was fitted with a 15-m HP-PLOT Molecular Sieve 5A column (ID 0.53 mm, film thickness 50 mm). The oven temperature was kept constant at 60°C. The temperature of the injection port and the detector was maintained constant at 250°C. Helium was used as the carrier gas.

5.2.3.2. VFAs and solvent analysis

VFAs, ethanol and butanol concentrations were analysed for each bottle from the liquid phase (1 mL) using high performance liquid chromatography (Agilent Co., Palo Alto, USA) equipped with a refractive index detector (RID) and an Agilent Hi-Plex H column (Internal diameter × length, 7.7 ×300 mm, size 8 μm). A H₂SO₄ solution (5 mM) was used as mobile phase at a flow rate of 0.7 ml/min and with a sample injection volume of 50 μl. The column temperature was set at 60°C and the RID detector at 55 °C.

5.2.3.3. Microbial analysis

DNA was extracted using a DNeasy® PowerSoil Kit (QIAGEN, Germany) following the manufacturer's protocol. Approximately 0.5 g of the solids from the samples was used for DNA

extraction. The extracted DNA was quantified and its quality was checked by a Nanodrop 2000c Spectrophotometer (Thermo Scientific, USA). A total of 1,103,482 sequences were obtained from all investigated samples (Table 5.1). For more details on microbial community analysis, please see section 3.2.3 (Chapter 3). The raw data is available in OneDrive NUIG.

Table 5.1 The operational taxonomic units (OTUs) sequence table per sample statistics for microbial community analysis. Samples taken from suspended sludge at 10 d, and the end of stage I, II, III (III-a, b and c are triplicates) and the granular sludge inoculum (G-a, G-b) at genus level. The two batch bottles used the sludge taken from the bioreactor as inoculum (stage I, day 26) (I-a, I-b).

Sample (V3V4a)	Input sequences	Sequences assigned to OTUs	Sequences assigned to taxa	Count after lineage-specific copy-number correction	Median sequence length after preprocessing
10 d	72702	66109	66109	19727	424
I	58761	53699	53699	17182	424
II	63815	57402	57402	18719	424
III-a	59467	52177	52177	15680	422
III-b	58181	51113	51113	15304	422
III-c	56605	49821	49821	15285	422
I-a	174983	126305	126305	30873	402
I-b	175270	134029	134029	32259	402
G-a	163540	136572	136572	74150	422
G-b	160028	129594	129594	73452	422
Total	1043352	856821	856821	312631	4186

5.3 Results

5.3.1 Enrichment of acetogenic sludge and production of acids and ethanol in gas fed reactor

During the reactor operation, after 10 days of adaption, acetic acid started to be produced and reached 35 mM (Fig. 5.2a, Eq. 1). Ethanol was detected at day 11 and increased to 1.35 mmol·L⁻¹ at day 12 but it was then degraded (Fig. 5.2a, Eq. 2). Instead, butyric acid started to be produced at day 12 when ethanol degradation occurred and increased to 0.5 mmol·L⁻¹ at day 26. Propionic acid started to be produced at day 14 and reached 1.82 mmol·L⁻¹ at day 26. The pH was decreased along with the accumulation of acetic acid and kept at 4.5–5.0 after day

21 (Fig. 5.2b). However, ethanol production was not observed when the pH was as low as 4.5 from day 21 to 26 (Fig. 5.2a).

To stimulate ethanol production from acetic acid, H₂/CO₂ was replaced by 100% H₂ at day 27 (Stage II, 27-50 d). Indeed, 100% H₂ addition induced ethanol production and it reached 1.2 mmol·L⁻¹ at day 37 (Fig. 5.2a, Eq. 4). Thereafter, ethanol production started to decrease and to a concentration of 0.5 mmol·L⁻¹ (Fig. 5.2a). Meanwhile, butyric acid accumulated and reached 2.4 mmol·L⁻¹ (Fig. 5.2a). After feeding 100% H₂, both ethanol and butyric acid production occurred from day 30 to 37, but butyric acid kept increasing along with the consumption of ethanol from day 37 to 50. The concentration of both acetic acid and propionic acid decreased at the end of the stage II.

At stage III, 10 μM tungsten addition induced both acetic acid and butyric acid degradation, accompanied with the production of valeric acid and caproic acid, respectively, 1.3 and 0.4 mmol·L⁻¹ at the end of incubation (Fig. 5.2a).

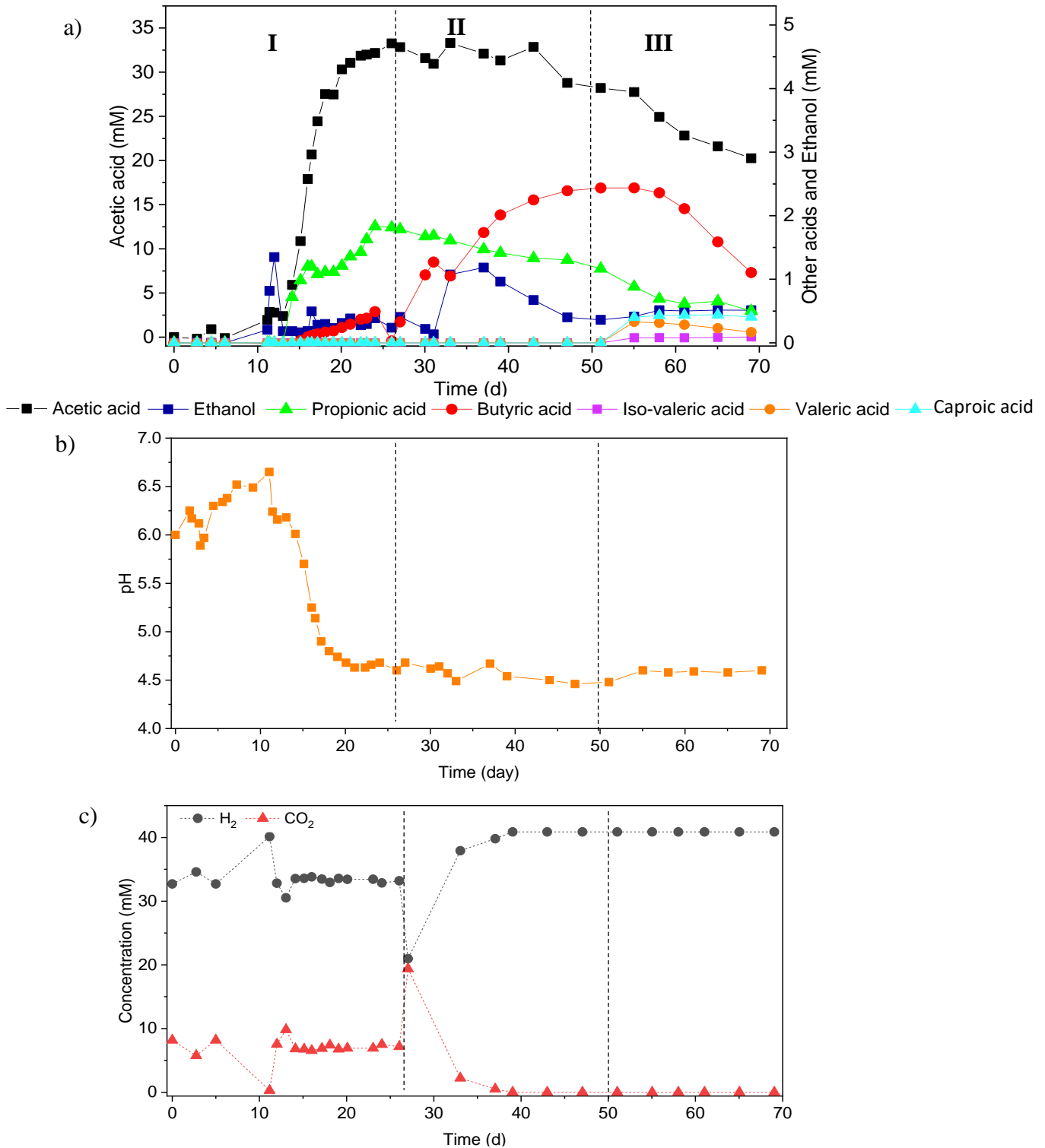


Fig. 5.2 H₂/CO₂ fermentation in a semi-continuous gas fed reactor by anaerobic granular sludge. a) acids and ethanol production, b) change of pH and c) H₂, CO₂ concentration from H₂/CO₂ or H₂ by granular sludge. The substrate of stage I, II and III are, respectively, H₂/CO₂, H₂ and H₂ + 10 μM tungsten.

5.3.2 Effect of exogenous acetate and tungsten addition on H₂/CO₂ conversion by enriched sludge

When using H₂/CO₂ as the substrate (the control) for the enriched sludge (day 70), acetic acid was produced with a final concentration of 6.1 mmol·L⁻¹ (Fig. 5.3a, Table 5.2). Methane production was observed along with the acetic acid production and 36.6 mmol·L⁻¹ methane had accumulated at the end of the incubation (Fig. 5.3a). H₂ and CO₂ consumption was, respectively, 160 and 40.6 mmol·L⁻¹ at the end of the incubation (Fig. 5.3a).

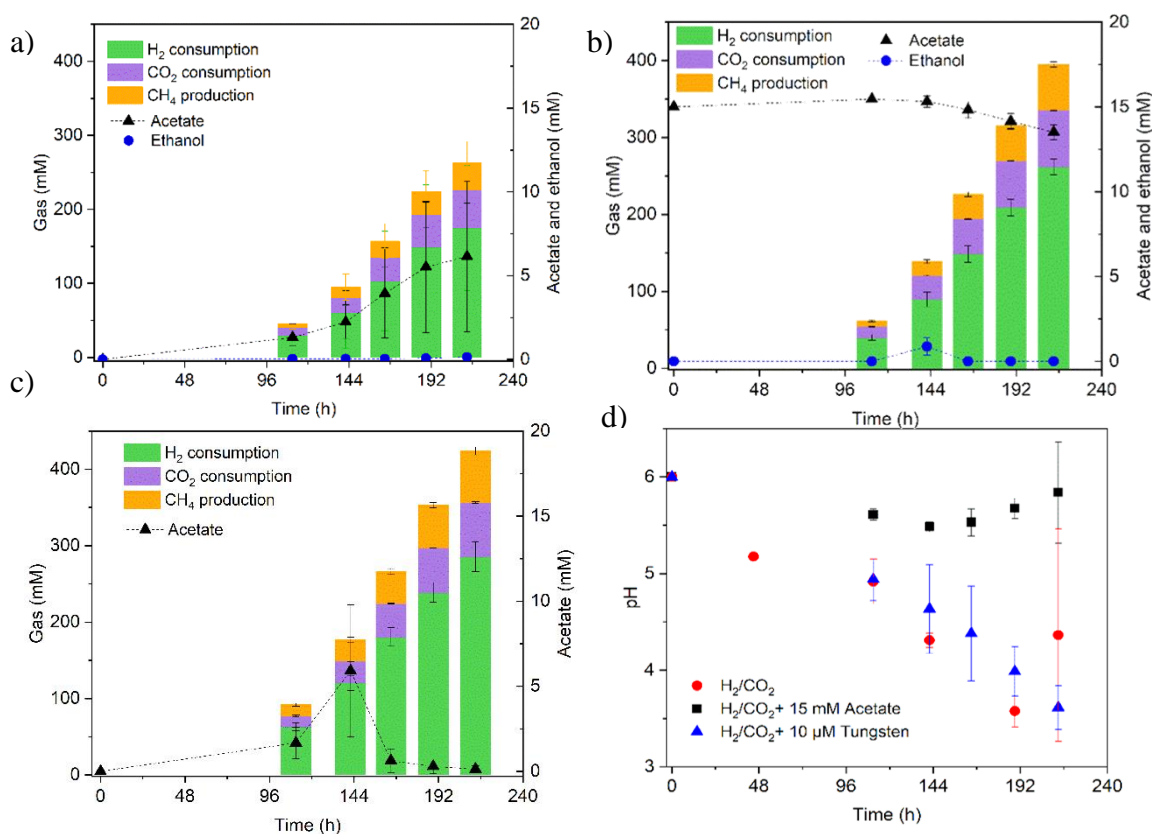


Fig. 5.3 H₂ and CO₂ consumption and CH₄, acetate and ethanol production by enriched sludge sampled on day 70 from the bioreactor using a) H₂/CO₂, b) H₂/CO₂ + 15 mM acetate and c) H₂/CO₂ + 10 μM tungsten as the substrate and d) change of pH in these incubations.

Table 5.2 The highest production of acetic acid and ethanol, CH₄ accumulation, H₂ and CO₂ consumption at the end of incubation by enriched sludge in batch tests.

Compound	H ₂ /CO ₂	H ₂ /CO ₂ + 15 mM Hac	H ₂ /CO ₂ + 10 μM W
Acetic acid (mM)	6.1±4.5	15.5±0.1	5.9±3.4
Ethanol (mM)	0.1±0.1	0.9 ±0.5	0
CH ₄ (mM)	36.6 ± 28.6	59.7 ± 3.4	67.6±5.2
H ₂ consumption (mM)	174.8±84.1	262.0 ± 10.4	285.5±19.4
CO ₂ consumption (mM)	51.7±18.2	73.3 ± 1.0	71.1±1.0

With 15 mmol·L⁻¹ acetate addition, 0.9 mmol·L⁻¹ ethanol was produced after 144 h but it was degraded after 192 h and did not accumulate at the end of the incubation. However, methane production was observed and accumulated to 60.0 mmol·L⁻¹ at the end of the incubation. The acetic acid concentration slightly decreased from initially 15 to 13 mmol·L⁻¹ at the end of the incubation (Fig. 5.3b). H₂ and CO₂ consumption was, respectively, 262.0 and 73.3 mmol·L⁻¹ at the end of the incubation (Fig. 5.3a) and was correspondingly 1.6 fold and 1.8 fold higher than the control to which no external acetate was provided. The H₂ and CO₂ consumption rate increased to, respectively, 0.85 and 0.26 mmol·L⁻¹·h⁻¹ compared to the control of 0.59 and 0.18 mmol·L⁻¹·h⁻¹ (Table 5.2).

The addition of 10 μM tungsten enhanced the H₂ and CO₂ consumption of 285.8 and 71.1 mmol·L⁻¹, respectively, at a H₂ and CO₂ consumption rate of 1.02 mmol·L⁻¹·h⁻¹ and 0.25 mmol·L⁻¹·h⁻¹, respectively, compared to the control. Methane (67.6 mmol·L⁻¹) was produced at the end of the incubation (Fig. 5.3c). The methane production was from acetate as the substrate since the produced acetic acid at 144 h (6.0 mmol·L⁻¹) was almost totally consumed in the 10 μM W+H₂/CO₂ incubation upon completion of the experiment (Fig. 5.3c, d). Surprisingly, the pH of the control and the 10 μM tungsten incubation decreased quickly even below 4 after 192 h but methane production was still detected (Fig. 5.4d).

5.3.3 Effect of exogenous acetate on with H₂/CO₂ conversion by enriched sludge

Initially, acetate was not significantly consumed while it slightly increased at the initial concentration of 15 and 30 mmol·L⁻¹ acetate (Fig. 5.4a). Methane production reached 14.9, 59.7, 5.2 and 14.0 mmol·L⁻¹ along with the increased initial 10, 15, 30 and 45 mmol·L⁻¹ acetate concentration. Correspondingly, CO₂ consumption was respectively, 27.7, 73.3, 19.8 and 25.4 mmol·L⁻¹, whereas the H₂ consumption amounted to 78.9, 261.9, 45.4 and 73.1 mmol·L⁻¹, respectively. Correspondingly, the pH decreased from initial 6 to 5.0-5.2 at both initial 15 and 30 mmol·L⁻¹ acetate due to the positive net acetic acid production (Fig. 5.4e). The gas pressure was decreased slowly during the incubation, because part of the gas pressure came from the methane production (Fig. 5.4f).

The 15 mM acetate addition reached the highest CH₄ production, CO₂ and H₂ consumption compared with 10, 30 and 45 mmol·L⁻¹ acetate, while the acetic acid concentration slightly decreased at the end (Fig. 5.4). 10 and 50 mmol·L⁻¹ acetate had a similar effect on the CH₄ production and H₂ and CO₂ consumption, while supplementing 30 mmol·L⁻¹ acetate obtained the lowest CH₄ production, CO₂ and H₂ consumption.

Further experiments demonstrated that when using 100% H₂ and in the absence of CO₂, the ethanol production process did not happen after 240 h incubation. The pH did not change during the incubation and the gas pressure did not decrease. The failure of acetate and H₂ utilization might be because the enriched acetogens were mostly autotrophic acetogens, which was further confirmed by the microbial community analysis (see below).

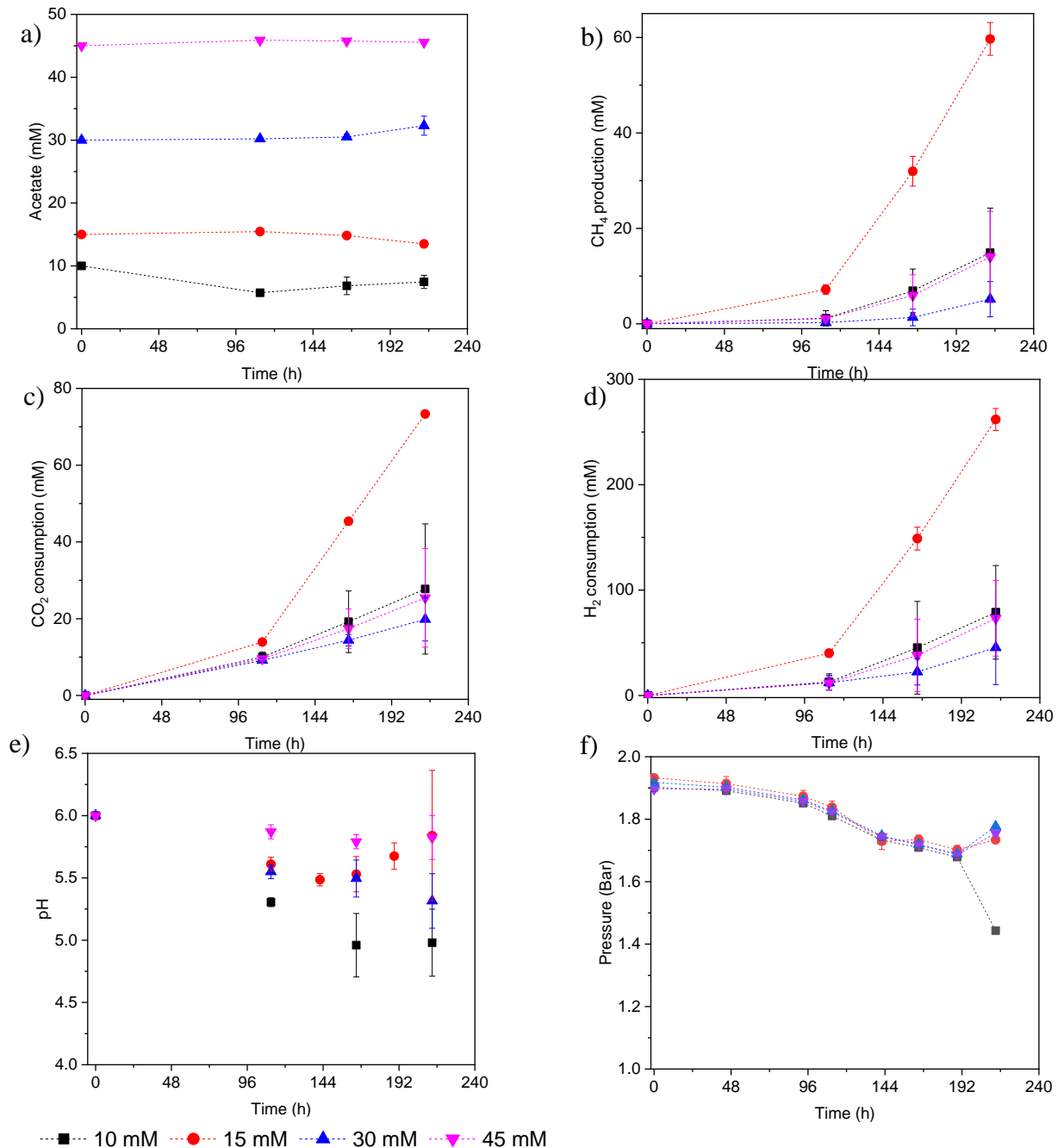


Fig. 5.4 Effect of 10, 15, 30 and 45 mM exogenous acetate on production profiles by enriched sludge (day 70 of bioreactor operation) using H₂/CO₂ as the substrate a) acetate concentration, b) CH₄, c) CO₂ and d) H₂ production, e) change of pH and f) gas pressure.

5.3.4 Acetate and ethanol conversion in the presence of H₂/CO₂ by enriched sludge

Acetate and ethanol were added to simulate the conversion process, i.e. the reverse β oxidation pathway, to further assess if longer chain VFA were produced, as observed in the reactor. With 15 HAc+5 EtOH and 30 HAc+15 EtOH, methane production was observed and reached, respectively, 54.1 and 46.3 mmol·L⁻¹. Neither ethanol nor longer chain fatty acids were produced during the incubation.

With 15 mmol·L⁻¹ acetate and 5 mmol·L⁻¹ ethanol addition, CH₄ production and CO₂ and H₂ consumption were all higher compared to the incubations supplied with 30 mmol·L⁻¹ acetate and 15 mmol·L⁻¹ ethanol addition (Fig. 5.5). Both the acetate and ethanol concentration slightly decreased during the incubation (Fig. 5.5a, b). The pH was slightly increased possibly due to the decreased dissolved CO₂ in the liquid medium induced by the consumption of headspace CO₂ (Fig. 5.5c). The gas pressure decreased slowly and showed a similar trend between the 15 HAc+5 EtOH and 30 HAc+15 EtOH groups.

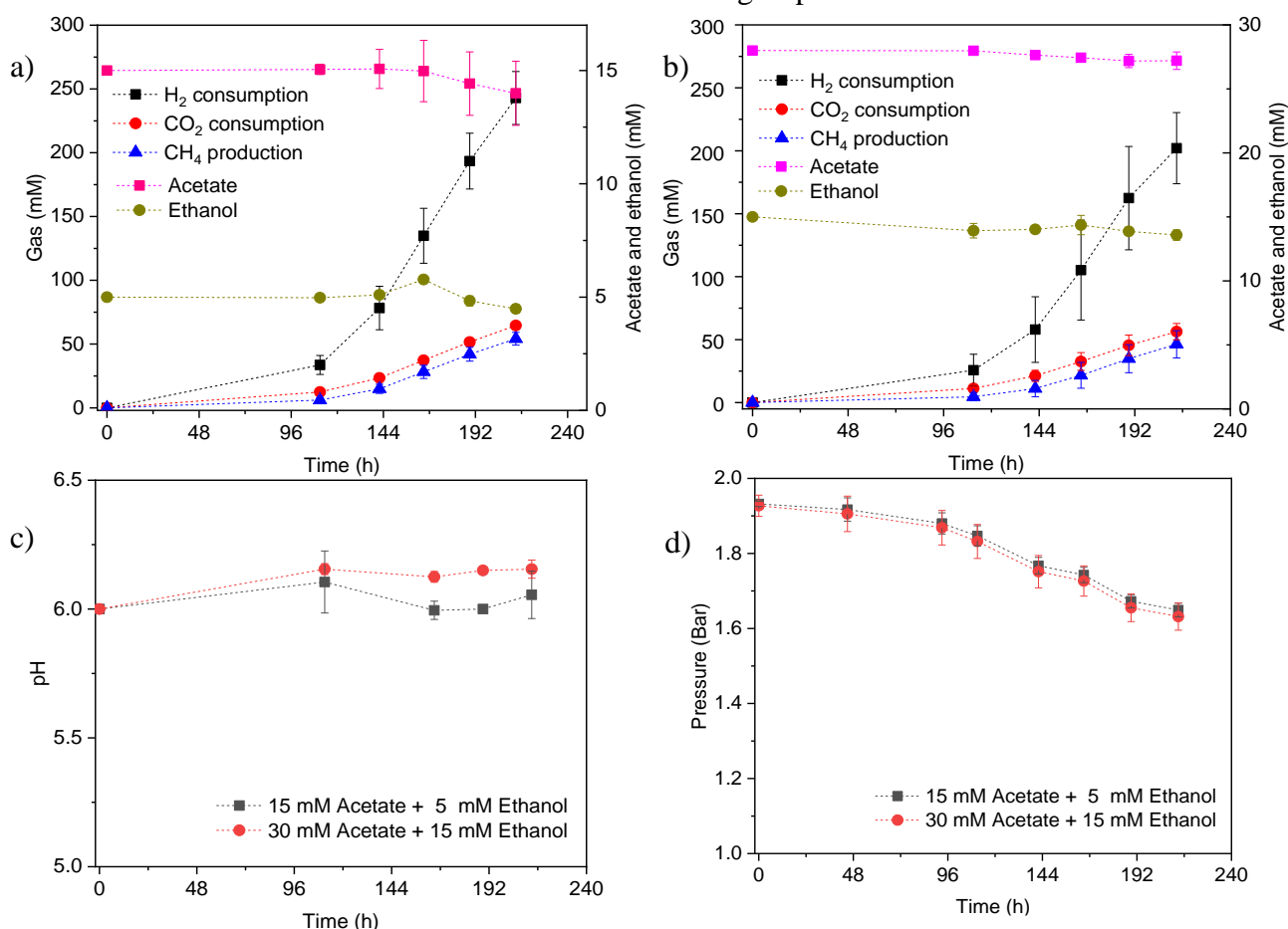


Fig. 5.5 H₂ and CO₂ consumption and CH₄, acetate and ethanol production in the presence of a) 15 mM acetate + 5 mM Ethanol and b) 30 mM Acetate + 15 mM Ethanol, c) pH and d) gas pressure change by enriched sludge sampled on day 70 using H₂/CO₂ as the substrate.

The enriched sludge was further checked for the addition of glucose to possibly enhance the biomass grow and mixotrophy. However, the ethanol production did not significantly enhance compared to the solely glucose fed incubation (Fig. 5.6).

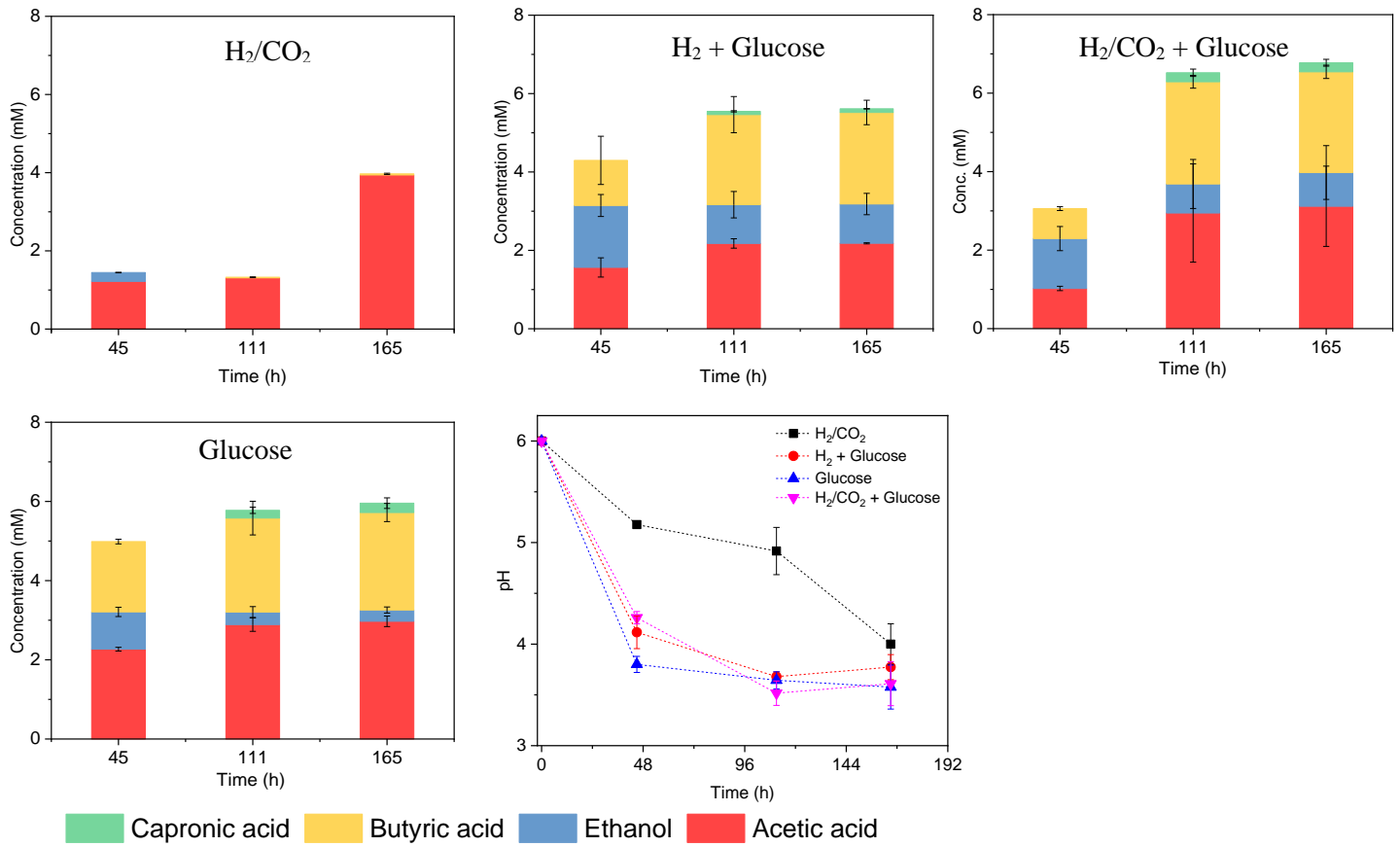


Fig. 5.6 Effect of glucose (0.5 g/L) on H_2/CO_2 bioconversion by enriched sludge.

5.3.5 Microbial analysis

Microbial analysis of the suspended sludge of the bioreactor showed the relative abundance of acetogens related at class level *Clostridia*. On day 10, when the acetic acid started to be produced, they comprised a relative abundance of 3.1%, it increased to 11.4% at the stage II and 9.4% at the stage III, finally reaching about 25-26% (Fig. 5.7a).

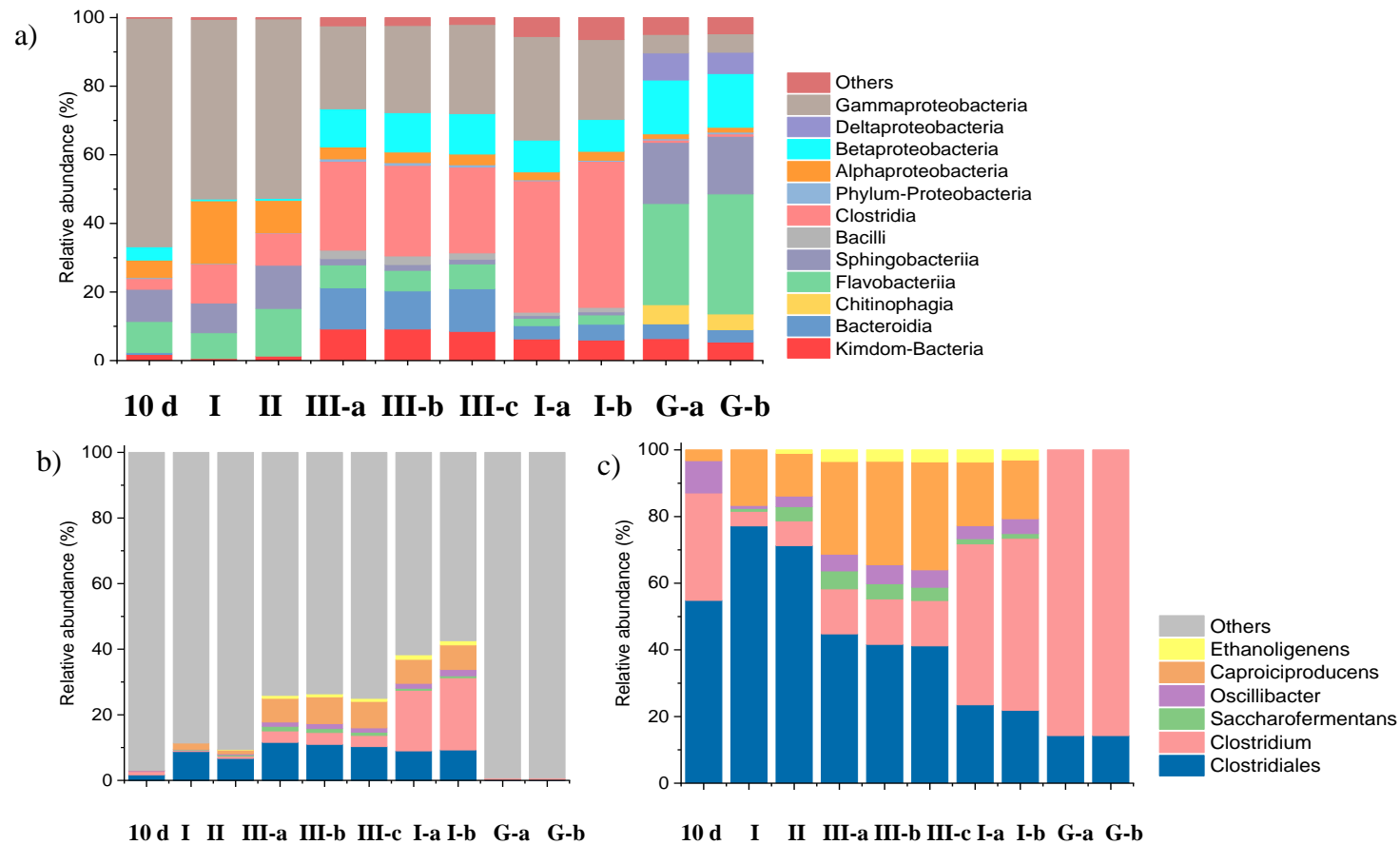


Fig. 5.7 Relative abundance of microorganism from suspended sludge at 10 d, and the end of stage I, II, III (III-a, b and c are triplicates) and the granular sludge inoculum (G-a, G-b) at genus level. The two batch bottles used the sludge taken from the bioreactor as inoculum (stage I, day 26) (I-a, I-b). a) Microbial analysis of all bacteria; b) Genus level in the *Clostridiales* order, the relative abundance is relative to all the bacteria, and c) Genus level in the *Clostridiales* order, the relative abundance is relative to the *Clostridiales* order.

For the *Clostridium* genus, the relative abundance with 0.1% at day 10 increased to, respectively, 0.5% at stage II, 0.7% at stage III and about 3.5% at the end of each stage (Fig. 5.7b). Fig. 5.8 shows the acetic acid and ethanol production in the batch bottles inoculated with enriched sludge from the bioreactor at day 70. The microbial analysis data (I-a, I-b of bottle 1, 2, respectively) showed that the higher relative abundance of the *Clostridium* genus compared to the reactor sludge sampled on day 10. *Clostridium* was enriched with a relative abundance of 3.5% in the bioreactor (day 70) and increased to 18.5 and 22.0 % in the enriched batch bottle 1 and 2 (Fig. 5.7b).

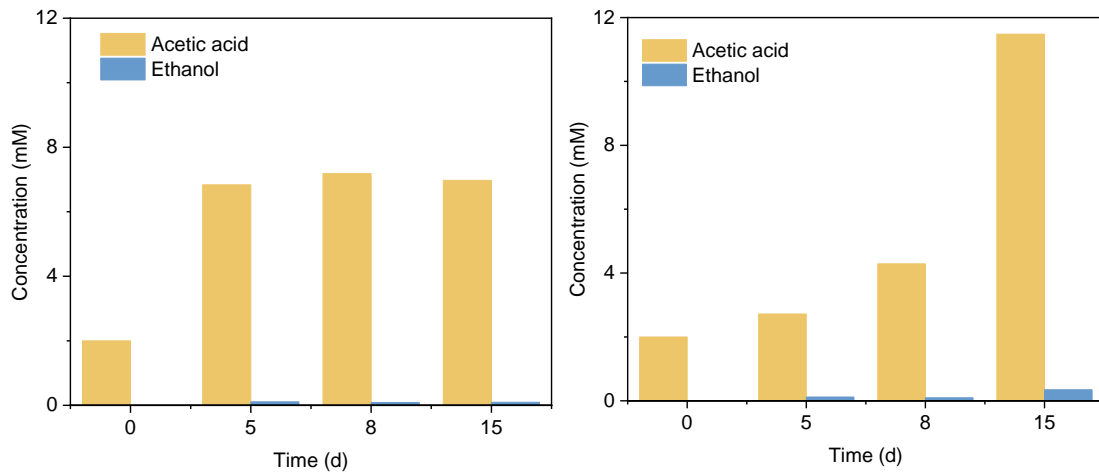


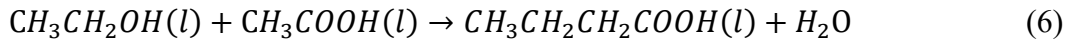
Fig. 5.8 Acetic acid and ethanol production of the two enriched bottles using sludge from the bioreactor (day 26, stage I) as inoculum.

Fig. 5.7c shows the distribution of the *Clostridium* genus. The *Clostridium* genus and other acetogens belonging to the *Clostridia* class occupied above 60% at the end of the incubation (III-a, b, c) (Fig. 5.7c). In the *Clostridia* class, the relative abundance of the *Caproiciproducens* genus increased from 3.2% on day 10 to about 30% at the end of the incubation. The increase and enrichment of *Caproiciproducens* was corresponding to the increased caproic acid production at the end of the incubation. Small amounts of the *Ethanoligenens* genus were enriched with around 3% at the end of the incubation (triplicates, III-a, b, c), which might have contributed to the ethanol production process during the fermentation. The *Oscillibacter* genus existed during the whole fermentation process with a relative abundance of 9.8% at day 10, then decreased to 5.8% at the end of the incubation (Fig. 5.7c). *Oscillibacter* is known to be involved in acidogenesis during dark fermentation (Goud et al., 2017) and this microorganism might play a role in the acetic acid accumulation during the adaption stage. change by enriched sludge sampled on day 70 using H_2/CO_2 as the substrate.

5.4 Discussion

5.4.1 VFAs and ethanol production by anaerobic granular sludge in the gas fed reactor

This study showed that 100% H₂ addition induced both butyric acid and ethanol production, while 10 μM tungsten induced caproic acid production at a pH as low as 4.5-5.0. Ethanol production was observed during the H₂/CO₂ fermentation process and 100% H₂ as electron donor, but it was subsequently degraded. Considering the inoculum applied was an undefined mixed culture, ethanol has been degraded to acetic acid in the presence of CO₂ (Eq. 5) or used as the electron donor for butyric acid production (Eq. 6).



The first ethanol degradation (day 11) was possibly due to its oxidation to acetic acid in the presence of CO₂ since butyric acid production was insignificantly observed at that time (Fig. 5.2a). The second ethanol decrease (day 37-50) possibly supplied butyric acid production via the reverse β oxidation pathway (Grootscholten et al. 2013), during which the butyric acid concentration increased along with the ethanol consumption (Fig. 5.2). Considering ethanol production occurred at pH of 6.5 at day 11, at the second ethanol decrease at pH 4.5, the pH increase might induce ethanol accumulation.

The presence of CO₂ on ethanol utilization could have induced formation of longer chain fatty acids. Roghair et al. (2018) reported butyric acid and caproic acid production via controlling the ethanol use under different CO₂ loading rates (0.5 and 2.5 LCO₂·L⁻¹·d⁻¹) by anaerobic granular sludge. However, our previous study using the same anaerobic granular sludge demonstrated that the ethanol oxidation to acetic acid was priority over chain elongation in the presence of CO₂ at initial pH 5.7 and 6.5 by the same anaerobic granular sludge (He et al., 2022).

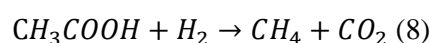
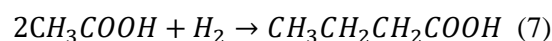
H₂ acted as electron donor for chain elongation process, which has been reported in the literature (Baleeiro et al., 2021). Tungsten enhanced chain elongation process at pH 4.0-4.5. Caproic acid production occurred at a pH as low as 4, which was seldom reported since chain elongation processes generally occur at high pH value (Ganigué et al., 2016). On the other hand, acetogens adding a carbon to the carbon chain could be enriched after the second ethanol degradation and further contributed to the chain elongation process. Further research is required with ¹³C NMR and labelled substrate (e.g., CO₂, ethanol and acetate) to elucidate the biochemical conversions in the sludge.

5.4.2 Methane production in batch tests by enriched sludge in batch tests

This study showed that, with gaseous H₂/CO₂, 15 mM acetic acid addition reached the highest methane production, CO₂ and H₂ consumption compared to the 0, 10, 30 and 45 mmol·L⁻¹ acetic acid addition by enriched sludge (day 70) (Fig. 5.3a, b, Fig. 5.4). Despite of the different extent of gas consumption, methane occupied the main product of the enriched sludge. An initial pH of 6 could be attributed to the methane production in batch tests by the enriched sludge while methane production was totally inhibited at pH 4.5-4.7 in the bioreactor. The inhibited methane production in the reactor could be attributed to the heat pre-treatment and the long-time operation at low pH of 4.5. However, along with the operation, methanogens could be enriched in the inoculum although the production of methane can be inhibited at a pH of 4.5 (Fernández-Naveira et al., 2017). Although methane production can be inhibited when the pH was lower than 6, its production has been observed in a few reactors operating at low pH, especially along with increased operation time (Chakraborty et al., 2019). Another reason might be the gas feeding mode or different mass transfer rate between 1 bar gas pressure in the reactor, whereas an initial 1.8 bar in the batch bottles. Higher gas pressure induced more CO₂ dissolution in the medium and may stimulate hydrogenotrophic methanogens (Roghair et al. 2018).

5.4.3 Effect of exogenous acetate on acetogenesis and methanogenesis by enriched sludge

This study showed that exogenous acetate with 10, 15, 30 and 45 mmol·L⁻¹ cannot be used for ethanol or methane production in the presence of 100% H₂ by the enriched sludge. Even with H₂/CO₂ as the gaseous substrate, the maximum acetate consumption occupied 13.3% (thus 2 mmol·L⁻¹) in the 15 mmol·L⁻¹ acetate incubation. Ethanol (Eq. 7) and methane (Eq. 8) production from exogenous acetate failed using 100% H₂ as electron donor by the enriched sludge. This might be because the enriched microorganisms after 70 days incubation in the bioreactor were autotrophic acetogens, such as the *Clostridia* and *Bacilli* class using CO₂ instead of acetate as the substrate.



5.5 Conclusion

Autotrophic acetogens were enriched in a H₂/CO₂ gas fed reactor for acetic acid, butyric acid and caproic acid production from heat-treated anaerobic granular sludge treating dairy wastewater. 100% H₂ induced butyric acid and ethanol production at pH 4.5-5, but ethanol was degraded and might have contributed to the butyric acid production. 10 μM tungsten addition induced caproic acid production at pH 4.0-4.5. The *Clostridia* order was enriched at the end of the gas fed reactor and contributed to VFAs and ethanol production. The enriched sludge mainly produced methane from H₂/CO₂, exogenous acetate and ethanol in batch incubations at pH 6 and 25°C. The enriched sludge failed to convert acetate and 100% H₂ to ethanol at an initial pH of 6.

5.6 References

Abrini, Jamal, Henry Naveau, and Edmond-Jacques Nyns. 1994. *Clostridium autoethanogenum*, sp. nov., an anaerobic bacterium that produces ethanol from carbon monoxide. Archives of Microbiology 161 (4): 345–51.

Andreesen, Jan R, and Kathrin Makdessi. 2008. Tungsten, the surprisingly positively acting heavy metal element for prokaryotes. Annals of the New York Academy of Sciences 1125 (1): 215–29.

Angly, F. E., Dennis, P. G., Skarszewski, A., Vanwonterghem, I., Hugenholtz, P. and Tyson, G. W., 2014. CopyRighter: a rapid tool for improving the accuracy of microbial community profiles through lineage-specific gene copy number correction. Microbiome 2 (1): 11.

Baleeiro, F., Struber, H. and Kleinstuber, S. 2021. Hydrogen as a co-electron donor for chain elongation with complex communities. Frontiers in Bioengineering and Biotechnology, 9: 251.

Bhatia, S. K., Bhatia, R. K., Jeon, J. M. , Kumar, G. and Yang, Y. H. 2019. Carbon dioxide capture and bioenergy production using biological system – a review. Renewable and Sustainable Energy Reviews, 110, 143-158.

Chakraborty, S., Rene, E.R., Lens, P. N. L., Veiga, M.C. and Kennes, C. 2019. Enrichment of a solventogenic anaerobic sludge converting carbon monoxide and syngas into acids and alcohols. Bioresource Technology, 272: 130-136.

Chakraborty, S., Rene, E. R., Lens, P. N. L., Rintala, J., and Kennes, C., 2020. Effect of tungsten and selenium on C₁ gas bioconversion by enriched anaerobic sludge and microbial community analysis. Chemosphere, 250: 126105.

Cotter, J. L., Chinn, M. S., and Grunden, A. M., 2009. Ethanol and acetate production by *Clostridium ljungdahlii* and *Clostridium autoethanogenum* using resting cells. *Bioprocess and Biosystems Engineering* 32 (3): 369–80.

Fernández-Naveira, Á., Veiga, M.C. and Kennes, C., 2017. H-B-E (hexanol-butanol-ethanol) fermentation for the production of higher alcohols from syngas/waste gas. *Journal of Chemical Technology & Biotechnology*, 92 (4): 712-731.

Ganigué, R., Sánchez-Paredes, P., Bañeras, L. and Colprim, J., 2016. Low fermentation pH is a trigger to alcohol production, but a killer to chain elongation. *Frontiers in Microbiology* 7: 702.

Goud, R. K., Arunasri, K., Yeruva, D. K., Krishna, K. V., Dahiya, S. and Mohan, S. V., 2017. Impact of selectively enriched microbial communities on long-term fermentative biohydrogen production. *Bioresource Technology* 242: 253-264.

Grootscholten, T., Steinbusch, K., Hamelers, H. and Buisman, C., 2013. Chain elongation of acetate and ethanol in an upflow anaerobic filter for high rate MCFA production. *Bioresource Technology* 135: 440–445.

Gunes, B. 2021. A critical review on biofilm-based reactor systems for enhanced syngas fermentation processes. *Renewable and Sustainable Energy Reviews*, 143, 110950.

He, Y., Cassarini, C., Marciano, F. and Lens P. N. L., 2020. Homoacetogenesis and solventogenesis from H₂/CO₂ by granular sludge at 25, 37 and 55°C. *Chemosphere*, 265: 128649.

He, Y., Lens, P. N., Veiga, M. C. and Kennes, C., 2022. Selective butanol production from carbon monoxide and syngas by an enriched anaerobic culture. *Science of the Total Environment*. 806, 150579.

Karekar, S. C., Srinivas, K. and Ahring, B. K. 2020. Continuous in-situ extraction of acetic acid produced by *Acetobacterium woodii* during fermentation of hydrogen and carbon dioxide using amberlite fpa53 ion exchange resins. *Bioresource Technology Reports*, 12, 100568.

Liou, J. S. C., Balkwill, D. L., Drake G. R. and Tanner R. S. 2005. *Clostridium carboxidivorans* sp. nov. a solvent-producing *Clostridium* isolated from an agricultural settling lagoon, and reclassification of the acetogen *Clostridium scatologenes* strain sl1 as *Clostridium drakei* sp. nov. *International Journal of Systematic and Evolutionary Microbiology*, 55(5), 2085-2091.

Liu, K., Atiyeh, H. K., Stevenson, B. S., Tanner, R. S. , Wilkins, M. R. and Huhnke, R. L. 2014. Mixed culture syngas fermentation and conversion of carboxylic acids into alcohols. *Bioresource Technology*, 152: 337-346.

Liu, R., Hao, X. and Wei, J. 2016. Function of homoacetogenesis on the heterotrophic methane production with exogenous H₂/CO₂ involved. *Chemical Engineering Journal*, 284, 1196-1203.

Modestra, J. A., Katakojwala, R., and Mohan, S. V. 2020. CO₂ fermentation to short chain fatty acids using selectively enriched chemolithoautotrophic acetogenic bacteria. *Chemical Engineer Journal*, 394:124759.

Mohammadi, M., Younesi, H., Najafpour, G. and Mohamed, A. R., 2012. Sustainable ethanol fermentation from synthesis gas by *Clostridium ljungdahlii* in a continuous stirred tank bioreactor. *Journal of Chemical Technology & Biotechnology* 87 (6): 837-843.

Padan, E., Zilberstein, D. and Schuldiner, S. 1981. pH homeostasis in bacteria. *Biochimica et Biophysica Acta (BBA)-Reviews on Biomembranes* 650 (2–3): 151–66.

Roghair, M., Hoogstad, T., Strik, D., Plugge, C. M., Timmers, P., Weusthuis, R. A., Bruins, M. E., Buisman, C., 2018. Controlling ethanol use in chain elongation by CO₂ loading rate. *Environmental Science & Technology*, 52 (3): 1496-1505.

Stoll, I. K., Herbig, S., Zwick, M., Bookish, N., Sauer, J., Neumann, A. and Oswald, F. 2018. Fermentation of H₂ and CO₂ with *Clostridium ljungdahlii* at elevated process pressure—first experimental results. *Chemical Engineering Transactions*, 64: 151-156.

Xu, H., Liang, C., Chen, X., Xu, J., Yu, Q., Zhang, Y. and Yuan, Z. 2020. Impact of exogenous acetate on ethanol formation and gene transcription for key enzymes in *Clostridium autoethanogenum* grown on CO. *Biochemical Engineering Journal*, 155: 107470.

Yamamoto, I., Saiki, T., Liu, S. M. and Ljungdahl, L. G. 1983. Purification and properties of NADP-dependent formate dehydrogenase from *Clostridium thermoaceticum*, a tungsten-selenium-iron protein. *Journal of Biological Chemistry*, 258 (3): 1826–1832.

Chapter 6 Selective butanol production from carbon monoxide by an enriched anaerobic culture

A modified version of this chapter has been published as:

He Y., Lens, P. N. L., Veiga, M. C. and Kennes, C. 2022. Selective butanol production from carbon monoxide by an enriched anaerobic culture. *Science of the Total Environment*, 806, 150579.

Abstract

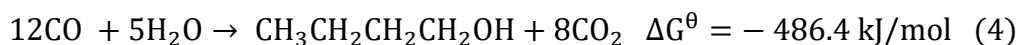
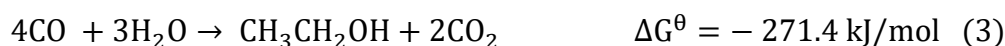
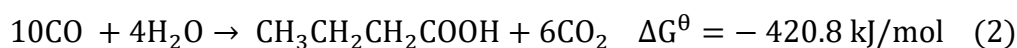
An anaerobic mixed culture able to grow on pure carbon monoxide (CO) as well as syngas (CO, CO₂ and H₂) that produced unusual high concentrations of butanol was enriched in a bioreactor with intermittent CO gas feeding. At pH 6.2, it mainly produced acids, generally acetic and butyric acids. After adaptation, under stress conditions of CO exposure at a partial pressure of 1.8 bar and low pH (e.g., 5.7), the enrichment accumulated ethanol, but also high amounts of butanol, up to 6.8 g/L, never reported before, with a high butanol/butyric acid molar ratio of 12.6, highlighting the high level of acid to alcohol conversion. At the end of the assay, both the acetic acid and ethanol concentrations decreased, with concomitant butyric acid production, suggesting C₂ to C₄ acid bioconversion, though this was not a dominant bioconversion process. The reverse reaction of ethanol oxidation to acetic acid was observed in the presence of CO₂ produced during CO fermentation. Interestingly, butanol oxidation with simultaneous butyric acid production occurred upon production of CO₂ from CO, which has to the best of our knowledge never been reported. Although the sludge inoculum contained a few known solventogenic *Clostridia*, the relative taxonomic abundance of the enriched sludge was diverse in *Clostridia* and Bacilli classes, containing known solventogens, e.g. *Clostridium ljungdhalii*, *Clostridium ragsdalei* and *Clostridium coskatii*, confirming their efficient enrichment. The relative abundance of unassigned *Clostridium* species amounted to 27% with presumably novel ethanol/butanol producers.

6.1 Introduction

Biofuels such as ethanol and butanol are commercially produced from sugars, corn starch and lignocellulosic biomass (Munasinghe and Khanal, 2010). Alternatively, these feedstocks can be gasified to syngas, a mixture of CO, CO₂ and H₂, which can then also be converted to ethanol, butanol or other valuable chemicals by biocatalysis (Kennes et al., 2016; Wang et al., 2014). Syngas fermentation has raised attention recently, among others for its advantage of using non-food feedstock (Devarapalli and Atiyeh, 2015). In addition, in biomass gasification the whole feedstock (cellulose, hemicellulose and lignin) is converted to syngas, while fermentation processes only use the cellulose and hemicellulose fractions of the lignocellulosic biomass. Also, syngas is an off gas of the steel industry, thus this cheap gas substrate can make syngas-based butanol production more economical (Yu et al., 2015). CO is one of the main components of syngas. Therefore, its biological conversion to biofuels such as ethanol and butanol has become a promising approach (Fernández-Naveira et al., 2017a). Butanol has a

similar energy content as gasoline and a higher commercial value than ethanol. It can potentially replace and reduce fossil fuel consumption (Fast et al., 2015).

The low energy density and toxicity of CO limit its use in biological processes, but some acetogens such as *Clostridium carboxidivorans*, *Clostridium autoethanogenum*, *C. ljungdahlii* and *Clostridium acetivum* can convert CO to acids, ethanol (Arslan et al., 2019; Devarapalli et al., 2016; Richter et al. 2013) and, occasionally, butanol (Phillips et al., 2015; Fernández-Naveira, 2016a). Acetogens possess the key enzyme carbon monoxide dehydrogenase to convert CO to CO₂, with acetyl-CoA as main intermediate, following the Wood-Ljungdahl metabolic pathway (WLP) (Fernández-Naveira et al., 2017a). The production of alcohols from CO takes place in two stages, i.e. acids (e.g. acetic acid and butyric acid) are produced first (acetogenesis, Eq. 1, 2) along with cell growth, followed by the production of alcohols such as ethanol and butanol (solventogenesis, Eq. 3, 4):



Solventogenesis has been shown to be triggered by stress conditions, such as high CO partial pressure, nutrient limitation or low pH (Benomar et al. 2015; Mohammadi et al. 2012). For example, *C. autoethanogenum* and *C. ljungdahlii* produced ethanol when the pH of the medium was around 4.75 to 5 under mesophilic conditions, while acids were produced at higher pH values (Guo et al., 2010; Fernández-Naveira et al., 2016a; Stoll et al., 2018). Besides *Clostridium* spp., some other bacteria have occasionally been reported to produce alcohols. For example, the alkaliphilic species *Alkalibaculum bacchi* grows at pH 6.5-10.5 and also produces ethanol and acetate from CO/CO₂ (Allen et al., 2010).

Limited studies have reported mixed culture C₁-gas fermentation for the production of alcohols, such as butanol, from 100% CO (Chakraborty et al., 2019). Only some *Clostridium* strains, such as pure cultures of *C. carboxidivorans* (Fernández-Naveira et al., 2016a, 2016b, 2017b) and co-cultures of *C. autoethanogenum* and *Clostridium kluyveri* (Diender et al., 2016) produce these alcohols from 100% CO. From a practical point of view, however, mixed culture fermentations are easier to implement at large scale compared to pure cultures, as they do not require sterile bioreactor conditions compared to pure cultures (Kamil et al., 2019). Moreover, they are more resistant to unfavorable environmental conditions, such as low pH, which enables easier implementation at large scale compared to pure cultures (Liu et al., 2014). On the other

hand, the production of butanol from CO by mixed cultures has been scarcely studied (Fernández-Naveira et al., 2017a; Humphreys and Minton, 2018).

Anaerobic sludges from wastewater treatment plants are a source of microbial species capable of CO to alcohol conversion (Arantes et al., 2020). CO can be metabolized by a variety of trophic groups present in these anaerobic sludges such as methanogens, hydrogenogens and acetogens (Li et al., 2020). Heat pretreatment is an effective way to inhibit methanogens and select spore-forming acetogens, converting CO into acids and solvents (Cai and Wei, 2004; Monlau et al., 2013). To date, studies that reached high butanol concentrations from C₁ gases are scarce (Fernández-Naveira 2017a). Concentrations exceeding 2.7 g/L have never been reported from syngas or pure CO bioconversion (Fernández-Naveira et al., 2016a). Therefore, this study aimed at obtaining higher and selective ethanol and butanol production using CO as the sole carbon source with an anaerobic granular sludge as inoculum in an intermittent gas-fed incubation to enrich for efficient CO converting solventogenic acetogens from anaerobic granular sludge. In addition, a pH shift from 6.2 to 5.7 was applied for inducing solventogenesis from CO. The conversion pathway for selective butanol production by the enriched sludge in CO fed batch reactor was elucidated.

6.2 Materials and methods

6.2.1 Biomass

Anaerobic granular sludge was obtained from a 200 m³ upflow anaerobic sludge bed reactor producing methane from dairy industry effluent (He et al., 2020) at 20 °C and a hydraulic retention time of 9-12 h (He et al. 2020). The total solids (TS) and volatile solids (VS) content were 42.7 (± 1.0) g/L and 24.8 (± 0.5) g/L, respectively. The anaerobic sludge was first centrifuged at 8000 g for 10 minutes to remove the supernatant and then heat treated at 90 °C for 15 minutes as described by Dessì et al. (2017).

6.2.2 Medium composition

The culture medium was prepared according to Stams et al. (1993) with some modifications as follows (/L): 408 mg KH₂PO₄, 534 mg Na₂HPO₄·2H₂O, 300 mg NH₄Cl, 300 mg NaCl, 100 mg MgCl₂·6H₂O, 110 mg CaCl₂·2H₂O; 1 mL trace metal and 1 mL vitamin stock solution (Stams et al., 1993). Once prepared, medium (except for CaCl₂·2H₂O and vitamins) was brought to boiling to remove O₂, then cooled down to room temperature under an oxygen-free N₂ flow. CaCl₂·2H₂O and the vitamins were subsequently added, as well as

Na₂S (0.24 g) as the reducing agent. To enhance the biomass growth, 0.5 g/L yeast extract was used from day 70 onwards in the fed batch reactor and in all batch experiments.

6.2.3 Experimental set-up

6.2.3.1 Gas-fed enrichment

Intermittent gas-fed enrichment experiments were carried out in two 1 L serum bottles (Fisherbrand, FB-800-1100, Waltham, U.S., fed batch reactors) with 300 mL medium and heat-treated anaerobic granular sludge at an initial VS concentration of 1.0 g/L (Fig. 6.1). The first fed batch reactor was set-up with no pH control for 127 days fermentation (FB1). Enriched sludge was obtained after 127 days fermentation in FB1 and used as the inoculum for a second, pH controlled, CO fed batch reactor (FB2, see 6.4.1.2) with pH controlled at 6.2 and 5.7 for 35 days fermentation, as well as several batch tests (see 6.4.2) to study its metabolic properties.

The fed batch reactors were sealed with a gas tight septum fitted with a pH probe (9,5×300 mm, VWR) in the middle. The pH probe was connected to a pH controller (Cole-Parmer 300, Cambridgeshire, UK) and pH was adjusted using either 1 M NaOH or HCl solutions by two pumps (Verdeflex, The Netherland). The fed batch reactors were agitated at 150 rpm by a shaker (Infors AG CH-4103, Bottmingen, Switzerland) at 33 °C in a thermostatic chamber. Considering the positive role of CO partial pressure of 1.7 or 2.5 bar on solventogenesis (Hurst and Lewis, 2010; Lanzillo et al., 2020) and for consistency with the gas pressure of 1.8 bar of our previous study (He et al., 2020), an initial CO pressure of 1.8 bar was used in this study. CO was supplied to the headspace of the reactor as the sole carbon source and electron donor to reach an initial gas pressure of 1.8 bar. When the gas pressure decreased below 1 bar, as a result of bacterial CO gas consumption (corresponding to one CO feeding), the reactor was flushed with fresh pure CO for about 5 minutes, until reaching again a gas pressure of 1.8 bar.

In FB1, CO was added 19 times in total. An initial pH of 6.2 was applied at stages I and V and an initial pH 5.7 was applied at stage II, III, IV and VI (Table 6.1). The pH was adjusted at the beginning of each CO feeding since the pH was not controlled (Table 6.1).

6.2.3.2 Batch experiments

Batch experiments of conversion pathway elucidation were conducted in 500 mL serum bottles with 100 mL medium and 10% enriched sludge taken from the first CO fed bioreactor operating for 127 days. Batch experiments of CO and syngas fermentation were conducted in 125 mL serum bottles with 30 mL medium and 10% enriched sludge. The bottles were sealed with rubber stoppers and capped with aluminum crimp caps. All bottles were pressurized with CO or syngas at an initial pressure of 1.8 bar and were incubated at 150 rpm and at 33°C.

Enriched sludge in this study refers to the sludge taken from the CO fed FB1 after 127 days of operation.

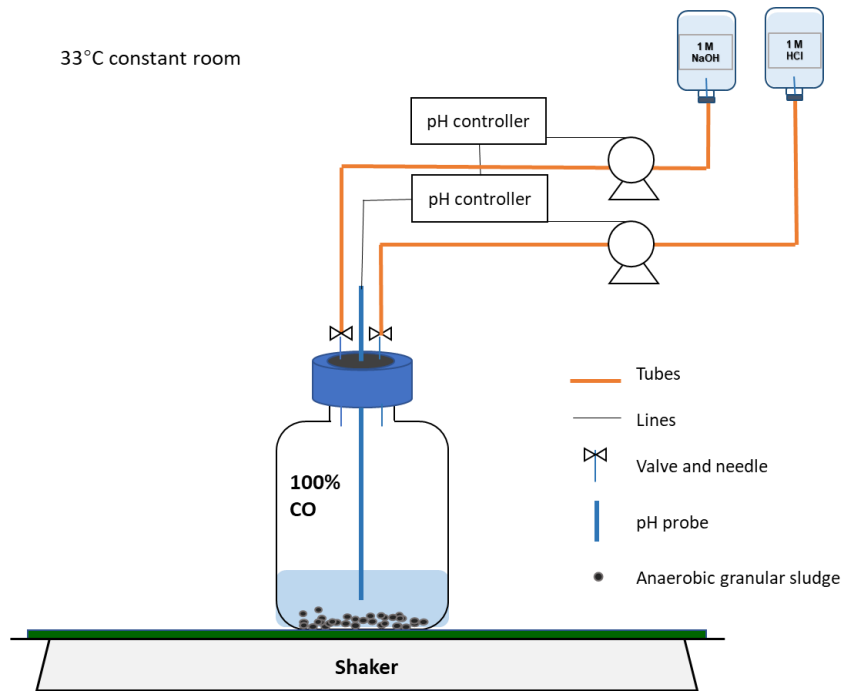


Fig. 6.1 Schematic diagram of the CO fed batch reactor set-up.

Table 6.1 The operational conditions and production profile, highest alcohol to acids ratio and highest concentration of acids and alcohols in period I (0- 99 d) and II (100-127 d) in FB1 using CO as the sole substrate by the heat treated enriched anaerobic culture.

	Duration	Period I (0-99 d)			Period II (100-127 d)		
Operational conditions		Stage I (15-33 d)	Stage II (34-40 d)	Stage III (41- 99 d) Storage at 4°C (40-70 d)	Stage IV (100- 106 d)	Stage V (107-110 d)	Stage VI (111-127 d)
	Initial pH	6.2	5.7	5.7	5.7	6.2	5.7
	Main products	H ₂	Acetic acid	Ethanol Butanol	Ethanol Butanol	Acetic acid Butyric acid	Butanol
	Yeast extract	0			150 mL fresh medium replacement and 0.5 g/L YE addition at 100 d		
Highest concentrations (g/L)	Acetic acid	4.5			7.2		
	Ethanol	1.0			2.2		
	Propionic acid	0.4			0.4		
	Butyric acid	0.9			3.0		
	Butanol	0.4			6.8		
	CO ₂ accumulation	151.9			261.0		
	pH	3.8-6.2			4.8-6.5		
Highest ratio	Ethanol/acetic acid	5.1			3.6		
	Butanol/butyric acid	0.6			12.6		
CO conversion efficiency to acids and alcohols (%)		30.3			21.4		
Carbon balance (%)		91.0			68.2		

6.2.4 Experimental design

6.2.4.1 Fed-batch reactor operation

6.2.4.1.1 Biomass enrichment and selective butanol production in FB1

The operation for the enrichment in FB1 had two periods. Period I lasted for 99 days and was comprised of several stages, i.e. H₂ production (stage I, 15-33 d), acetic acid accumulation (stage II, 34–40 d) and ethanol and butanol production (stage III, 41 – 100 d) stage. Along with acetic acid accumulation, the FB1 reactor pH was adjusted back to pH 4.8-5.2 at day 36-40 to avoid the pH decreasing further and stimulate ethanol production (Ganigué et al., 2016) and the pH was sustained at 4.8-5.2 till 69 d. At day 40 (the beginning of stage III), the reactor was maintained at 4°C in the fridge for 30 days and later put back at 33°C. Therefore, a 10 days adaptation period was required from day 70 to 80 (Fig. 6.2).

After 99 days CO feeding (the start of Period II), considering only limited activity of acid and alcohol production was detected and exhaustion of some nutrients was expected, 150 mL medium was removed and replaced by 150 mL fresh medium with initial pH of 6.2. 0.5 g/L yeast extract (YE) was added to the medium in order to obtain a higher biomass concentration and reduce the adaptation period, as YE is well known to stimulate CO converting bacterial growth (Diender et al., 2016). Period II comprised of an acetic acid accumulation (stage IV, 100-106 days), butyric acid production (stage V, 107-110 d) and butanol accumulation (stage VI, 111-127 d) stage.

6.2.4.1.2 Controlled pH at 6.2 and 5.7 in the FB2

To better understand the effect of pH on ethanol and butanol production, FB2 was operated with pH control at high pH 6.2 to obtain acetic acid and butyric acid production and low pH 5.7 to stimulate solventogenesis. FB2 was inoculated with 10% enriched sludge from FB1. In total, 12 times CO was added to this bioreactor, which was operated for 35 days.

6.2.4.2 Batch tests

6.2.4.2.1 Metabolic pathway elucidation in enrichment

Experiments were performed to test if some of the observed bioconversions with the enriched sludge (sampled day 127 d in FB1) follow the reverse β -oxidation pathway and to try to elucidate why ethanol and butanol concentrations occasionally decreased during the fermentation process in case of CO₂ accumulation. Four experimental assays were conducted with 2.2 g/L acetic acid and 6 g/L ethanol and with either 100% N₂ or 100% CO₂ at initial pH 5.7 and 6.2, using 10% enriched sludge as inoculum.

To investigate the effect of accumulated CO₂ on butanol oxidation during the fermentation process, a batch experiment was set up with 3.8 g/L butanol and with CO₂ in the gas phase, at

either initial pH 6.5 or 5.7 with 10% enriched sludge (sampled on day 127) as inoculum to investigate possible butanol oxidation to butyric acid by CO₂.

6.2.4.2.2 Ethanol and butanol production from CO/syngas by enriched sludge in batch tests

The enriched sludge taken from FB1 (127 d) was tested for syngas bioconversion in 125 ml serum bottles with 10% inoculum and 30 ml culture medium with 0.5 g/L yeast extract addition. The headspace was flushed with syngas, i.e. CO/CO₂/H₂/N₂ (v/v, 20/20/10/50) or 100 % CO to an initial pressure of 1.8 bar. Control bottles were set up with 100% N₂ at the initial pressure of 1.8 bar and 10% enriched sludge as inoculum. All experiments were performed in duplicate.

6.2.4.3 Sampling

In FB1 and FB2, the gas pressure was measured daily. 1 mL of liquid sample was withdrawn daily for measuring the cell concentration (OD₆₀₀) and pH. It was then centrifuged at 8000×g for 5 min and the supernatant was used to analyze the short chain volatile fatty acids, ethanol and butanol concentrations. 1 mL gas sample was taken at the end of each CO feeding to determine the H₂, CO, CO₂ and CH₄ concentrations in FB1. In the batch tests, the cell concentration, pH, short chain volatile fatty acids, ethanol and butanol concentrations were analyzed every two days after cell growth was observed.

6.2.5 Carbon balance calculation

The change of the total amount of carbon was defined as the carbon concentration at time 0 compared to time t. The change of the total amount of carbon of the substrate equals the sum of the total amount of carbon of the products and biomass (Eq. 5). The carbon recovery α was calculated by the ratio between the total amount of carbon of the products and the substrates (Eq. 6):

$$\sum_{i=1}^m C_{s_i}(0) - \sum_{i=1}^m C_{s_i}(t) = \sum_{j=1}^m C_{p_j}(t) + C_b(t) \quad (5)$$

$$\alpha = \frac{\sum \Delta C_{p_j}}{\sum \Delta C_{s_i}} \times 100\% \quad (6)$$

where C_{s_i} is the substrate carbon, C_{p_j} the product carbon and C_b the carbon concentration of the biomass

6.2.6 Microbial analysis

DNA was extracted using a DNeasy® PowerSoil Kit (QIAGEN, Germany) following the manufacturer's protocol. 10 mL enriched sludge taken from the CO fed FB1 after 127 days of operation was used for DNA extraction. The extracted DNA was analyzed by Metagenomics-Seq (Illumina PE150, Q30 \geq 80%) (Novogene, UK). Taxonomic annotation analysis involved comparing metagenomic reads to the database of taxonomically informative gene families (NR database) to annotate each metagenomic homolog (Mende et al., 2012). Taxonomic diversity involves identifying those reads that are marker gene homologs to a database of taxonomically informative gene families, using sequence or phylogenetic similarity to the database sequences (NR database; Buchfink et al., 2015) to taxonomically annotate each metagenomic homolog (MEGAN; Huson et al., 2011). According to the abundance table of each taxonomic level, various analyses were performed including Krona analysis, bar plot for abundant species and heatmap of abundance (Ondov et al., 2011). For more details on the analysis procedure, please see the following:

6.2.6.1 Experimental procedures of Metagenomic sequencing

1) Sample testing. There are mainly three methods for DNA samples: (1) DNA degradation degree and potential contamination was monitored on 1% agarose gels. (2) DNA purity (OD_{260}/OD_{280} , OD_{260}/OD_{230}) was checked using the NanoPhotometer® spectrophotometer (IMPLEN, CA, USA). (3) DNA concentration was measured using Qubit® dsDNA Assay Kit in Qubit® 2.0 Fluorometer (Life Technologies, CA, USA). OD value is between 1.8~2.0, DNA contents above 1 μ g are used to construct a library.

2) Library construction. A total amount of 1 μ g DNA per sample was used as input material for the DNA sample preparations. Sequencing libraries were generated using NEBNext® Ultra™ DNA Library Prep Kit for Illumina (NEB, USA) following the manufacturer's recommendations and index codes were added to attribute sequences to each sample. Briefly, the DNA sample was fragmented by sonication to a size of 350bp, then DNA fragments were end-polished, A-tailed, and ligated with the full-length adaptor for Illumina sequencing with further PCR amplification. At last, PCR products were purified (AMPure XP system) and libraries were analysed for size distribution by Agilent2100 Bioanalyzer and quantified using real-time PCR.

3) Sequencing. The library preparations were sequenced on an Illumina NovaSeq platform and paired-end reads were generated.

6.2.6.2 Bioinformatic Analysis

1) Data Quality Control: Raw Data contained a certain percentage of low-quality data after sequencing. To ensure the accuracy and reliability of the subsequent information analysis, quality control and host filtering of the raw data were carried out to obtain effective data (Clean Data);

2) Metagenome Assembly: Metagenome was assembled based on Clean Data after quality control of each sample, and put the unutilized reads of each sample together for mixed assembly to explore the information of low-abundance species of the samples;

3) Gene Prediction: The gene prediction was carried out by MetaGeneMark based on the scaftigs which were assembled by single and mixed samples. Pool the predicted genes together for dereplication to construct gene catalogue. Based on the Clean Data of each sample from the gene catalogue, the abundance information of the gene catalogue for each sample could be obtained;

4) Taxonomy Annotation: This procedure involved comparing metagenomic reads to the database of taxonomically informative gene families (NR database) to annotate each metagenomic homolog. The abundance tables of different taxonomic ranks were based on gene abundance table.

The raw data is available in OneDrive NUIG.

6.2.7 Analytical methods

Gas pressure was measured by a pressure gauge (LEO1, Keller, Winterthur, Switzerland). Acetic, propionic and butyric acid as well as ethanol and butanol were determined by high performance liquid chromatography (HPLC, HP1100, Agilent Co., Palo Alto, USA) equipped with a refractive index detector and Agilent Hi-Plex H Column (300×7.7 mm) as described by Arslan et al. (2019). A 5 mmol·L⁻¹ H₂SO₄ solution was used as the mobile phase at a flow rate of 0.80 mL/min. The sample injection volume was 20 μL and the column temperature 45 °C. The cell concentration was determined with a spectrophotometer (Hitachi, Model U-200, Pacisa & Giralt, Spain) at a wavelength of 600 nm (Arslan et al., 2019).

H₂ and CO were determined on a HP 6890 gas chromatograph (GC, Agilent Technologies, Madrid, Spain) equipped with a thermal conductivity detector (TCD) and a 15-m HP-PLOT Molecular Sieve 5A column (ID 0.53 mm; film thickness 50 μm) as described by Arslan et al. (2019). The initial oven temperature was kept constant at 50 °C for 5 min and then raised by 20 °C/min for 2 min, to reach a final temperature of 90 °C. The temperature of the injection port and the detector were maintained constant at 150 °C. Helium was used as the carrier gas

at a flow rate of 2 mL/min. CO₂ and CH₄ were measured on an HP 5890 gas chromatograph (GC, Agilent Technologies, Spain) equipped with a TCD (Arslan et al., 2019). The injection, oven, and detection temperatures were maintained at 90, 25, and 100 °C, respectively. The area obtained from the GC was correlated with the concentration of the gases as described by Chakraborty et al. (2019).

6.3 Results

6.3.1 Enrichment and selective butanol production by anaerobic granular sludge in FB1

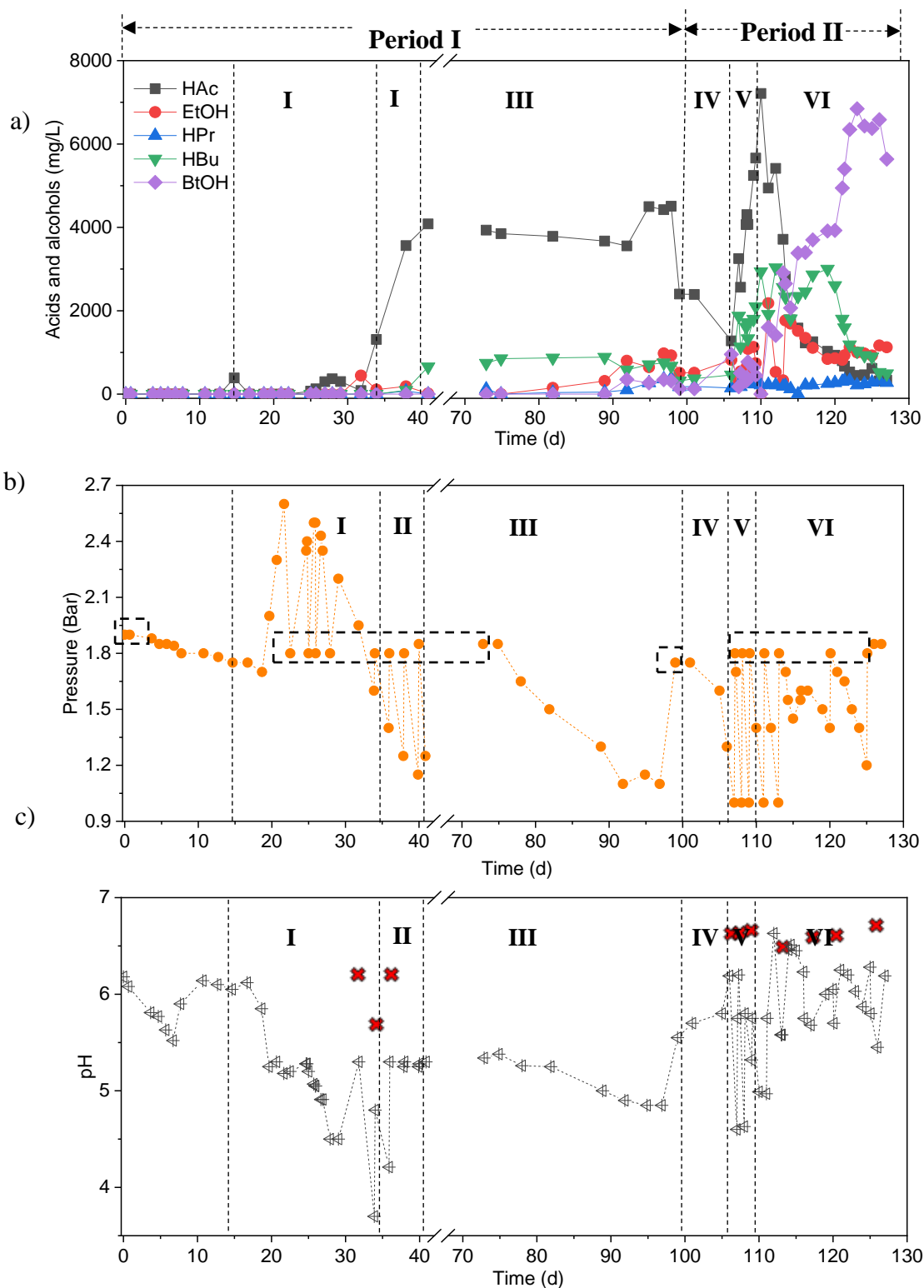
6.3.1.1 Acetic acid and butyric acid production from CO at initial pH 6.2 (Period I)

During Stage I (15-33 d) of Period I, H₂ production was initially observed, with a transient accumulation of 0.39 g/L acetic acid after two weeks (Fig. 6.2a). H₂ started being produced concomitantly with CO consumption and this lasted till 33 d (Fig. 6.2d), suggesting an initial enrichment of H₂ producing bacteria. After that, hydrogen accumulation leveled off with a simultaneous boost in acetic acid production (Fig. 6.2a). The gas pressure increased from 1.8 bar initially to a maximum of 2.6 bar due to H₂ and CO₂ production (Fig. 6.2b). The pH of the enrichment medium decreased from an initial pH 6 to pH 5.3 when H₂ started being produced (Fig. 6.2c). The CO consumption rate increased from 2.89 to 31.12 mmol·L⁻¹·d⁻¹ and both the H₂ and CO₂ production rate increased, respectively, from 1.89 to 41.27 mmol·L⁻¹·d⁻¹ and 1.48 and 25.37 mmol·L⁻¹·d⁻¹ from 21 to 27 d (Fig. 6.2e). When H₂ production levelled off, the accumulation of H₂ and CO₂ reached, respectively, 66.7 and 66.6 mmol·L⁻¹ and the amount of CO consumed reached 88.8 mmol·L⁻¹ (Fig. 6.2d).

Stage II (34–40 d) was dominated by acetic acid accumulation. The highest concentration of acetic acid reached 4.2 g/L at 40 d, together with 0.66 g/L butyric acid. A small peak of 0.45 g/L ethanol was found at day 32, but then gradually decreased to reach 0.01 g/L on day 40. The CO consumption rate decreased at 27-33 d, but then increased from 5.14 to 15.15 mmol·L⁻¹·d⁻¹ at 33-40 d (Fig. 6.2e).

Stage III (41 – 99 d) was characterized by ethanol and butanol production after a 10 days adaptation period from day 70 to 80, subsequent the 30 day storage of the sludge at 4 °C (Fig. 6.2a). The highest ethanol, butanol and butyric acid concentrations were, respectively, 0.98, 0.35 and 0.89 g/L (Fig. 6.2a). Acetic acid showed a slight decrease (3.79 to 3.56 g/L), while ethanol increased from 0.15 g/L to 0.80 g/L from 81 to 91 d (Fig. 6.2a). Thereafter, the acetic acid concentration increased from 3.56 g/L at 61 d to 4.50 g/L at 94 d during which the CO pressure slowly decreased (Fig. 6.2d). The ethanol concentration increased to 0.98 g/L at 96 d

(Fig. 6.2a, c). After day 96, another stable phase of acetic acid and ethanol production established till the end of Period I (day 99).



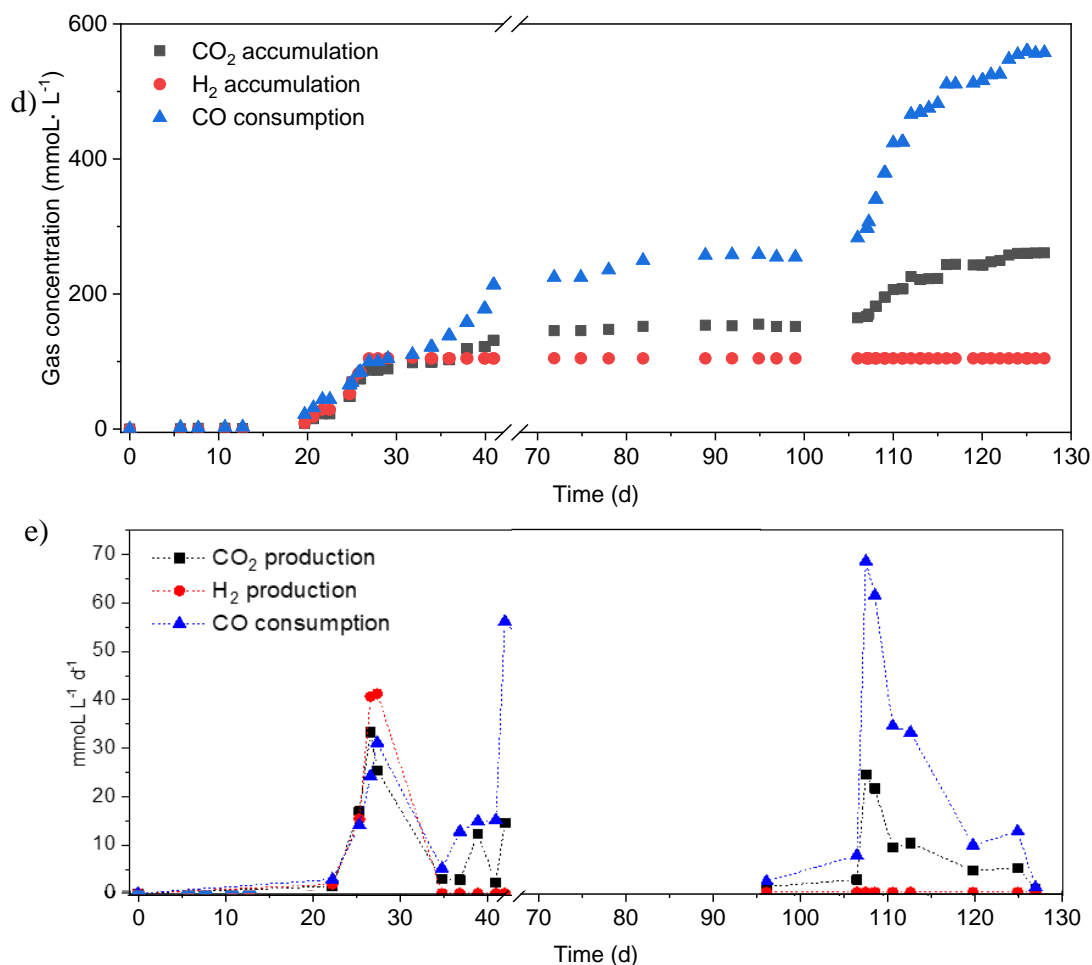


Fig. 6.2 CO bioconversion for ethanol and butanol production by heat-treated granular sludge in an intermittent gas-fed bioreactor (FB1) with initial CO gas pressure of 1.8 bar. a) Production of acetic acid (HAc), propionic acid (HPr), butyric acid (HBu), ethanol (EtOH) and butanol (BtOH), b) gas pressure, c) pH, d) CO₂ and H₂ production and CO consumption and e) CO₂ and H₂ production and CO consumption (mmol L⁻¹ d⁻¹) at each CO feeding. The orange dots inside the dash box in panel represent 1.8 bar CO feeding. The red cross mark in panel c) represents pH adjustment to 5.7 each time CO was added.

6.3.1.2 Selective butanol production from CO at pH 5.7–6.5 (Period II)

After one week incubation in a culture medium with initial pH of 5.7 (stage IV, 100-106 days), the acetic acid concentration decreased from 2.4 to 1.3 g/L, while 0.82 and 0.95 g/L of, respectively, ethanol and butanol were produced along with a pH increase from 5.7 to 6.0 (Fig. 6.2a). The pH increase was due to the consumption of acetic acid with concomitant production of neutrally charged ethanol and butanol. The CO consumption rate and CO₂ production rate reached their highest value of, respectively, 68.60 and 24.42 mmol L⁻¹ d⁻¹ at 109 d (Fig. 6.2e).

During stage V (107-110 d), acetic acid and butyric acid concentrations increased again, up to 7.21 g/L acetic acid and 2.94 g/L butyric acid till 110 d, which was attributed to the

transient pH increase, known to stimulate acidogenesis. During this stage, the accumulation of these acids induced a pH decrease to 4.5-5.

Stage VI (111-127 d), at pH often below 5, was a high butanol production stage. On 111-119 d, acetic acid was rapidly consumed, dropping from 7.21 to 1.0 g/L. Interestingly, the ethanol concentration also decreased from 2.2 to 0.8 g/L (discussed below, see 3.3.1 and 4.2), while the butyric acid concentration increased slowly up to its highest concentration of 3.0 g/L. Simultaneously, the butanol concentration increased rapidly up to 4.0 g/L at 119 d, while the butyric acid concentration remained stable. After day 119, both acetic acid and ethanol concentrations decreased to below 1.0 g/L, and also butyric acid was quickly consumed. This was accompanied by a second fast increase of the butanol concentration, which reached 6.8 g/L at 127 d. It was observed that butanol production occurred when the medium pH was 5.7, though it raised to 6.4 due to the consumption of acetic acid and butyric acid (Fig. 6.2c). To sustain continuous butanol production, the pH was regularly, manually, adjusted to 5.7, each time CO was added (Fig. 6.2c).

6.3.1.3 Carbon balance of FB1

In Period I (0-99 d), the carbon balance was almost closed and reached 91.0%, to which the unaccounted carbon used for cell growth should be added (Table 6.1). The level of CO bioconversion to organic compounds (acids and alcohols) and CO₂ (mmol carbon) in Period II (100-127 d) was 21.4% and 46.8%, respectively, reaching 68.2% in total at the end of the incubation period (Fig. 6.3).

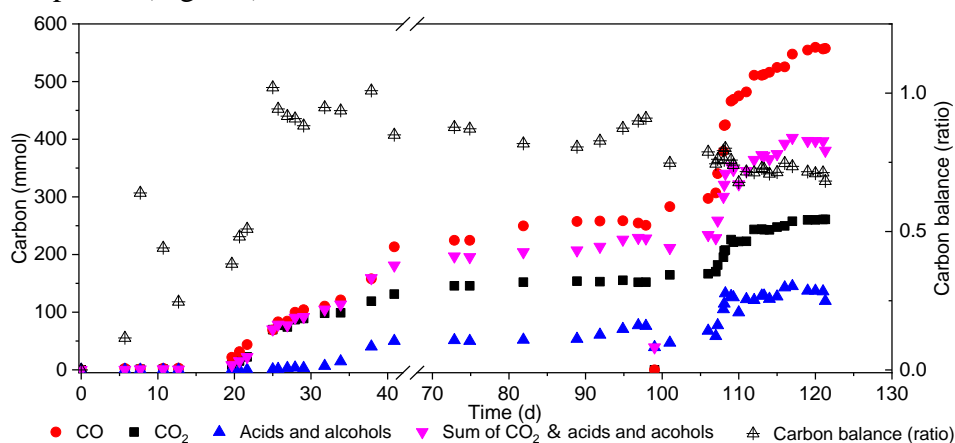


Fig. 6.3 Carbon balance for ethanol and butanol production using CO as the sole carbon source by heat-treated granular sludge in an intermittent gas-fed bioreactor (FB1). The input mmol carbon of CO consumption and distributed as CO₂ and acids and alcohols production, produced carbon as sum of CO₂, acids and alcohols.

6.3.2 Conversion pathways for selective butanol production by enriched sludge

6.3.2.1 CO and syngas conversion

The enriched sludge from FB1 at 127 d was tested in batch assays using pure CO and syngas (CO/CO₂/H₂/N₂, 20/20/10/50, v/v) as the substrates. After two weeks incubation with CO as the substrate, 1.30 g/L ethanol and 0.30 g/L butanol were produced, while 2.40 g/L ethanol and 0.33 g/L butanol were obtained from syngas (Fig. 6.4 a, b). The partial pressure of CO in the syngas in this study was 0.36 bar, which is much lower than in 100% CO at 1.8 bar. The presence of 1.8 bar CO extended the lag phase of bacterial growth (Fig. 6.4), but the cell concentration reached an OD₆₀₀ of 1.72 after 14 days incubation was higher than in the OD (1.56) obtained using syngas at the end of the incubation (Fig. 6.4c, d). These batch tests confirmed that the enriched sludge from CO fed FB1 enabled ethanol and butanol production from both CO and syngas.

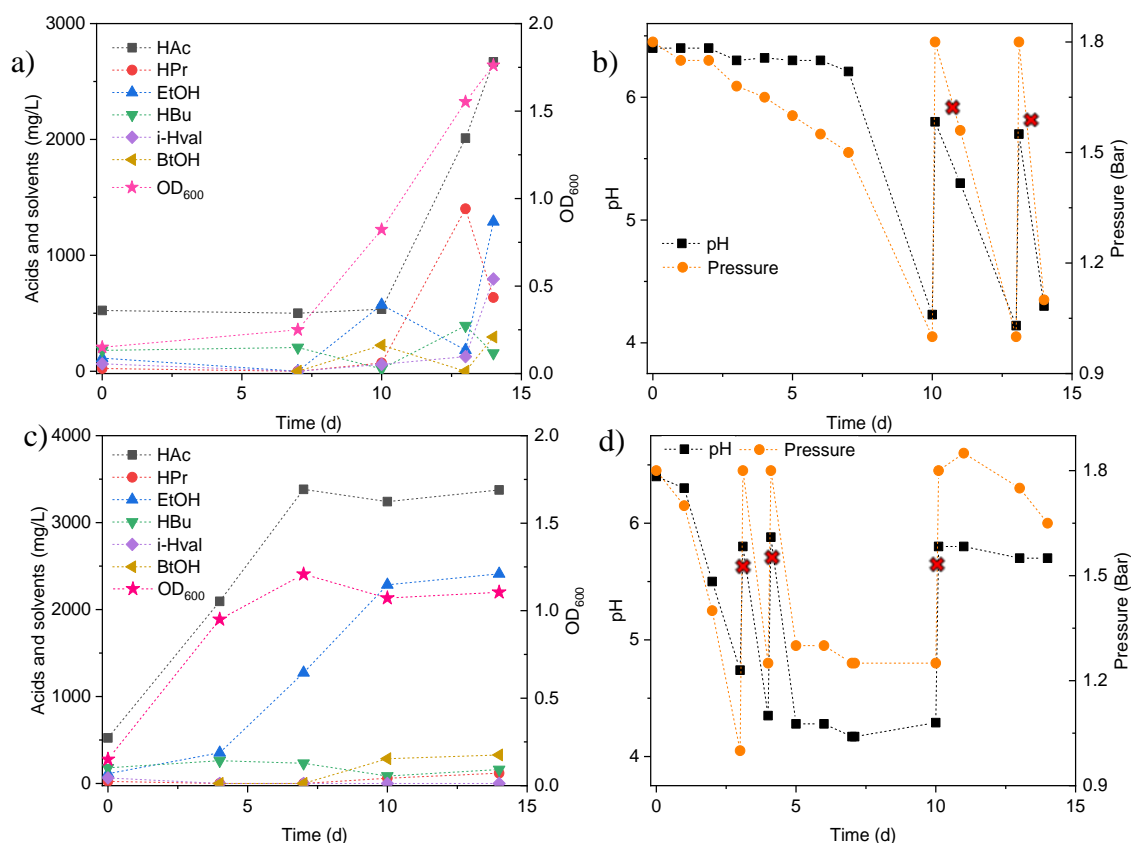


Fig. 6.4 Studies of CO (a, b) and syngas (c, d) bioconversion by enriched sludge sampled day 127 at initial pH 6.2 in batch experiments. a) and c) products profiles; b) and d) change of pH and gas pressure by enriched sludge in batch tests with initial CO/syngas gas pressure 1.8 bar. Red cross marks in panel b) and d) represent pH adjustment to 5.7 each time CO was added.

6.3.2.2 Ethanol oxidation in the presence of CO₂ by enriched sludge

At high or low initial pH (6.5 or 5.7) with N₂ in the headspace, neither exogenous acetic acid nor ethanol were significantly consumed after 11 days of incubation (Fig. 6.5a, b). However, after 30 days incubation, 1.5 g/L ethanol was consumed with the concomitant production of 0.4 g/L acetic acid, 0.6 g/L butyric acid and 0.8 g/L butanol along with the pH dropping to 5.67 from the initial pH 6.5 (Fig. 6.5a). The production of acetic acid could be from ethanol oxidation, and the production of butyric acid demonstrated a C₂ to C₄ acid conversion process occurred during the long time (30 d) incubation. At initial pH 5.7, 0.9 g/L ethanol was consumed, while 0.5 g/L acetic acid was produced, and both the butyric acid and butanol concentrations showed a slight increase (<0.1 g/L), while the pH decreased to 5.24 at day 30 (Fig. 6.5b). The highest cell concentration at initial pH 6.5 and 5.7 reached, respectively, an OD of 0.25 and 0.3 (Fig. 6.5a, b).

With N₂ in the headspace, at 30 d, the produced carbon was in total 83.8 mmol·L⁻¹ C distributed over 13.3 mmol·L⁻¹ C acetic acid, 27.2 mmol·L⁻¹ C butyric acid and 43.2 mmol·L⁻¹ C butanol, while the total carbon consumed was 82.0 mmol·L⁻¹ C with 65.2 mmol·L⁻¹ C being ethanol and 16.7 mmol·L⁻¹ C likely to be 0.5 g/L YE. Thus, the carbon balance of this batch test from consumed ethanol and YE to acetic acid, butyric acid and butanol was almost closed. Hence, part of the ethanol was converted to C₄ compounds.

In the presence of CO₂, ethanol started to be converted to acetic acid after 5 d at initial high pH 6.5 (Fig. 6.5c) and 7 d at initial low pH 5.7 (Fig. 6.5d), eventually reaching a total conversion of ethanol to acetic acid. The mole ratio of consumed ethanol to acetic acid, in the presence of CO₂, was 0.80 and 0.76, respectively, at initial pH 6.5 or pH 5.7 (Fig. 6.5e). This is close to the theoretical ratio of acetic acid production from ethanol and CO₂ (Eq.7) (Bao et al., 2019).



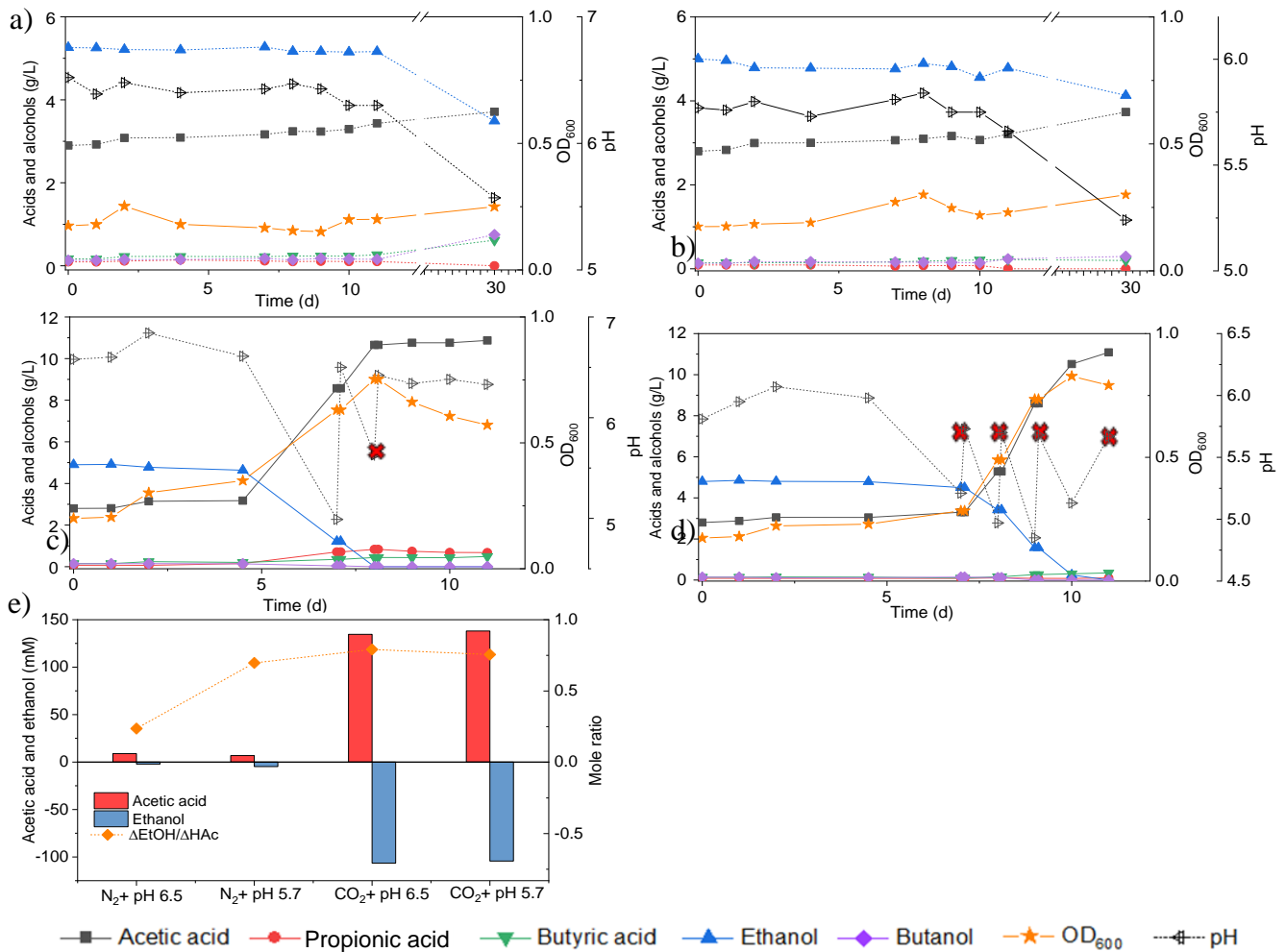


Fig. 6.5 Effect of exogenous acetic acid and ethanol addition on the production of acetic acid, propionic acid, butyric acid, ethanol and butanol, change of pH and OD₆₀₀ by enriched sludge (sampled day 127 from FB1) in batch tests. a) N₂ + initial pH 6.5, b) N₂ + initial pH 5.7, c) CO₂ + initial pH 6.5 and d) CO₂ + initial pH 5.7 as well as e) Net production of acetic acid and ethanol and molar ratio of consumed ethanol and produced acetic acid. Red cross marks in panel c) and d) represent manual pH adjustment.

6.3.2.3 Butanol oxidation in the presence of CO₂ by the enriched sludge

With initial pH 6.5, the butanol concentration decreased while the butyric acid concentration was produced along with the pH slightly decreasing after 5 days incubation (Fig. 6.6a, c). Thereafter, the butanol concentration further decreased to 2.5 g/L while the pH decreased to 6.2 at day 10. Butanol was subsequently completely consumed within 1 day (Fig. 6.6a, c). At initial pH 5.7, butanol decreased to 3.1 g/L at day 5 and was then quickly consumed, reaching 0.6 g/L (85% consumption) within 2 days (Fig. 6.2b, d). Acetic acid and butyric acid accumulated to, respectively, 2.0 and 3.6 g/L along with the pH decrease to 4.5 (Fig. 6.6b, d). The pH was then adjusted to 5.7 at day 7 (Fig. 6.6d). Butanol was completely consumed after 12 days and 2.5 g/L acetic acid and 4.5 g/L butyric acid were obtained at the end of the incubation (Fig. 6.6b). The cell concentration reached the highest OD₆₀₀ of 0.4 at both initial pH 6.5 and 5.7 (Fig. 6.6c, d). The mole ratio of butanol consumption to butyric acid production was 0.92 and 1.08, respectively, at initial pH 6.5 and 5.7, which is close to the theoretical ratio of 1 (Eq. 8) (Schaefer et al., 2010; Fernández-Naveira et al., 2017a).

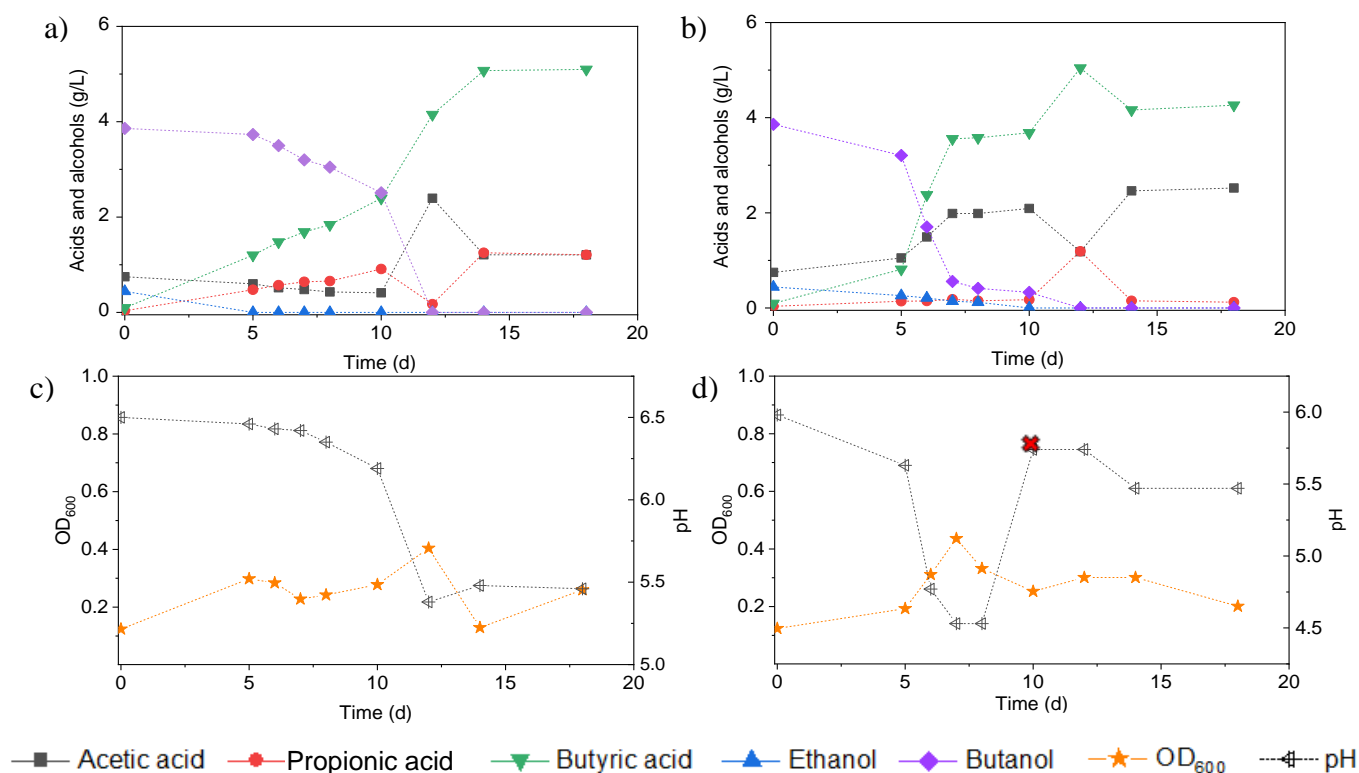
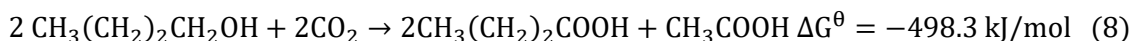


Fig. 6.6 Production of acetic acid, propionic acid, butyric acid, ethanol, and butanol from exogenous butanol + CO₂ by the enriched sludge sampled at day 127 from FB1. Initial pH of a) 6.5 and b) 5.7 and corresponding changes in pH and OD₆₀₀ of c) and d). Red cross mark represents manual pH adjustment.

6.3.3 Ethanol and butanol production by the enriched culture at pH 6.2 and 5.7 in FB2

Fig. 6.7b shows that the gas pressure decreased in incubations of the enriched sludge (sampled day 127 from FB1), when the pH was controlled at 6.2, from 1.8 bar to 1 bar during days 14 of incubation, during which 0.9 g/L acetic acid and 0.3 g/L butyric acid were produced. After a 2nd CO feeding (pressurization to 1.8 bar) on day 14 at the same pH value, the gas pressure decreased again to 1.1 bar within 24 h and 3.2 g/L acetic acid and 1.0 g/L butyric acid accumulated. It is noteworthy to observe that the small amount of ethanol (0.48 g/L) originating from the inoculum was also completely consumed by day 15 (Fig. 6.7a). With the high CO consumption, the cell concentration doubled between the 1st and 2nd CO supply, i.e., the OD₆₀₀ increased from 1.0 to 2.0 between days 14-16 (Fig. 6.7a).

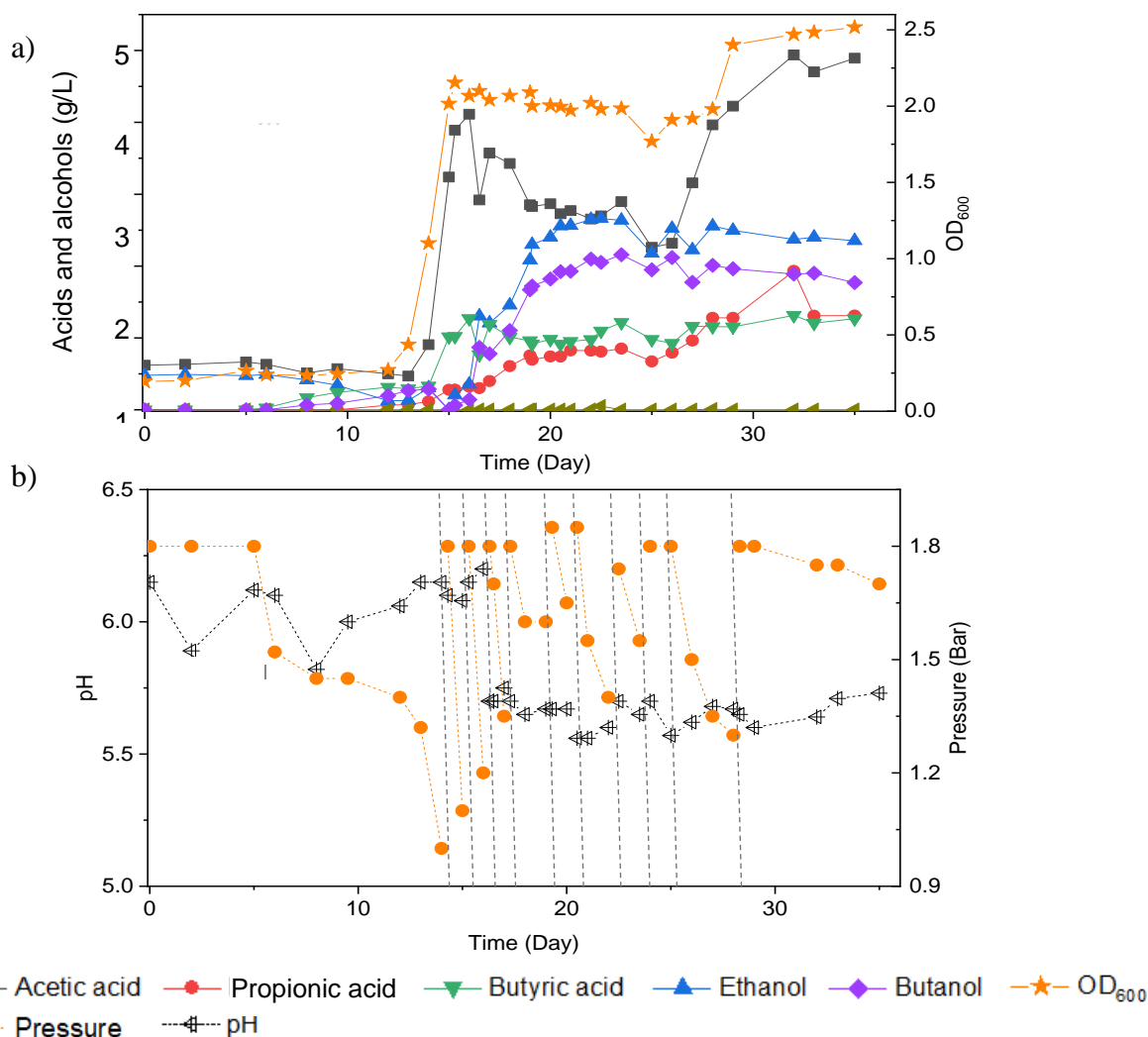


Fig. 6.7 a) Acetic acid, propionic acid, ethanol, butyric acid, butanol and cell concentrations (OD₆₀₀) and b) change of pH and gas pressure using CO as the sole substrate by the enriched sludge (sampled day 127) with intermittent CO gas feeding (FB2) on days 0, 14, 16, 17, 18, 19, 21, 22, 24, 26 and 28 d. Dash line in panel b represent CO feeding.

Considering the dominant production of acetic and butyric acids, but without any significant ethanol and butanol accumulation at pH 6.0-6.2, the pH was decreased to 5.7 on day 16 to observe its possible effect on solventogenesis (Fig. 6.7b). 1.8 bar CO decreased to 1.2 bar after 24 h and the concentrations of acetic acid and butyric acid reached, respectively, 4.0 and 1.3 g/L, whereas the ethanol concentration increased to 0.4 g/L at 17 d (Fig. 6.7a). Subsequently, both ethanol and butanol concentrations increased to, respectively, 2.7 and 2.1 g/L at day 24 after the 8th CO addition (Fig. 6.7a). Thereafter, the production of both acids and alcohols stabilized (Fig. 6.7a). Therefore, 50 mL fresh medium was added to re-supply nutrients. From then onwards, the cell concentration increased to an OD₆₀₀ of 2.5 and the acetic acid concentration increased to 4.9 g/L at day 35, while the ethanol and butanol concentrations did not further increase (Fig. 6.7a).

When operating at a pH of 5.7, alcohols were produced, though it was noted that ethanol and butanol production was inhibited when the gas pressure decreased from 1.8 bar to 1.35 bar (days 16.5-17). This was attributed to the accumulation of CO₂ and the possible reverse reaction of conversion of alcohols back to acids (Eq. 7, 8), as observed in previous tests (Fig. 6.5 and 6.6). Therefore, 1.8 bar CO was subsequently added every 24 h to avoid CO₂ accumulation since the accumulation of CO₂ may cause ethanol and butanol oxidation (Fig. 6.5 and 6.6).

6.3.5 Microbial community analysis

The relative taxonomic abundance of the enriched sludge sampled from the bioreactor (day 127) when reaching 6.8 g/L butanol is shown in a Krona figure (simplified as Fig. 6.8). The relative abundance was 61% bacteria, 5% archaea and 34% unknown. The *Firmicutes* phylum occupied 75% of the bacteria, mainly represented by the *Clostridia* (47%) and *Bacilli* (49%) class (Fig. 6.8a). The *Clostridiales* order occupied 98% in the *Clostridia* class, which was mainly distributed over the *Ruminococcaceae* 14%, *Clostridiaceae* 21% and 40% *Oscillospiraceae* families (Fig. 6.8a). The *Clostridium* genus occupied 91% of the *Clostridiaceae* family, distributed as *Clostridium* strain W14A (29%), *C. ragsdalei* (10%), *C. estertheticum* (5%) and *C. ljungdahlii* (3%) (Fig. 6.8b). Some well-studied solventogenic species such as *C. autoethanogenum*, *C. carboxidivorans* and *C. kluyveri* occupied, respectively, 1%, 0.6% and 0.6% of the *Clostridium* genus (Fig. 6.8b). The relative abundance in the *Clostridiaceae* family (8%) and *Clostridium* genus (7%) of bacteria in the enriched

sludge is much higher than, respectively, 1.7% and 0.3% of the bacteria in the granular sludge inoculum (Fig. 6.9) (He et al., 2020).

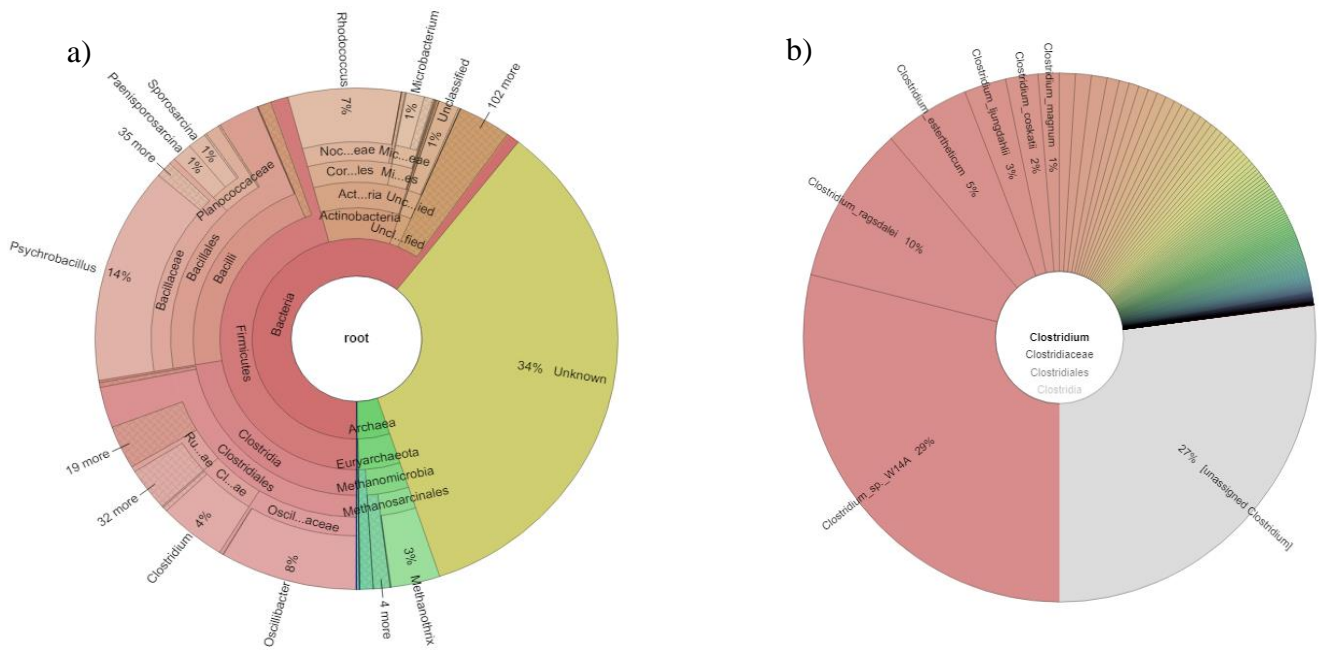


Fig. 6.8 Relative taxonomic abundance at a) genus and b) *Clostridium* species level of the enriched sludge from FB1 at day 127.

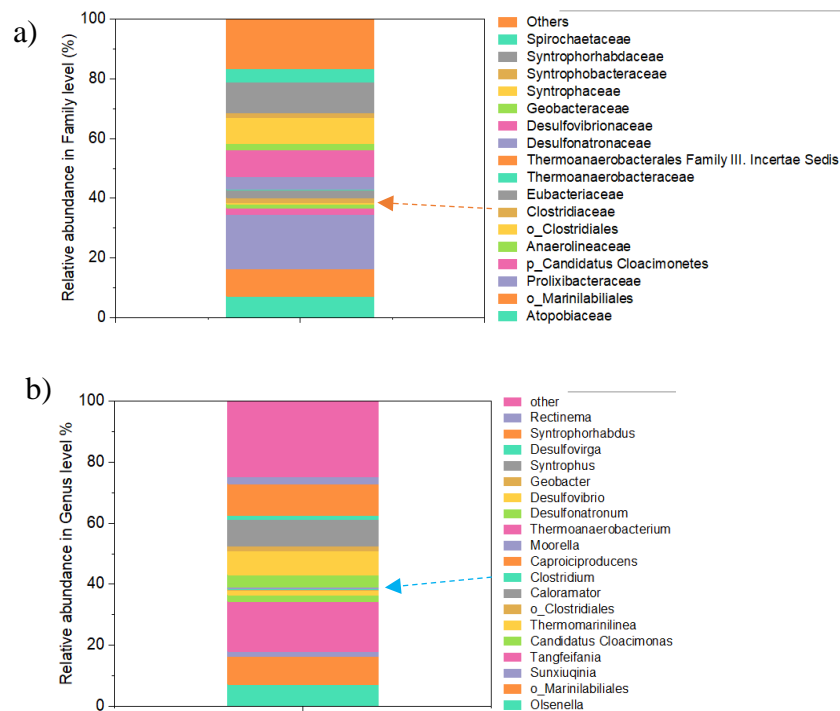


Fig. 6.9 Relative taxonomic abundance at family (a) and genus (b) level of the inoculum granular sludge.

6.4 Discussion

6.4.1 Selective butanol production by CO fed anaerobic sludge

6.4.1.1 Selective butanol production

This study showed a CO gas-fed enrichment can produce a butanol concentration as high as 6.8 g/L (Fig. 6.2) with a butanol/butyric acid ratio of 12.6 (Table 6.1). This is, to the best of our knowledge, the thus far highest reported butanol concentration (Table 6.2). The much higher selective production of butanol with the microbial culture enriched in this study can be explained by the broader metabolic potential of the enriched mixed populations compared to pure cultures, in combination with the pH value and the stressful environmental conditions such as increased CO partial pressure (Fig. 6.2a, b). Indeed, the microbial community analysis showed that various *Clostridium* species were enriched, including *C. carboxidivorans* in the class *Clostridia* and other CO converting acetogens in the class *Bacilli*. The positive effect of increased CO partial pressure on cell growth and ethanol production has been reported for some pure strains, e.g. *C. carboxidivorans* (Lanzillo et al., 2020). Hurst and Lewis (2010) studied the effect of the CO partial pressure (P_{CO}) on ethanol production in *C. carboxidivorans* and found that cell growth increased by 440% when increasing the P_{CO} from 0.35 to 2 bar. Ethanol production was not observed when the P_{CO} was 0.35 bar (Hurst and Lewis, 2010). When the P_{CO} was 0.5, 0.7 and 1.05 bar, ethanol was produced in the non-growth phase. Conversely, if P_{CO} was increased to 2 bar, ethanol production was growth-associated. Lanzillo et al. (2020) investigated the cell growth and ethanol/butanol production by *C. carboxidivorans* at a CO pressure varying between 0.5 and 2.5 bar. The best condition for alcohol production was an initial 1.7 bar CO, yielding 0.4 g/L ethanol and 0.13 g/L butanol (Lanzillo et al., 2020). Similarly, this study obtained a selective butanol production in FB1 as well as 2.7 g/L ethanol and 2.1 g/L butanol in FB2 using 1.8 bar CO as the substrate, of which the gas pressure (1.8 bar) was consistent with the reported optimum CO partial pressure (1.7-2.0 bar) (Hurst and Lewis, 2010; Lanzillo et al., 2020).

Fig. 6.2a shows that the increase in butanol concentration in the bioreactor with intermittent CO gas feeding occurred in two steps: the first butanol increase occurred at 111-119 d, when the acetic acid and ethanol concentrations decreased, while the butyric acid concentration remained relative stable. The stable butyric acid concentration was assumed to be due to its simultaneous production from the C_1 gas and conversion to butanol via the WLP pathway (Fernández-Naveira et al., 2017a). The second butanol increase was observed at pH 5.7 along with the decrease in butyric acid concentration and reached 6.8 g/L at the end of the

incubation (Fig. 6.2a). The optimal pH for solventogenesis is generally slightly acidic in most acetogenic bacteria, though some strains, e.g. *C. aceticum*, have recently been shown to produce alcohols at near neutral pH (Arslan et al., 2019).

It should be noted that 0.5 g/L yeast extract addition in Period II might also have played a positive role in biomass growth, which can be seen from the shorter adaption time than in Period I (Fig. 6.2). Yeast extract is an important, partly undefined, source of nutrients and micronutrients required for microorganisms (Abubackar et al., 2015), especially for syngas fermenting microorganisms, e.g. strain *C. carboxidivorans* P7 (Wan et al., 2017) and *C. autoethanogenum* DSM 10061 (Abubackar et al., 2012). Abubackar et al. (2012) investigated the effect of the yeast extract concentration (0.6–1.6 g/L) on biological solvent production by *C. autoethanogenum* DSM 10061 and used the Minitab analysis with a two level four factor (2^4). Lowering the YE concentration resulted in the production of more reduced compounds such as ethanol. Diender et al. (2016) investigated the production of fatty acids and solvents by a synthetic co-culture of *C. autoethanogenum* and *C. kluyveri* grown on CO. The co-culture was only capable of growing efficiently with 0.5 g/L yeast extract. Yeast extract concentrations lower than 0.5 g/L resulted in strong negative effects on the acid and alcohol production rates, and significantly increased the lag phase. Yeast extract can somewhat favor the biomass growth at unfavorable pH. For instance, in a bioreactor with continuous CO supply and 1 g/L yeast extract at low pH 5.75, the maximum biomass concentration obtained was comparable to the maximum biomass concentration at pH 6.0 (Abubackar et al., 2015). Therefore, 0.5 g/L yeast extract addition from day 100 onwards (start of Period II) might have played a positive role on the cell growth and alcohol production in this study.

6.4.1.2 Ethanol and butanol production by pH shift from 6.2 to 5.7

The pH control of the CO fed FB2 demonstrated that the shift of pH from 6.2 to 5.7 stimulated both ethanol and butanol production by the enriched sludge (Fig. 6.7). This agrees with the intermittent gas-fed FB1 experiment, suggesting enhanced butanol production (Period II) when the pH was manually adjusted around 5.7 (Fig. 6.2a, c). This shift at pH 5.7 in this study is slightly higher than previously reported pH values, between 4.5-5.5, that induce solventogenesis in syngas fermentation. Low pH does stimulate ethanol production from CO and syngas as shown by Chakraborty et al. (2019), who achieved ethanol production by anaerobic granular sludge after decreasing the pH from 6.2 to 4.9. The highest butanol concentration of 1.18 g/L was reached after 41 days of incubation at pH 4.9 (Chakraborty et al., 2019).

6.4.1.3 Carbon balance

The CO conversion efficiency was higher in Period I (91%) compared to Period II (68%) (Table 6.1). The frequent pH decreases in Period II might have damaged or killed the cells, resulting in the low carbon utilization. Mohammadi et al. (2012) reported a CO conversion efficiency of 93% with *C. ljungdahlii* in a reactor with continuous syngas (55% CO) feeding. In another experiment with *C. ljungdahlii* in a bubble column bioreactor, the CO bioconversion was only 60% from syngas (25% CO) (Morinaga and Kawada, 1990).

6.4.1.4 Microbial community analysis

C. carboxidivorans is the only reported *Clostridium* species that can produce butanol from C₁ gases (Fernández-Naveira et al., 2016a), although its relative abundance is very low in the enriched sludge (0.6%) (Fig. 6.8b). It should be noted that the relative abundance of unassigned *Clostridium* is 27% of the *Clostridium* genus and thus some unassigned *Clostridium* spp. might have contributed to the butanol production (Fig. 6.8b). Considering the diversity of the *Clostridium* genus in the enriched sludge, a broad range of acetogenic organisms can be involved in CO bioconversion to metabolites such as butanol through species interactions, that are not possible in pure cultures. For instance, *Clostridium* species such as *C. autoethanogenum* and *C. kluyveri* have never been observed to produce butanol or hexanol individually in pure monocultures. However, a co-culture of both organisms was found to accumulate both butanol and hexanol (Diender et al., 2016). Considering the mixed culture in the enriched sludge, the positive role of mixed *Clostridium* strains might have contributed to enhanced alcohol production in FB1.

Concerning the other detected bacteria, *Ruminococcus* species of the *Ruminococcaceae* family have been shown to produce H₂ (Kotay et al., 2008). In the *Oscillospiraceae* family, the relative abundance of the *Oscillibacter* genus reached 97% (Fig. 6.8a), which is known to be involved in acidogenesis during dark fermentation (Goud et al., 2017) and butyric acid production by microbial electrosynthesis using CO₂ as the substrate (Dessi et al., 2021). Besides the class *Clostridia*, the *Psychrobacillus psychrotolerans* species occupied as high as 57% of the class *Bacilli* and 20% of bacteria (Fig. 6.8a). The relative abundance of the *Rhodococcus* genus reached 12% of the bacterial population and some species of *Rhodococcus*, such as *Rhodococcus erythropolis* N9T-4 can utilize CO to CO₂ under oligotrophic conditions (Fig. 6.8a) (Ohhata et al., 2007).

6.4.2 Ethanol and butanol oxidation in the presence of CO₂

Attempts of metabolic pathway elucidation in the enrichment experiments (Fig. 6.3) suggest that ethanol consumption during butanol production was due to its conversion back to acetic acid in the presence of CO₂. However, ethanol was completely oxidized to acetic acid with CO₂ only after 11 days (Fig 3c, d), while part of the ethanol was used for C₄ compound production in a N₂ atmosphere (without CO₂) after 30 days of incubation (Fig 3a, b). Hence, ethanol oxidation to acetic acid was dominant compared to its utilization for C₄ acid conversion with the accumulation of CO₂. The same ethanol oxidation process to acetic acid has been demonstrated in solventogenic acetogens such as *C. aceticum* (Arslan et al., 2019). ¹³C-labeled ethanol and acetate experiments with another strain, *C. ljungdahlii*, revealed that ethanol production occurred during the exponential phase and that ethanol could then be oxidized to acetate via the aldehyde ferredoxin oxidoreductase pathway in the presence of 1 bar CO and at controlled pH 6.0 (Liu et al., 2020). Though ethanol oxidation to acetic acid had been reported in pure cultures of solventogenic *Clostridia* (Arslan et al., 2019; Liu et al., 2020), butanol oxidation to butyric acid has to the best of our knowledge not been reported before.

Table 6.2 Maximum ethanol and butanol concentrations achieved during syngas and CO fermentation by pure and mixed cultures in batch and continuous bioreactor systems.

Microorganism	Reactor configuration	Gas composition	Working volume (L)	Time/d	Temperature/°C	pH	Maximum alcohols (g/L)		Reference
							Ethanol	Butanol	
<i>Alkalibaculum bacchi</i> CP15	CSTR	CO/CO ₂ /H ₂ /N ₂ (20/15/5/60)	3.3/7	51	37	8.0	6.0	1.1	Liu et al., 2014
<i>C. carboxidivorans</i> P7	Bubble column	CO/CO ₂ /N ₂ (25/15/60)	4.5 /6.2	10	37	5.3~5.75	1.6	0.6	Rajagopalan et al. 2002
	HFR	CO/CO ₂ /H ₂ /N ₂ (20/15/5/60)	8	15	37	6	24.0	NA	Shen et al. 2014
	CSTR	CO/CO ₂ /H ₂ /N ₂ (20/15/5/60)	3/7.5	11	37	5.7	1.5	0.5	Ukpong et al. 2012
	CSTR	100% CO	1.2/2	21	33	5.75, 4.75	5.55	2.66	Fernández-Naveira et al. 2016
	CSTR	CO/CO ₂ /H ₂ /N ₂ (30/10/20/40)	1.2/2	14	33	6.2, 5.2	5.9	2.1	Fernández-Naveira et al. 2019
	Batch	CO/CO ₂ /H ₂ /Ar (56/20/9/15)	0.03/0.125	5	37	NA	3.64	1.35	Shen et al. 2020
	Batch	CO/CO ₂ /H ₂ (70/20/10)	0.03/0.282	25	37	No control	3.0	1.0	Phillips et al. 2015
	Batch	CO/CO ₂ /H ₂ (40/30/30)	0.045/0.25	15	37	5.0-7.0	3.6	1.0	Sun et al. 2018
<i>C. autoethanogenum</i>	CSTR	100% CO	1.2/2	7	30	6.0, 4.75	0.9	NA	Abubackar et al. 2015
	Batch	100% CO	0.075 /0.2	NA	30	5.75, 4.75	0.65	NA	Abubackar et al. 2012
<i>C. ljungdahlii</i>	CSTR Bubble column (BC)	CO/CO ₂ /H ₂ (60/5/35)	1/2 (CSTR) 4/6 (BC)	83	35	5.5 (CSTR) 4.3~4.8 (BC)	20.7	NA	Richter et al. 2013
<i>C. aceticum</i>	CSTR	CO/CO ₂ /H ₂ /N ₂ (30/5/15/50)	1.2/2	52	30	6.98	5.6	NA	Arslan et al. 2019
<i>C. ragsdalei</i>	Trickling bed reactor	CO/CO ₂ /H ₂ /N ₂ (38/28.5/28.5/5)	1	70	37	5.8-4.6	5.7	NA	Devarapalli et al. 2016
<i>Anaerobic sludge</i>	Fed batch reactor	CO	0.2/1	127	33	5.7-6.45	2.2	6.8	This study

Based on the observed compounds consumed and produced during butanol production (Fig. 6.2), different scenarios of conversion pathways for selective butanol production were considered. Firstly, it was checked (see section 3.2) if some bacterial populations could have converted acetic acid and ethanol to butyric acid via the reversed β -oxidation pathway, since those two C₂ compounds were sometimes consumed while the concentration of butyric acid increased (Fig. 6.2a). As a result, butyric acid could then have been converted to butanol via the acetyl-CoA pathway by solventogenic acetogens in the intermittent gas-fed reactor. The reverse β -oxidation pathway using acetate (C₂) as carbon backbone and ethanol (C₂) as an electron donor can lead to *n*-butyrate (C₄) production, which has been described in species such as *C. kluyveri* (Aglar et al., 2012; Richter et al., 2016; San Valero et al., 2019). However, our experiments with exogenous acetate, ethanol and either CO₂ or N₂ showed that butyric acid production from acetic acid and ethanol was not a relevant mechanism (Fig. 6.5), while ethanol oxidation to acetic acid in the presence of CO₂ was feasible instead (Fig. 6.5). Further research on the carbon flow and the biochemical mechanisms of C₂ and C₄ compound formation from CO and CO₂ is thus required, e.g., using nuclear magnetic resonance (NMR) spectroscopy with ¹³C CO labelled substrates (Gurudata, 2011).

6.4.3 H₂ production during start-up period

H₂ production was observed during the initial 15-33 days, but then shifted to acetic acid production (Fig. 6.2d). At each CO feeding, the molar ratio of H₂ production to CO consumption was close to 1 (Fig. 6.10), which is in accordance with the theoretical ratio of H₂ production from CO (Eq. 7). One explanation is that hydrogen-utilizing acetogens were slowly enriched to become dominant after 30 days of operation along with the accumulation of H₂ and the presence of CO and CO₂ (Fig. 6.5). Hydrogenic acetogens can indeed be enriched from anaerobic sludge in the presence of CO (Liu et al., 2016).

Considering the accumulation of CO₂ during the fermentation process, it is not possible to discriminate between a direct conversion of CO to acetate (Eq. 1) and an indirect conversion via H₂ and CO₂ as intermediates (Eq. 9 and Eq. 10):



This could be elucidated by NMR spectroscopy with ^{13}C labelled substrates in future studies.

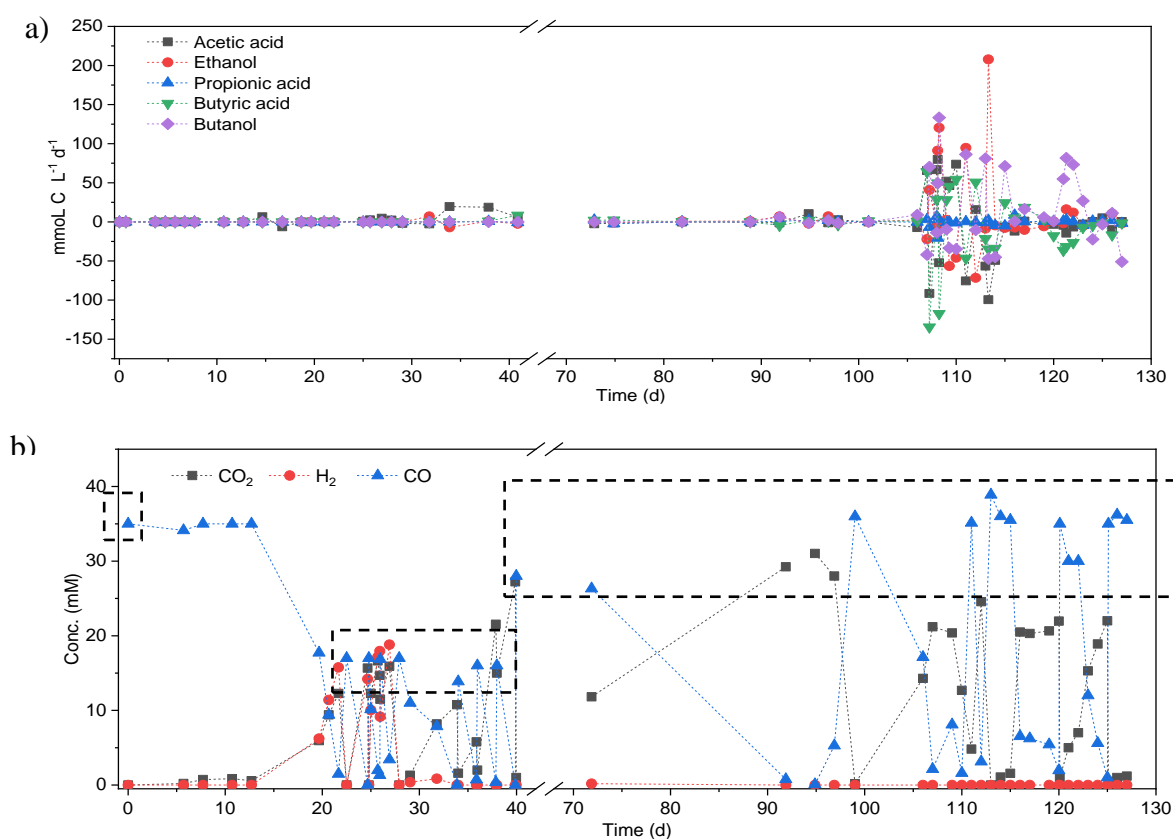


Fig. 6.10 a) Net production rates of acetic acid, propionic acid, butyric acid, ethanol and butanol in the intermittently fed reactor in $\text{mmol C L}^{-1} \text{d}^{-1}$ and b) CO consumption and production of CO_2 and H_2 . The blue triangle inside the dash square means CO feeding.

H_2 production from CO by both pure or mixed cultures has been reported under mesophilic, thermophilic and hyper-thermophilic conditions in pure cultures of *Carboxydotherrmus hydrogenoformans*, *Carboxydocella thermoautotrophica* and *Thermincola carboxydiphila* (Table 6.3). CO is oxidized by carbon monoxide dehydrogenase (CODH retaining a Ni–Fe active site) to produce CO_2 , and electrons are transferred by ferredoxin to an energy-converting hydrogenase that reduces protons to molecular H_2 (Simon et al., 2015). Generally, the growth rates of mesophilic hydrogenogenic bacteria on CO are low and enough biomass needs to develop before the phase of anaerobic CO conversion to H_2 production can start (Parshina et al., 2005). Thermophilic conditions are generally more favorable leading to a higher biohydrogen yield (Table 6.3).

From an energetic point of view, the Gibbs free energy of hydrogen production from CO (-20.1 kJ/mol , Eq. 9) and water is much higher than both acetic acid production from CO and water (-154.6 kJ/mol , Eq. 1) or CO_2 and H_2 (-75.4 kJ/mol , Eq. 10). The optimal growth pH of

the known CO converting hydrogenic strains (Table 6.3) is near neutral under both mesophilic and thermophilic conditions. None of these strains were observed in the enriched sludge from the bioreactor at day 127 (Table 6.3). The *Rhodospirillales* order with relative abundance lower than 0.1% was identified in the enriched sludge. However, H₂ production was observed at pH 5.3-5.5 in this study (Fig. 6.2c). One possible explanation could be the presence of specific CO-utilizing/H₂-producing strains considering the diverse microbial populations present in anaerobic sludge (Wan et al., 2016). It should be noted that the molar ratio of CO consumption to H₂ production was conform to the theoretical ratio of 1 (Eq. 9) (Fig. 6.2d), which confirms that H₂ production originates from CO and not from acetic acid bioconversion.

Table 6.3 Environmental conditions of H₂ production using CO as substrate by pure cultures and enrichments.

Biocatalysts	Substrate	Growth Temperature/ °C	Optimum Temperature/ °C	pH	Optimum pH	Reference
<i>Carboxydothemus hydrogenoformans</i>	100% CO	40-78	70-72	--	6.8-7.0	Svetlichny et al. 1991
<i>Carboxydocella thermoautotrophica</i>	100% CO	40-68	58	6.5-7.6	7.0	Sokolova et al. 2002
<i>Thermincola carboxydiphila</i>	100% CO	37-68	55	6.7-9.5	8.0	Sokolova et al. 2005 Parshina et al. 2005
<i>Desulfotomaculum nigrificans</i>	100% CO	30-68	55	6.0-8.0	6.8-7.2	Visser et al. 2014 (DOI: 10.4056/sigs.4718645)
<i>Rhodospirillum rubrum</i>	100% CO	--	30	--	7.5	Dadak et al., 2016
<i>Rhodopseudomonas palustris</i> PT	60% CO	--	30	--	7	Pakpour et al. 2014
Anaerobic sludge	100% CO	55	--	--	--	Simpa et al 2004
Activated sludge	100% CO	55	--	10	--	Wan et al. 2016
Anaerobic granular sludge	100% CO	33	--	5.5	--	This study

Note: '--' represents data not reported.

6.5 Conclusions

CO and syngas metabolizing solventogenic bacteria were enriched from heat-treated anaerobic granular sludge treating dairy wastewater at pH 5.7-6.5 and produced up to 6.8 g/L butanol with initial CO pressure of 1.8 bar in an intermittent gas-fed bioreactor. The high selective production of butanol with the enriched culture could be explained by the broader metabolic potential of the mixed bacterial inoculum compared to pure cultures. Upon the accumulation of CO₂ in the bioreactor, the enriched mixed culture also occasionally reoxidized

ethanol and butanol to acetic acid and butyric acid, respectively. Additional tests under controlled pH demonstrated that a low pH (5.7) stimulated ethanol and butanol production by the enriched culture. Although the original sludge hardly contained acetogenic/solventogenic *Clostridia*, the microbial analysis of the enriched ethanol/butanol producing community showed the applied enrichment procedure efficiently selected for a range of *Clostridium* species, including several alcohol producers, such as *C. ljungdhalii*, *C. ragsdalei* and *C. coskatii*, in addition to other unidentified species which could include new solventogenic strains.

6.6 References

Abubackar, H.N., Veiga, M.C. and Kennes, C., 2012. Biological conversion of carbon monoxide to ethanol: effect of pH, gas pressure, reducing agent and yeast extract. *Bioresource Technology*, 114: 518-522.

Abubackar, H.N., Veiga, M.C. and Kennes, C., 2015. Ethanol and acetic acid production from carbon monoxide in a *Clostridium* strain in batch and continuous gas-fed bioreactors. *International Journal of Environmental Research & Public Health*, 12(1): 1029-1043.

Agler, M.T., Spirito, C.M., Usack, J.G., Werner, J.J. and Angenent, L.T., 2012. Chain elongation with reactor microbiomes: upgrading dilute ethanol to medium-chain carboxylates. *Energy & Environmental Science*, 5(8): 8189-8192.

Allen, Toby D., Matthew E. Caldwell, Paul A. Lawson, Raymond L. Huhnke, and Ralph S. Tanner. 2010. *Alkalibaculum bacchi* gen. nov., sp. nov., a CO-oxidizing, ethanol-producing acetogen isolated from livestock-impacted soil. *International Journal of Systematic and Evolutionary Microbiology* 60 (10): 2483-2489.

Arantes Ana L., Moreira João P. C., Diender Martijn, Parshina Sofiya N., Stams Alfons J. M., Alves M. Madalena, Alves Joana I., Sousa Diana Z. 2020. Enrichment of anaerobic syngas-converting communities and isolation of a novel carboxydophilic *Acetobacterium wieringae* strain JM. *Frontiers in Microbiology*.11:58

Arslan, K., Bayar, B., Abubackar, H.N., Veiga, M.C., Kennes, C. 2019. Solventogenesis in *Clostridium aceticum* producing high concentrations of ethanol from syngas. *Bioresource Technology*, 292:121941.

Bao, S., Wang, Q., Zhang, P., Zhang, Q., Wu, Y., and Li, F., Tao, X. Wang, S., Nabi, M., Zhou, Y., 2019. Effect of acid/ethanol ratio on medium chain carboxylate production with different VFAs as the electron acceptor: insight into carbon balance and microbial community. *Energies*, 12 (19): 3720.

Buchfink B., Xie C., Huson D.H. Fast and sensitive protein alignment using DIAMOND. 2015. *Nature Methods*, 12:59-60.

Cai, M., Liu, J. and Wei, Y., 2004. Enhanced biohydrogen production from sewage sludge with alkaline pretreatment. *Environmental Science & Technology*, 38(11): 3195-3202.

Chakraborty, S., Rene, E.R., Lens, P.N.L., Veiga, M.C. and Kennes, C. 2019. Enrichment of a solventogenic anaerobic sludge converting carbon monoxide and syngas into acids and alcohols. *Bioresource Technology*, 272: 130-136.

Dadak, A., Aghbashlo, M., Tabatabaei, M., Younesi, H. and Najafpour, G. 2016. Exergy-based sustainability assessment of continuous photobiological hydrogen production using anaerobic bacterium *Rhodospirillum rubrum*. *Journal of Cleaner Production*, 139: 157-166

Dessi, P., Lakaniemi, A.M. and Lens, P.N., 2017. Biohydrogen production from xylose by fresh and digested activated sludge at 37, 55 and 70°C. *Water Research*, 115: 120-129.

Dessi P., Sánchez C., Mills S., Francesco G. C., Isipato M., Umer Z. I., Collins G., Piet N.L. Lens. 2021. Carboxylic acids production and electrosynthetic microbial community evolution under different CO₂ feeding regimens. *Bioelectrochemistry*, 137, 107686.

Devarapalli M. and Atiyeh H K. 2015. A review of conversion processes for bioethanol production with a focus on syngas fermentation. *Biofuel Research Journal*, 2(3): 268-280.

Devarapalli, M., Atiyeh, H.K., Phillips, J.R., Lewis, R.S., and Huhnke, R.L., 2016. Ethanol production during semi-continuous syngas fermentation in a trickle bed reactor using *Clostridium ragsdalei*. *Bioresource Technology*, 209: 56–65.

Diender, M., Stams, A. and Sousa, D. Z. 2016. Production of medium-chain fatty acids and higher alcohols by a synthetic co-culture grown on carbon monoxide or syngas. *Biotechnology for Biofuels*, 9 (1): 82.

Fast, A. G., Schmidt, E. D., Jones, S. W. and Tracy, B. P., 2015. Acetogenic mixotrophy: novel options for yield improvement in biofuels and biochemicals production. *Current Opinion in Biotechnology*, 33: 60-72.

Fernández-Naveira, Á., Abubackar, H.N., Veiga, M.C. and Kennes, C., 2016a. Efficient butanol-ethanol (BE) production from carbon monoxide fermentation by *Clostridium carboxidivorans*. *Applied Microbiology and Biotechnology*, 100(7): 3361-3370.

Fernández-Naveira, Ánxela, Haris Nalakath Abubackar, María C. Veiga, and Christian Kennes. 2016b. Carbon monoxide bioconversion to butanol-ethanol by *Clostridium carboxidivorans*: kinetics and toxicity of alcohols. *Applied Microbiology and Biotechnology* 100 (9): 4231-4240.

Fernández-Naveira, Á., Veiga, M.C. and Kennes, C., 2017a. H-B-E (hexanol-butanol-ethanol) fermentation for the production of higher alcohols from syngas/waste gas. *Journal of Chemical Technology & Biotechnology*, 92(4): 712-731.

Fernández-Naveira, Á., Abubackar, H.N., Veiga, M.C. and Kennes, C. 2017b. Production of chemicals from C₁ gases (CO, CO₂) by *Clostridium carboxidivorans*. *World Journal of Microbiology and Biotechnology*, 33 (3): 43.

Fernández-Naveira, Á., Veiga, M.C. and Kennes, C., 2019. Selective anaerobic fermentation of syngas into either C₂-C₆ organic acids or ethanol and higher alcohols. *Bioresource Technology*, 280:387-395.

Ganigué, R., Sánchez-Paredes, P., Bañeras, L. and Colprim, J. 2016. Low fermentation pH is a trigger to alcohol production, but a killer to chain elongation. *Frontiers in Microbiology*, 7, 702.

Goud, R.K., Arunasri, K., Yeruva, D.K., Krishna, K.V., Dahiya, S. and Mohan, S.V., 2017. Impact of selectively enriched microbial communities on long-term fermentative biohydrogen production. *Bioresource Technology*, 242: 253-264.

Guo, Y., Xu, J., Zhang, Y., Xu, H., Yuan, Z. and Li, D., 2010. Medium optimization for ethanol production with *Clostridium autoethanogenum* with carbon monoxide as sole carbon source. *Bioresource technology*, 101 (22): 8784-8789.

Gurudata, N. 2011. ¹³C nuclear magnetic resonance of oximes. i. solvent and isotope effects on the ¹³C chemical shifts of acetoxime. *Canadian Journal of Chemistry*, 50(12): 1956-1958.

He, Y., Chiara C., Flora M., and Piet N.L. Lens. 2020. Homoacetogenesis and solventogenesis from H₂/CO₂ by granular sludge at 25, 37 and 55°C. *Chemosphere*, 128649.

Humphreys, C.M. and Minton N.P., 2018. Advances in metabolic engineering in the microbial production of fuels and chemicals from C₁ gas. *Current Opinion in Biotechnology* 50: 174-181.

Hurst, Kendall M., and Randy S. Lewis. 2010. Carbon monoxide partial pressure effects on the metabolic process of syngas fermentation. *Biochemical Engineering Journal* 48 (2): 159-165.

Huson, D.H., Mitra, S., Ruscheweyh, H.J., Weber, N. and Schuster, S.C., 2011. Integrative analysis of environmental sequences using MEGAN4. *Genome Research*, 21(9): 1552-1560.

Kennes, D., Abubackar, H.N., Diaz, M., Veiga, M.C. and Kennes, C. 2016. Bioethanol production from biomass: carbohydrate vs syngas fermentation. *Journal of Chemical Technology and Biotechnology*, 91: 304-317.

Kotay, S.M. and Das, D., 2008. Biohydrogen as a renewable energy resource—prospects and potentials. *International Journal of Hydrogen Energy*, 33(1): 258-263.

Lanzillo, F., Giacomo R., Francesca R., Russo E. M., and Marzocchella, A. 2020. Batch Syngas Fermentation by *Clostridium carboxidivorans* for Production of Acids and Alcohols. *Processes* 8 (9): 1075.

Liu, K., Hasan K. Atiyeh, Bradley S. Stevenson, Ralph S. Tanner, Mark R. Wilkins, and Raymond L. Huhnke. 2014. Mixed culture syngas fermentation and conversion of carboxylic acids into alcohols. *Bioresource Technology*, 152: 337-346.

Liu Y., Wan J., Han S., Zhang S., Luo G. 2016. Selective conversion of carbon monoxide to hydrogen by anaerobic mixed culture. *Bioresource Technology*, 202: 1-7.

Liu, Z., Jia D., Zhang K., Zhu H., Zhang Q., Jiang W., Gu Y., and Li F., 2020. Ethanol metabolism dynamics in *Clostridium ljungdahlii* grown on carbon monoxide. *Applied and Environmental Microbiology*, 86 (14): e00730-20.

Mende , D. R., Waller, A. S., Sunagawa, S., AI Järvelin, Chan, M. M., Arumugam, M., Raes, J. and Bork, P., 2012. Assessment of metagenomic assembly using simulated next generation sequencing data. *PloS one*, 7 (2): e31386.

Mohammadi, M., Habibollah Y., Ghasem N., and Abdul R. M. 2012. Sustainable ethanol fermentation from synthesis gas by *Clostridium ljungdahlii* in a continuous stirred tank bioreactor. *Journal of Chemical Technology & Biotechnology* 87 (6): 837-843.

Monlau, F., Trably, E., Barakat, A., Hamelin, J., Steyer, J.P. and Carrere, H., 2013. Two-stage alkaline–enzymatic pretreatments to enhance biohydrogen production from sunflower stalks. *Environmental Science & Technology*, 47(21): 12591-12599.

Morinaga, T. and Naoki Kawada. 1990. The production of acetic acid from carbon dioxide and hydrogen by an anaerobic bacterium. *Journal of Biotechnology* 14 (2): 187-194.

Munasinghe, P.C. and Khanal, S.K., 2010. Biomass-derived syngas fermentation into biofuels: opportunities and challenges. *Bioresource Technology*, 101(13): 5013-5022.

Ohhata, N., Yoshida, N., Egami, H., Katsuragi, T., Tani, Y. and Takagi, H., 2007. An extremely oligotrophic bacterium, *Rhodococcus erythropolis* N9T-4, isolated from crude oil. *Journal of Bacteriology*, 189(19): 6824-6831.

Ondov B. D., Bergman N. H. and Phillippy A. M., 2011. Interactive metagenomic visualization in a Web browser. *BMC bioinformatics*, 12 (1): 385.

Pakpour, F., Najafpour, G., Tabatabaei, M., Tohidfar, M. and Younesi, H., 2014. Biohydrogen production from CO-rich syngas via a locally isolated *Rhodospseudomonas palustris* PT. *Bioprocess and Biosystems Engineering*, 37(5): 923-930.

Park, S., Muhammad, Y., Jeong J., Cha, M., Kang, H., Jang, N., Choi I., and Chang., I., 2017. Acetate-assisted increase of butyrate production by *Eubacterium limosum* KIST612 during carbon monoxide fermentation. *Bioresource Technology*, 245: 560-566.

Parshina, S. N., Sipma, J., Nakashimada, Y., Henstra, A. M., Smidt, H., Lysenko, A. M., Lens, P. N., Lettinga, G. and Stams, A. J., 2005. *Desulfotomaculum carboxydivorans* sp. nov., a novel sulfate-reducing bacterium capable of growth at 100% CO. *International Journal of Systematic and Evolutionary Microbiology*, 55 (5): 2159-2165.

Phillips, J. R., Atiyeh, H. K., Tanner, R. S., Torres, J. R., Saxena, J., Wilkins, M. R. and Huhnke, R. L., 2015. Butanol and hexanol production in *Clostridium carboxydivorans* syngas fermentation: medium development and culture techniques. *Bioresource Technology*, 190: 114-121.

Richter, H., Molitor, B., Diender, M., Sousa, D. Z. and Angenent, L. T., 2016. A narrow pH range supports butanol, hexanol, and octanol production from syngas in a continuous co-culture of *Clostridium ljungdahlii* and *Clostridium kluyveri* with in-line product extraction. *Frontiers in Microbiology*, 7: 1773.

San-Valero, P., Fernández-Naveira, Á., Veiga, M.C. and Kennes, C., 2019. Influence of electron acceptors on hexanoic acid production by *Clostridium kluyveri*. *Journal of Environmental Management*, 242: 515-521.

Schaefer, C. E., Yang, X., Pelz, O., Tsao, D. T., Streger, S. H. and Steffan, R. J., 2010. Anaerobic biodegradation of iso-butanol and ethanol and their relative effects on BTEX biodegradation in aquifer materials. *Chemosphere*, 81 (9): 1111-1117.

Simon, K. M. R., Lee, H. S., Lim, J. K., Kim, T. W., Lee, J. H. and Kang, S. G., 2015. One-carbon substrate-based biohydrogen production: microbes, mechanism, and productivity. *Biotechnology Advances*, 33 (1): 165-177.

Sipma, J., Meulepas, R. J. W., Parshina, S. N., Stams, A. J. M., Lettinga, G. and Lens, P. N. L., 2004. Effect of carbon monoxide, hydrogen and sulfate on thermophilic (55°C) hydrogenogenic carbon monoxide conversion in two anaerobic bioreactor sludges. *Applied Microbiology and Biotechnology*, 64 (3): 421-428.

Sokolova, T. G., Kostrikina, N. A., Chernyh, N. A., Tourova, T. P., Kolganova, T. V. and Bonch-Osmolovskaya, E. A., 2002. *Carboxydocella thermautotrophica* gen. nov., sp. nov., a novel anaerobic, CO-utilizing thermophile from a Kamchatkan hot spring. *International Journal of Systematic and Evolutionary Microbiology*, 52(6): 1961-1967.

Sokolova, T.G., Kostrikina, N.A., Chernyh, N.A., Kolganova, T.V., Tourova, T.P. and Bonch-Osmolovskaya, E.A., 2005. *Thermincola carboxydiphila* gen. nov., sp. nov., a novel

anaerobic, carboxydophilic, hydrogenogenic bacterium from a hot spring of the Lake Baikal area. *International Journal of Systematic and Evolutionary Microbiology*, 55(5): 2069-2073.

Stams, A.J., Van Dijk, J.B., Dijkema, C., Plugge, C.M., 1993. Growth of syntrophic propionate-oxidizing bacteria with fumarate in the absence of methanogenic bacteria. *Applied and Environmental Microbiology*. 59 (4): 1114–1119.

Stoll, I.K., Herbig, S., Zwick, M., Boukis, N., Sauer, J., Neumann, A. and Oswald, F., 2018. Fermentation of H₂ and CO₂ with *Clostridium ljungdahlii* at elevated process pressure—first experimental results. *Chemical Engineering Transactions*, 64: 151–56.

Sun, X., Atiyeh, H.K., Kumar, A., Zhang, H. and Tanner, R.S., 2018. Biochar enhanced ethanol and butanol production by *Clostridium carboxidivorans* from syngas. *Bioresource Technology*, 265: 128-138.

Svetlichny, V.A., Sokolova, T.G., Gerhardt, M., Ringfeil, M., Kostrikina, N.A. and Zavarzin, G.A., 1991. *Carboxydotherrmus hydrogeniformans* gen. nov., sp. nov., a CO-utilizing thermophilic anaerobic bacterium from hydrothermal environments of Kunashir Island. *Systematic and Applied Microbiology*, 14(3): 254-260.

Wan, J., Jing, Y., Zhang, S., Angelidaki, I. and Luo, G., 2016. Mesophilic and thermophilic alkaline fermentation of waste activated sludge for hydrogen production: focusing on homoacetogenesis. *Water Research*, 102: 524-532.

Wan, N., Sathish, A., You, L., Tang, Y.J., Wen, Z., 2017. Deciphering *Clostridium* metabolism and its responses to bioreactor mass transfer during syngas mass transfer during syngas fermentation. *Scientific Reports*, 7, 10090–10100.

Wang, J., Yang, X., Chen, C. C. and Yang, S. T. 2014. Engineering *Clostridia* for butanol production from biorenewable resources: from cells to process integration. *Current Opinion in Chemical Engineering*, 6: 43–54.

Yu, J., Liu, J., Jiang, W., Yang, Y. and Sheng, Y. 2015. Current status and prospects of industrial bio-production of n-butanol in China. *Biotechnology Advances*, 33 (7):1943-1501.

Chapter 7 Enhanced ethanol production from carbon monoxide by enriched *Clostridium* bacteria

A modified version of this chapter has been published as:

He Y., Lens, P. N. L., Veiga, M. C. and Kennes, C. 2022. Enhanced ethanol production from carbon monoxide by enriched *Clostridium* bacteria. *Frontiers in Microbiology* 12, 754713.

Abstract

Carbon monoxide metabolizing *Clostridium* spp. were enriched from the biomass of a butanol-producing reactor. After six successive biomass transfers, ethanol production reached as much as 11.8 g/L with minor accumulation of acetic acid, under intermittent gas feeding conditions and over a wide pH range of 6.45 to 4.95. The molar ratio of ethanol to acetic acid exceeded 1.7 after the lag phase of 11 days and reached its highest value of 8.6 during the fermentation process after 25 days. Although butanol production was not significantly enhanced in the enrichment, the biomass was able to convert exogenous butyric acid (3.2 g/L) into butanol with nearly 100% conversion efficiency using CO as reducing power. This suggested that inhibition of butanol production from CO was caused by the lack of natural butyric acid production, expectedly induced by unsuitable pH values due to initial acidification resulting from the acetic acid production. The enriched *Clostridium* population also converted glucose to formic, acetic, propionic, and butyric acids in batch tests with daily pH adjustment to pH 6.0. The *Clostridium* genus was enriched with its relative abundance significantly increasing from 7% in the inoculum to 94% after five successive enrichment steps. Unidentified *Clostridium* species showed a very high relative abundance, reaching 73% of the *Clostridium* genus in the enriched sludge (6th transfer).

7.1 Introduction

A significant portion of biomass sources like straw and wood is poorly degradable, but the gasification of these carbon rich waste materials to produce synthesis gas mainly with carbon monoxide (CO) and H₂ as a starting substrate for fermentation could offer a solution to this problem (Mohammadi et al., 2011). CO is a toxic gas and is present in several industrial gaseous emissions such as those of steel plants (Yu et al, 2016). Its microbiological conversion to (bio)fuels such as ethanol and butanol via the water-gas shift reaction by microorganisms has gained increased attention recently (Fernández-Naveira et al., 2017a).

The low energy density and toxicity of CO limits its application in environmental biotechnology, but a limited number of acetogens can convert CO to acids, ethanol and, occasionally, butanol and even hexanol (Fernández-Naveira et al., 2017a). These acetogens possess the key carbon monoxide dehydrogenase enzyme, which converts CO to CO₂, with acetyl-CoA as main intermediate, following the Wood-Ljungdahl pathway (WLP) (Fernández-Naveira et al., 2017a). The production of alcohols from CO takes place in two stages; i.e. first accumulation of volatile fatty acids takes place and then solventogenesis occurs (Richter et al., 2013; Abubackar et al., 2018). Only a low number of solventogenic carboxydrotrophic

acetogens have been isolated so far from a variety of environments such as soil, sediments, anaerobic sludge and animal manure, including *Clostridium ljungdahlii* (Tanner et al., 1993), *Clostridium autoethanogenum* (Abrini et al., 1994), *Clostridium carboxidivorans* (Liou et al., 2005) and *Butyribacterium methylotrophicum* (Lynd et al., 1982). Other acetogenic bacteria, known to produce acetic acid, have only recently been shown to have solventogenic potential with the accumulation of high amounts of ethanol, including *Clostridium aceticum* (Arslan et al. 2019), *Acetobacterium wieringae* Strain JM grown on 1.70 bar CO (Arantes et al., 2020) and *Clostridium sp.* AWRP grown on syngas (Lee et al., 2019).

Although syngas bioconversion has been studied with several pure strains, mixed culture fermentations may be easier to implement at large scale compared to pure cultures, as they may be more resistant and do not require sterile conditions (Charubin et al., 2019). More importantly, the presence of a broad range of acetogenic organisms in mixed cultures could have the potential to achieve metabolic yields that are theoretically not possible in pure cultures. Although mixed cultures may raise challenges of stability of the microbial composition, these can be overcome by controlling parameters such as pH and CO substrate concentration. Mixed cultures may exhibit syntrophic or complementary behaviour and may thus better withstand poor environmental conditions such as a low pH or nutrient limitation and have better abilities for adaptation. For instance, *C. autoethanogenum* can convert CO or syngas to ethanol and acetate, but when co-cultured with *Clostridium kluyveri*, the co-culture ends up producing butanol or hexanol with CO as reducing power, not found in any of those individual strains (Diender et al., 2016).

Despite this huge potential, hardly any study has reported and optimized ethanol and butanol production in mixed cultures using 100% CO as the carbon source. Chakraborty et al. (2019) investigated a two stage fermentation using anaerobic sludge as inoculum, in which first 6.18 g/L acetic acid was produced from continuous CO gas feeding by an enriched anaerobic sludge at a controlled pH of 6.2. Then, in the same continuous stirred tank reactor (CSTR), 11.1 g/L ethanol and 1.8 g/L butanol accumulated when the pH was decreased to 4.9. The aim of this study was to first enrich CO metabolizing, solvent producing acetogens using 100% CO as the carbon and energy source. The enriched bacteria were then determined and the functional acetogens were identified via microbial community analysis. Secondly, this study further explored the effect of exogenous butyric acid and glucose on enhanced butanol production as well as the effect of pH regulation on enhanced ethanol and butanol production by the enriched acetogenic bacteria.

7.2 Materials and methods

7.2.1 Source of inoculum

The inoculum was obtained from a fed batch incubation producing for 6.8 g/L butanol operated with intermittent gas feeding using CO as the sole carbon and energy source after 127 days operation (He et al., 2022). The microbial community of the inoculum was mainly composed of *Clostridia* (37%) and *Bacilli* (36%) class (He et al., 2022) and 7% *Clostridium* genus (Table 7.2).

7.2.2 Medium composition

The culture medium was prepared as described previously (He et al., 2021). A 1 L culture medium was prepared according to Stams et al. (1993) and modified as follows: 408 mg/L KH_2PO_4 , 534 mg/L $\text{Na}_2\text{HPO}_4 \cdot 2\text{H}_2\text{O}$, 300 mg/L NH_4Cl , 300 mg/L NaCl , 100 mg/L $\text{MgCl}_2 \cdot 6\text{H}_2\text{O}$, 110 mg/L $\text{CaCl}_2 \cdot 2\text{H}_2\text{O}$; 1 mL trace metal and 1 mL vitamin stock solution (Stams et al., 1993). Once prepared, the 1 L medium (except for $\text{CaCl}_2 \cdot 2\text{H}_2\text{O}$ and vitamins) was brought to boiling in order to remove O_2 , and it was later cooled down to room temperature under an oxygen-free N_2 flow. Then $\text{CaCl}_2 \cdot 2\text{H}_2\text{O}$ and the vitamins were added, as well as Na_2S (0.24 g) as the reducing agent.

7.2.3 Experimental set-up

7.2.3.1 Enrichment of CO converting acetogens

Enrichments were obtained by successive transfer of active cultures (10% v/v) into fresh medium with a headspace CO pressure of 1.8 bar. 100 mL medium was dispensed into 500 mL flasks, 10 mL enriched sludge was added as inoculum, and the pH was adjusted to 6.2 with 2 M HCl under CO gas flow. The bottles were then sealed with rubber stoppers, capped with screw caps, and incubated with steady agitation (150 rpm) in the dark. When the gas pressure decreased below 1 bar, as a result of bacterial C_1 -gas consumption, the bottle was flushed with fresh pure CO for about 5 minutes, until again reaching a gas pressure of 1.8 bar. To avoid inhibition of solventogenesis at low pH, its value was adjusted to 6.0-6.4 at the beginning of each CO addition. To enhance cell growth, yeast extract was added, after filtration through a 0.22 μm filter, to reach a final concentration of 0.5 g/L. As soon as microbial growth was observed, i.e. OD_{600} increased and acetic acid and alcohols were produced, 10 mL inoculum was transferred into another flask under the same conditions.

In the 6th transfer, the last CO addition started with an initial CO gas pressure of only 1.5 bar, as the glass serum bottles started after 27 days fermentation under gas pressures as high as 1.8 bar. In the 7th and 8th transfer, the CO pressure was further decreased to 1.2 bar.

7.2.3.2 Enhanced butanol production from exogenous butyric acid by enriched *Clostridium* populations

To assess and demonstrate the butanol production potential of the enriched culture after the 5th transfer on CO, the enriched sludge was further inoculated in a 1L serum bottle with 200 mL culture medium and with the addition of 3.2 g/L exogenous butyric acid. The initial pH was 6.2 and 100% CO was introduced as electron donor to reach an initial gas pressure of 1.8 bar. The same CO feeding procedure was used as described in section 2.3.1.

7.2.3.3 Exogenous glucose consumption by the enriched sludge

To investigate the sugar utilization and possible endogenous acid production used for ethanol and butanol production, the enriched biomass of the 6th transfer with dominant *Clostridium* spp. was incubated with either pure glucose or glucose and CO as the substrates. 25 mL medium was dispensed into 125 mL conical flasks, 2.5 mL enriched sludge was added as inoculum (10%) and the pH was adjusted to 6.2 with 2 M HCl under N₂ gas flow. The headspace was flushed with N₂ or CO, glucose was added to reach a final concentration of 5 g/L in duplicate experiments. The bottles were then sealed with rubber stoppers, capped with screw caps, and incubated with steady agitation (150 rpm) in a dark environment.

7.2.3.4 Ethanol production from CO with pH control at 6.2 and 5.7 in intermittent gas-fed bioreactors

The poor butanol production among the transfers was expected to be due to the low butyric acid production, likely induced by unfavourable pH values and the natural pH drop. Therefore, CO conversion by the enriched culture was further investigated under pH controlled conditions at pH 5.7 and 6.2, and also without pH control using 10% enriched sludge from the 7th transfer. pH control experiments were carried out in two 1 L serum bottles with 200 mL culture medium and with pH control at either pH 5.7 or 6.2 by supplying 1M HCl or 1M NaOH. The same CO feeding procedure was used as described in section 2.3.1.

7.2.3.5 Sampling

The gas pressure was measured daily. Liquid samples (1 mL) were withdrawn for measuring the cell concentration (OD₆₀₀), then centrifuged at 8000×g for 5 min and the supernatant was used to quantify the concentrations of acids and solvents.

7.2.4 Analytical methods

The cell concentration was determined with a spectrophotometer (Hitachi, Model U-200, Pacisa & Giralt, Spain) at a wavelength of 600 nm with medium solution as the blank (Arslan et al., 2019). pH was measured by pH meter (Mettler Toledo, Zurich, Switzerland).

Acetic acid, propionic acid, butyric acid, ethanol and butanol were determined on a high performance liquid chromatography (HPLC, HP1100, Agilent Co., USA) equipped with a refractive index detector using an Agilent Hi-Plex H Column (300×7.7 mm). A 5 mM H₂SO₄ solution was used as mobile phase at a flow rate of 0.80 mL/min, with a sample injection volume of 20 µL and a column temperature of 45 °C (Arslan et al., 2019).

7.2.5 Microbial analysis

The microbial community composition of different successive transfers of the inoculum, 2nd, 4th, 5th, 6th, 7th, 8th, exogenous butyric acid addition (HBU), glucose fermentation (Glucose), pH 6.2 and pH 5.7 were analyzed. DNA was extracted using a DNeasy® PowerSoil Kit (QIAGEN, Germany) following the manufacturer's protocol. 10 mL sludge was used for DNA extraction at the end of the incubations of successive transfers. The extracted DNA was quantified and its quality was checked by a Nanodrop 2000c Spectrophotometer (Thermo Scientific, USA). The extracted DNA were analyzed by Metagenomics -Seq (Illumina PE150, Q30 ≥ 80%) (Novogene, UK). The procedures of metagenomic sequencing are detailed in <https://en.novogene.com/services/research-services/metagenomics/shotgun-metagenomic-sequencing/> and Zhang et al. (2018) and section 6.2.6 (Chapter 6). The raw data is available in OneDrive NUIG.

Table 7.1 The Statistic of gene catalogues

ORFs NO.	954,675
integrity: start	150,041(15.72%)
integrity: none	39,733(4.16%)
integrity: all	547,831(57.38%)
integrity: end	217,070(22.74%)
Total Len.(Mbp)	590.04
Average Len. (bp)	618.06
GC percent	48.03

Note: "ORFs NO." means number of genes in gene catalogue. "integrity :start" represents amount and percentage of genes only containing start codon. "integrity: end" represents amount and percentage of genes only containing stop codon. "integrity: none" represents amount and percentage of genes not containing start or stop codon. "integrity: all" represents amount and percentage of genes containing both start and stop codon. "Total Len. (Mbp)" means the total length of gene catalogue (million).

"Average Len." means the average length of genes in gene catalogue. "GC Percent" means the prediction of GC content of genes in gene catalogue.

The gene catalogues have been depicted in Table 7.1 and Fig. 7.1. Taxonomy annotation analysis involved comparing metagenomic reads to the database of taxonomically informative gene families (NR database) to annotate each metagenomic homolog. Taxonomic diversity involves identifying those reads that are marker gene homologs to a database of taxonomically informative gene families using sequence or phylogenetic similarity to the database sequences (NR database) (Buchfink et al., 2015) to taxonomically annotate each metagenomic homolog (MEGAN, Huson et al., 2011).

According to the abundance table of each taxonomic level, various analyses were performed including Krona analysis, bar plot for abundant species and heatmap of abundance. Principal-component analysis (PCA) based on Bray-Curtis distance was used to evaluate the similarity of samples. The distance was calculated according to relative taxonomic abundance (Buchfink et al., 2015). The final results were exhibited by combining the clustering result and relative abundance of different samples at the phylum level.

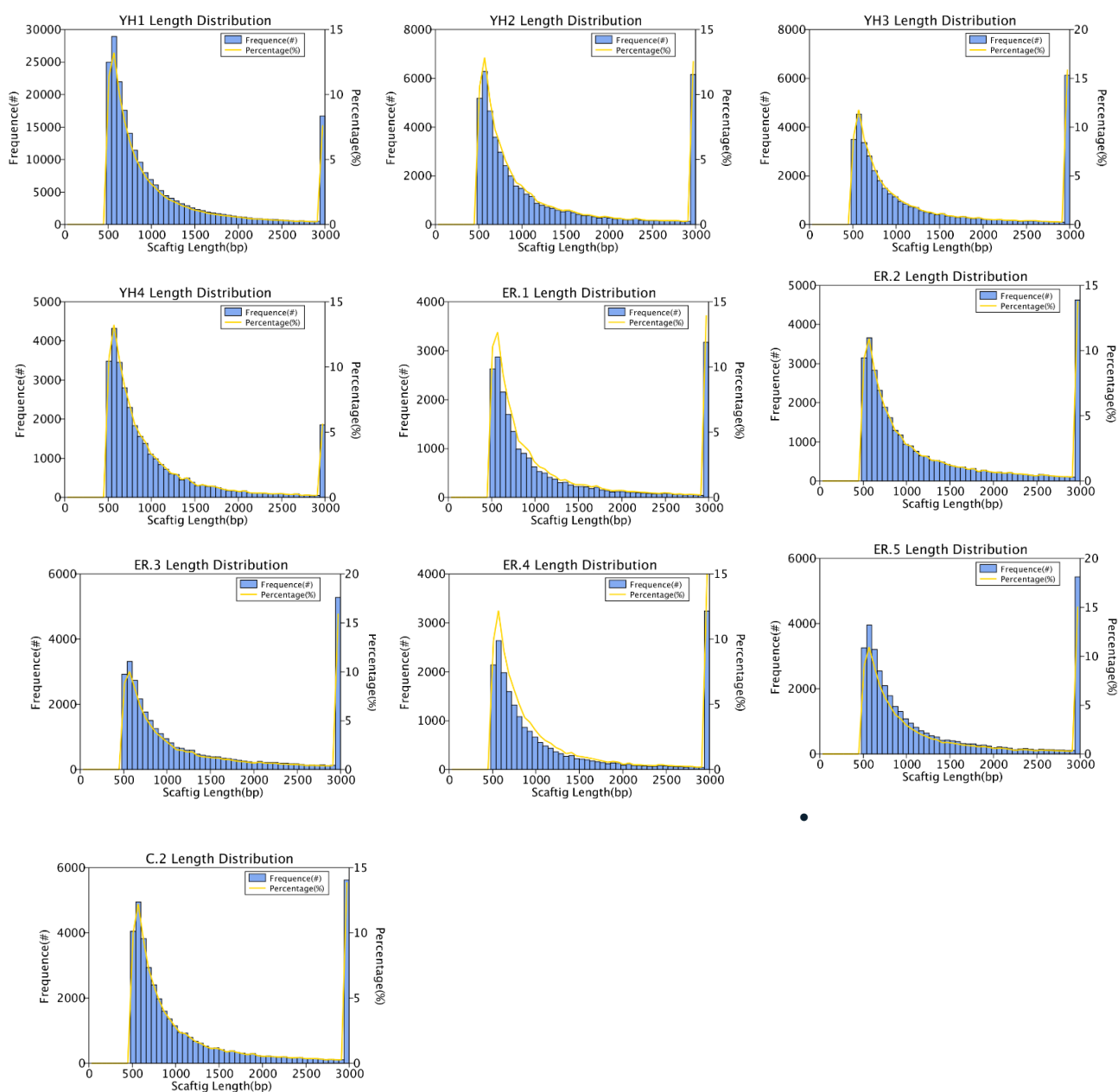


Fig. 7.1 Distribution of scaftig length (≥ 500 bp)

(YH1- The enriched sludge at the end of the bioreactor for 6.8 g/L butanol production, YH2- 2nd transfer, YH3- 4th transfer, YH4- 5th transfer, ER1- 6th transfer, ER2- 7th, ER3- 8th, ER4- 5 HBU (Exogenous 3.2 g/L butyric acid), ER5- 6th transfer grows on 5 g/L glucose, C1- pH 6.2, C2- pH 5.7).

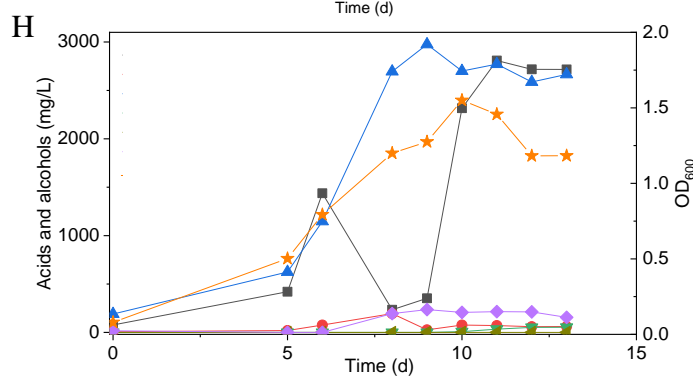
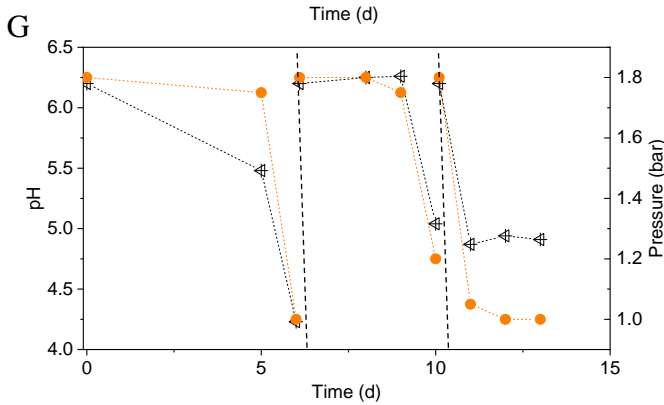
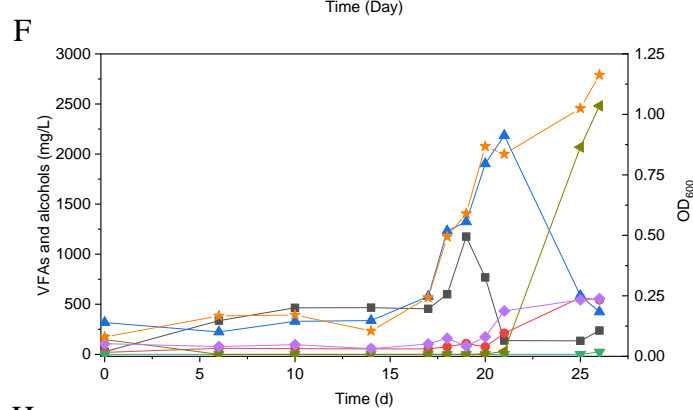
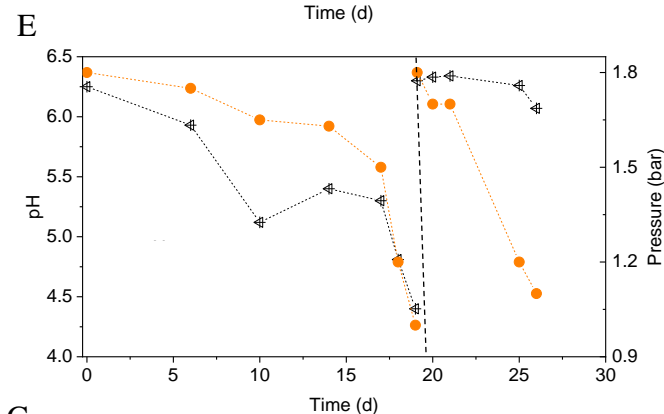
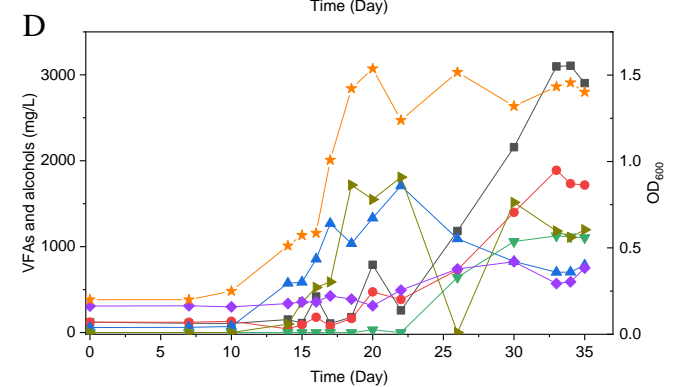
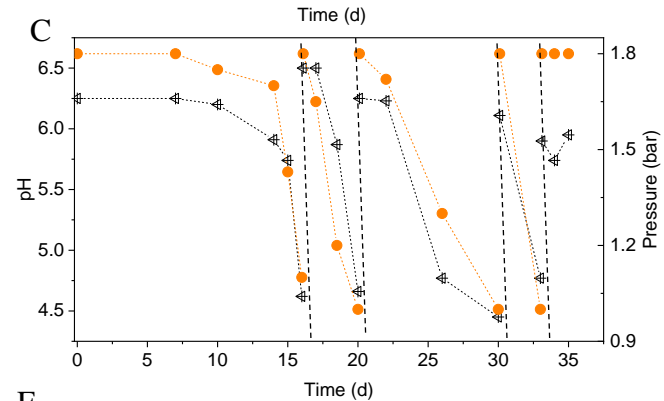
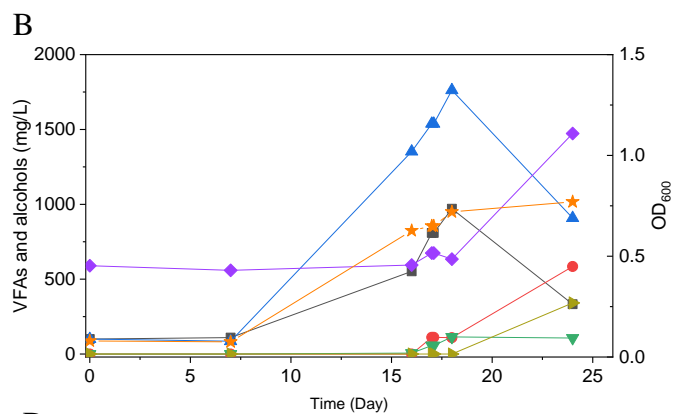
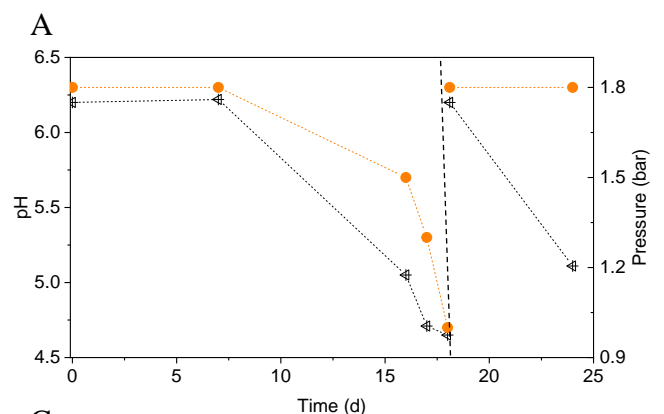
7.3 Results

7.3.1 Enrichment of CO-converting acetogens

In the 1st transfer, CO was added twice (i.e., two CO additions) at 0 and 18 d (Fig. 7.2A). After 16 days of fermentation, 0.6 g/L acetic acid and 1.3 g/L ethanol were produced (Fig. 7.2B). Both the acetic acid and ethanol concentration reached their highest value of 0.9 and 1.7 g/L, respectively, at day 18 along with a gas pressure decrease from 1.8 to 1.0 bar and the pH dropped to 4.65 (Fig. 7.2A, B). Then both the acetic acid and ethanol concentration decreased to, respectively, 0.5 and 1.0 g/L at day 24. The OD₆₀₀ gradually increased to a maximum value of 0.72 after 24 days of incubation. 0.1 g/L butyric acid had accumulated at day 18 and kept stable till the end of incubation day 24, while butanol production was stimulated during the second CO fermentation and reached 1.0 g/L at day 24. Some other acids were detected as well, such as 0.6 g/L propionic acid and 0.3 g/L valeric acid, which further contributed to induce a pH decrease to 5.11 at the end of the incubation (Fig. 7.2A).

In the 2nd transfer, CO was added at 0, 16, 21, 30 and 33 d, respectively (i.e. five CO additions) (Fig. 7.2C). Ethanol started being produced and reached 0.9 g/L at day 16 while the acetic acid concentration remained low, with only 0.4 g/L being detected, and the pH dropped to 4.6 (Fig. 7.2D). Then the ethanol concentration kept increasing to 1.7 g/L, while the acetic acid concentration was 0.3 g/L along with the pH decreased to 4.7 and the OD₆₀₀ reached its highest value of 1.537 at day 22 (Fig. 7.2D). Thereafter, acetic acid started to accumulate quickly and reached 3.1 g/L, while the ethanol concentration decreased to 0.7 g/L at the end of the incubation (Fig. 7.2D). Meanwhile, the net amounts of butyric acid and butanol increased to 1.1 and 0.8 g/L, respectively (Fig. 7.2D). The concentrations of propionic and valeric acid were, respectively, 1.7 and 1.2 g/L, at the end of the incubation (Fig. 7.2D).

During the 3rd transfer, CO was supplied twice, at day 0 and 19. After approximately 17 days of adaption, the net acetic acid and ethanol concentrations increased to reach 1.1 and 1.0 g/L, respectively, at day 19, with the pH dropping to 4.4 (Fig. 7.2E, F). The net amount of ethanol reached its highest concentration of 1.8 g/L, along with a steep decrease of the acetic acid concentration to 0.1 g/L at day 22 when the gas pressure decreased from 1.8 to 1.7 bar (Fig. 7.2E, F). However, the ethanol and acetic acid concentrations decreased to 0.4 g/L at day 26 (Fig. 7.2E). The butanol concentration increase occurred after adding CO at pH 6.2 at day 19, then it remained stable at 0.6 g/L (Fig. 7.2F). Both 0.5 g/L propionic acid and 2.5 g/L valeric acid were also found at day 26 (Fig. 7.2E, F), when the highest cell concentration of 1.163 (OD₆₀₀) was obtained.



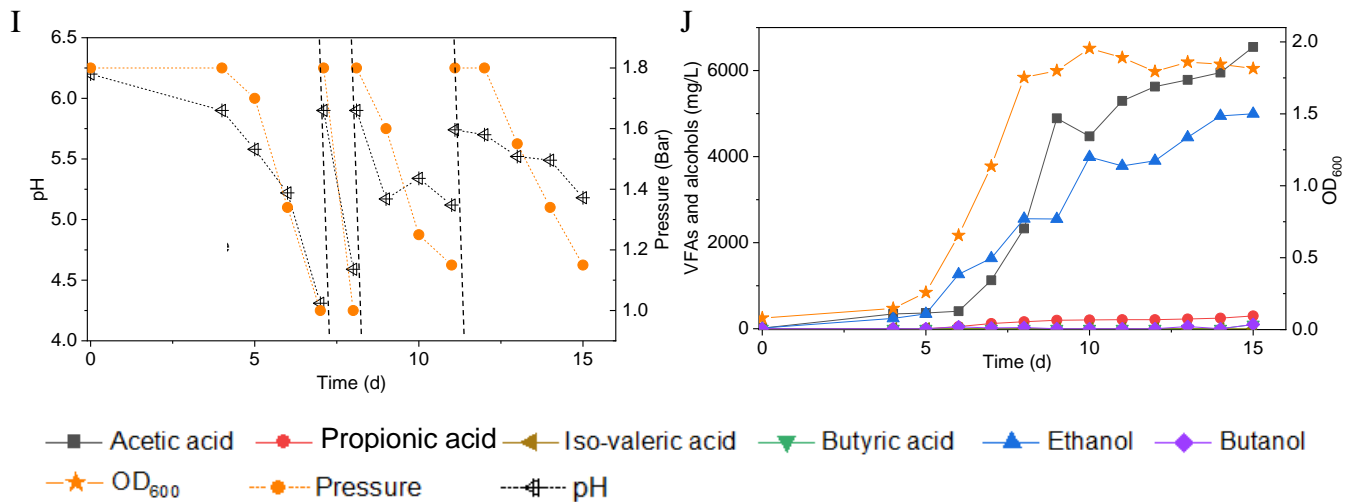


Fig. 7.2 Enrichment of CO converting solventogenic bacteria among the five transfers using CO as the carbon source by enriched sludge with initial CO gas pressure of 1.8 bar. (A), (C), (E), (G) and (I) represent the changes of gas pressure and pH of the 1st, 2nd, 3rd, 4th and 5th transfer, respectively. (B), (D), (F), (H) and (J) represent cell concentration (OD₆₀₀) acetic acid (HAc), propionic acid (HPr), butyric acid (HBu), ethanol (EtOH), isovaleric acid (i-Hval) and butanol (BtOH) production of the 1st, 2nd, 3rd, 4th and 5th transfer, respectively. The dash lines in Figure (A), (C), (E), (G) and (I) represent 1.8 bar CO addition and pH adjustment.

With the 4th transfer, CO was supplied at day 0, 6 and 10, respectively. The net ethanol and acetic acid production reached 1.0 and 1.4 g/L, respectively, along with the pH decreasing to 4.23 at day 6 (Fig. 7.2G, H). The ethanol concentration kept increasing and reached 2.4 g/L, with the pH dropping to 5.0 (Fig. 7.2G, H). Finally, the ethanol concentration slightly increased to 2.8 g/L at day 11 of the last CO addition (Fig. 7.2G, H). The cell concentration increased to 0.793 after the first CO addition and reached the highest value of 1.55 after the second CO addition (Fig. 7.2G, H).

Acetic acid and ethanol production were dominant in the 5th transfer but with a quite higher ethanol concentration than in all previous transfers (Fig. 7.2I). CO was supplied four times at day 0, 7, 8 and 12 (Fig. 7.2I). After 5 days adaption to the 5th transfer, the acetic acid and ethanol concentrations increased to 0.4 and 1.3 g/L, respectively, with the pH decreasing to 5.22, while the OD₆₀₀ increased to 0.655 at day 7 (Fig. 7.2I, J). The second CO addition lasted only one day, with a very fast gas consumption, and the acetic acid and ethanol concentrations increasing to 2.3 and 2.6 g/L, respectively, with the pH dropping to 4.31 and the OD₆₀₀ increasing to 1.753 at day 8 (Fig. 7.2I, J). With the last two CO additions in the 5th transfer, the

cell concentration remained roughly stable, while acetic acid and ethanol concentrations increased to 6.5 and 5.0 g/L, respectively (Fig. 7.2I, J).

The enrichment strategy of five successive transfers had efficiently selected for acetic acid/ethanol producing organisms, with only minor concentrations of other metabolites, such as propionic and valeric acid. The unstable propionic acid and valeric acid production at the 1st, 2nd and 3rd transfer could be attributed to the change of microbial community composition during the enrichment, for instance, the relative abundance of *Clostridium* bacteria was enriched 52% at the 2nd transfer, while it was increased to 78% of the 4th transfer (Table 7.2). The exponential biomass growth phase led to an exponential production of metabolites, while the accumulation of end products slowed down once the steady biomass concentration was reached (Fig. 7.2). Ethanol consumption, which was observed towards the end of each incubation period during the first three transfers, was not observed anymore from the fourth transfer onwards (Fig. 7.2). The net ethanol production was enhanced 3 fold at the 5th transfer compared to the first one. The relatively high production of 5.0 g/L ethanol in batch tests using CO as the carbon source was seldomly reported so far, except some studies conducted in bioreactors using syngas as the substrate (Table 7.3). This high ethanol concentration can be even significantly increased further, as shown in the additional experiments described hereafter.

Table 7.2 Relative abundance of *Clostridium spp.* at genus level in the initial inoculum sludge and the 2nd, 4th, 5th, 6th, 7th and 8th transfer as well as in the incubation with exogenous butyric acid (HBu) and glucose addition (Glucose), controlled pH 6.2 and pH 5.7.

	Inoculum sludge	2 nd transfer	4 th transfer	5 th transfer	6 th transfer	7 th transfer	8 th transfer	HBu	Glucose	pH 6.2	pH 5.7
Inoculum source								5 th transfer enriched sludge	6 th transfer enriched sludge	7 th transfer enriched sludge	
The relative abundance of <i>Clostridium</i> genus in bacteria	7	52	78	94	81	84	88	88	9	81	88
The relative abundance of <i>Clostridium</i> genus in the total sample	4	43	66	85	73	73	81	82	7	69	76
Species name	<i>Clostridium</i> (Genus level) %										
<i>Clostridium strain W14A</i>	29	0.7	2	0.9	2	1	1	0.4	11	2	1
<i>Clostridium ragsdalei</i>	10	2	4	4	4	4	4	4	3	4	4
<i>Clostridium estertheticum</i>	5	0.008	0.007	0.009	0.0007	0.002	0.002	0.0007	0.05	0.005	0.01
<i>Clostridium ljungdahlii</i>	3	8	8	8	8	8	8	8	0.9	8	8
<i>Clostridium coskatii</i>	2	4	4	5	4	4	4	4	0.6	4	4
<i>Clostridium magnum</i>	1	0.3	0.3	0.1	0.06	0.08	0.3	0.1	4	0.4	0.5
<i>Clostridium autoethanogenum</i>	1	5	5	6	6	6	6	6	0.4	5	5
<i>Clostridium sp. PI S10 A1B</i>	0.9	0.2	0.07	0.01	0.01	0.07	0.02	0.05	2	0.1	0.03
<i>Clostridium amylolyticum</i>	0.8	0.2	0.09	0.03	0.05	0.04	0.04	0.03	2	0.08	0.06
<i>Clostridium botulinum</i>	0.7	0.2	0.3	0.2	0.2	0.2	0.2	0.2	2	0.2	0.2
<i>Clostridium homopropionicum</i>	0.4	0.02	0.04	0.01	0.004	0.003	0.1	0.01	10	0.05	0.03
<i>Clostridium carboxidivorans</i>	0.6	0.4	0.4	0.4	0.3	0.7	0.6	0.3	0.8	0.4	0.4
<i>Clostridium kluyveri</i>	0.6	0.3	0.4	0.3	0.3	0.3	0.4	0.3	0.4	0.3	0.3
<i>Clostridium tyrobutyricum</i>	0.5	0.7	0.8	0.8	0.7	0.7	0.8	0.7	0.2	0.7	0.7
<i>Clostridium sp. C105KSO15</i>	0.08	0.009	0.08	0.002	0.01	0.04	0.04	0.4	3	0.01	0.004
<i>Clostridium cadaveris</i>	0.07	0.5	0.7	0.1	0.2	0.2	0.2	1	14	0.5	0.4
<i>Clostridium butyricum</i>	0.07	0.009	0.02	0.005	0.0006	0.002	0.02	0.003	1	0.03	0.06
<i>Clostridium sp. BNLI100</i>	0.03	0.002	0.003	0.0001	0.0003	0.002	0.007	0.008	1	0.03	0.01
Other identified <i>Clostridium spp.</i>	17.3	6.5	2.8	1.1	1.2	2.7	1.3	1.5	14.7	2.2	3.3
Unidentified <i>Clostridium spp.</i>	27	71	71	73	73	72	73	73	29	72	72

Note: The bolded values in Glucose column represent the increased relative abundance of *Clostridium spp.* compared to the successive transfers. The bolded values in the last row represent the high relative abundance of unidentified *Clostridium spp.*

Table 7.3 Highest ethanol and butanol concentrations during syngas/CO fermentation using various biocatalysts.

Microorganism	Reactor configuration	Gas composition	Working volume (L)	Time/d	pH	Highest alcohols (g/L)		Reference
						Ethanol	Butanol	
<i>Alkalibaculum bacchi</i> CP15	CSTR	CO/CO ₂ /H ₂ /N ₂ (20/15/5/60)	3.3/7	51	8.0	6.0	1.1	Liu et al., 2014
<i>C. carboxidivorans</i> P7	Bubble column	CO/CO ₂ /N ₂ (25/15/60)	4.5 /6.2	10	5.3~5.75	1.6	0.6	Rajagopalan et al., 2002
	HFR	CO/CO ₂ /H ₂ /N ₂ (20/15/5/60)	8	15	6	24.0	NA	Shen et al., 2014
	CSTR	CO/CO ₂ /H ₂ /N ₂ (20/15/5/60)	3/7.5	11	5.7	1.5	0.5	Ukpong et al., 2012
	CSTR	100% CO	1.2/2	21	5.75, 4.75	5.55	2.66	Fernández et al., 2016
	Batch	CO/CO ₂ /H ₂ /Ar (56/20/9/15)	0.03/0.125	5	NA	3.64	1.35	Shen et al., 2020
<i>C. autoethanogenum</i>	CSTR	100% CO	1.2/2	7	6.0, 4.75	0.9	NA	Abubackar et al., 2015
	Batch	100% CO	0.075 /0.2	NA	5.75, 4.75	0.65	NA	Abubackar et al., 2012
<i>C. ljungdahlii</i>	CSTR+ Bobble column	CO/CO ₂ /H ₂ (60/5/35)	1/2 (CSTR) 4/6 (BC)	83	5.5 (CSTR) 4.3~4.8 (BC)	20.7	NA	Richter et al., 2013
<i>Clostridium aceticum</i>	CSTR	CO/CO ₂ /H ₂ /N ₂ (30/5/15/50)	1.2/2	52	6.98	5.6	NA	Arslan et al., 2019
<i>C. ragsdalei</i>	Tricking bed reactor	CO/CO ₂ /H ₂ /N ₂ (38/28.5/28.5/5)	1	70	5.8-4.6	5.7	NA	Devarapalli et al., 2016
<i>Clostridium</i> Strain P11	CSTR	CO/CO ₂ /H ₂ /N ₂ (20/15/5/60)	3.5 / 7.5	15	6.1	5.0	0.6	Maddipati et al., 2011
Anaerobic sludge from industry wastewater treatment	CSTR	100% CO	1.2/2	42	6.2, 4.9	11.1	1.8	Chakraborty et al., 2019
Enriched sludge in fed batch (6 th transfer)	Fed batch	100% CO	0.1/0.5	29	5.0-6.3	11.8	1.0	This study

7.3.2 Enhanced ethanol production with minor acetic acid accumulation

In the 6th transfer, CO converting acetogens with enhanced ethanol production were successfully enriched compared to the previous five transfers. Six CO supplies were performed in the 6th transfer, at 0, 13, 15, 19, 21 and 26 d, with the initial CO gas pressure set at 1.8 bar (Fig. 7.3A).

In the first CO addition (0-13 d), 11 days adaption were required and then 0.8 g/L acetic acid and 2.2 g/L ethanol were produced, with an ethanol to acetic acid molar ratio of 3.32 (Fig. 7.3B). This lag phase of several days, just after inoculation, was typically observed in all transfers indicating gradual adaption to the conditions, while subsequent fast gas consumption occurred at each new CO supply. The pH value decreased to 4.95 and the gas pressure decreased to 1 bar at day 13 (Fig. 7.3A). The second CO addition (13-15 d) lasted only 48 h as the gas pressure quickly dropped to 1.2 bar and the pH decreased to 5.5 (Fig. 7.3A) and yielded 2.1 g/L acetic acid and 3.0 g/L ethanol. The molar ratio of ethanol to acetic acid decreased to 1.87, due to the high acetic acid accumulation in the biomass log phase (Figure 2B). The cell concentration increased to 1.685 (OD₆₀₀) (Fig. 7.3B).

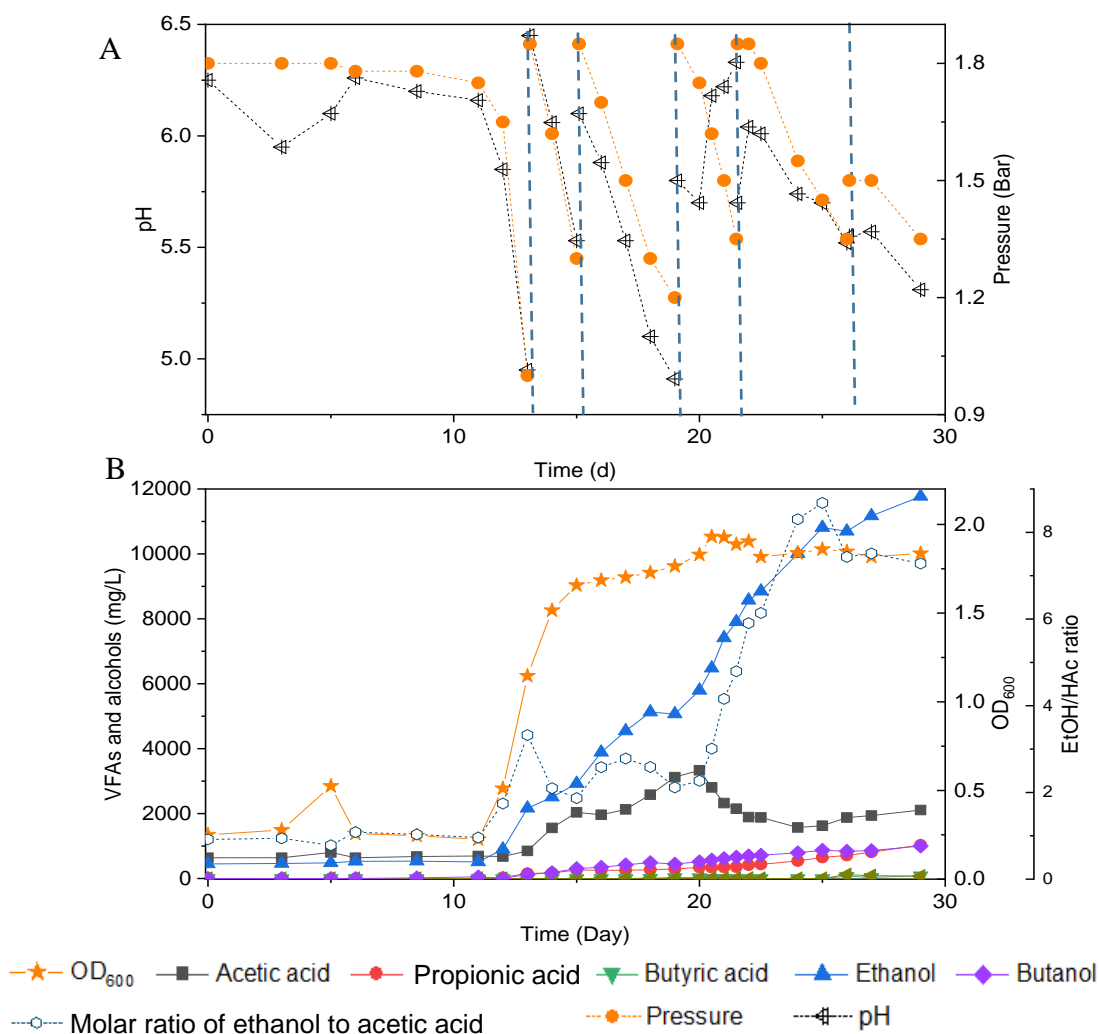


Fig. 7.3 Changes of pH and gas pressure (A) and cell concentration (OD_{600}), acetic acid, propionic acid, butyric acid, ethanol, butanol and molar ratio of ethanol to acetic acid (B) using CO as the carbon source with initial CO gas pressure of 1.8 bar in the 6th transfer by enriched sludge. The dash lines in Fig. 7.2A represent 1.8 bar CO addition and pH adjustment.

At the third CO addition (15-19 d), the pH decreased to 4.91, ethanol kept accumulating up to 5.1 g/L, while the acetic acid concentration only slowly increased to 3.1 g/L (Fig. 7.3B). Around this period, biomass growth and the acetic acid concentration levelled off; while ethanol production kept increasing at high rates, except for a short stable period at day 18-19, corresponding to a gas pressure that decreased to 1.2 bar and a pH value that reached its lowest value ($pH < 5$) of the whole experiment (Fig. 7.3). A similar slowing down in the ethanol production was observed at the end of the first CO addition from the 1st to 5th transfer, at low gas pressure and pH 4.95 (Fig. 7.2). A minor increase in cell concentration was observed, up to 1.765 (OD_{600}), at day 19. At the fourth CO addition (19-21 d), the acetic acid concentration decreased for the first time, along with the pH increasing from 5.7 to 6.18 at day 20 (Fig. 7.3B).

To sustain acetic acid consumption and minimize any potential ethanol oxidation sometimes reported in the presence of CO₂ (Arslan et al., 2019; He et al., 2022), the pH was readjusted to 5.7. The accumulation of ethanol reached then 7.9 g/L, while the acetic acid concentration decreased to 2.1 g/L and the ethanol to acetic acid molar ratio reached 4.80 (Fig. 7.3B). The highest cell concentration of 1.932 (OD₆₀₀) was then measured at day 21 and cell growth entered a steady phase. The gas pressure decreased to 1.35 bar at day 21 (Fig. 7.3A).

During the fifth CO addition (21- 26 d) of the 6th transfer, ethanol was the only compound with increasing concentration, up to 10.7 g/L, with the highest ethanol/acetic acid molar ratio of 8.68 at day 25 (Fig. 7.3B). A final, high ethanol concentration of 11.8 g/L was obtained with only 2.1 g/L acetic acid, 1.0 g/L propionic acid and 1.0 g/L butanol, and insignificant butyric acid production (0.07 g/L) at the end of the incubation (Fig. 7.3B).

The highest net ethanol concentrations of the 1st, 2nd, 3rd, 4th, 5th and 6th transfer were, respectively, 1.7, 1.7, 1.9, 2.8, 5.0 and 11.8 g/L (Fig. 7.4A). Conversely, the highest net butanol production during the six transfers, were, respectively, 0.9, 0.5, 0.5, 0.2, 0.1 and 1.0 g/L from the first to the last transfer (Fig. 7.4A). The ethanol concentration was enhanced 6.9 fold between the 1st and the 6th transfer. The butanol concentration at the 5th transfer reached only 1/9 of the value corresponding to the 1st transfer (Fig. 7.4A). The net butyric acid production also decreased along with the enrichments, which reached its highest concentration of 0.2 g/L in the 1st transfer and 1.1 g/L in the 2nd transfer; then it remained below 0.1 g/L at the 3rd, 4th, 5th and 6th transfer (Fig. 7.4B). Despite the low butanol production, interestingly, its concentration increased slowly although butyric acid was not significantly produced after six enrichments (Fig. 7.4A). The highest butanol concentration reached 1.0 g/L and with only 0.085 g/L butyric acid production at the end of the incubation period (Fig. 7.4A, B).

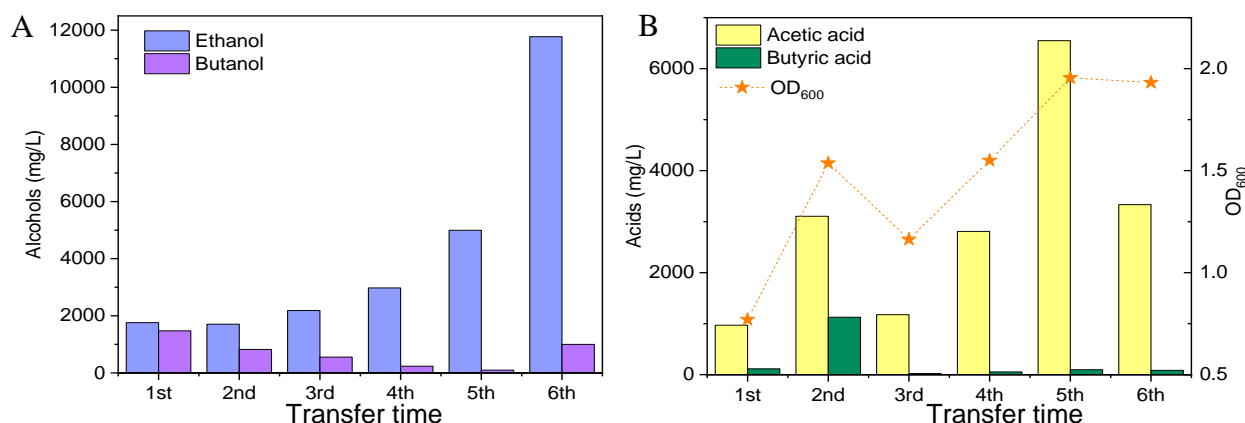


Fig. 7.4 Comparison of the maximum ethanol and butanol concentration (A) and acetic acid, butyric acid and cell concentration (OD₆₀₀) (B) of the 1st, 2nd, 3rd, 4th and 5th transfer using CO as the carbon source by enriched sludge.

The relative abundance of the initial inoculum was 61% bacteria, 5% archaea and 34% unknown. The phylum Firmicutes occupied 75% of the bacteria, mainly represented by the *Clostridia* (47%) and *Bacilli* (49%) class (Fig. 7.5A). The *Clostridiales* order occupied 98% in the *Clostridia* class, which was mainly distributed over the *Ruminococcaceae* (14%), *Clostridiaceae* (21%) and *Oscillospiraceae* (40%) family (Fig. 7.5A). After successive transfers and enrichments, the *Clostridium* genus increased from 7% in the inoculum sludge to 52, 78 and 94 and 81%, respectively, in the 2nd, 4th and 5th and 6th transfer of the enriched cultures (Fig. 7.5, Table 7.2).

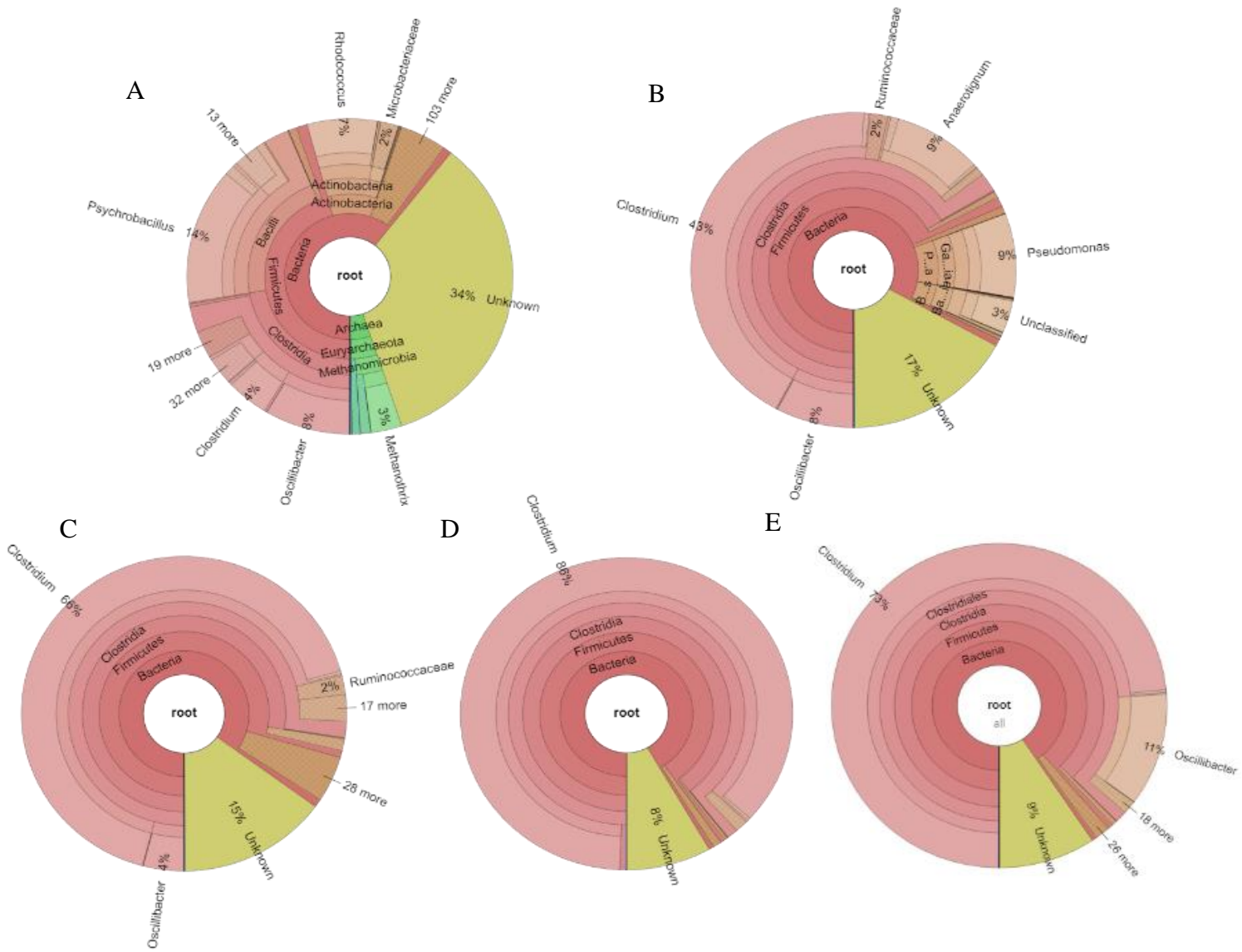


Fig. 7.5 Relative abundance at genus level of (A) the initial inoculum, (B) 2nd, (C) 4th, (D) 5th and (E) 6th transfers for enriched acetogens using CO as the carbon source.

Among the *Clostridium* genus, some identified species such as *C. autoethanogenum* increased from 1% to 6%, which is known to convert CO to acetic acid and ethanol via the

WLP pathway (Tables 7.2 and 7.3). The relative abundance of *C. ljungdahlii* increased from 3% to 8% after enrichment, which is also a species producing acetate and ethanol from syngas via the WLP (Mohammadi et al., 2012) (Tables 7.2 and 7.3). *C. carboxidivorans* produces butanol from CO (Fernández-Naveira et al., 2016), besides ethanol, but its relative abundance did not significantly increase and even slightly decreased to 0.4% in the 5th transfer (Tables 7.2 and 7.3). Unidentified *Clostridium* species occupied a very high relative abundance, increasing from 27% in the inoculum to 71, 71, 74 and 73% of the *Clostridium* genus, respectively, in the 2nd, 4th, 5th and 6th transfer (Table 7.2). The 7th and 8th transfers were further conducted in successive transfers and the relative abundance of the *Clostridium* genus occupied as high as, respectively, 73% and 81%, similar to the 5th and 6th transfer (Fig. 7.6 and Fig. 7.7).

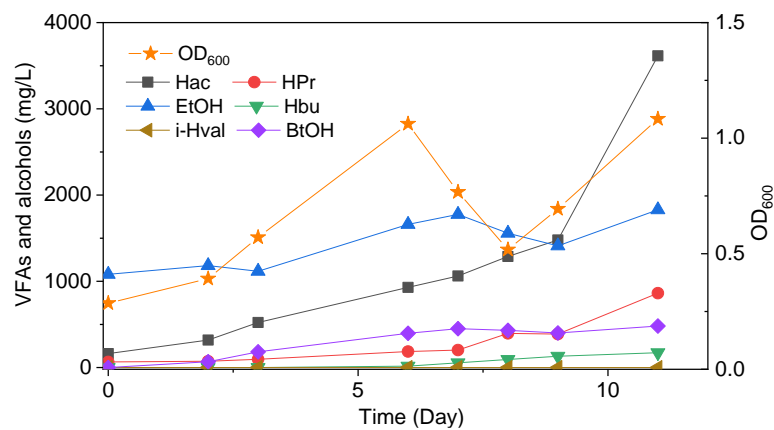


Fig. 7.6 Production of acetic acid (Hac), propionic acid (HPr), butyric acid (Hbu), ethanol (EtOH), isovaleric acid (i-Hval) and butanol (BtOH) of different transfer times and change of gas pressure and pH at 7th using CO as the carbon source by enriched sludge with initial CO.

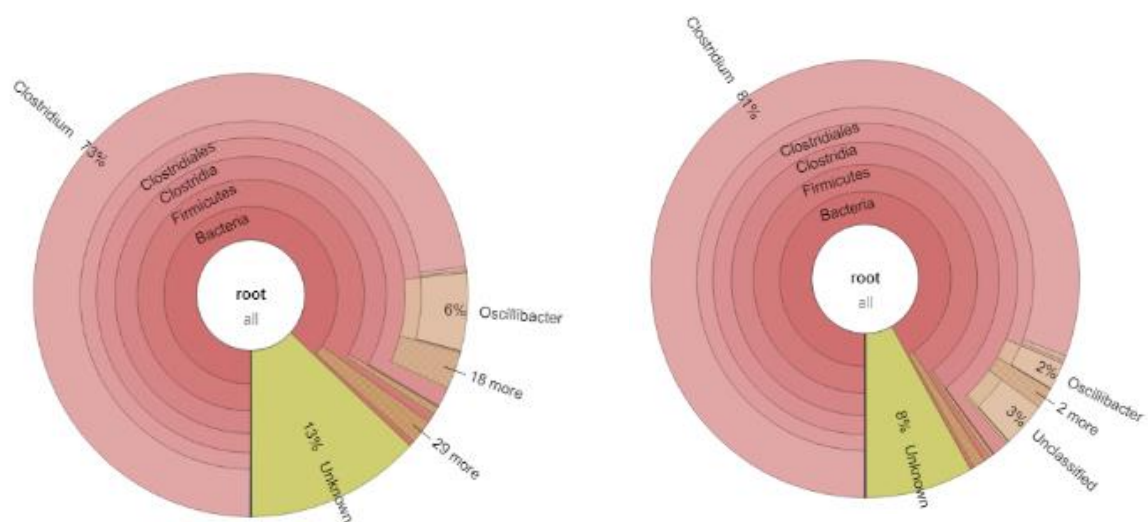


Fig. 7.7 Relative abundance at genus level of the a) 7th and b) 8th transfer to enrich CO converting acetogens.

Fig. 7.8 shows a clustering tree based on Bray-Curtis dissimilarity and the relative abundance at phylum level among the initial inoculum and the successive transfers. The initial inoculum had a high dissimilarity with the successive transfers, while the 2nd transfer had high dissimilarity with the subsequent transfers, which corresponds to the high differences in the relative abundance at genus level (Fig. 7.8, Table 7.2). The highest dissimilarity was observed between glucose fermentation (see section 3.4) and the other assays. The common and special genes (the genes not shared) among the transfers are shown in the Venn diagrams (Fig. 7.9). In the common core genome of 21,338, specific genes were decreased along with the successive transfers. For instance, the inoculum had the highest number of genes (306,946), while the 6th transfer had the least specific genes (296) (Fig. 7.9A). Considering the high abundance of the *Clostridium* genus, a Venn figure for gene analysis at *Clostridium* genus level was analyzed. Interestingly, the 5th and 6th transfers contained only, respectively, 17 and 7 special genes in the *Clostridium* genus (Fig. 7.9B).

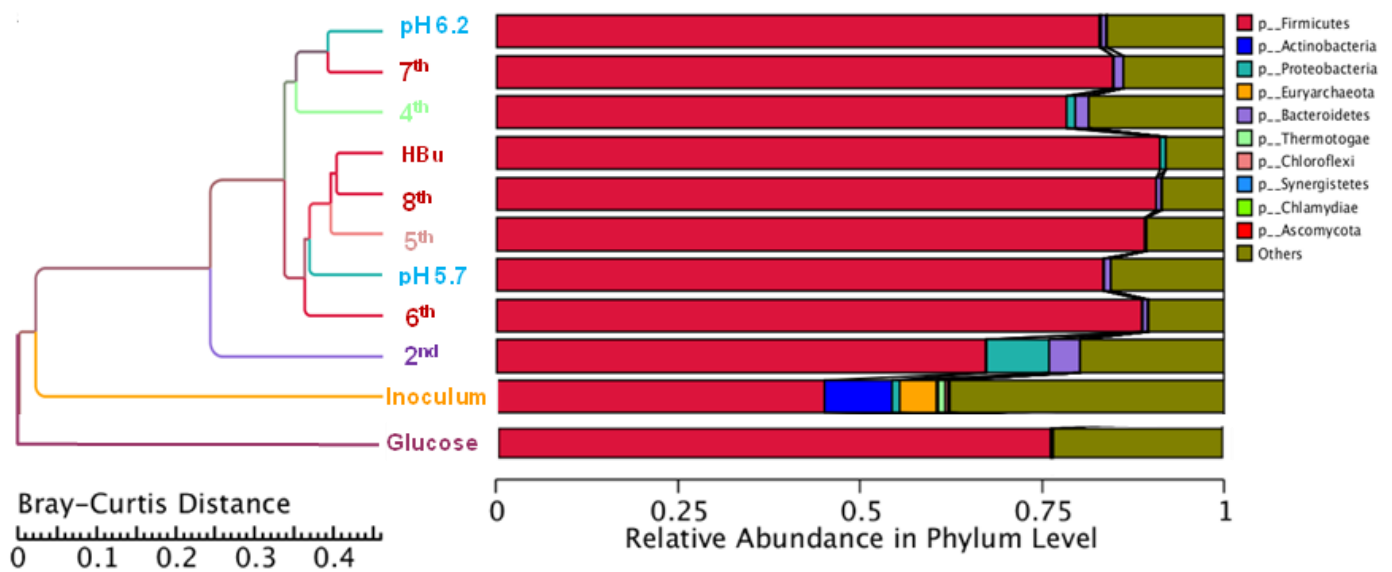


Fig. 7.8 Clustering tree based on Bray-Curtis distance of the inoculum, 2nd, 4th, 5th, 6th, 7th, 8th and exogenous butyric acid addition.

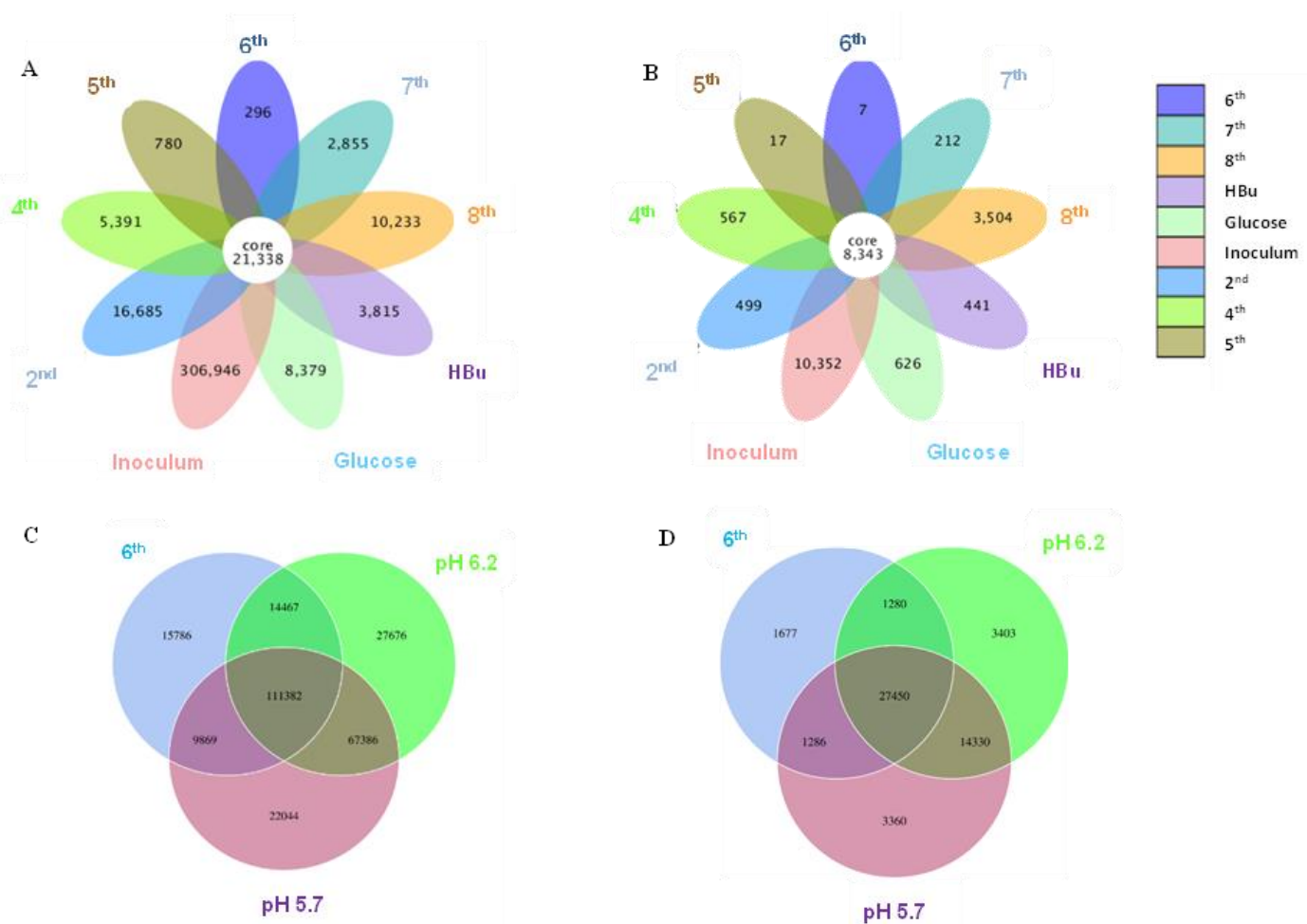


Fig. 7.9 Venn diagrams of (A) the whole genes and (B) genes in *Clostridium* genus level present in the inoculum, 2nd, 4th, 5th, 6th, 7th, 8th and exogenous butyric acid addition of enrichment study; (C) the whole genes and (D) genes in *Clostridium* genus level pH 5.7, pH 6.2 and 6th transfer enriched sludge for ethanol production under pH control. The overlapping parts represent the number of common genes among samples (groups); the other parts represent the number of special genes present in a particular sample.

7.3.3 Butanol production from exogenous butyric acid using CO as reducing power

Upon the addition of exogenous butyric acid inoculated with the 5th transfer enriched sludge taken at the end of incubation and twice CO addition (day 0 and 16), the cell growth entered the log phase after 14 days adaption: fast and high butanol production was observed and reached 1.8 g/L in less than one day, while butyric acid decreased from its initial value of 3.2 g/L to 1.1 g/L at day 15 (Fig. 7.10A). Meanwhile, acetic acid and ethanol production reached 1.1 and 1.3 g/L, respectively, at the end of the first CO addition (day 16) suggesting simultaneous butanol production from exogenous butyric acid together with acetic acid and ethanol production from CO (Fig. 7.10A).

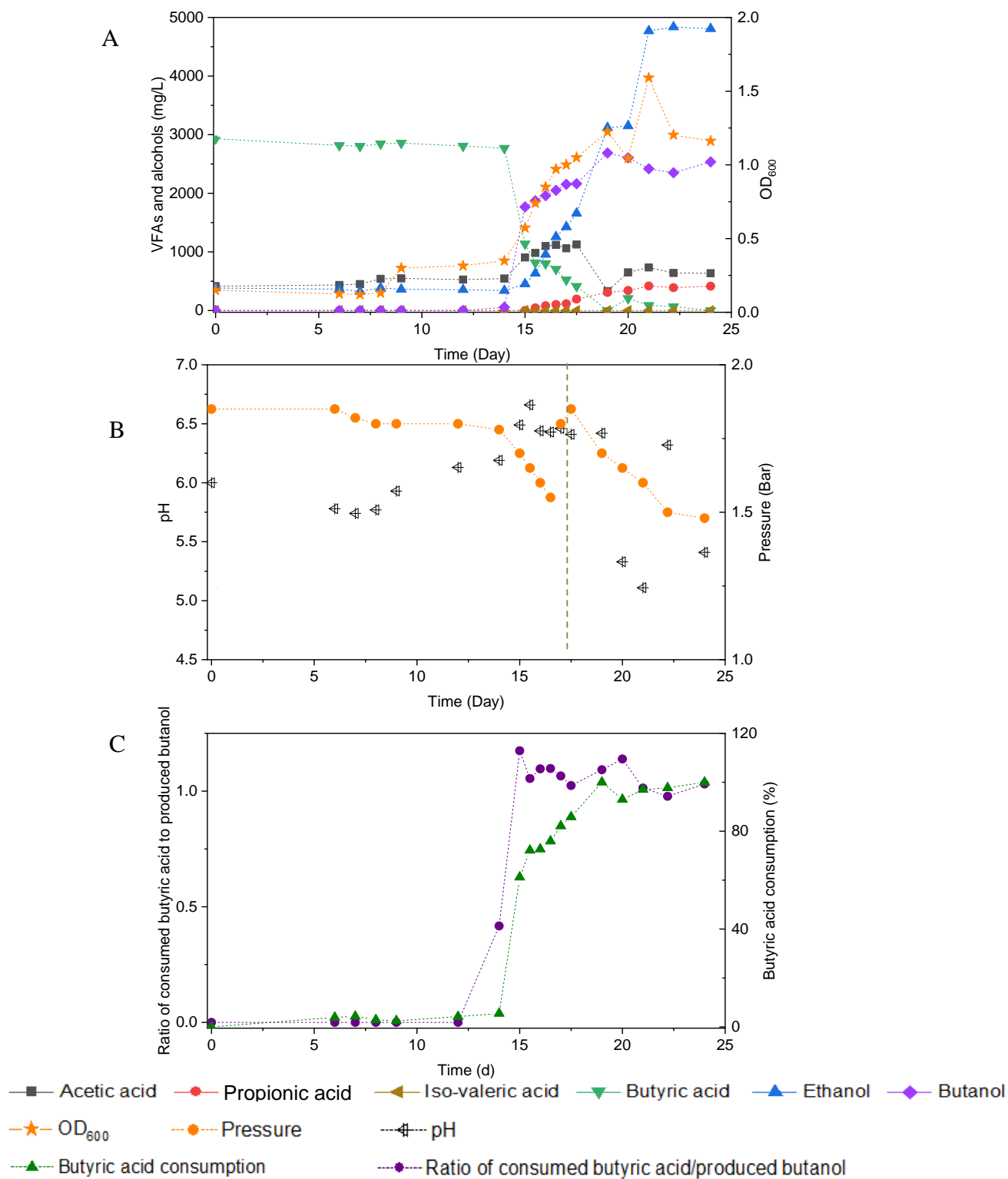


Fig. 7.10 Effect of exogenous 3.2 g/L butyric acid on acetic acid, propionic acid, iso-valeric acid, butyric acid, ethanol, butanol production and cell concentration (OD₆₀₀) (A), change of pH and gas pressure (B) and molar ratio of butyric acid consumption/butanol production and butyric acid consumption percentage (C) using CO as the carbon source with initial CO gas pressure of 1.8 bar by enriched sludge.

Considering the possible ethanol consumption in the presence of accumulated CO₂, and thus to avoid CO₂ build-up, 1.8 bar CO was added in the headspace on day 17 (Fig. 7.10B). The amount of butanol kept increasing, reaching its highest concentration of 2.7 g/L at the end of the incubation, while butyric acid got meanwhile completely exhausted. Complete exogenous butyric acid consumption and the end of butanol production occurred simultaneously. At the end of the incubation period, ethanol had reached its highest concentration of 4.8 g/L and acetic acid remained at a relatively low concentration of 0.6 g/L (Fig. 7.10A). The pH was adjusted manually to 6.2 each time its value either exceeded 6.5 or decreased below 5.2. The production of butanol from butyric acid and CO was observed over the pH range 6.2- 6.5 (Fig. 7.10B). When the pH exceeded 6.5 or was lower than 5.2 (20-24 d), butanol production was insignificantly increased (Fig. 7.10B).

For the enriched sludge after converting butyric acid to butanol, with 100% conversion efficiency, the relative abundance of the *Clostridium* genus increased from 73% to 82%, but the relative abundance at species level, such as *C. ljungdahlii*, *C. autoethanogenum*, *Clostridium ragsdalei* and *Clostridium coskatii* did not change much compared to the enriched sludge of the 6th transfer (Table 7.2). The genus *Oscillibacter* with 11% in the 6th transfer inoculum disappeared after exogenous butyric acid conversion, while the relative abundance of the *Anaerotignum* genus and *Lachnoclostridium* genus were both slightly increased to 2% in the sludge after converting exogenous butyric acid to butanol (Fig. 7.11A).

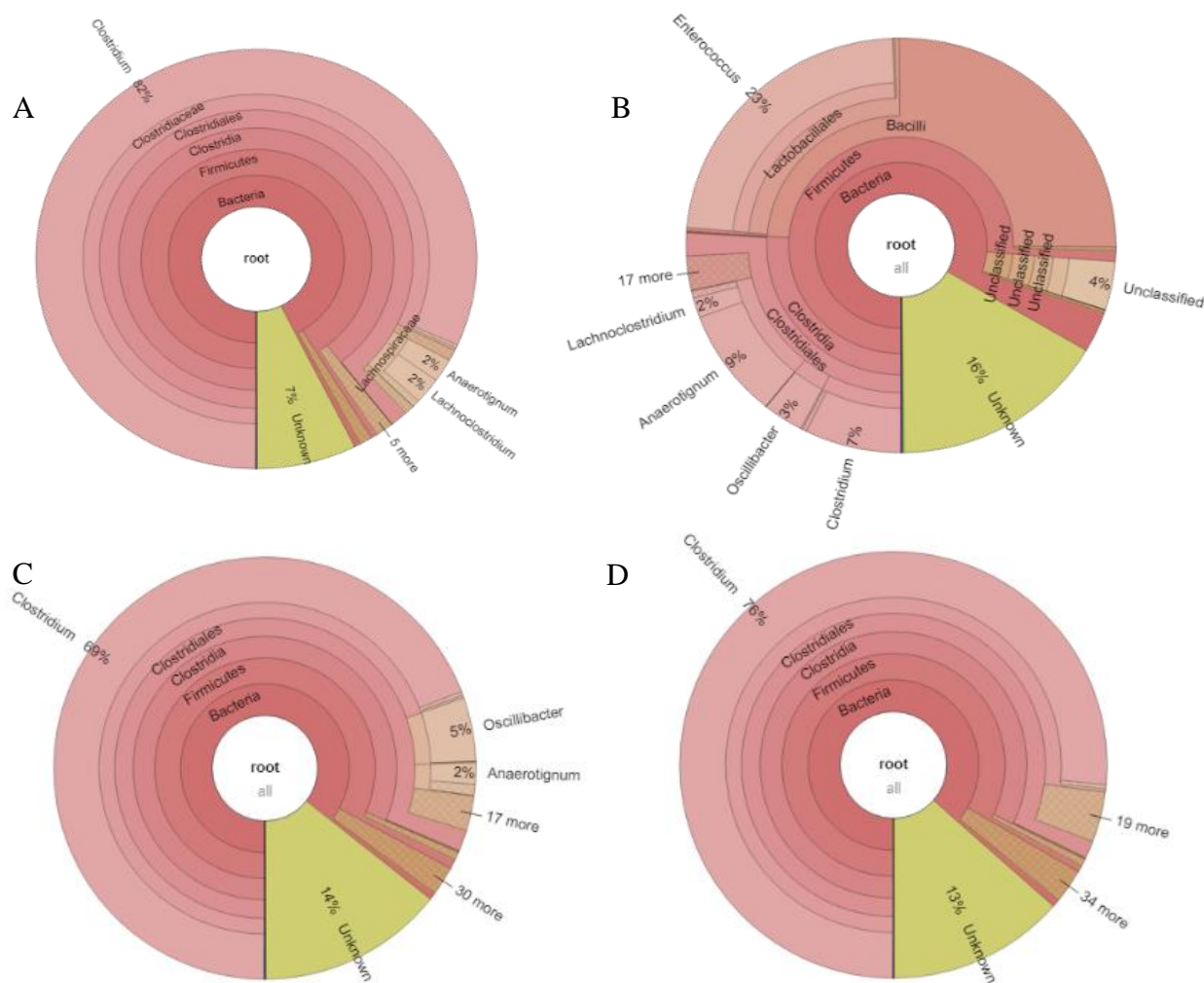


Fig. 7.11 Microbial community analysis of (A) exogenous 3.2 g/L butyric acid addition inoculated with the 5th transfer enriched sludge, (B) exogenous 5 g/L glucose addition inoculated with 6th transfer enriched sludge; (C) pH 6.2 and (D) pH 5.7 inoculated with 7th enriched sludge.

7.3.4 Glucose and CO co-fermentation

When using 5 g/L glucose ($166 \text{ mmol}\cdot\text{L}^{-1} \text{ C}$) as the sole substrate (with N_2 as the gas phase), it was totally consumed with production of formic acid at 120 h and formic acid accumulation ($163 \text{ mmol}\cdot\text{L}^{-1} \text{ C}$) was observed at 216 h. Then formic acid was further converted to acetic acid, followed by propionic acid (Fig. 7.12A). Glucose was consumed in 120 h (Fig. 7.10A and Fig. 7.10B) and the presence of CO did not influence much the glucose consumption rate compared with N_2 as the gas phase. The $\text{mmol}\cdot\text{L}^{-1}$ carbon balance kept relative stable during glucose consumption and formic acid production, although a small part of carbon could be used for cell growth. When glucose was completely consumed, 10-15% carbon loss was observed in the total $\text{mmol}\cdot\text{L}^{-1}$ carbon after 240 h, which was possibly due to

the carbon lost as CO₂ during solventogenesis (Eq. 1) (Fig. 7.12A, B). Biomass growth was very similar in both cases and reached an OD₆₀₀ of about 0.5 at 44 h and then later the highest OD₆₀₀ of 0.71 and 1.08, respectively, in the incubation with solely glucose or glucose and CO (Fig. 7.12C). The enriched acetogens can thus also use glucose as the carbon source, which results in the accumulation of formic acid, followed by the slow production of acetic acid and propionic acid (Fig. 7.12).

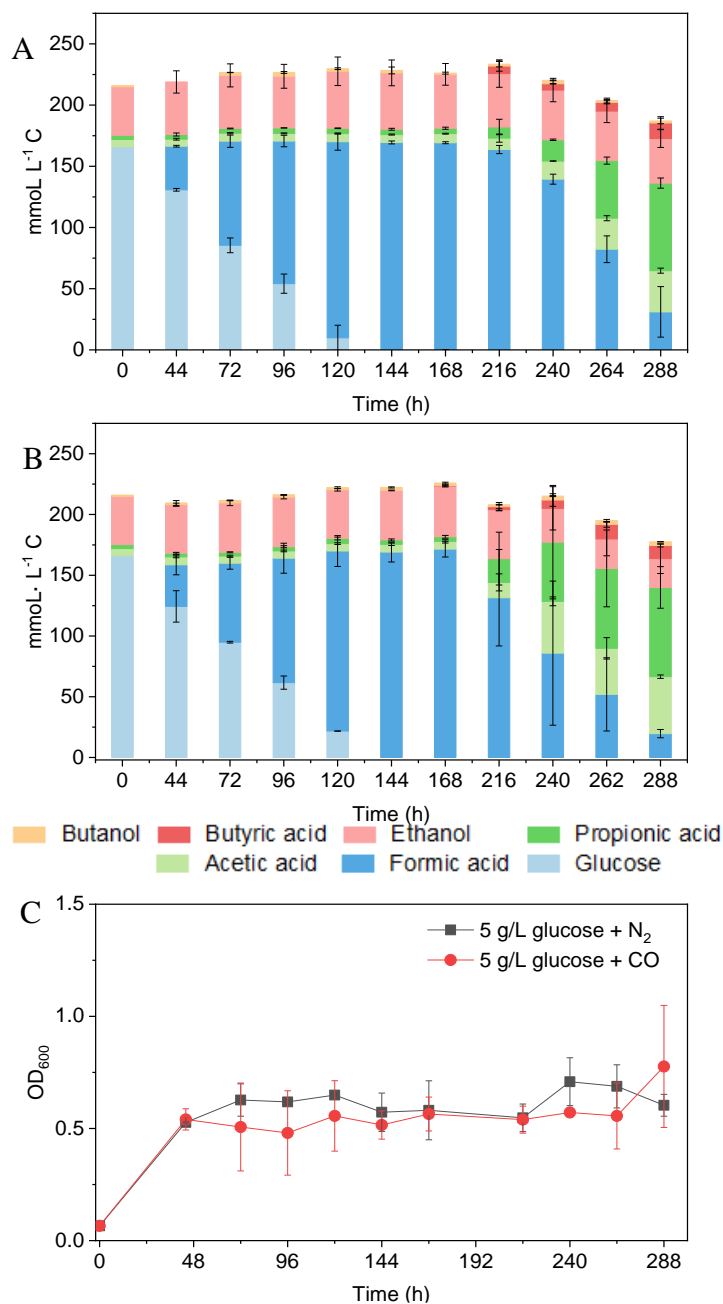


Fig. 7.12 Glucose consumption and acetic acid, propionic acid, butyric acid, ethanol, butanol production in mmol·L⁻¹ C using (A) 5 g/L glucose + N₂ and (B) 5 g/L glucose + CO as the substrate by the enriched sludge (6th transfer) and (C) cell concentration (OD₆₀₀).

After glucose bioconversion, the microbial community significantly changed: the *Clostridia* class occupied only 26%, while the *Bacilli* class occupied as high as 49% of the total. In the *Clostridia* class, the genus *Anaerotignum* occupied 9%, the *Oscillibacter* genus 3%, while the *Clostridium* genus was remarkably decreased from 73% in the 6th transfer to 7% after glucose bioconversion (Fig. 7.5E and Fig. 7.11B). The increased relative abundance of known *Clostridium* spp. compared to the 6th transfer, were, respectively, *Clostridium* strain W14A from 2 to 11%, *Clostridium homopropionicum* from 0.004 to 10%, *Clostridium cadaveris* from 0.2 to 14%, compared to the 6th transfer inoculum (Table 7.2). The relative abundance of *Clostridium butyricum* and *Clostridium* sp. BNL1100 both increased from 0.002 to 1% compared to the 6th transfer inoculum (Table 7.2). On the other side, the abundance of *C. ljungdahlii*, *C. autoethanogenum* and *Clostridium coskatii* decreased below 1% (Table 7.2). In the *Bacilli* class, the genus *Enterococcus* occupied 47% with 27% of *Enterococcus faecalis* and unidentified *Bacilli* occupying 52% (Fig. 7.11B).

7.3.5 CO conversion with pH controlled at 5.7 and 6.2

At pH controlled at 5.7 using the 7th transfer enriched sludge as the inoculum, the incubation entered the log phase on day 7 and reached an OD₆₀₀ of 1.478 during the first CO addition (0-7 d) (Fig. 7.13A). The acetic acid concentration increased to 4.6 g/L, while no increase in ethanol concentration was observed, and the butyric acid concentration reached 0.45 g/L at day 7. Considering the unfavorable ethanol production but high acetic acid accumulation, the pH was adjusted to 5.2 in order to try to stimulate solvent production at the second CO addition on day 7. However, the acetic acid concentration kept increasing and reached its highest concentration of 6.9 g/L at day 12. The butyric acid concentration increased to 0.66 g/L. The pH was adjusted to 4.9 at the third CO addition at day 12. Both acetic acid and the cell concentrations remained stable until the end of the incubation. The pH was adjusted back to 5.7 at the fourth CO addition, but it did not enhance acetic acid or ethanol production (Fig. 7.13A, B).

At pH controlled at 6.2, a longer adaption time of 12 days was observed than at pH 5.7 (Fig. 7.13C). The acetic acid concentration increased to 0.99 g/L, while 0.3 g/L ethanol, carried over from the inoculum, was completely consumed by day 14. The butyric acid and butanol concentration increased both to 0.3 g/L during the first CO addition (0-14 d) (Fig. 7.13C). The second CO addition occurred at 14 – 18 d (Fig. 7.13D). The concentrations of acetic, propionic and butyric acid increased to 2.4, 0.2 and 0.5 g/L, respectively, while ethanol was not produced and butanol remained stable at 0.3 g/L (Fig. 7.12). The highest cell concentration reached an

OD₆₀₀ of 1.23 (Fig. 7.13C). In the last CO addition (18 -21 d), the acetic acid concentration increased to 3.1 g/L, while 0.2 g/L ethanol was produced.

The control incubation with initial pH 6.2 showed the same 12 days adaption time as the incubations with the pH controlled at 6.2. Three CO additions were applied at 0, 15 and 18 d. During the first CO addition (0-14 d), acetic acid production increased to 1.1 g/L along with a pH decrease to 4.35 and gas pressure decrease to 1 bar (Fig. 7.13E, 10F). Ethanol increased to 0.5 g/L and butanol to 0.4 g/L, and the butyric acid concentration was 0.1 g/L. In the second CO addition (14-18 d), the acetic acid and ethanol concentration increased to, respectively, 3.2 and 0.6 g/L along with the pH decreasing to 5.29. The propionic acid concentration reached 0.6 g/L. The highest cell concentration reached an OD₆₀₀ of 1.114 at day 17. In the third CO addition, the acetic acid and ethanol concentration slightly increased to, respectively, 3.6 and 0.7 g/L (Fig. 7.13E).

For the enriched sludge, at pH controlled at 6.2 or 5.7 using the 7th transfer as inoculum, in the family level, the relative abundance of *Clostridiaceae*, *Oscillospiraceae* and *Lachnospiraceae* occupied, respectively, 70%, 5% and 3% of the total sample at pH 6.2, while the values were, respectively, 77, 1 and 0.6% at pH 5.7, compared to the inoculum in which they reached 74, 10 and 0.4%, respectively (Fig. 7.11C, D). The relative abundance of the *Clostridium* genus occupied the highest value, with 69% and 76%, respectively, at pH 6.2 and 5.7, which are both close to the initial inoculum value of 73% (Fig. 7.11C, D). The relative abundance of identified *Clostridium* spp. did not significantly change (Table 7.2). The differences among the *Clostridium* spp. in gene number and similarity among samples is shown in a Venn diagram (Fig. 7.9C, D). Compared to the inoculum, the special gene numbers increased from 1677 to 3403 and 3360, respectively, at pH 6.2 and 5.7 (Fig. 7.9D).

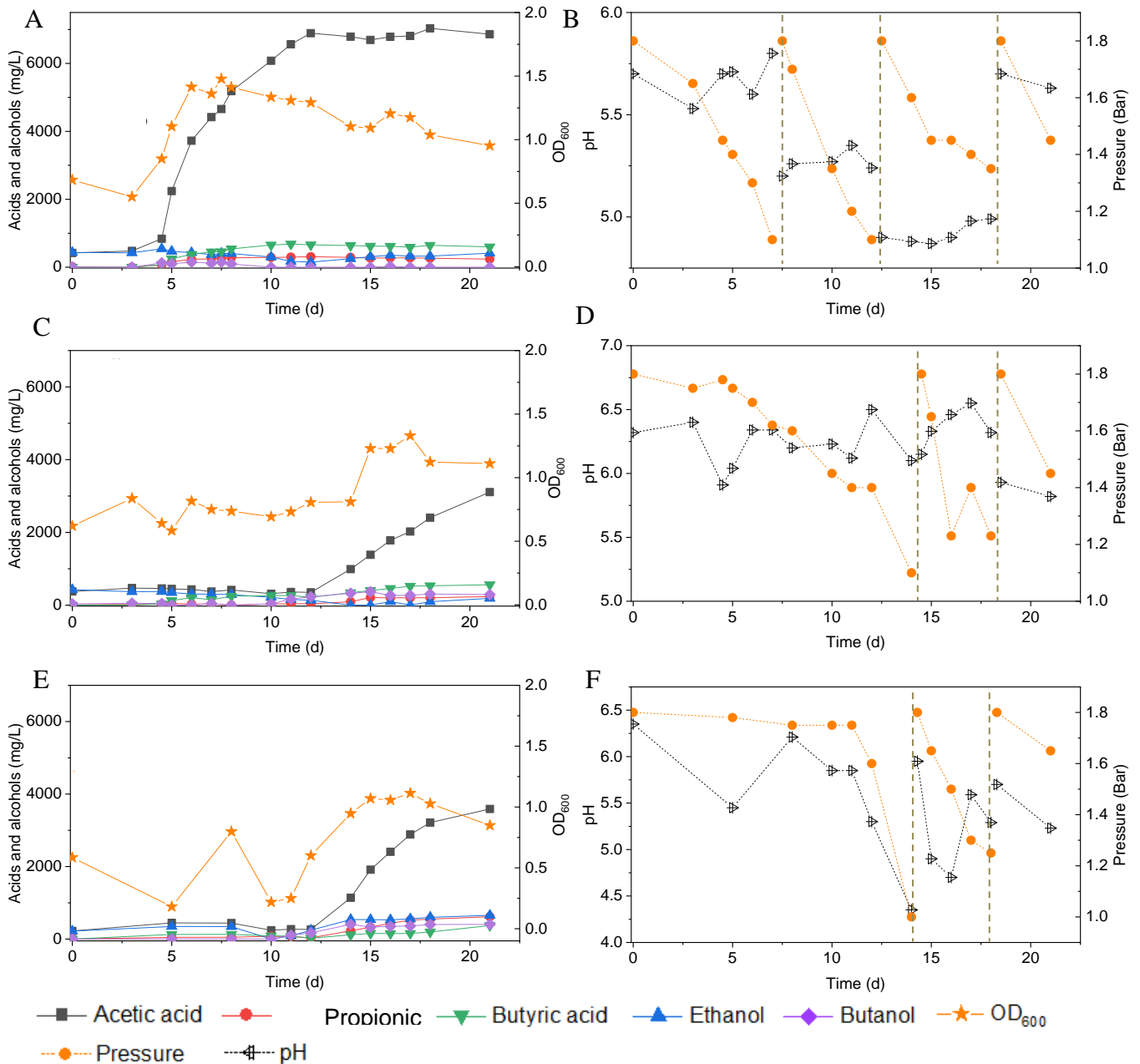


Fig. 7.13 Acetic acid, propionic acid, butyric acid, ethanol and butanol production and change of gas pressure and pH, respectively, under pH control of 5.7 (A) and (B), 6.2 (C) and (D) and manually pH adjustment (E) and (F) using CO as the carbon source with initial CO gas pressure 1.8 bar by the enriched sludge from the 7th transfer.

7.4 Discussion

7.4.1 Enhanced ethanol production with minor accumulation of acetic acid by highly enriched *Clostridium* sludge

This study showed that enhanced ethanol production was achieved with intermittent gas feeding and reached a maximum concentration of 11.8 g/L, with a high ethanol/acetic acid

molar ratio of 8.68 in the 6th transfer (Fig. 7.3B). The ethanol/acetic acid molar ratio was higher than 1 during the whole incubation and kept increasing after the adaption stage (Fig. 7.3B). It should be noted that such high ethanol production was, to the best of our knowledge, never reported from 100% CO bioconversion under a wide pH range from 4.95 to 6.45 (Table 7.3). Lee et al. (2019) isolated a novel strain *Clostridium* sp. AWRP from a wetland using syngas as the substrate. This strain produced 5.4 g/L ethanol and 0.9 g/L butanol in a batch bioreactor. Abubackar et al. (2015) compared pH 6 and 4.75 on ethanol production from CO in a CSTR by *C. autoethanogenum* and found that pH 4.75 favoured ethanol production together with a negligible acetic acid concentration (<50 mg/L), but with the highest ethanol concentration of 0.867 g/L, which is quite lower than that obtained in the present research.

The present study shows that enhanced ethanol accumulation was achieved under a wide pH range from 6.45 to 4.95 (Fig. 7.3A), and it can be concluded that the pH decreases induced a metabolic shift from acetogenesis to solventogenesis and allowed stepwise ethanol increases with low acetic acid accumulation, which may provide an efficient strategy for enhanced ethanol production. Moreover, the natural pH decrease could reduce ethanol oxidation in the presence of CO₂ accumulation (Arslan et al., 2019) and thus further induce more ethanol production (He et al., 2021b).

Ethanol production occurred both in the biomass log phase (11-19 d) with 5.1 g/L and stable phase (19-29 d) with 11.8 g/L of cell growth (Fig. 7.3B). The increase in ethanol concentration in the steady growth phase was about 1.3-fold higher than in the log phase. The decrease in acetic acid concentration was first observed when cell growth entered its stable phase at day 19 (Fig. 7.3B). It is commonly assumed that solventogenesis occurs and is mainly promoted under non-growth conditions of homoacetogens (Mohammadi et al., 2011). For instance, *C. ljungdahlii* produced acetic acid and adenosine triphosphate (ATP) in the growth stage and ethanol production generally occurs during the non-growth stage from CO, H₂ and CO₂ in the pH range of 4.0 to 7.0 via the acetyl-CoA pathway (Abubackar et al., 2011). However, this is not necessarily always the case. Cotter et al. (2009) observed little to no ethanol production in non-growing *C. ljungdahlii* cultures in a nitrogen-deficient medium. Besides, alcohol production during the biomass growth stage has also been observed (Fig. 7.3B) (Fernández-Naveira et al., 2017b).

From the genes analysis at *Clostridium* genus level, of the 8343 shared genes present in the inoculum, the special genes in the 5th transfer amounted to 0.20% (17 special genes) and 6th transfer only occupied 0.08% (7 special genes) (Fig. 7.9B). Therefore, such high ethanol production with low acetic acid accumulation in the 6th transfer may not be related too much

with the difference in *Clostridium* species with 5th transfer, although both contain a high relative abundance of unidentified *Clostridium* (Table 7.2). Instead, the natural pH drop along with acetic acid accumulation triggers solventogenesis and the timely pH adjustment at each CO addition prevented inhibition of biomass growth that can be caused by a further pH drop and thus allowed solventogenesis to prevail continuously. On the other hand, the stability of the microbial community was also demonstrated during the 4th, 5th and 6th transfer with high numbers of the *Clostridium* genus.

Compared to the previous six transfers, neither ethanol nor butanol production were enhanced when this enrichment was incubated at a pH controlled at 5.7 or 6.2. The inhibition of ethanol production was first suspected to be related to the changes in microbial populations (Figure FIG. 7.6). However, the relative abundance of the *Clostridium* genus was hardly affected in the assay at pH 5.7 compared to the inoculum; instead, it even showed a slight increase in *Clostridium* genus from 69% to 73% (Fig. 7.11). The relative abundance of the *Oscillospiraceae* family decreased at both pH 6.2 and 5.7 compared to the inoculum, while the *Lachnospiraceae* family slightly increased. Esquivel-Elizondo et al. (2017) enriched *Oscillospiraceae* from CO or CO and H₂ for mainly acetate production by anaerobic sludge. Considering the high abundance of unidentified *Clostridium* (Table 7.2), the failure of ethanol production might be due to differences of the unidentified *Clostridium* spp. among the enriched transfers at pH 6.2 and pH 5.7.

7.4.2 Enrichment of CO-converting microorganisms for enhanced ethanol production

This study showed that the successive transfer procedure exerts a strong selective pressure on the microbial populations, with extreme enrichment of the *Clostridium* genus to end up representing >90% of the whole microbial community (Table 7.2). This resulted in a significantly higher ethanol accumulation, though butyric acid and butanol production became marginal, enriching thus for highly specific and efficient ethanol producers. To the best of our knowledge, to date, this paper is the first report providing such extensive microbial community analysis related to solventogenic CO fermentation, describing such a high amount unidentified *Clostridium* species enriched on CO (1.8 bar) from an anaerobic sludge. Chakraborty et al. (2019) conducted enrichments on CO and syngas for ethanol production from anaerobic sludge in a continuous stirred tank reactor and the species *C. autoethanogenum* was selectively enriched at pH 4.9 after 42 days fermentation. Esquivel-Elizondo et al. (2017) investigated microbial community changes under different CO gas partial pressures (0, 8.1, 18.2, 40.5 and

81.1 kPa) and enriched mainly *Eubacteriaceae*, *Ruminococcaceae*, *Oscillospira* and *Bacteroidales* with acetate as the main product.

Solventogenesis can be stimulated to obtain a high ethanol production at the non-growth phase in *C. ljungdahlii* (Mohammadi et al., 2012). In this study, ethanol was produced and its concentration increased in the log phase along with cell growth (Fig. 7.12), which could be attributed to the high CO partial pressure (P_{CO} , 1.8 bar) used in these experiments. Other authors also observed simultaneous alcohol production and biomass growth in species such as *C. autoethanogenum* (Abubackar et al., 2015) and *C. carboxidivorans* (Fernández-Naveira et al., 2017a) grown on C_1 gases in bioreactors. Hurst and Randy (2010) reported that ethanol production was initiated at earlier times when increasing P_{CO} (from 0.35 to 2.0 bar), i.e. high P_{CO} changed ethanol production from non-growth-associated to growth-associated in *Clostridium carboxidivorans* P7^T.

Clostridium spp. were dramatically enriched with a majority of unidentified *Clostridium* species after successive transfers using CO with initial pressure of 1.8 bar as the carbon source and electron donor. The 4th, 5th and 6th transfers showed less difference compared to the 2nd one, which corresponds to the enhancement of ethanol production after the 4th transfer. For instance, the relative abundance of the *Lachnospiraceae* family, medium chain fatty acid producers such as propionic acid, decreased from 11% in the 2nd transfer to below 1% after the 4th transfer (Fig. 7.10). No significant clustering was observed from the 4th to the 8th transfer demonstrating the stability of the enriched solvent producing acetogens, i.e. *Clostridium* spp. using CO as the substrate. However, no significant change of known *Clostridium* spp. were observed in the 4th, 5th and 6th transfer although high ethanol production was observed in the 6th enrichment transfer with low accumulation of acetic acid throughout the whole fermentation process (Table 7.2). On the other hand, the mixed culture composed of identified and unidentified *Clostridium* spp. could withstand pH changes and showed efficient solventogenesis over a wide pH range, which also explained the high ethanol production during 5th and 6th transfer co-feedings. Therefore, pH fluctuations in a mixed culture of *Clostridium* spp. may result in high, enhanced ethanol production, in which a high amount of unidentified strains may play a relevant role, concomitant with an only minor amount of residual acetic acid and a high ethanol/acetic acid ratio.

Nevertheless, the unfavourable butanol production observed here is likely due to unfavourable conditions, such as a low butyric acid production (precursor of butanol production), rather than the loss of butanol-producing acetogens considering the similar relative abundance of both *Clostridium* genus (81%) and *Clostridium* species in the incubations

with exogenous butyric acid (88%) (Table 7.2). CO can be converted to acetic acid and ethanol via the acetyl-CoA by different enzymes of the WLP, and then acetyl-CoA can be further enzymatically transformed into butyryl-CoA from which butyric acid and butanol are produced (Fernández-Naveira et al., 2017a). Acid production in the acidogenic stage is necessary for alcohol production in the solventogenic stage (Worden et al., 1991). Butyric acid (C₄) production occurs from the acetic acid (C₂) carbon chain, which generally requires higher pH (above 5.7) than solventogenesis (4.5-5.0) (He et al., 2022; Ganigué et al., 2016). Therefore, despite of the diversity of the microbial community, the differences in butanol production among the different enrichments might be due to the different extents of pH fluctuation (Fig. 7.2 and Fig. 7.3). Environmental conditions may play a key role in different production profiles of metabolites, besides changes in microbial populations. Thus, it is suspected that the low butanol production among the transfers may be due to the low butyric acid concentration, which was possibly partly induced by unstable and unfavourable pH conditions.

7.4.3 Enhanced butanol production from exogenous butyric acid by enriched *Clostridium* populations

This study showed that the addition of exogenous butyric acid stimulated butanol production by the enriched culture with nearly 100% conversion efficiency in the assay, although butanol production was inhibited during the successive transfers (Fig. 7.2 and Fig. 7.3) using the same inoculum. This further demonstrated the inhibition of butanol production during the enrichment process is possibly attributed to the lack of suitable conditions, such as the absence of butyric acid production. On the other hand, the failure of natural butyric acid production was most probably induced by the excessive pH drop under uncontrolled experimental pH conditions, such as the natural pH drop from 6.2 to 4.95 among the transfers (Fig. 7.3). Thus, the pH value is considered to play an important role for obtaining butanol. Previous assays using the same enriched sludge yielded first 1.3 g/L butyric acid at controlled pH 6.2, with the accumulation of 2.1 g/L butanol when the pH was adjusted to 5.7 (He et al., 2022).

The molar ratio of butyric acid consumption to butanol production was close to 1, which matched with the theoretical molar ratio (Eq. 1) after 15 d (Fig. 7.10C), and the butyric acid to butanol conversion efficiency reached almost 100%. Therefore, two metabolic reactions can be assumed to co-exist in the fermentation process: one being butanol production from exogenous butyric acid and CO (Liu et al., 2020), and the other being acetic acid production from CO with ethanol production via the WLP (Fernández-Naveira et al., 2017a). Interestingly,

the molar ratio of ethanol/acetic acid reached 9.86 at the end of the incubation (Fig. 7.10C), which is much higher than in other commonly reported studies of ethanol production from CO (Table 7.3).

From a microbial community point of view, the relative abundance of one of the only known butanol-producing species, *C. carboxidivorans*, was below 1% of the *Clostridium* genus in all the samples, which pointed to another possibility that the non-butanol producing *Clostridium* strain, such as *C. autoethanogenum*, may change their metabolic pathway and produce butanol in the presence of butyric acid in a mixed culture (Diender et al., 2016). In the *Clostridium* genus level, the special genes of the enriched sludge after converting exogenous butyric acid to butanol (441 special genes) were much higher than those present in the inoculum (7 special genes), i.e. biomass from the 6th transfer (Fig. 7.9B). The known *Clostridium* spp. were similar with the inoculum, the extra special genes in the enriched sludge after converting butyric acid to butanol might be due to the difference in unidentified *Clostridium*. Therefore, it was suspected that the numerous unidentified *Clostridium* spp. might explain the different behaviour among samples considering that they exceeded 70% relative abundance in the *Clostridium* genus among the transfers (Table 7.2). The special genes of the enriched acetogens with exogenous butyric acid amounted to 441 and shared 95.0% of the genes with the biomass of the 6th transfer (8343 common genes) (Fig. 7.9B).

7.4.4 Bioconversion of glucose or glucose and CO co-fermentation by the enriched culture

It has been reported that somewhat different metabolites may be obtained, even for a same bacterial pure culture, when either grown autotrophically on C₁ gases or heterotrophically on sugars, e.g. glucose (Fernández-Naveira et al., 2017b, 2017c). Formic acid accumulation was observed in both the glucose or the glucose and CO co-fermentation process (Fig. 7.12). Similarly, significant early accumulation of formic acid from glucose was also observed in pure cultures of *C. carboxidivorans* (Fernández-Naveira et al., 2017c), while this was not found when that strain was grown on C₁ gases (Fernández-Naveira et al., 2017b).

From the microbial community point of view, after glucose fermentation, the relative abundance of the *Clostridium* genus remarkably decreased to less than 1/10 compared to the inoculum within 12 days (288 h) of incubation (Fig. 7.12 and Fig. 7.11). *Enterococcus faecalis*, with increased relative abundance, can produce short chain fatty acids such as acetic acid using glucose as the substrate (Urdaneta et al., 1995). Despite the decrease in *Clostridium* genus, the relative abundance of *Clostridium* spp. varied at species level, with an increase of the

abundance of *Clostridium* strain W14A, *Clostridium homopropionicum* and *Clostridium cadaveris* (Table 7.2). *Clostridium* strain W14A was isolated from a cellulose degrading biofilm in a landfill leachate microcosm (Ransom-Jones and McDonald, 2016). Similarly with glucose as the substrate, *Clostridium* strain W14A was enriched reaching as high as 11% of the *Clostridium* genus in this study (Table 7.2). With sugar substrates, such as fructose, *Clostridium homopropionicum* was observed to produce acetate, butyrate, butanol and H₂ (Dörner and Schink, 1990).

7.5 Conclusions

This study describes a possible suitable strategy to enrich homoacetogens from anaerobic sludge for solventogenic ethanol and butanol production using CO as the carbon source after successive transfers and fed batch CO addition. The enriched acetogens with high *Clostridium spp.* abundance produced as much as 11.7 g/L ethanol with low accumulation of acetic acid over a wide pH range of 6.45-4.95. This selective ethanol production has been seldomly reported, especially with the low acetic acid accumulation under the pH range in the mixed culture. Besides, the enriched acetogens in the present study produced 2.7 g/L butanol from exogenous butyric acid with 100% conversion efficiency using CO as reducing power. Six successive transfers successfully enriched the *Clostridium* genus increasing from 7% in the inoculum to 94% in the solventogenic enrichment, including several well known alcohol producers such as *C. ljungdhalii*, *C. autoethanogenum* and *C. coskatii*, but with also unidentified *Clostridium* species occupying as high as 74% of the *Clostridium* genus.

7.6 References

- Abrini, J., Naveau, H. and Nyns, E. J. (1994). *Clostridium autoethanogenum*, sp. nov., an anaerobic bacterium that produces ethanol from carbon monoxide. *Arch. Microbiol.* 161 (4), 345–51.
- Abubackar, H.N., Veiga, M.C. and Kennes, C. (2011). Biological conversion of carbon monoxide: rich syngas or waste gases to bioethanol. *Biofuel Bioprod. Bior.* 5 (1), 93-114.
- Abubackar, H.N., Veiga, M.C. and Kennes, C. (2012). Biological conversion of carbon monoxide to ethanol: effect of pH, gas pressure, reducing agent and yeast extract. *Bioresour. Technol.* 114, 518-522.
- Abubackar, H.N., Veiga, M.C. and Kennes, C. (2015). Carbon monoxide fermentation to ethanol by *Clostridium autoethanogenum* in a bioreactor with no accumulation of acetic acid. *Bioresour. Technol.* 186, 122-127.

Abubackar, H.N., Veiga, M.C. and Kennes, C. (2018). Production of acids and alcohols from syngas in a two-stage continuous fermentation process. *Bioresour. Technol.* 253, 227-234.

Arantes, A. L., Moreira, J. P., Diender, M., Parshina, S. N., Stams, A. J., Alves, M. M., Alves, J. I. and Sousa, D. Z. (2020). Enrichment of anaerobic syngas-converting communities and isolation of a novel carboxydophilic *Acetobacterium wieringae* strain JM. *Front. Microbiol.* 11, 58.

Arslan, K., Bayar, B., Abubackar, H. N., Veiga, M. C. and Kennes, C. (2019). Solventogenesis in *Clostridium aceticum* producing high concentrations of ethanol from syngas. *Bioresour. Technol.* 292, 121941.

Buchfink B., Xie C., Huson D.H. (2015). Fast and sensitive protein alignment using DIAMOND. *Nat Methods*, 12,59-60.

Chakraborty, S., Rene, E.R., Lens, P. N. L., Veiga, M.C. and Kennes, C. (2019). Enrichment of a solventogenic anaerobic sludge converting carbon monoxide and syngas into acids and alcohols. *Bioresour. Technol.* 272, 130-136.

Charubin, K., & Papoutsakis, E. T. 2019. Direct cell-to-cell exchange of matter in a synthetic *Clostridium* syntrophy enables CO₂ fixation, superior metabolite yields, and an expanded metabolic space. *Metab. Eng.* 52, 9–19.

Cotter, J. L., Chinn, M. S. and Grunden, A. M. (2009). Ethanol and acetate production by *Clostridium ljungdahlii* and *Clostridium autoethanogenum* using resting cells. *Bioproc. Biosyst. Eng.* 32 (3), 369-380.

Devarapalli, M., Atiyeh, H. K., Phillips, J. R., Lewis, R. S. and Huhnke, R. L. (2016). Ethanol production during semi-continuous syngas fermentation in a trickle bed reactor using *Clostridium ragsdalei*. *Bioresour. Technol.* 209, 56–65.

Diender, M., Stams, A. J. and Sousa, D. Z. (2016). Production of medium-chain fatty acids and higher alcohols by a synthetic co-culture grown on carbon monoxide or syngas. *Biotechnol. Biofuels* 9 (1), 82.

Dörner, C., Schink, B. (1990). *Clostridium homopropionicum* sp. nov., a new strict anaerobe growing with 2-, 3-, or 4-hydroxybutyrate. *Arch. Microbiol.* 154 (4), 342-348.

Esquivel-Elizondo, S., Delgado, A. G. and Krajmalnik-Brown, R. (2017). Evolution of microbial communities growing with carbon monoxide, hydrogen and carbon dioxide. *FEMS Microbiol. Ecol.* 93 (6), 1-12.

Fernández-Naveira, Á., Veiga, M. C. and Kennes, C. (2017a). H-B-E (hexanol-butanol-ethanol) fermentation for the production of higher alcohols from syngas/waste gas. *J. Chem. Technol. Biot.* 92 (4), 712-731.

Fernández-Naveira, Á., Veiga, M. C. and Kennes, C. (2017b). Effect of pH control on the anaerobic H-B-E fermentation of syngas in bioreactors. *J. Chem. Technol. Biot.* 92, 1178-1185.

Fernández-Naveira, Á., Veiga, M. C., Kennes, C. (2017c). Glucose bioconversion profile in the syngas-metabolizing species *Clostridium carboxidivorans*. *Bioresour. Technol.* 244, 552-559.

Fernández-Naveira, Á., Abubackar, H. N., Veiga, M. C. and Kennes, C. (2016). Efficient butanol-ethanol (BE) production from carbon monoxide fermentation by *Clostridium carboxidivorans*. *Appl. Microbiol. Biot.* 100 (7), 3361-3370.

Ganigué, R., Sánchez-Paredes, P., Bañeras, L. and Colprim, J. (2016). Low fermentation pH is a trigger to alcohol production, but a killer to chain elongation. *Front. Microbiol.* 7, 702.

He, Y., Cassarini, C., Marciano, F. and Lens, P. N. L. (2021). Homoacetogenesis and solventogenesis from H₂/CO₂ by granular sludge at 25, 37 and 55°C. *Chemosphere* 265, 128649.

He, Y., Lens, P. N. L., Veiga, M. C., and Kennes, C. (2022). Selective butanol production from carbon monoxide and syngas by an enriched anaerobic culture. *Sci. Total Environ.* 806, 150579.

Hurst, Kendall M, and Randy S Lewis. (2010). Carbon Monoxide Partial Pressure Effects on the Metabolic Process of Syngas Fermentation. *Biochem. Eng. J.* 48 (2), 159–65.

Huson, D. H., Mitra, S., Ruscheweyh, H. J., Weber, N. and Schuster, S. C. (2011). Integrative analysis of environmental sequences using MEGAN4. *Genome Res.* 21 (9), 1552-1560.

Lee, J., Lee, J. W., Chae, C. G., Kwon, S. J., Kim, Y. J., Lee, J. H. and Lee, H. S. (2019). Domestication of the novel alcohologenic acetogen *Clostridium* sp. AWRP: from isolation to characterization for syngas fermentation. *Biotechnol. Biofuels* 12 (1), 228.

Liou, J. S. C., Balkwill, D. L., Drake, G. R. and Tanner, R. S. (2005). *Clostridium carboxidivorans* sp. nov., a solvent-producing *Clostridium* isolated from an agricultural settling lagoon, and reclassification of the acetogen *Clostridium scatologenes* strain SL1 as *Clostridium drakei* sp. nov. *Int. J. Syst. Evol. Microbiol.* 55 (5), 2085–91.

Liu, C., Wang, W., O-Thong, S., Yang, Z., Zhang, S., Liu, G. and Luo, G. (2020). Microbial insights of enhanced anaerobic conversion of syngas into volatile fatty acids by co-fermentation with carbohydrate-rich synthetic wastewater. *Biotechnol. Biofuels* 13.

- Liu, K., Atiyeh, H. K., Stevenson, B. S., Tanner, R. S., Wilkins, M. R. and Huhnke, R. L. (2014). Continuous syngas fermentation for the production of ethanol, n-propanol and n-butanol. *Bioresour. Technol.* 151, 69-77.
- Lynd, Lee, R. Kerby and J. G. Zeikus. (1982). Carbon monoxide metabolism of the methylotrophic acidogen *Butyribacterium methylotrophicum*. *J. Bacteriol.* 149 (1), 255-263.
- Maddipati, P., Atiyeh, H. K., Bellmer, D. D. and Huhnke, R. L. (2011). Ethanol production from syngas by *Clostridium* strain p11 using corn steep liquor as a nutrient replacement to yeast extract. *Bioresour. Technol.* 102 (11), 6494–6501.
- Mohammadi, M., Najafpour, G. D., Younesi, H., Lahijani, P., Uzir, M. H. and Mohamed, A. R. (2011). Bioconversion of synthesis gas to second generation biofuels: a review. *Renew. Sust. Energ. Rev.* 15 (9), 4255-4273.
- Mohammadi, M., Younesi, H., Najafpour, G. and Mohamed, A. R. (2012). Sustainable ethanol fermentation from synthesis gas by *Clostridium ljungdahlii* in a continuous stirred tank bioreactor. *J. Chem. Technol. Biot.* 87 (6), 837-843.
- Rajagopalan, S., Datar, R. P. and Lewis, R. S. (2002). Formation of ethanol from carbon monoxide via a new microbial catalyst. *Biomass Bioenerg.* 23 (6), 487–93.
- Ransom-Jones, E. and McDonald, J. E. (2016). Draft genome sequence of *Clostridium* sp. strain W14A isolated from a cellulose-degrading biofilm in a landfill leachate microcosm. *Genome Announcements* 4 (5).
- Richter, H., Martin, M. E. and Angenent, L. T. (2013). A two-stage continuous fermentation system for conversion of syngas into ethanol. *Energies* 6 (8), 3987–4000.
- Shen, S., Wang, G., Zhang, M., Tang, Y., Gu, Y., Jiang, W., Wang, Y. Zhuang, Y. (2020). Effect of temperature and surfactant on biomass growth and higher-alcohol production during syngas fermentation by *Clostridium carboxidivorans* P7. *Bioresour. Bioprocess.* 7 (1), 1-13.
- Shen, Y., Brown, R. and Wen, Z. (2014). Syngas fermentation of *Clostridium carboxidivoran* P7 in a hollow fiber membrane biofilm reactor: Evaluating the mass transfer coefficient and ethanol production performance. *Biochem. Eng. J.* 85, 21-29.
- Stams, A., Dijk, Dijkema, C., and Plugge, C. M. (1993). Growth of syntrophic propionate-oxidizing bacteria with fumarate in the absence of methanogenic bacteria. *Appl. Environ. Microbiol.* 59 (4), 1114-1119.
- Tanner, R. S., Miller, L. M. and Yang, D. (1993). *Clostridium ljungdahlii* sp. nov., an acetogenic species in *Clostridial* RRNA homology group I. *Int. J. Syst. Evol. Microbiol.* 43 (2), 232–236.

Ukpong, M. N., Atiyeh, H. K., De Lorme, M. J., Liu, K., Zhu, X., Tanner, R. S., Wilkins, M. R. and Stevenson, B. S. (2012). physiological response of *Clostridium carboxidivorans* during conversion of synthesis gas to solvents in a gas-fed bioreactor. *Biotechnol. Bioeng.* 109 (11), 2720–28.

Urdaneta, D., Raffae, D., Ferrer, A., de Ferrer, B. S., Cabrera, L. and Pérez, M. (1995). Short-chain organic acids produced on glucose, lactose, and citrate media by *Enterococcus faecalis*, *Lactobacillus casei*, and *Enterobacter aerogenes* strains. *Bioresour. Technol.* 54 (2), 99-103.

Worden, R. M., Grethlein, A. J., Jain, M. K. and Datta, R. (1991). Production of butanol and ethanol from synthesis gas via fermentation. *Fuel* 70 (5):615-619.

Yu, J., Liu, J., Jiang, W., Yang, Y. and Sheng, Y. (2015). Current status and prospects of industrial bio-production of n-butanol in China. *Biotechnol. Adv.* 33(7), 1493-1501.

Zhang, W., Liu, W., Hou, R., Zhang, L., Schmitz-Esser, S., Sun, H., Xie, J., Zhang, Y., Wang, C., Li, L., Yue, B., Huang, H., Wang, H., Shen, F. and Zhang, Z. (2018). Age-associated microbiome shows the giant panda lives on hemicelluloses, not on cellulose. *ISME J* 12, 1319–1328.

Chapter 8 Effect of endogenous and exogenous butyric acid on butanol production with CO by enriched *Clostridia*

A modified version of this chapter has been published as:

He Y., Lens, P. N. L., Veiga, M. C. and Kennes, C. 2022. Effect of endogenous and exogenous butyric acid on butanol production from CO by enriched *Clostridia*. *Frontiers in Bioengineering and Biotechnology*. Accepted.

Abstract

Butanol exhibits a similar energy content as gasoline and has a higher energy density than ethanol and can potentially mitigate fossil fuels consumption. To increase the selectivity for butanol production during CO fermentation, exogenous acetic acid and ethanol, exogenous butyric acid as well as endogenous butyric acid from glucose fermentation have been investigated using CO as reducing power by a highly enriched *Clostridium* sludge. Addition of 3.2 g/L exogenous butyric acid reached the highest 1.9 g/L butanol concentration with a conversion efficiency of 67%. With exogenous acetate and ethanol supply, butanol reached 1.6 g/L at the end of the incubation. However, the presence of acetic acid and ethanol favoured butanol production to 2.6 g/L from exogenous butyric acid by the enriched sludge. Finally, exogenous 14 g/L butyric acid reached the highest butanol production of 3.4 g/L, which also is the highest butanol concentration from CO/syngas fermentation reported. CO addition triggered butanol production from endogenous butyric acid (produced from glucose, Glucose+N₂) with as high as 58.6% conversion efficiency and 62.1% butanol yield. However, butanol production was not efficiently produced by glucose and CO co-fermentation (Glucose+CO), although a similar amount of endogenous butyric acid was produced compared to Glucose+N₂. The *Clostridium* genus occupied a relative abundance as high as 82% from the initial inoculum, while the *Clostridia* and *Bacilli* class were both enriched and dominated in Glucose +N₂ and Glucose +CO incubations. This study showed supply of butyric acid is a possible strategy for enhancing butanol production by CO fed anaerobic sludge, either via exogenous butyric acid, or via endogenous production by sugar fermentation, such as from wastewater containing low sugar concentrations.

8.1 Introduction

Carbon monoxide (CO) is one of the main components from industrial gas emissions such as steel plants and gasification of biomass or municipal solid waste (Yu et al, 2016). ‘Syngas-aided’ fermentation, which combines syngas and microorganism together for production valuable chemicals, including butanol, has received incredible attention since the last decade (Mohammadi et al., 2011; Baleeiro et al., 2019). Butanol (butyl alcohol and 1-butanol, C₄H₉OH) is an alternative liquid fuel because of its similar characteristics to gasoline. Thus, it can be used directly in any gasoline engines without modification and/or substitution thus gains more value than ethanol for biofuels (Lee et al. 2008; Knoshaug and Zhang, 2009). CO fermentation has the advantage of using non-food feedstocks compared to traditional fermentation

(Devarapalli and Atiyeh, 2015). In addition, CO is present in off gas of the steel industry, thus this cheap gas substrate can make syngas-based butanol production more economical.

The conversion of CO follows the Wood–Ljungdahl pathway (WLP) to synthesize acetyl-CoA, that can be further converted to acetic acid, biomass and ethanol production (Fernández-Naveira et al., 2017a; Teixeira et al., 2018). Several microorganisms convert CO/syngas to ethanol, including *Acetobacterium woodii*, *Clostridium ljungdahlii*, *Clostridium autoethanogenum*, *Clostridium carboxidivorans* and *Butyribacterium methylotrophicum*, but very few can produce higher alcohols like butanol (Cheng et al., 2019; Fernández-Naveira et al., 2017a; Liu et al., 2014a). The known *Clostridium* strains hardly produced butanol at concentrations higher than 2.7 g/L from syngas or CO (Fernández-Naveira et al., 2016). Considering the inhibited butanol production in pure cultures, CO conversion to butanol by a broad range of acetogenic mixed cultures has received little attention (Alves et al., 2013). Mixed cultures have the advantages of non-sterilization and resistance to unfavorable environmental conditions, such as a wide pH range for alcohol production. This enables an easier implementation at large scale compared to pure cultures (Liu et al., 2019).

Acid production in the acidogenic stage is necessary and even enhances solvent production in the solventogenic stage (Worden et al., 1991), such as enhanced ethanol production with exogenous acetate by *C. autoethanogenum* (Xu et al., 2020). Exogenous butyric acid has been used for enhancing butanol production in acetone-butanol-ethanol (ABE) fermentation from organic carbon (Munch et al., 2020; Lu et al., 2017; Luo et al., 2015; Gao et al. 2016), but CO/syngas fermentation has been seldom reported although CO is a potential reductant for the reduction of butyric acid to butanol. Therefore, one appealing way for enhancing butanol production is first to induce butyric acid production, either exogenously supplied or endogenously produced. There, butyric acid could be further used for butanol production following butyryl-CoA in the Wood-Ljungdahl pathway (WLP) (Fernández-Naveira et al., 2017a).

In addition, acetic acid can be converted into the higher added value compound butyric acid through carbon chain elongation in which ethanol can be used as electron donor promoting the reverse β -oxidation pathway (Baleeiro et al., 2019). The addition of acetic acid and ethanol can be converted to butyric acid by some mid chain acid producers, then, endogenous butyric acid can be converted to butanol by solventogenic acetogens. Some co-fermentation examples have been studied in co-cultures, such as acetogenic *Clostridium kluyveri* and solventogenic *C. autoethanogenum* (Diender et al., 2016). The addition of acetate also prevented strain degeneration in *Clostridium* spp. (Chen and Blaschek 1999).

Endogenous butyric acid production from sugar fermentation could be an alternative source for butyric acid and enhanced butanol production (Munch et al., 2020). Glucose, as the typical carbohydrate for synthetic carbohydrate rich wastewater can be converted to butyric acid by *Clostridium* spp, such as *C. carboxidivorans* (Fernández-Naveira et al., 2017b). A few reports focused on CO and glucose co-fermentation for methane and hydrogen production, but not for acids and alcohol production (Jing et al., 2017; Liu et al., 2020). Additionally, butanol production from co-fermentation of CO/syngas and glucose by anaerobic fermentation by mixed cultures is an attractive and economical process (Baleeiro et al., 2019).

To date, selective butanol production from CO and exogenous acids and ethanol on butanol selectivity by mixed cultures has not yet been reported. To enhance and select butanol production by enriched sludge with high a large *Clostridium* spp. population using CO as reducing power, this study outlined different strategies to increase the butyric acid concentration, i.e., via exogenous acetic acid and ethanol supply as well as exogenous and endogenous butyric acid supply. This study further investigated the microbial community and identified the dominant strains regulating butanol production via endogenous butyric acid under solely glucose fermentation followed by CO addition (Glucose + N₂) and co-fermentation of glucose and CO (Glucose + CO) by the enriched sludge.

8.2 Materials and methods

8.2.1 Source of inoculum

The inoculum was obtained from a CO fed enriched sludge after six successive biomass transfers described in detail by He et al. (2021, 2022). The inoculum contained 81% of the *Clostridium* genus reaching an ethanol production as much as 11.8 g/L with minor accumulation of acetic acid at pH 6.45 to 4.95. The inoculum can convert exogenous butyric acid into butanol using CO as the reducing power (He et al., 2021).

8.2.2 Medium composition

The culture medium was prepared as described previously (He et al., 2022). A 1 L culture medium was prepared according to Stams et al. (1993) and modified as follows: 408 mg/L KH₂PO₄, 534 mg/L Na₂HPO₄·2H₂O, 300 mg/L NH₄Cl, 300 mg/L NaCl, 100 mg/L MgCl₂·6H₂O, 110 mg/L CaCl₂·2H₂O; 1 mL trace metal and 1 mL vitamin stock solution (Stams et al., 1993). Once prepared, the 1 L medium (except for CaCl₂·2H₂O and vitamins) was brought to boiling in order to remove O₂, and it was later cooled down to room temperature

under an oxygen-free N₂ flow. Then CaCl₂·2H₂O and the vitamins were added, as well as Na₂S (0.24 g) as reducing agent.

8.2.3 CO fed batch reactor set-up

All experiments were carried out in 1 L fed batch reactors (Fisherbrand, FB-800-1100, Waltham, U.S.), with 10% enriched sludge in 200 mL medium. The fed batch reactors were sealed with a gas tight septum fitted with a pH probe (9,5×300 mm, VWR) in the middle. The pH probe was connected to a pH controller (Cole-Parmer 300, Cambridgeshire, UK) and the pH was adjusted using either 1 M NaOH or HCl solutions by two pumps (Verder International BV, Utrecht, the Netherlands). The fed batch reactors were agitated at 150 rpm by a shaker (Infors AG CH-4103, Bottmingen, Switzerland) at 33 °C in a thermostatic chamber. 100% CO was supplied to the headspace of the reactor as the sole carbon and energy source with an initial gas pressure of 1.8 bar. When the gas pressure decreased below 1 bar, as a result of bacterial CO gas consumption (corresponding to one CO feeding), the reactor was flushed with fresh pure CO for about 5 minutes, until reaching again a gas pressure of 1.8 bar.

8.2.4 Experimental design

8.2.4.1 Exogenous acetic acid, ethanol and butyric acid

The effect of exogenous acetic acid, butyric acid and ethanol on the production of butanol by enriched sludge was evaluated in four 1 L fed batch reactors with 200 mL culture medium and inoculated with 10% enriched sludge (section 2.2). The medium was supplied with acetic acid and ethanol (HAc+EtOH), acetic acid, ethanol and butyric acid (HAc+EtOH+HBu), or butyric acid (HBu), respectively, besides the control described below (Fig. 8.1a).

In the HAc+EtOH experiment, acetate and ethanol addition was designed to stimulate the butyric acid production via the reverse β oxidation pathway and further induced butanol production using CO as reducing power. In the HAc+EtOH+HBu experiment, acetate and ethanol addition was designed to increase butyric acid production (reverse β oxidation pathway) with the presence of exogenous butyric acid, which can possibly result in enhanced butanol production using CO as reducing power.

An initial pH of 5.9 was applied and the pH was adjusted to 5.9 at each CO addition. The final concentrations of acetic acid, butyric acid and ethanol were, respectively, 2.2, 3.2 and 6 g/L (Table 8.1). The acetic and butyric acid concentrations were chosen to obtain a molar relationship of ethanol to acid of around 3.5 that has been shown for enhanced butyric acid production. The control contained the same gas pressure and inoculum, but without acids and ethanol addition.

CO was added at day 0, 11, 14, 15, 16 and 27 in the HAc+EtOH+HBu experiment; at 0, 11, 13, 15, 17, 20, 27 and 32 d in the HAc+EtOH experiment; at day 0, 17, 19, 20, 23, 25 and 30 in the HBu experiment; and at day 0, 20, 25, 27 and 35 in the control.

8.2.4.2 Exogenous butyric acid addition

Two 1 L CO fed batch reactors were used with 7 and 14 g/L butyric acid externally supplied at the same CO gas pressure and inoculum as described in section 2.2. The pH value was maintained at 5.5-6.0 by 1 M HCl or 1 M NaOH. CO was added at day 0, 15 and 21 d in the 7 g/L HBu and at day 0, 20 and 25 d in the 14 g/L HBu incubation.

8.2.4.3 Influence of endogenous butyric acid from glucose on butanol production using CO as gaseous substrate

(1) Batch tests of endogenous butyric acid from glucose

Endogenous butyric acid production from glucose was first tested in a batch test with 30 mL medium in 125 mL serum bottles with initially 5 g/L glucose and N₂ as the headspace. When glucose had been totally consumed and butyric acid produced (glycolysis), the headspace was flushed with 100% CO for 5 min up to a final CO pressure of 1.8 bar. CO acts as reducing power to stimulate butanol production from endogenous butyric acid by the enriched *Clostridium* bacteria. CO was added at day 5, 9 and 11.

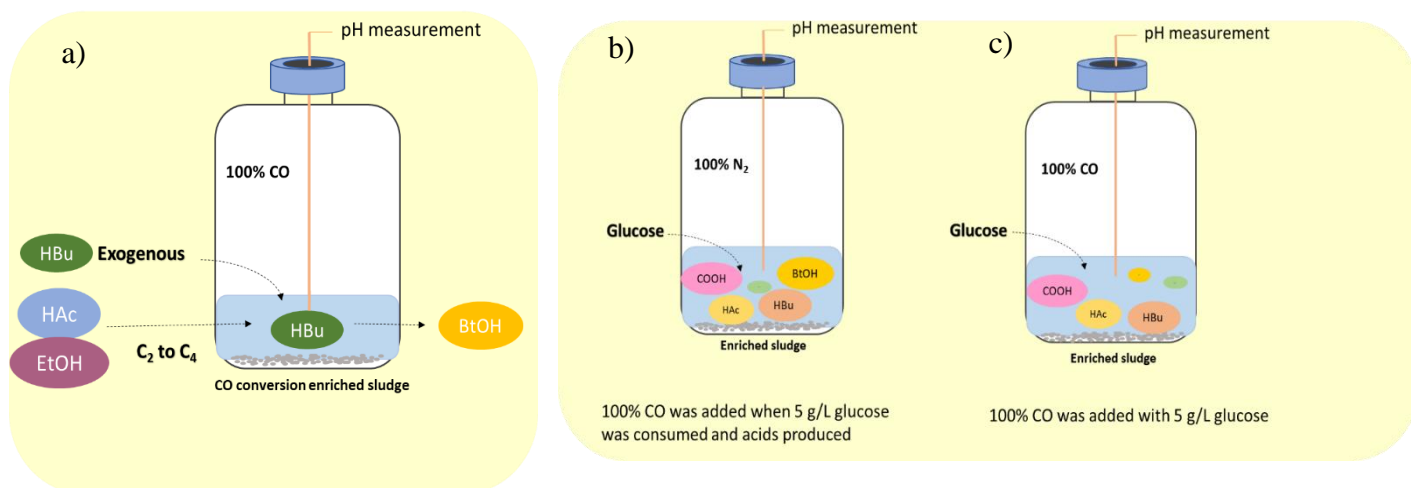


Fig. 8.1 Schematic diagram of a) influence of exogenous acetate, butyrate and ethanol on butanol production using CO as gaseous substrate, b) endogenous butyric acid from glucose (Glucose +N₂) and c) co-fermentation of CO and glucose (Glucose+CO).

Table 8.1 The highest net acids and alcohol production, mole ratio of ethanol to acetic acid and butanol to butyric acid, butyric acid conversion and butanol yield of experiments on the influence of acetate, butyrate and ethanol on butanol production using CO as gaseous substrate.

No.	Gas	Exogenous acids and ethanol (g/L)			Molar ratios		Highest net production (g/L)						Ratio		Butanol yield (%)	Butyric acid conversion (%)
		Acetic acid	Butyric acid	Ethanol	Ethanol/Acetic acid	Ethanol/Butyric acid	Acetic acid	Butyric acid	Ethanol	Butanol	Propionic acid	Valeric acid	EtOH/H Ac	BtOH/H Bu		
I. Exogenous acetic acid, ethanol and butyric acid																
1	CO	2.2	0	6	3.55	-	11.2	1.1	4.3	1.6	1.3	0.2	1.79	3.84	-	-
2	CO	2.2	3.2	6	3.55	3.59	10.7	0.1	0.5	2.6	0.9	0.0	0.46	-	100.2	76.2
3	CO	0	3.2	0	-	-	6.9	0.1	4.3	1.9	1.3	0.1	0.33	-	67.0	53.7
4 Control	CO	0	0	0	-	-	8.3	0.6	2.7	0.2	0.4	0.0	3.45	-	-	-
II. Exogenous 7 and 14 g/L butyric acid																
5	CO	0	7	0	--	--	7.1	--	0.2	2.3	0.2	0	0.01	2.04	15.8	32.2
6	CO	0	14	0	--	--	3.9	--	0.1	3.4	0.1	0	0.05	1.16	58.0	67.5

(2) Endogenous butyric acid from glucose in CO fed reactor

The sequential conversion of glucose (glycolysis) and then CO (WLP) or the co-fermentation of glucose and CO by the enriched sludge were further investigated in two gas fed reactors (Fig. 8.1b and 1c). pH was controlled at 5.5-6.2 by 1 M NaOH or 1 M HCl. Glucose was added initially to reach a concentration of 5 g/L and the headspace was flushed with either N₂ or CO, i.e. Glucose + N₂ and Glucose + CO. In the Glucose + N₂ experiment, when glucose was totally consumed and butyric acid accumulated ((G + N)₁), the headspace was flushed with CO for 5 min to reach a gas pressure of 1.8 bar at 180, 252, 360 and 432 h, respectively, to stimulate butanol accumulation ((G+N)₂). In CO and glucose co-fermentation, CO was flushed at 0, 180, 276 and 432 h in the Glucose + CO experiment.

The microbial community of the four enriched sludge samples were analyzed: two samples from the Glucose + N₂ experiment, when glucose was totally consumed and butyric acid accumulated ((G+N)₁) and at the end of the incubation ((G+N)₂) after CO was added as well as two samples from the Glucose + CO experiment, when glucose was totally consumed and butyric acid accumulated ((G+C)₁), and at the end of the incubation ((G+C)₂).

8.2.5 Analytical methods

Acetic, propionic, and butyric acids, ethanol and butanol were determined on a high performance liquid chromatography (HPLC, HP1100, Agilent Co., Palo Alto, USA) equipped with a refractive index detector, using an Agilent Hi-Plex H Column (300×7.7 mm). A 5 mM H₂SO₄ solution was used as mobile phase at a flow rate of 0.80 mL/min, with a sample injection volume of 20 μL, and a column temperature of 45 °C (Arslan et al., 2019). The cell concentration was determined with a spectrophotometer (Hitachi, Model U-200, Pacisa & Giralt, Pacisa & Giralt, Spain) at a wavelength of 600 nm (Arslan et al., 2019). pH was measured using a pH meter (Mettler Toledo, Zurich, Switzerland).

8.2.6 Calculations

The butyric acid (HBu) conversion efficiency and butanol (BtOH) yield were calculated according to Eq. (1) and (2), respectively:

$$HBu \text{ conversion efficiency} = \frac{C_{in} - C_{out}}{C_{in}} \quad (1)$$

Where C_{in} = the total carbon from exogenous butyric acid addition; C_{out} = the carbon from the butyric acid at the end of the incubation after conversion to butanol.

$$BtOH \text{ yield} = \frac{\text{Real butanol production}}{\text{Theoretical butanol}} \times 100\% \quad (2)$$

Where *Real butanol production* and *Theoretical butanol* were calculated in $\text{mmol} \cdot \text{L}^{-1} \text{ C}$.

8.2.7 Microbial analysis

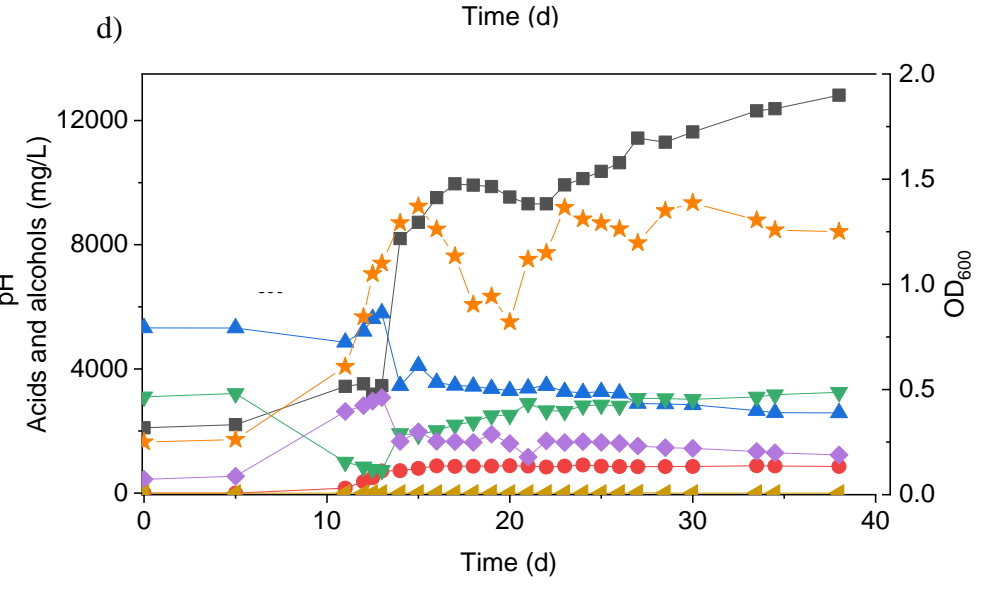
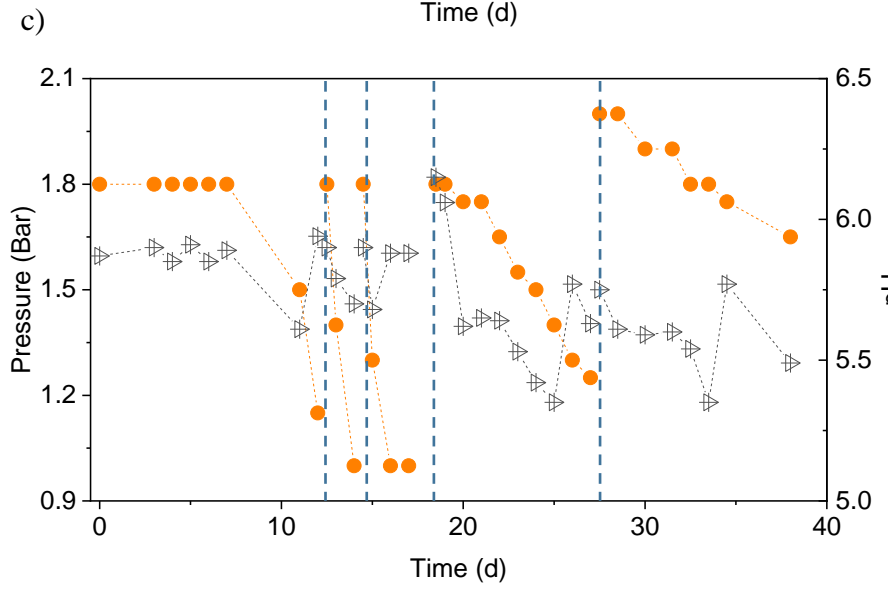
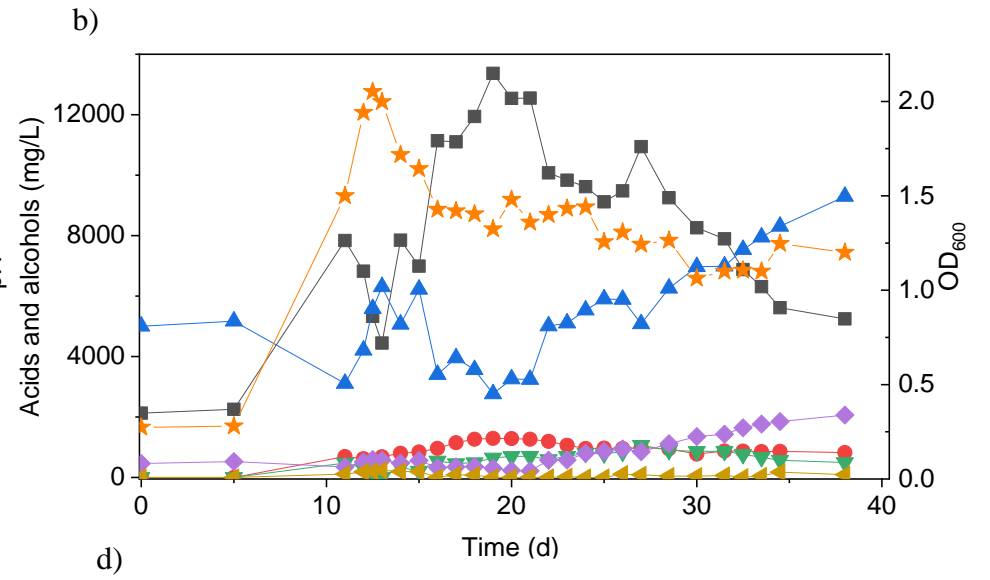
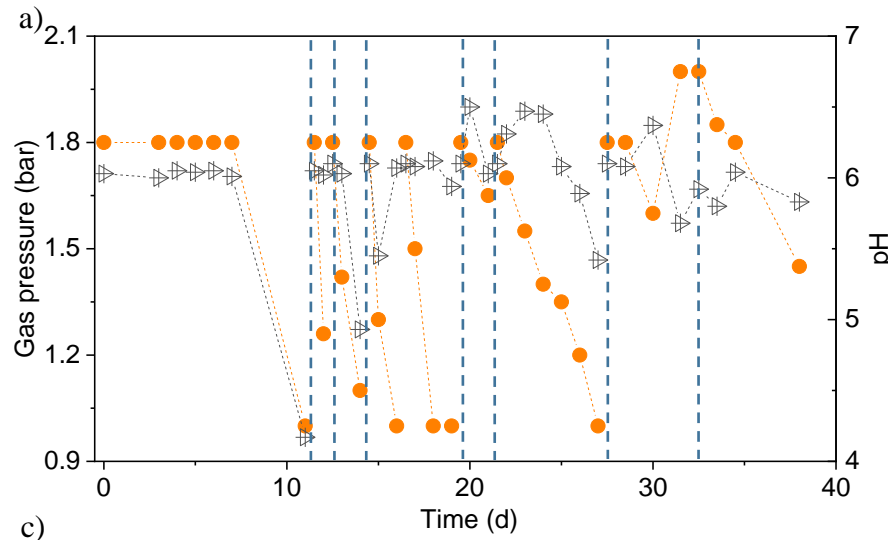
DNA was extracted using a DNeasy® PowerSoil Kit (QIAGEN, Germany) following the manufacturer's protocol. 10 mL sludge was used for DNA extraction at the end of the incubations. The extracted DNA was quantified and its quality was checked with a Nanodrop 2000c Spectrophotometer (Thermo Scientific, USA). The extracted DNA was analyzed by Metagenomics -Seq (Illumina PE150, Q30 \geq 80%) (Novogene, UK). The analysis procedure has been described in He et al. (2021).

8.3 Results

8.3.1 Ethanol and butanol production with exogenous acetic acid, ethanol and butyric acid using CO as the carbon source

8.3.1.1 Exogenous acetic acid and ethanol supply

In the HAC+EtOH experiment, butanol production was not observed till day 20 (Fig. 8.2a, b). Thereafter, interestingly, butanol production increased and reached a final concentration of 2.1 g/L with a net production of 1.6 g/L at the end of the incubation (day 38), during which the pH ranged between 5.4 to 6.5 (Fig. 8.2a, b). However, acetic acid was produced first and increased from 2.2 g/L to 7.8 g/L and simultaneously the ethanol concentration decreased from 5.0 g/L to 3.1 g/L at day 11. The pH dropped to 4.07 due to the accumulation of acetic acid and the biomass reached an OD_{600} of 1.5 (Fig. 8.2a, b). Thereafter, acetic acid accumulated to its maximum concentration of 12.5 g/L (Fig. 8.2b), while the ethanol concentration quickly increased to 6.3 g/L at day 15 to finally decrease again to as low as 3.5 g/L at day 20. At the seventh CO addition (day 20-25), ethanol increased again to 5.9 g/L at 25 d (Fig. 8.2b). At the last CO addition, the CO gas pressure was increased to 2.0 bar, ethanol increased again and reached its highest concentration of 9.3 g/L at pH 5.8-6.4. The highest net production of acetic acid, ethanol, butyric acid and butanol reached, respectively, 11.2, 4.3, 1.1 and 1.6 g/L (Table 8.1). Other acids such as propionic acid with the highest concentration of 1.3 g/L and a small amount of valeric acid (0.2 g/L) were obtained during the fermentation (Table 8.1).



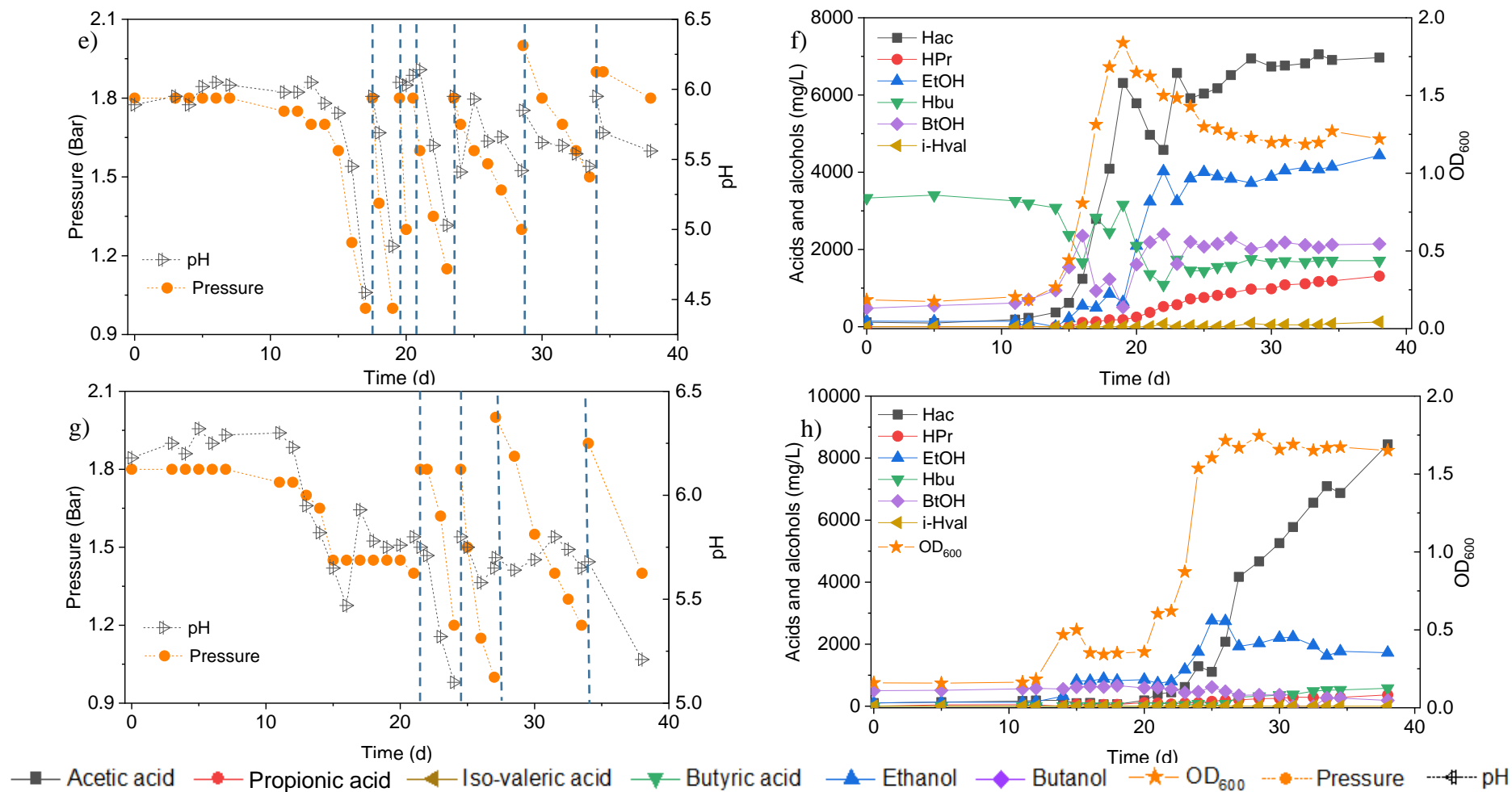


Fig. 8.2 Production of acids and alcohols, cells concentration and change of gas pressure in semi-gas feeding reactors by enriched sludge from 6th transfer using CO as the carbon source. a) and b) exogenous acetic acid and ethanol; c) and d) exogenous acetic acid, ethanol and butyric acid; e) and f) exogenous butyric acid; g) and h) control without exogenous acids or ethanol. The dashed lines represent CO addition and pH regulation.

8.3.1.2 Exogenous acetic acid, ethanol and butyric acid supply

In the HAc+EtOH+HBU experiment, the butanol concentration increased to 2.8 g/L along with the butyric acid concentration dropping from 3.1 to 1.0 g/L, with the pH ranging from 5.9 to 5.6, at the first CO addition (Fig. 8.2c, d). Ethanol slightly decreased while acetic acid increased after a few days of adaption, which exhibits a similar trend as in the HAc+EtOH experiment (Fig. 8.2b, d). On the second CO addition (day 11- 14), butanol increased to 3.1 g/L at 13 d, when the gas pressure dropped to 1.4 bar (Fig. 8.2c, d). During the gas pressure decrease from 1.4 bar to 1 bar, the concentrations of both butanol and ethanol decreased, respectively, from 3.1 to 1.7 g/L and 8 to 3.5 g/L at day 13-14. Conversely, the butyric acid concentration increased from 0.7 to 1.9 g/L and acetic acid accumulated quickly to 8.2 g/L (Fig. 8.2c, d). Thereafter, acetic acid reached 10.0 g/L at day 16 while butyric acid increased continuously until the end of the incubation (Fig. 8.2c, d). After 38 days incubation, the highest net acetic acid concentration of 10.7 g/L was obtained; while the highest net production of ethanol, butyric acid, and butanol reached, respectively, 0.5, 0.1, and 2.6 g/L (Table 8.1).

8.3.1.3 Exogenous butyric acid supply

In the exogenous HBU experiment, the butanol concentration increased to 2.4 g/L along with the exogenous butyric acid concentration dropping from 3.2 to 1.7 g/L, at pH 5.9, on day 16 (Fig. 8.2f). However, later on, the butanol concentration decreased from 2.4 to 1.0 g/L, at day 17, with a pH drop from 5.45 to 4.45, and the gas pressure decreasing from 1.25 to 1.0 bar (Fig. 8.2e, f). Acetic acid increased to 2.8 g/L, while the pH value decreased to 4.55 and ethanol slightly increased to 0.5 g/L. At the second CO addition (17-19 d), butanol dropped again to its lowest concentration of 0.5 g/L, while butyric acid increased to 3.2 g/L at day 19 (Fig. 8.2f). The acetic acid concentration increased to 6.3 g/L, along with the pH drop to 4.88 (Fig. 8.2e). At the third and fourth CO addition (19 - 23 d), ethanol and butanol increased again accompanied by the decrease of acetic acid and butyric acid concentrations, reaching 6.9 g/L acetic acid, 4.4 g/L ethanol, 1.7 g/L butyric acid and 2.1 g/L butanol at day 38 (Fig. 8.2f). The propionic acid concentration increased after day 20 and reached 1.3 g/L at day 38 (Fig. 8.2f).

In the control, five CO additions were amended (Fig. 8.2g). Acetic acid and ethanol were mainly produced, with the highest concentrations of, respectively, 8.2 and 2.8 g/L (Fig. 8.2h). Biomass growth was also observed (Fig. 8.2h). Both butyric acid and butanol were insignificantly produced, with only 0.6 g/L butyric acid and 0.2 g/L butanol production at day 38 (Fig. 8.2h).

8.3.2 Effect of exogenous butyric acid supply on butanol production

Upon 7 g/L butyric acid addition, the butanol concentration increased to 2.2 g/L at day 13 while butyric acid decreased from 7.0 to 5.0 g/L (Fig. 8.3b). Simultaneously, acetic acid increased to 1.9 g/L at day 13 and 4.0 g/L at day 15 and biomass growth entered into the log phase and with the OD₆₀₀ reached the highest value of 1.1 (Fig. 8.3b). Then, the butanol concentration slightly decreased to 1.1 g/L while acetic acid increased to its highest concentration of 7.8 g/L at day 38 (Fig. 8.3b). A small amount of hexanoic acid was observed with the highest concentration of 0.2 g/L at day 25 and propionic acid increased to 0.3 g/L at day 38 (Fig. 8.3b).

In a second assay, with 14 g/L exogenous butyric acid supply, butanol increased to 2.9 g/L at day 20 along with the amount butyric acid dropping (Fig. 8.3d). Butanol kept increasing to 3.5 g/L at day 25 and finally reached 3.6 g/L at the third CO addition, at day 27 (Fig. 8.3d). The acetic acid concentration increased to 2.3 g/L at day 20, with the cell concentration reaching its highest absorbance of 1.000 (Fig. 8.3d). At the end of the incubation (day 38), acetic acid had increased to its highest concentration of 4.5 g/L, while the cell concentration (OD₆₀₀) decreased to 0.661 (Fig. 8.3d). The butanol production pattern was similar to the exogenous supply of 7 g/L butyric acid, except that the butanol accumulation was twice as high. The butanol production slowed down and even stopped after the first CO addition, but acetic acid production and biomass growth continued.

Fig. 8.2 and Table 8.1 thus show that the butanol production was significantly enhanced in the presence of exogenous butyric acid. The amount of accumulated butanol increased up to 1.2 and 1.8 fold, respectively, with 7 and 14 g/L HBU, compared to 3.2 g/L HBU. Although the butanol yield reached its highest value of 67.0% with 3.2 g/L HBU, it decreased to, respectively, 15.8 and 58.0% with 7 and 14 g/L HBU (Table 8.1). The butyric acid conversion efficiency reached its highest value of 67.5% with 14 g/L HBU, correspondingly 1.3 and 2.1 fold higher than, respectively, than 7 and 3.2 g/L HBU (32.2 and 53.7%, respectively) (Table 8.1). However, in the presence of HAc + EtOH + HBU, the butanol yield and butyric acid conversion efficiency reached, respectively, 100% and 76.2% which are both higher than with HBU (Table 8.1).

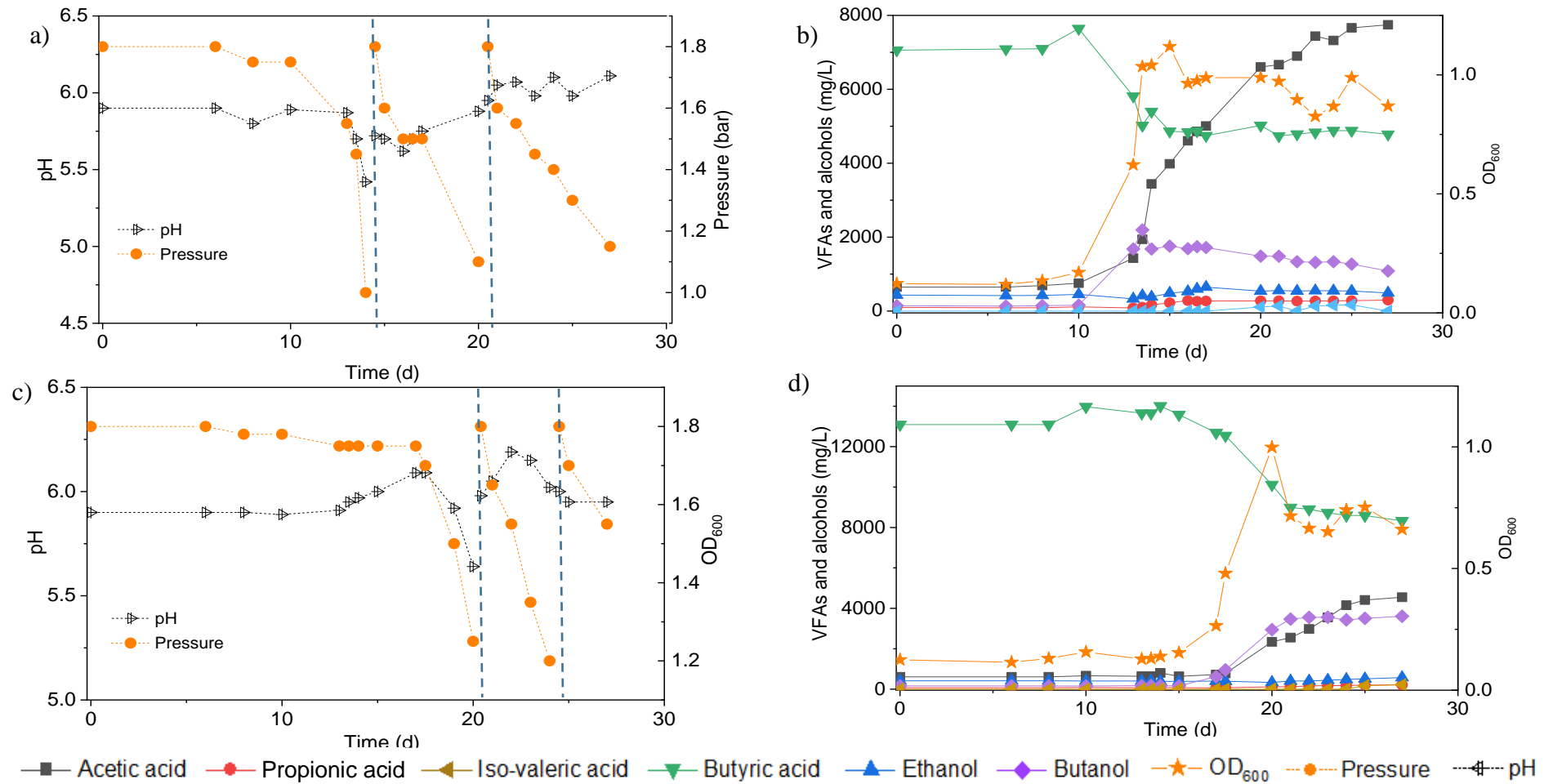


Fig. 8.3 Production of acids and alcohols, cells concentration and change of gas pressure in semi-gas feeding reactors by enriched sludge from 6th transfer (He et al. 2021b) using CO as the carbon source. a) and b) exogenous 7 g/L butyric acid; c) and d) exogenous 14 g/L butyric acid.

The dashed lines represent CO addition and pH regulation.

8.3.3 Fermentation with endogenous butyric acid from glucose

8.3.3.1 Batch tests

To better understand the carbon flow, the liquid products are shown in $\text{mmol L}^{-1} \text{ C}$ in a bar chart (Fig. 8.4). Initially $154 \text{ mmol} \cdot \text{L}^{-1} \text{ C}$ was added in the form of glucose (5 g/L) with a small amount of additional carbon carried over from the inoculum (Fig. 8.4). After 44 h, the accumulation of $24 \text{ mmol} \cdot \text{L}^{-1} \text{ C}$ formic acid was detected, which was then quickly converted to acetic acid, butyric acid and propionic acid with, respectively, 23.4, 54.0 and $2.1 \text{ mmol} \cdot \text{L}^{-1} \text{ C}$ at 72 h, when glucose was totally consumed (Fig. 8.4a). Butyric acid reached a concentration of $59.2 \text{ mmol} \cdot \text{L}^{-1} \text{ C}$ at 96 h and remained relatively stable thereafter (Fig. 8.4a). Therefore, CO was added at 120 h when all the original substrate (glucose) was exhausted. Then, butanol was produced and increased from $8 \text{ mmol} \cdot \text{L}^{-1} \text{ C}$ at 120 h to, respectively, 21 and $30 \text{ mmol} \cdot \text{L}^{-1} \text{ C}$ at 144 and 168 h. To stimulate butanol production, CO was again added at 168, 216 and 264 h (Fig. 8.4a). Correspondingly, the butanol concentration continuously increased to $61 \text{ mmol} \cdot \text{L}^{-1} \text{ C}$, representing a net production of $53.6 \text{ mmol} \cdot \text{L}^{-1} \text{ C}$, at the end of the incubation (Fig. 8.4a, Table 8.2). Ethanol production was also observed with the CO addition, reaching $34 \text{ mmol} \cdot \text{L}^{-1} \text{ C}$ at the end of the incubation (Fig. 8.4a).

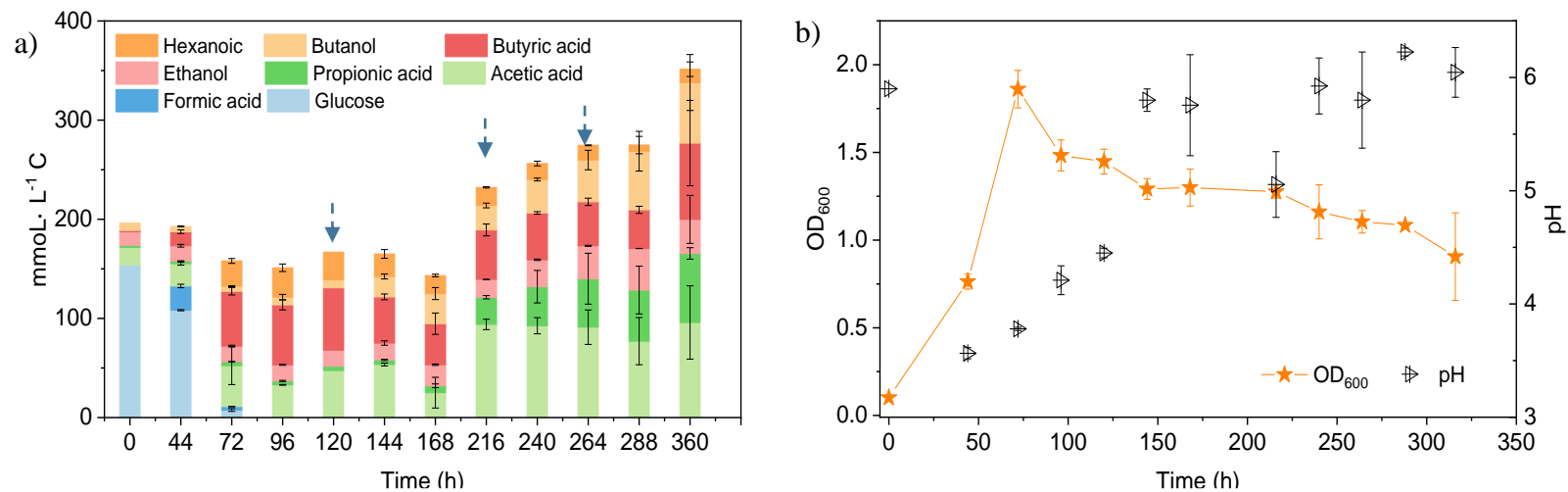


Fig. 8.4 a) Production of acids and alcohols and b) cell concentration and pH by enriched sludge using 5 g/L glucose as the substrate in batch tests. Down arrows in a) represent 1.1 bar CO addition at 120, 216 and 264 h. pH was adjusted to 5.9 on a daily basis.

Table 8.2 The highest net production of acids and alcohol, mole ratio of butanol to butyric acid and butanol yield.

Experimental conditions		The highest net production (mmol·L ⁻¹ C)							BtOH/HBu	HBu conversion efficiency (%)	Butanol yield (%)
		Formic acid	Acetic acid	Butyric acid	Ethanol	Butanol	Hexanoic acid	Propionic acid			
pH control	5 g/L Glucose + N ₂ then CO	95.4	17.5	42.9	6.6	26.6	33.0	4.7	1.50	58.6	62.1
	5 g/L Glucose + CO	70.3	60.4	50.3	1.0	11.1	0	34.2	0.35	45.3	22.1
Batch tests	5 g/L Glucose + N ₂ then CO	24.5	77.9	75.7	82.0	53.6	29.9	67.7	0.71	--	--

8.3.3.2 Endogenous butyric acid production from glucose and its conversion to butanol in a gas fed reactor with pH control

When using 5 g/L glucose as the substrate, glucose was totally consumed after 58 h, with a production of 95.4 mmol·L⁻¹ C formic acid, 0.7 mmol·L⁻¹ C acetic acid and 16.1 mmol·L⁻¹ C butyric acid (Fig. 8.5a). Formic acid was then subsequently consumed and converted to 6.9 mmol·L⁻¹ C acetic acid, 41.0 mmol·L⁻¹ C butyric acid and 31.2 mmol·L⁻¹ C hexanoic acid at 135 h (Fig. 8.5a). The pH value decreased to 5.5 at 180 h, due to the accumulation of acids, and it was then adjusted back to 6.0 (Fig. 8.5b). After CO addition at 180 h, butanol production was triggered and increased from 1.1 mmol·L⁻¹ C at 180 h to 4.2 mmol·L⁻¹ C, at 204 h, and later 8.7 mmol·L⁻¹ C, at 252 h (Fig. 8.5a). CO was then supplied again later, at 252, 360 and 432 h to potentially stimulate butanol production. Consequently, the net butanol production increased to 17.4 mmol·L⁻¹ C, at 360 h, and finally 26.6 mmol·L⁻¹ C at the end of the incubation and the butanol yield reached 62.1% (Fig. 8.5a, Table 8.2). The remaining butyric acid concentration was 17.8 mmol·L⁻¹ C at the end of the incubation, and the net butyric acid consumption was 24.7 mmol·L⁻¹ C, calculated from the difference with 42.5 mmol·L⁻¹ C at 180 h, when CO was first added. This almost equals the net butanol production of 25.5 mmol·L⁻¹ C at the end of the incubation (Fig. 8.5a).

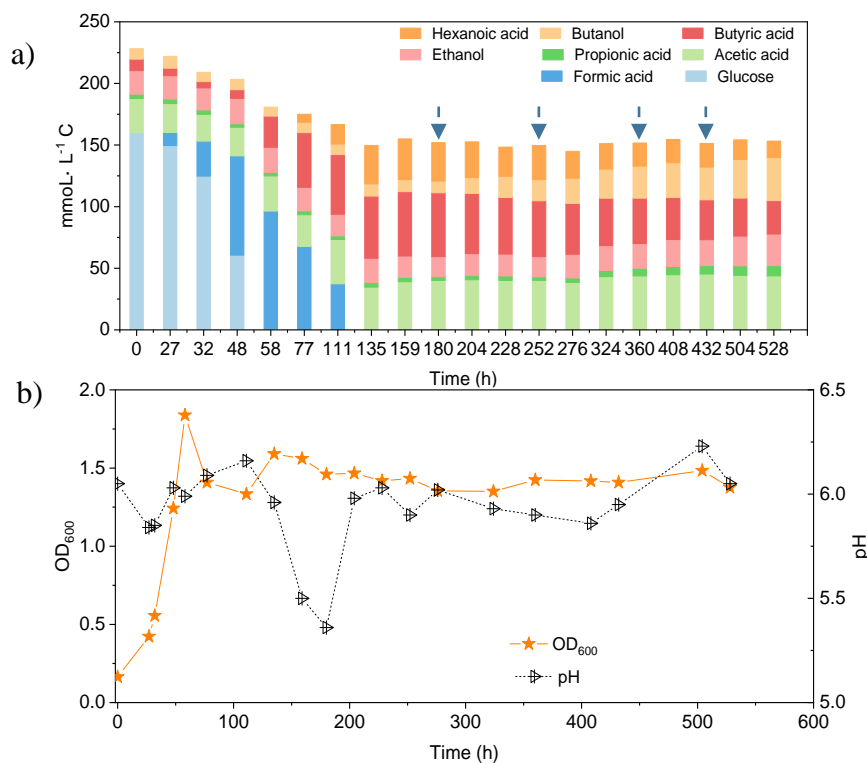


Fig. 8.5 a) Production of acids and alcohols and b) cell concentration and pH by enriched sludge using 5 g/L glucose as the substrate in a gas fed reactor (Glucose+N₂). Down arrows represent 1.1 bar CO addition at 180, 252, 360 and 432 h. pH was controlled at 5.5 – 6.2.

8.3.3.3 Co-fermentation of glucose and CO in a bioreactor with pH control

In the co-fermentation of CO and glucose (5 g/L), half the amount of glucose was consumed after 58 h, along with the production of 70 mmol·L⁻¹ C formic acid, as the major end product (Fig. 8.6a). Later, glucose was totally consumed, at 111 h, and 19.5 mmol·L⁻¹ C formic acid, 21.2 mmol·L⁻¹ C propionic acid and 50.3 mmol·L⁻¹ C butyric acid were produced (Fig. 8.6a). CO was added at 180, 276 and 432 h to enhance butanol production. The butanol concentration did indeed increase to 6.8 mmol·L⁻¹ C, after 276 h, 5.3 mmol·L⁻¹ C, after 432 h, and 9.7 mmol·L⁻¹ C at the end of the incubation (Fig. 8.6a). Both acetic acid and propionic acid reached as high as 60.4 and 34.2 mmol·L⁻¹ C, respectively, at the end of the incubation. Besides, the butanol yield reached 22.1% at the end of the incubation (Fig. 8.6a).

8.3.4 Microbial analysis

When supplying glucose + N₂, the relative abundance of the *Clostridia* and *Bacilli* class in the initial inoculum was, respectively, 82 and 1%, and reached, respectively, 58 and 33% when glucose was totally consumed ((G+N)₁, glycolysis). Then, both decreased to, respectively, 51 and 17% and unassigned bacteria occupied 8% at the end of the incubation (after replacing the headspace with CO, (G+N)₂) (Fig. 8.7). In the *Clostridia* class, the *Clostridium* genus decreased from 54% to 33%, while *Oscillibacter* genus increased from 0.6 to 9% at the end of the incubation. In the *Bacilli* class, the *Enterococcus* genus decreased from 15 to 8% (Fig. 8.7).

At the *Clostridium* genus level, *Clostridium butyricum* increased from 0.003% in the initial inoculum to 16% when glucose was totally consumed, while it decreased to 6% at the end of the incubation, after replacing the headspace with CO (Table 8.3). *C. carboxidivorans* was enriched from 0.3% of the whole *Clostridium* genus in the inoculum to, respectively, 6% when glucose was totally consumed and 4% at the end of the incubation (Table 8.3). The relative abundance of other known *Clostridium* species with relative abundance higher than 2% increased much at the end of the incubation compared to when glucose was totally consumed (Table 8.2). For instance, the relative abundance of *Clostridium sp.* W14A increased from 0.04 to 3%, *Clostridium ragsdalei* from 0.07 to 4%, *C. ljungdahlii* from 0.1 to 4%, *C. autoethanogenum* from 0.03 to 2%, and *Clostridium coskatii* from 0.07 to 2% (Table 8.3).

In CO and glucose co-fermentation (Glucose+CO), the enriched sludge was dominated by both *Clostridia* and *Bacilli* classes with relative abundance of 71% and 24%, respectively, when glucose was totally consumed ((G+C)₁). Then, it changed to, respectively, 59% and 29% at the end of the incubation ((G+C)₂) (Fig. 8.7). In the *Clostridia* class, although the *Clostridiaceae* family still occupied as high as 47% at the end of the incubation, an increase of

other families was also observed, such as the *Lachnospiraceae* family increasing from 0.8%, in (G+C)₁ to 9% and the *Oscillospiraceae* family increasing from 0.08 to 1% in (G+C)₂ (Fig. 8.7).

At the *Clostridium* genus level, the relative abundance of *Clostridium butyricum* reached 17% in (G+C)₁ but it then decreased to 2% in (G+C)₂ (Table 8.3). *C. carboxidivorans* significantly increased to 6% in (G+C)₂ compared to 0.1% in (G+C)₁ (Table 8.3). The relative abundance of other species such as *Clostridium* sp. W14A increased from 0.08 to 0.8%, *Clostridium ragsdalei* from 0.006 to 3%, *C. ljungdahlii* from 0.006 to 6%, *C. autoethanogenum* from 0.02 to 4%, and *Clostridium coskatii* from 0.003 to 3% (Table 8.3).

Fig. 8.8 shows the clustering tree based on Bray-Curtis dissimilarity and the relative abundance at phylum level among (G+N)₁, (G+N)₂, (G+C)₁ and (G+C)₂. (G+N)₁ had high dissimilarity with (G+C)₁, while (G+N)₂ had high similarity with (G+C)₂, but these four enriched sludges still exhibited close distances (Fig. 8.8). The common and special genes among the transfers is shown in the Venn figure (Fig. 8.9). In the core common genome of 56463 genes, special genes increased at the end of the incubation. For instance, 2905 special genes appeared in (G+C)₁ while they increased significantly, to 35257, in (G+C)₂ (Fig. 8.9a). Considering the high abundance of the *Clostridium* genus, a Venn figure for gene analysis at *Clostridium* genus level was done. Special genes that increased at the end of the incubation also showed a similar trend at *Clostridium* genus level (Fig. 8.9b).

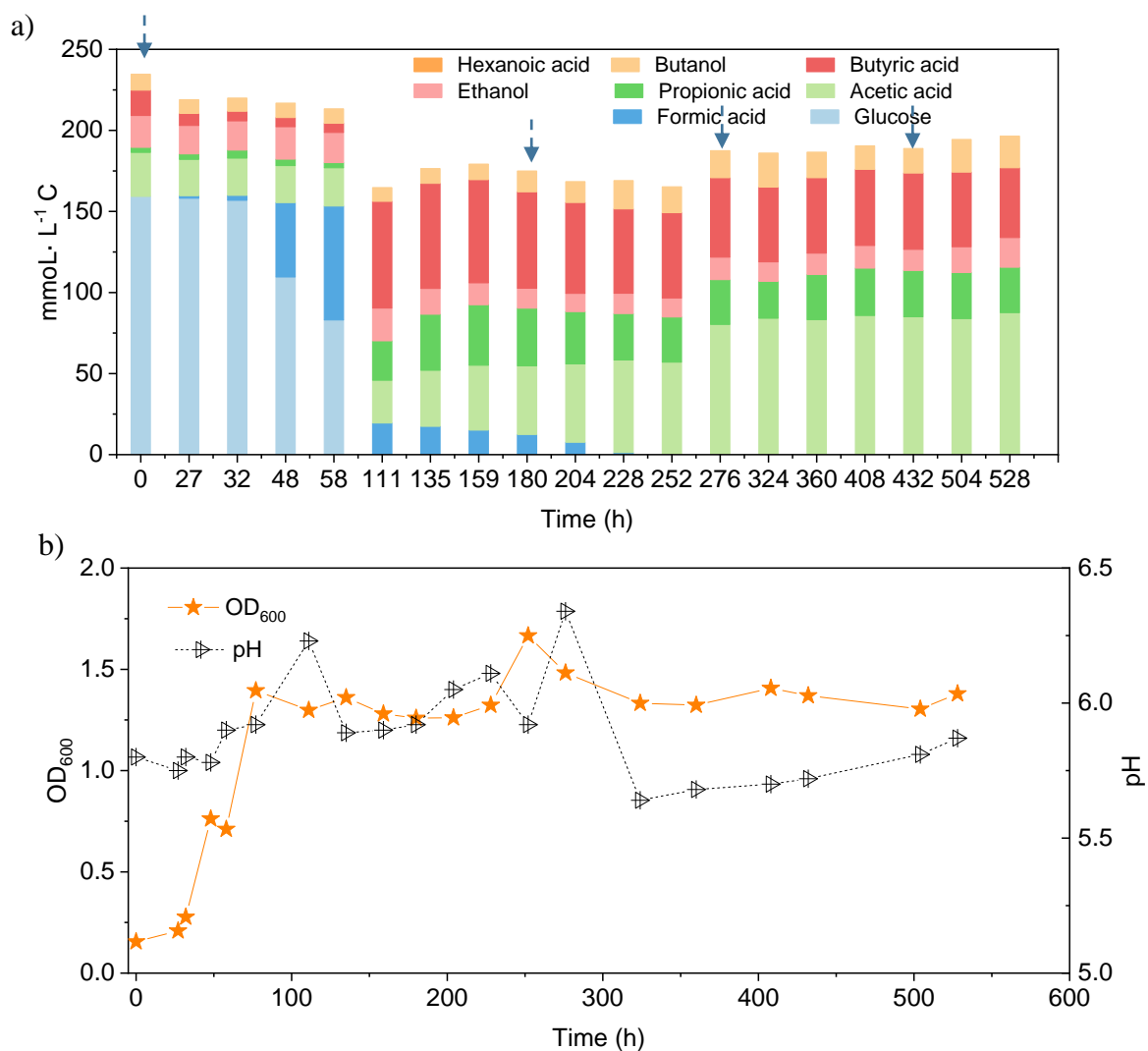


Fig. 8.6 a) Production of acids and alcohols and b) cell concentration and pH by enriched sludge from 6th transfer using 5 g/L glucose and CO as substrate in a gas fed reactor with intermittent CO gas feeding (Glucose+CO). Down arrows in a) represent 1.1 bar CO addition at 0, 180, 276 and 432 h, respectively. pH was controlled at 5.5 – 6.2.

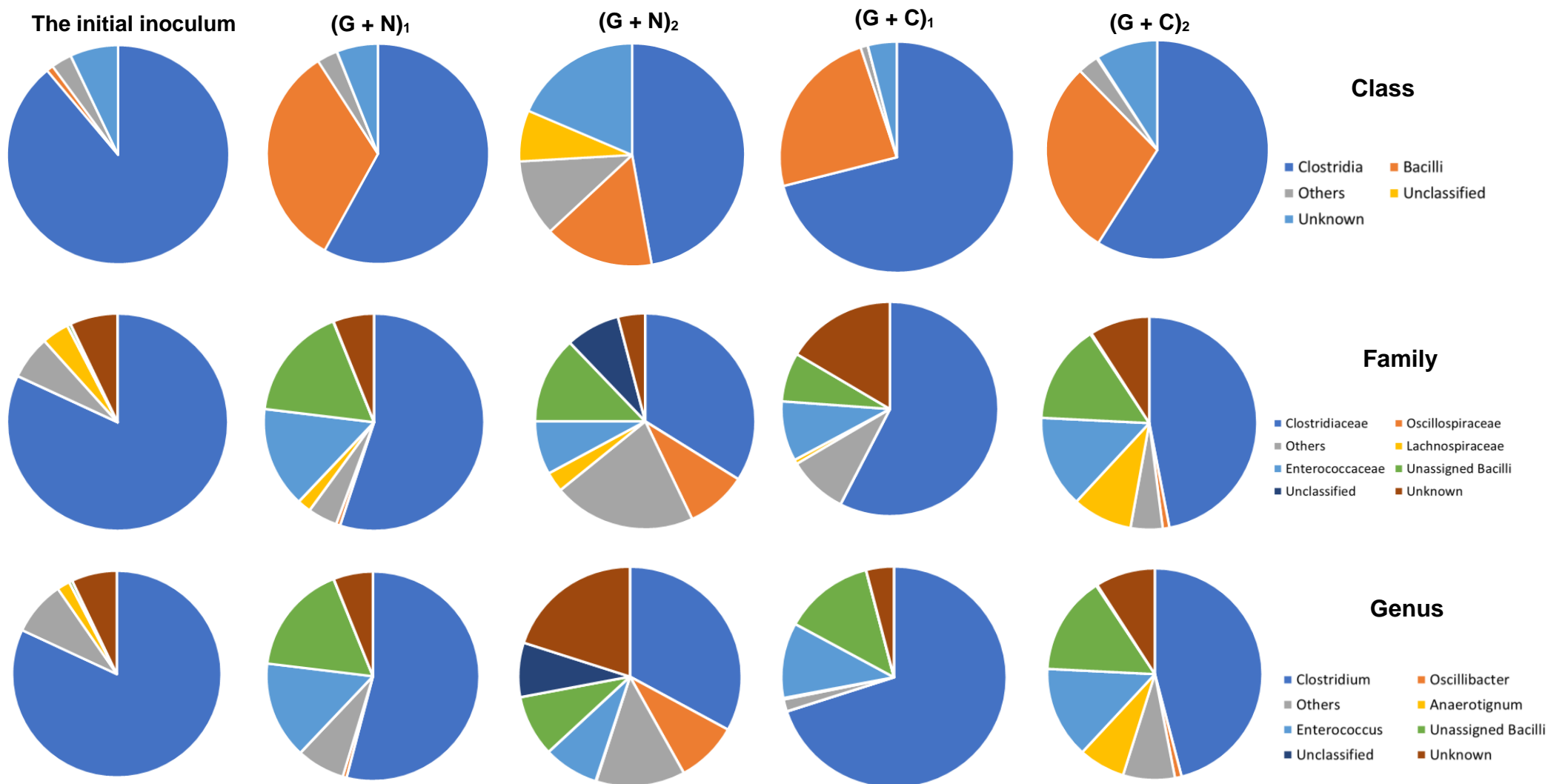


Fig. 8.7 The microbial community analysis of the initial inoculum, after glucose fermentation and CO and glucose co-fermentation from 6th transfer. ‘(G+N)₁’ represent when glucose was totally consumed using glucose as substrate and ‘(G+N)₂’ represent at the end of the incubation after CO was added. ‘(G+C)₁’ represent when glucose was totally consumed and ‘(G+C)₂’ represent at the end of the glucose and CO co-fermentation incubation.

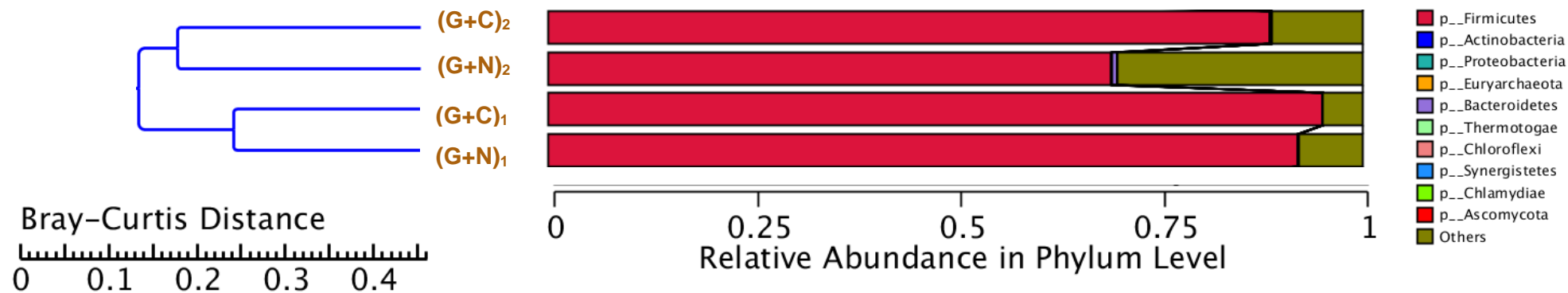


Fig. 8.8 Clustering tree based on Bray-Curtis distance of the microbial community after G+N and G+C fermentation by enriched sludge from 6th transfer. '(G+N)₁' represent when glucose totally consumed using glucose as substrate and '(G+N)₂' represent at the end of the incubation after CO was added. '(G+C)₁' represent when glucose totally consumed and '(G+C)₂' represent at the end of the incubation in glucose and CO co-fermentation.

Table 8.3 Relative abundance of *Clostridium* spp. at species level in Glucose+CO and Glucose +N₂ by enriched sludge from 6th transfer.

		Initial inoculum	Glucose		Glucose+ CO	
			(G+N) ₁	(G+N) ₂	(G+C) ₁	(G+C) ₂
Clostridium genus	Of bacteria	88	58	42	72	51
	Of root	82	54	33	70	46
Species name		<i>Clostridium</i> (Genus level) %				
<i>Clostridium butyricum</i>		0.003	16	6	17	2
<i>C. carboxidivorans</i>		0.3	6	4	0.1	6
<i>Clostridium</i> <i>sp. C8</i>		0.006	3	3	0.5	0.3
<i>Clostridium</i> <i>sp. IBUN125C</i>		0.00001	2	0.8	4	0.5
<i>Clostridium</i> <i>Cadaveris</i>		0.1	3	0.9	0.008	0.4
<i>Clostridium sp. W14A</i>		0.4	0.04	3	0.08	0.8
<i>Clostridium ragsdalei</i>		4	0.07	4	0.006	3
<i>C. ljungdahlii</i>		8	0.1	4	0.006	6
<i>C. autoethanogenum</i>		6	0.03	2	0.002	4
<i>Clostridium coskatii</i>		4	0.07	2	0.003	3
<i>Clostridium kluyveri</i>		0.3	0.02	0.3	0.004	0.2
Other identified <i>Clostridium spp.</i>		3.9	10.7	12.0	3.3	8.8
Unassigned <i>Clostridium spp.</i>		73	59	58	75	65

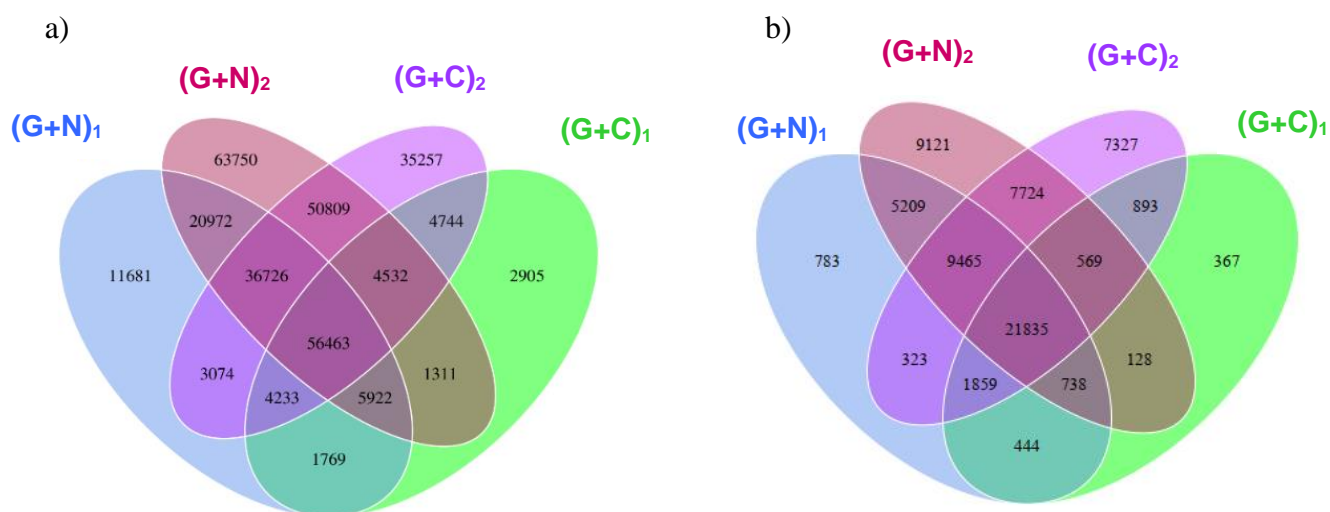


Fig. 8.9 Venn diagrams of gene number of a) the total genes and b) the genes in *Clostridium* genus level. The overlap parts represent the number of common genes between/among samples (groups); the other parts represent the number of special genes of samples (groups). ‘(G+N)₁’ represent when glucose was totally consumed using glucose as substrate and ‘(G+N)₂’ represent at the end of the incubation after CO was added. ‘(G+C)₁’ represent when glucose was totally consumed and ‘(G+C)₂’ represent at the end of the incubation in glucose and CO co-fermentation.

8.4 Discussion

8.4.1 Exogenous butyric acid enhanced butanol production using CO as reducing power

This study showed that butanol production was enhanced in the presence of exogenous butyric acid using CO as reducing power by the enriched sludge. Butanol production was increased along with increasing exogenous butyric acid concentration (Table 8.1), which can be attributed to the increased extent of acid to alcohol conversion, according to Eq. 3.



The highest butanol production of 3.4 g/L, with the exogenous supply of 14 g/L butyric acid is, to the best of our knowledge, the highest reported butanol concentration using CO as the gaseous substrate. Previous research reported a butanol production of 2.66 g/L, together with 5.55 g/L ethanol from CO fermentation, with *C. carboxidivorans* at pH 5.75 (Fernández-Naveira et al., 2016). Butanol production occurred along with exogenous butyric acid consumption and kept increasing when cell growth entered the log phase (Fig. 8.2). Acetic acid accumulation occurred rather later and accumulated fast after butanol reached a high concentration (Fig. 8.2). This indicates the preference for butanol production in the presence

of butyric acid and a 1.8 bar CO gas pressure, compared to acetic acid production. Furthermore, butanol production increased very quickly and reached close to the highest concentration at the end of the first CO addition (Fig. 8.2 and Fig. 8.3). However, it did not increase, instead, even slightly decreased after the first CO addition, which occurred almost in every experiment supplied with exogenous butyric acid (Fig. 8.2). During the fermentation process, CO can be used as both carbon source for acetic acid production and reducing power to reduce butyric acid to butanol by the enriched sludge. When exogenous butyric acid was present in the medium at the start of the fermentation, acetogens took first advantages of the existing butyric acid, using CO as reducing power and reduced butyric acid to butanol. Along with the biomass growth adaption, acetogens obtained energy from acetic acid production (ATP released process), thus CO acted more as the carbon source inducing increased acetic acid production than reducing power for butanol production from butyric acid (Mock et al., 2015; Zhu et al., 2020).

Butanol production occurred at pH 5.9 and with a CO gas pressure as high as 1.8 bar; but when the pH was lower than 5.5, butanol production was inhibited (Fig. 8.2). This pH range for alcohol production is in agreement with previous studies, in which the pH ranged from 5.7 to 6.4 for selective butanol production by the same enriched sludge as used in this study (He et al., 2022). Instead, the pH range is different from other previous reports, in which solventogenesis was stimulated at lower pH, varying between 4.5-5.5 (Ganigué et al., 2016; Chakraborty et al., 2019). The wide pH range for butanol production might be due to the mixed *Clostridium* spp. present in the inoculum used in this study. For instance, the relative abundance of *C. autoethanogenum* and *C. ljungdahlii* occupied, respectively, 6% and 8%, which are known to convert CO to acetic acid and ethanol via the WLP while butanol-producing *C. carboxidivorans* observed less than 1% (He et al., 2021b). However, the relative abundance of unidentified *Clostridium* species occupied as high as 73% of the *Clostridium* genus (He et al., 2021b).

The mole ratio of butanol production and butyric acid consumption in exogenous 3.2 g/L HBU is close to 1 during the fermentation process (Fig. 8.2d, f), which is conform the theoretical conversion ratio (Eq. 3), demonstrating the conversion occurs according to the stoichiometry given in Eq. 3. The mole ratio of butanol to butyric acid reached 2.04 with the exogenous supply of 7 g/L butyric acid, which is higher than 1.16 with exogenous supply of 14 g/L butyric acid (Table 8.1).

In addition, the adaption stage for cell growth and the end production was also shorter compared to the control, which all indicated that exogenous butyric acid can somewhat relief

CO toxicity for acetogens and thus allow these acetogens to use the existing butyric acid to produce butanol using CO as reducing power. Besides, with higher exogenous butyric acid concentrations, acetic acid production was somewhat inhibited and, simultaneously, longer adaptation times were observed for butanol production. For instance, the highest acetic acid production with exogenous supply of 3.2 and 7.0 g/L HBU is both 1.8 fold higher (7.1 and 6.9 g/L) than with 14 g/L HBU (3.9 g/L) (Fig. 8.3b, d, Table 8.1).

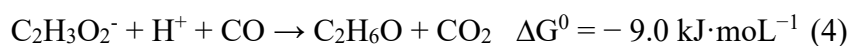
8.4.2 The presence of acetate and ethanol favored butanol production from butyric acid using CO as reducing power

This study showed that the presence of acetic acid and ethanol played a positive role in accelerating butanol conversion from exogenous butyric acid. In the HAc+EtOH+HBU experiment, the butanol yield and butyric acid conversion efficiency reached 100% and 76.2% , respectively, which were both higher than in the HBU experiment (Table 8.1). However, seldom studies have investigated the role of exogenous acetate and ethanol on butanol production using CO as gaseous substrate, except a few studies on exogenous butyric acid production by pure strains (Luo et al., 2015; Xu et al., 2020). Isom et al. (2015) conducted conversion efficiency studies of butyric acid to butanol, reaching 100% with *Clostridium ragsdalei*. In that study, the reduction was independent of growth in an optimized medium with headspace CO gas exchange every 48 h and with a gas pressure of 207 kPa. Perez et al. (2013) investigated exogenous 15 mM (1.32 g/L) butyric acid addition on butanol production by *C. ljungdahlii* ERI-2 using syngas, CO/H₂/CO₂ (60/35/5, v/v/v), and reached 13.3 mM (0.99 g/L) *n*-butanol and 91% of the theoretical yield from butyric acid. Liu et al. (2014b) reported 74.7% butyric acid conversion to *n*-butanol by a mixed culture of *Alkalibaculum bacchi* strain CP15 and *Clostridium propionicum* and obtained 0.8 g/L butanol with 1.5 g/L exogenous butyric acid, using syngas (CO/CO₂/H₂, 40/30/30, v/v) as gaseous substrate.

Both the butanol and ethanol concentration decreases were observed during the fermentation process when the gas pressure decreased below 1.3 bar (Fig. 8.2). This was induced by the production and accumulation of CO₂ during CO consumption (Eq. 1, 2). More CO₂ dissolved into the medium than CO due to its higher solubility, which further caused a decrease in gas pressure. Butanol and ethanol oxidation occurred in the presence of CO₂ according to our previous tests using the same inoculum as used in this study (He et al., 2022a). Besides, the reverse reaction of alcohols to acids has (sometimes) also been observed (Arslan et al., 2019). It seems that ethanol and butanol production, or reversely, oxidation, are regulated by, respectively, the CO and CO₂ concentration. Indeed, when CO was added at the beginning

of each CO addition (1.8 bar) and CO₂ was removed at the same time, alcohol production was favored (Fig. 8.2). The increased CO pressure may play a positive role inducing solventogenesis. For instance, increasing the CO pressure to 2 bar in the last two CO additions of the exogenous HAc+EtOH+HBu experiment, induced a higher ethanol production (Fig. 8.2b).

It was noted that a longer adaption time was required in the control bottle compared to the bottles with acids and ethanol addition. This might be because the added acetic acid, ethanol and butyric acid can act as carbon sources and thus somewhat relieve the possible toxicity caused by CO at a pressure as high as 1.8 bar. The mole ratios of ethanol production to acetic acid consumption are all close to 1, which is conform the theoretical mole ratio of the WLP (Fig. 8.3a, Eq. 4):



8.4.3 CO triggered butanol production from endogenous butyric acid produced from glucose with no significant microbial community change

This study showed that endogenous butyric acid was successfully produced from glucose and CO addition triggered butanol production from the existing endogenous butyric acid (Fig. 8.4) and the mole ratio of butanol production to butyric acid consumption was close to 1 (Eq. 3). Publications on exogenous acids addition for enhanced alcohol production are rather scarce. The highest butanol production reached 0.5 g/L with *Alkalibaculum bacchi* strain CP15, and it was further enhanced to 0.8 g/L with *Clostridium propionicum* using syngas CO/CO₂/H₂ (40/30/30, v/v/v) as the substrate (Liu et al., 2014b). This study promoted ‘syngas-aided’ alcohol production, i.e. enhancing butanol and longer chain alcohol production by taking advantage of the CO reducing power in triggering alcohol production with exogenous acids or acids produced from waste organic compounds.

The microbial community does not show large differences in (G+N)₁ and (G+N)₂ in terms of *Clostridia* and *Bacilli* classes. The *Oscillibacter* genus, belonging to the *Clostridia* class, was enriched at the end of the incubation ((G+N)₂) and has been observed to be involved in acidogenesis during dark fermentation (Goud et al., 2017). It was surprising that *Clostridium carboxidivorans*, known as one of the autotrophic CO-converting acetogens, was enriched in (G+N)₁, while its abundance decreased compared to the inoculum (Table 8.3). *C. carboxidivorans* can grow with glucose to produce formic, acetic, butyric and hexanoic acids at a relatively high pH of 6.2, while a low pH did not favour alcohol production (Fernández-Naveira et al., 2017b). *Clostridium butyricum* can produce acetate and butyrate using glucose

as the substrate and has also been shown to produce H₂ (Crabbendam et al., 1985; Jiang et al., 2016). The heterotrophic *Clostridium butyricum* species was enriched when glucose was totally consumed. However, thereafter, when CO was used as the substrate, the relative abundance of *Clostridium butyricum* decreased, while observing the enrichment of autotrophic acetogens such as *C. ljungdahlii*, *C. autoethanogenum*, *Clostridium sp.* W14A and *Clostridium ragsdalei*, which increased again using CO as the substrate (Table 8.3).

8.4.4 Glucose and CO co-fermentation enhanced butyric acid but not butanol production

Interestingly, butanol was insignificantly produced in glucose and CO co-fermentation, although butyric acid accumulated and reached 50.3 mmol·L⁻¹ C, which is even slightly higher than the highest butyric acid concentration (42.9 mmol·L⁻¹ C) reached with only glucose (Fig. 8.6, Table 8.2). In other words, different ways of adding CO may lead to different butanol concentrations: observing almost 2.4 fold more butanol (26.6 compared to 11.1 mmol·L⁻¹ C) when adding CO after endogenous butyric acid than initially adding CO (CO and glucose co-fermentation) under pH both controlled at 5.8-6.0. Co-fermentations of CO or syngas with glucose has only been reported with few pure cultures as mentioned above, e.g. *C. carboxidivorans* (Fernández-Naveira, et al. 2017b). It was supposed that in Glucose+N₂, when the sole carbon source (glucose) was consumed along with acids produced, another inorganic carbon source (CO) addition, stimulated autotrophic acetogens converted butyric acid to butanol due to its reductant role (Fig. 8.5). This is similar with the exogenous butyric acid experiments, butyric acid was first consumed and converted to butanol using CO as reducing power by enriched sludge, earlier than acetic acid production from CO (Fig. 8.2b, c, Fig. 8.3). In G+C, CO acted more as the carbon source instead of reducing power, resulted in higher acetic acid production.

The presence of CO decreased the glucose consumption rate with only half of the initial amount of glucose consumed after 58 h, when glucose was totally consumed in Glucose+N₂ (Fig. 8.6a). Secondly, both acetic acid and propionic acid concentrations were much higher compared to Glucose+N₂. Hexanoic acid production was inhibited in the Glucose+CO incubation, while its production reached as high as 33 mmol·L⁻¹ C in Glucose+N₂. The highest hexanoic acid production of 31.2 mmol·L⁻¹ C in Glucose+N₂ occupied 18.9% of the initial carbon of 165.9 mmol·L⁻¹ C from 5 g/L glucose (Table 8.2). Although butanol was not efficiently produced, the glucose and CO co-fermentation might provide another possible way for short chain fatty acid production by the enriched sludge with high *Clostridium* spp.

The microbial community in the Glucose + CO incubation did not show large changes compared to Glucose+N₂ (Fig. 8.8). In the Glucose + CO incubation, the abundance of the *Clostridium* genus increased, i.e. the relative abundance of *Clostridium* genus with Glucose + CO (70%) was higher than with Glucose + N₂ (54%) (Fig. 8.8). The relative abundance at the genus level was distributed as follows (Fig. 8.7): *Clostridium* 33%, *Oscillibacter* 8% and *Anaerotignum* 0.1% in (G+C)₁ while *Clostridium* genus 46%, *Oscillibacter* 1% and *Anaerotignum* 7% in (G+N)₁. The *Bacilli* class occupied 29% in G (G+C)₂ and 17% in (G+N)₂. At the *Clostridium* species level, the relative abundance of common autotrophic strains, such as *Clostridium carboxidivorans*, *C. autoethanogenum*, *Clostridium ragsdalei* and *C. ljungdahlii*, did not show much difference (Table 8.3). Liu et al. (2020) investigated the microbial community for 5 g/L glucose and syngas co-fermentation using the inoculum from a mesophilic anaerobic reactor. *Clostridium* spp. was enriched with a low relative abundance, and with the presence of mainly *Clostridium formicoaceticum*. However, butyrate was detected during the syngas and glucose co-fermentation, but not in the solely glucose fermentation and hexanoic acid was not reported in their study.

8.5 Conclusions

The exogenous supply of 3.2 g/L butyric acid resulted in the production of 1.9 g/L butanol, while in the presence of exogenous acetic acid and ethanol, butanol production was enhanced to 2.6 g/L by an enriched sludge with a high abundance of *Clostridium* spp. using CO as the gaseous substrate. The presence of acetate and ethanol enhanced the butyric acid conversion efficiency compared to exogenous butyric acid. When increasing the exogenous butyric acid concentration to 14 g/L, the highest butanol concentration (3.4 g/L) was produced. Butanol accumulation was significantly enhanced up 2.4 fold when adding CO after endogenous butyric acid production from glucose compared to when adding CO initially with glucose (co-fermentation), from which butanol was not efficiently produced with a similar amount of endogenous butyric acid production. The *Clostridia* and *Bacilli* class were dominantly enriched after glucose fermentation and at the end of the incubation. There is no big change in microbial community when comparing the end enriched sludge in Glucose+CO and Glucose + N₂.

8.6 References

Baleeiro, F. C., Kleinstaubler, S., Neumann, A. and Sträuber, H., 2019. Syngas-aided anaerobic fermentation for medium-chain carboxylate and alcohol production: the case for microbial communities. *Applied Microbiology and Biotechnology*, 103 (6): 8689-8709.

Chakraborty, S., Rene, E. R., Lens, P. N. L., Veiga, M. C. and Kennes, C., 2019. Enrichment of a solventogenic anaerobic sludge converting carbon monoxide and syngas into acids and alcohols. *Bioresource Technology*, 272: 130-136.

Chen, C. K. and Blaschek, H. P., 1999. Acetate enhances solvent production and prevents degeneration in *Clostridium beijerinckii* BA101. *Applied Microbiology and Biotechnology*, 52 (2): 170-173.

Cheng, C., Li, W., Lin, M. and Yang, S. T., 2019. Metabolic engineering of *Clostridium carboxidivorans* for enhanced ethanol and butanol production from syngas and glucose. *Bioresource Technology*, 284: 415-423.

Crabbendam, P. M., Neijssel, O. M. and Tempest, D. W., 1985. Metabolic and energetic aspects of the growth of *Clostridium butyricum* on glucose in chemostat culture. *Archives of Microbiology*, 142 (4): 375-382.

Devarapalli M. and Atiyeh H K. 2015. A review of conversion processes for bioethanol production with a focus on syngas fermentation. *Biofuel Research Journal*, 2 (3): 268-280.

Diender, M., Stams, A. and Sousa, D. Z., 2016. Production of medium-chain fatty acids and higher alcohols by a synthetic co-culture grown on carbon monoxide or syngas. *Biotechnology for Biofuels*, 9 (1), 82.

Fernández-Naveira, Á., Abubackar, H. N., Veiga, M.C. and Kennes, C., 2016. Carbon monoxide bioconversion to butanol-ethanol by *Clostridium carboxidivorans*: kinetics and toxicity of alcohols. *Applied Microbiology and Biotechnology*, 100 (9): 4231-4240.

Fernández-Naveira, Á., M.C. and Kennes, C., 2017a. H-B-E (hexanol-butanol-ethanol) fermentation for the production of higher alcohols from syngas/waste gas. *Journal of Chemical Technology and Biotechnology*, 92 (4): 712-731.

Fernández-Naveira, A., Veiga, M. C., Kennes, C., 2017b. Glucose bioconversion profile in the syngas-metabolizing species *Clostridium carboxidivorans*. *Bioresource Technology*, 244: 552-559.

Ganigué, R., Sánchez-Paredes, P., Bañeras, L. and Colprim, J., 2016. Low fermentation pH is a trigger to alcohol production, but a killer to chain elongation. *Frontiers in Microbiology*, 7, 702.

Gao, M., Tashiro, Y., Wang, Q., Sakai, K. and Sonomoto, K., 2016. High acetone–butanol–ethanol production in pH-stat co-feeding of acetate and glucose. *Journal of Bioscience and Bioengineering*, 122 (2): 176–182.

Goud, R. K., Arunasri, K., Yeruva, D. K., Krishna, K.V., Dahiya, S. and Mohan, S.V., 2017. Impact of selectively enriched microbial communities on long-term fermentative biohydrogen production. *Bioresource Technology*, 242: 253-264.

He, Y., Cassarini, C., Marciano, F. and Lens, P. N. L., 2020. Homoacetogenesis and solventogenesis from H₂/CO₂ by granular sludge at 25, 37 and 55°C. *Chemosphere*, 265: 128649.

He Y., Lens, P. N. L., Veiga, M. C. and Kennes, C. 2022. Selective butanol production from carbon monoxide by an enriched anaerobic culture. *Science of the Total Environment*, 806, 150579.

He Y., Lens, P. N. L., Veiga, M. C. and Kennes, C. 2021. Enhanced ethanol production from carbon monoxide by enriched *Clostridium* bacteria. *Frontiers in Microbiology* 754713.

Isom, Catherine E., Mark A. Nanny, and Ralph S. Tanner. 2015. Improved conversion efficiencies for n-fatty acid reduction to primary alcohols by the solventogenic acetogen *Clostridium ragsdalei*. *Journal of Industrial Microbiology & Biotechnology*, 42 (1): 29-38.

Jiang, D., Fang Z., Chin S. X., Tian, X. F. and Su T. C., 2016. Biohydrogen production from hydrolysates of selected tropical biomass wastes with *Clostridium butyricum*. *Scientific Reports*, 6 (1): 27205.

Jing, Y. , Campanaro, S. , Kougias, P. , Treu, L. , Angelidaki, I. and Zhang, S. , Luo G. 2017. Anaerobic granular sludge for simultaneous biomethanation of synthetic wastewater and co with focus on the identification of co-converting microorganisms. *Water Research*, 126, 19-28.

Knoshaug, E.P., Zhang, M., 2009. Butanol tolerance in a selection of microorganisms. *Applied Biochemistry and Biotechnology*, 153: 13–20.

Lee, S.Y., Park, J. H., Jang, S. H., Nielsen, L. K., Kim, J., Jung, K. S., 2008. Fermentative butanol production by *Clostridia*. *Biotechnology and Bioengineering* 101: 209–228.

Liu, C., Wang, W., O-Thong, S., Yang, Z., Zhang, S., Liu, G. and Luo, G., 2020. Microbial insights of enhanced anaerobic conversion of syngas into volatile fatty acids by co-fermentation with carbohydrate-rich synthetic wastewater. *Biotechnology for Biofuels*. 13 (1): 53.

Liu, K., Atiyeh, H. K., Stevenson, B. S., Tanner, R. S., Wilkins, M. R. and Huhnke, R. L., 2014a. Mixed culture syngas fermentation and conversion of carboxylic acids into alcohols. *Bioresource Technology*, 152: 337-346.

Liu, K., Atiyeh, H. K., Stevenson, B. S., Tanner, R. S., Wilkins, M. R. and Huhnke, R. L., 2014b. Continuous syngas fermentation for the production of ethanol, n-propanol and n-butanol. *Bioresource Technology*, 151: 69-77.

Liu, Y., Wan, J., Han, S., Zhang, S. and Luo, G. 2016. Selective conversion of carbon monoxide to hydrogen by anaerobic mixed culture. *Bioresource Technology*, 202:1-7.

Luo, H., Ge, L., Zhang, J., Zhao, Y., Jian, D., Li, Z., He, Z., Chen, R. and Shi, Z., 2015. Enhancing butanol production under the stress environments of co-culturing *Clostridium acetobutylicum*/*Saccharomyces cerevisiae* integrated with exogenous butyrate addition. *PLoS One* 10 (10): e0141160.

Luo, H., Zeng, Q., Han, S., Wang, Z., Dong, Q., Bi, Y. and Zhao, Y., 2017. High-efficient n-butanol production by co-culturing *Clostridium acetobutylicum* and *Saccharomyces cerevisiae* integrated with butyrate fermentative supernatant addition. *World Journal of Microbiology & Biotechnology*, 33(4):76.

Mohammadi, M., Najafpour, G. D., Younesi, H., Lahijani, P., Uzir, M. H. and Mohamed, A. R., 2011. Bioconversion of synthesis gas to second generation biofuels: a review. *Renewable & Sustainable Energy Reviews*, 15 (9): 4255-4273.

Mock, J. , Zheng, Y. , Mueller, A. P. , Ly, S. and Thauer, R. K., 2015. Energy conservation associated with ethanol formation from H₂ and CO₂ in *Clostridium autoethanogenum* involving electron bifurcation. *Journal of Bacteriology*, 197 (18): 2965-2980.

Munch, G., Mittler, J. and Rehmann, L., 2020. Increased selectivity for butanol in *Clostridium pasteurianum* fermentations via butyric acid addition or dual feedstock strategy. *Fermentation* 6 (3):67.

Perez, J. M., Richter, H., Loftus, S. E. and Angenent, L. T., 2013. Biocatalytic reduction of short-chain carboxylic acids into their corresponding alcohols with syngas fermentation. *Biotechnology and Bioengineering*, 110 (4): 1066-1077.

Teixeira, L. V., Moutinho, L. F. and Romão-Dumaresq, A. S. 2018. Gas fermentation of C₁ feedstocks: commercialization status and future prospects. *Biofuels, Bioproducts and Biorefining*, 12 (6): 1103-1117.

Worden, R. M., Grethlein, A. J., Jain, M. K. and Datta, R., 1991. Production of butanol and ethanol from synthesis gas via fermentation. *Fuel*, 70 (5):615-619.

Xu, H., Liang, C., Chen, X., Xu, J., Yu, Q., Zhang, Y. and Yuan, Z. 2020. Impact of exogenous acetate on ethanol formation and gene transcription for key enzymes in *Clostridium autoethanogenum* grown on CO. *Biochemical Engineering Journal*, 155: 107470.

Yu, J., Liu, J., Jiang, W., Yang, Y. and Sheng, Y., 2015. Current status and prospects of industrial bio-production of n-butanol in China. *Biotechnology Advances*, 33 (7): 1493-1501.

Zhu, H. F. , Liu, Z. Y. , X Zhou, Yi, J. H. and Li, F. L., 2020. Energy conservation and carbon flux distribution during fermentation of CO or H₂/CO₂ by *Clostridium ljungdahlii*. *Frontiers in Microbiology*, 11.

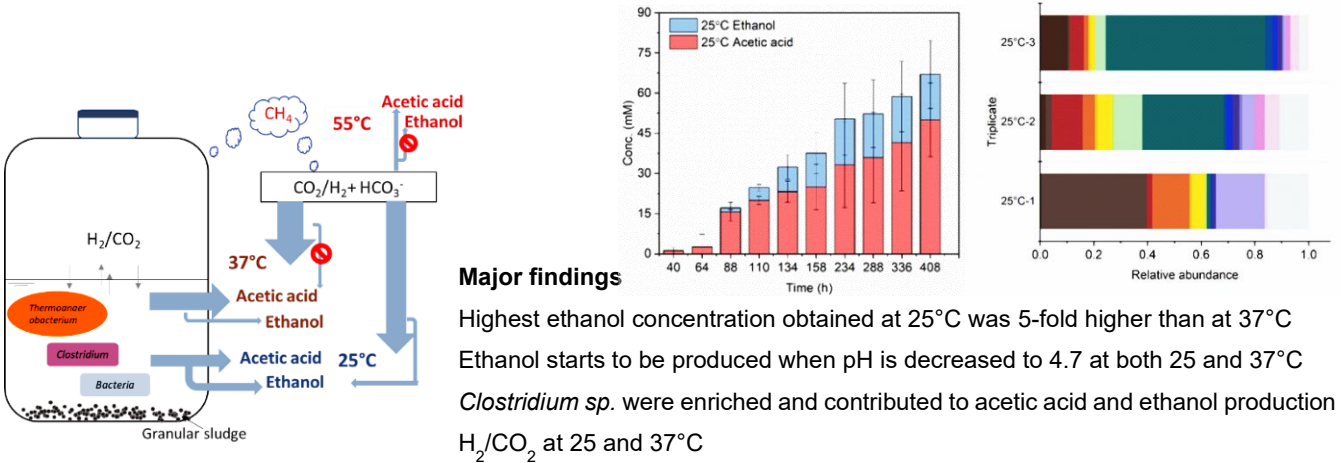
Chapter 9 General Discussion and Future Perspectives

9.1 General discussion

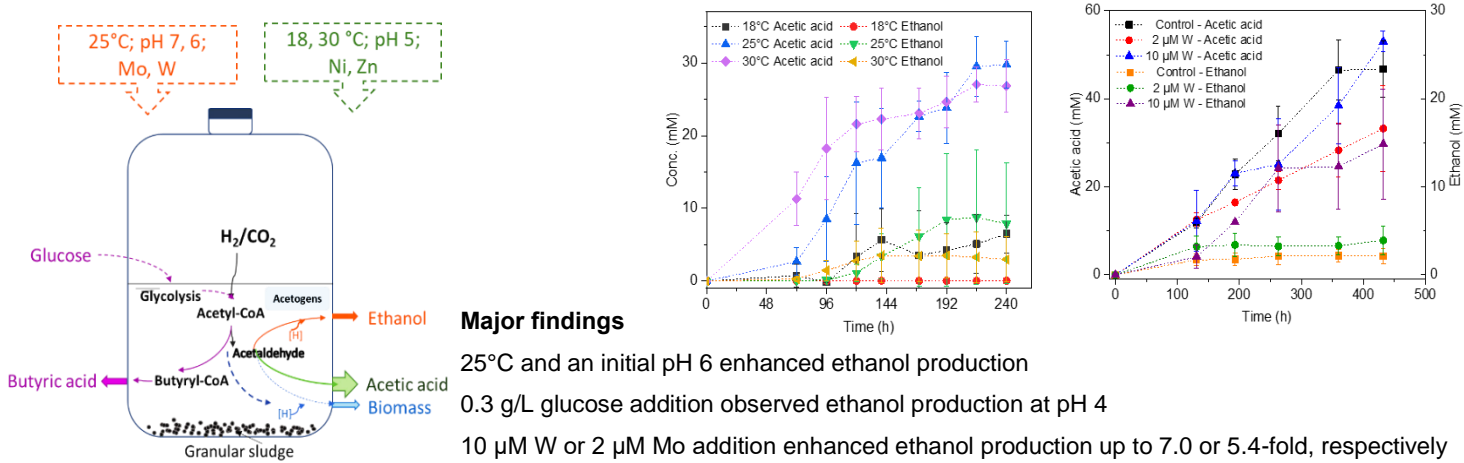
Syngas (CO, H₂ and CO₂) bioconversion for biofuel production, such as ethanol and butanol by acetogens, either directly or indirectly, simultaneously mitigates carbon emissions and generates valuable bioenergy products (Devarapalli and Atiyeh, 2015). Syngas bioconversion for solvent production has been paid increased attention in the last decades ever since the isolation of the first syngas conversion acetogen in 1990s (Abrini et al., 1994; Phillips et al., 1993). Studies on bioconversion of CO, the main syngas compound, for solvent production are rare, except for a few *Clostridium* strains (Fernández-Naveira et al., 2017). Syngas bioconversion to ethanol and butanol production raised limited interest till now, especially by mixed cultures (Chakraborty et al., 2019). The low concentration of ethanol and butanol production from syngas conversion remained a problem (Sun et al., 2019). Considering these challenges and limitations, the current research bridged the gap between the enhanced ethanol and butanol production, the process parameters and the enrichment of *Clostridium* bacteria using syngas/CO as the carbon source from anaerobic sludge.

Considering various factors influencing syngas fermentation, **chapter 2** reviewed the solventogenesis factors during the syngas fermentation. Low temperature, low pH, trace metal tungsten, yeast extract, biochar and nanoparticles have been reported to play a positive role for ethanol and butanol production by pure cultures, co-cultures and undefined mixed cultures. Temperature, C/H ratio, pH and trace metals have been considered in **chapters 3 and 4**. A fed batch gas fed reactor has been set-up in the CO bioconversion to ethanol and butanol production in **chapters 6, 7 and 8**. High and selective butanol production from CO by anaerobic sludge has been obtained in **chapter 6**. Furthermore, exogenous and endogenous butyric acid on enhanced butanol production has been demonstrated using CO as reducing power in **chapter 8**. The enrichment of CO converting solventogenic acetogens with high amount of *Clostridium spp.* has been achieved in **chapter 7**. The major findings from individual chapters of this PhD are shown in **Fig. 9.1 and Fig. 9.2**. **Fig. 9.3** outlines the link of these findings from **chapter 3** to **chapter 8**.

A. Homoacetogenesis and solventogenesis from H_2/CO_2 by granular sludge at 25, 37 and 55°C (Chapter 3)



B. Bioethanol production from H_2/CO_2 by solventogenesis using anaerobic granular sludge: effect of process parameters (Chapter 4)



C. Enrichment of homoacetogens converting H_2/CO_2 into acids and ethanol in bioreactor (Chapter 5)

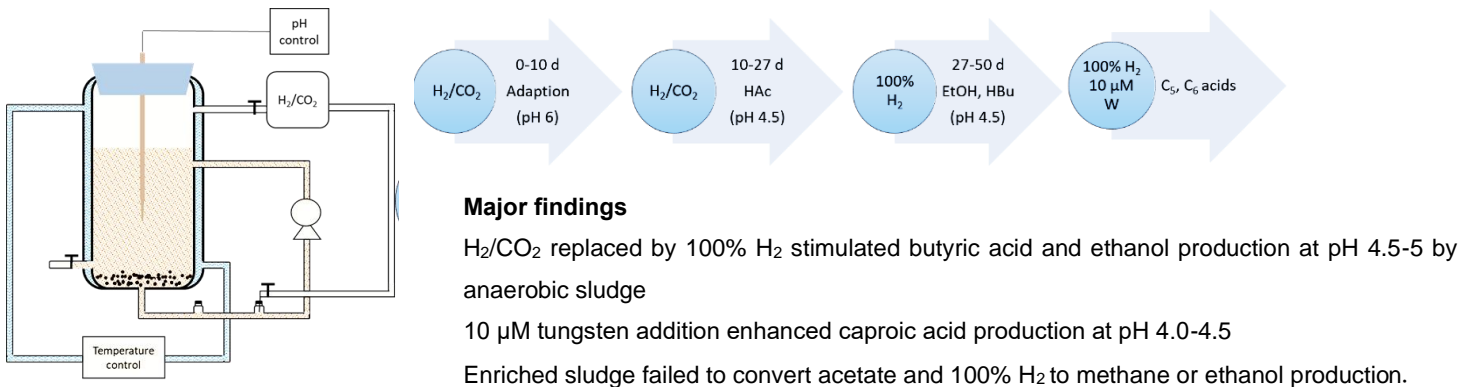
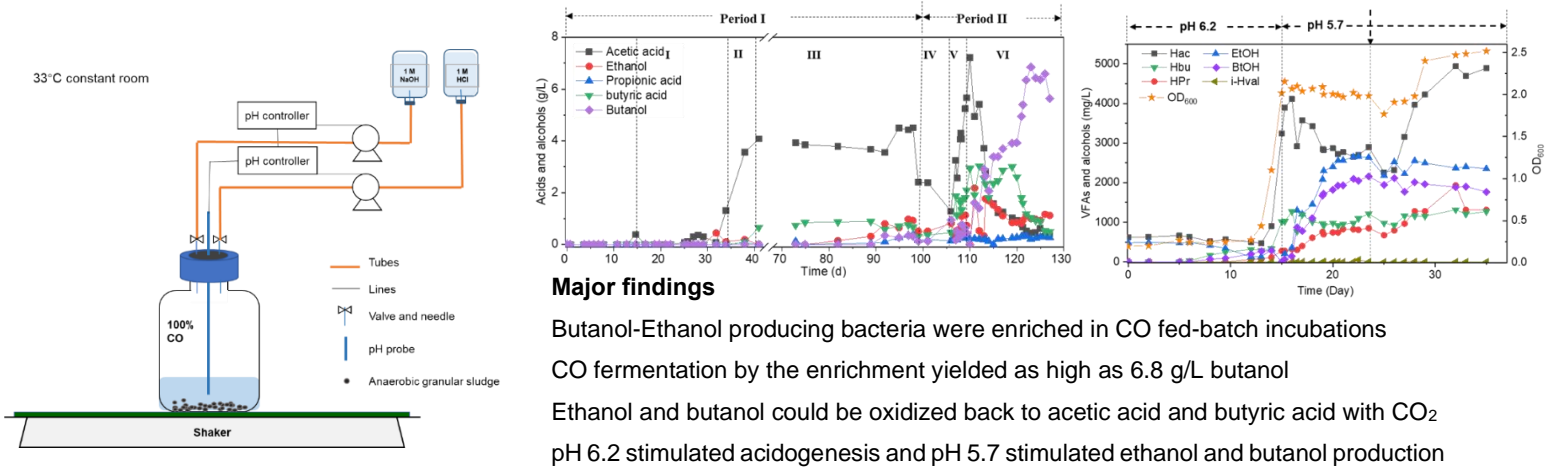
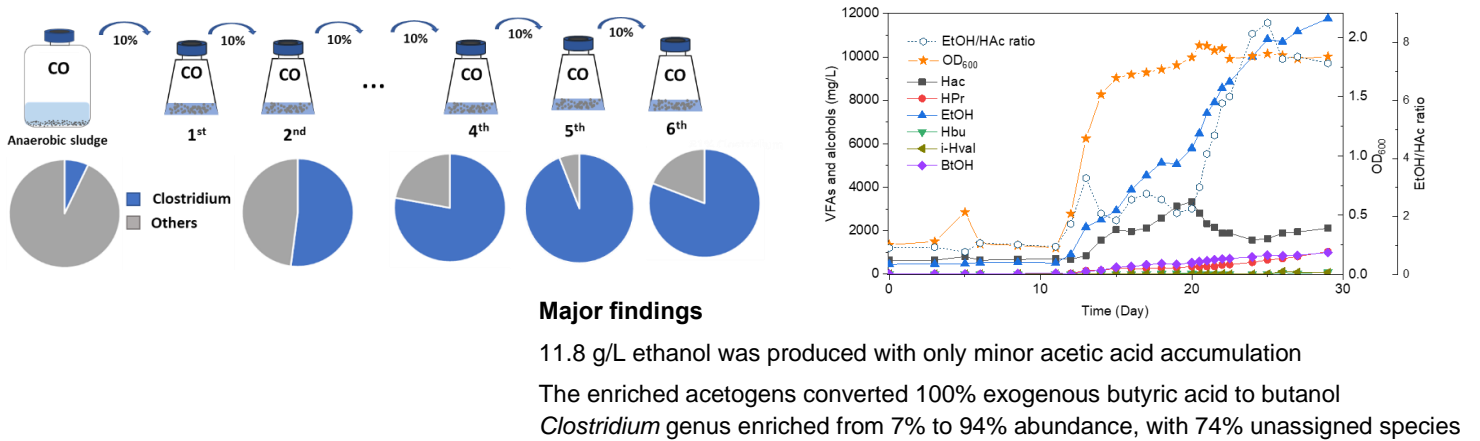


Fig. 9.1 Integrated process parameters for bioethanol production from H_2/CO_2 using anaerobic granular sludge of a) chapter 3, chapter 4 and c) chapter 5.

A. Selective butanol production from carbon monoxide by an enriched anaerobic culture (Chapter 6)



B. Enhanced ethanol production from carbon monoxide by enriched *Clostridium* bacteria (Chapter 7)



C. Influence of acetate, butyrate and ethanol on butanol production using CO as gaseous substrate (Chapter 8)

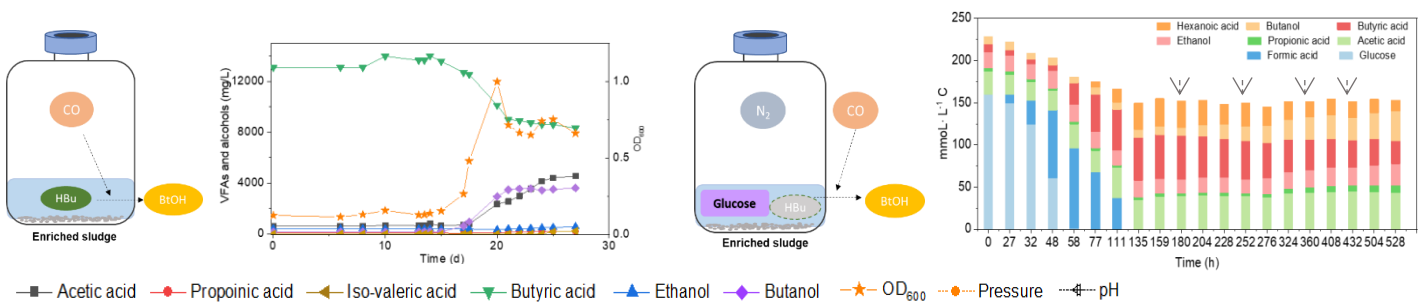


Fig. 9.2 Overview of CO fermentation for ethanol and butanol production and enrichment of CO converting *Clostridium* bacteria present in anaerobic granular sludge in a) chapter 6, b) chapter 7 and c) chapter 8.

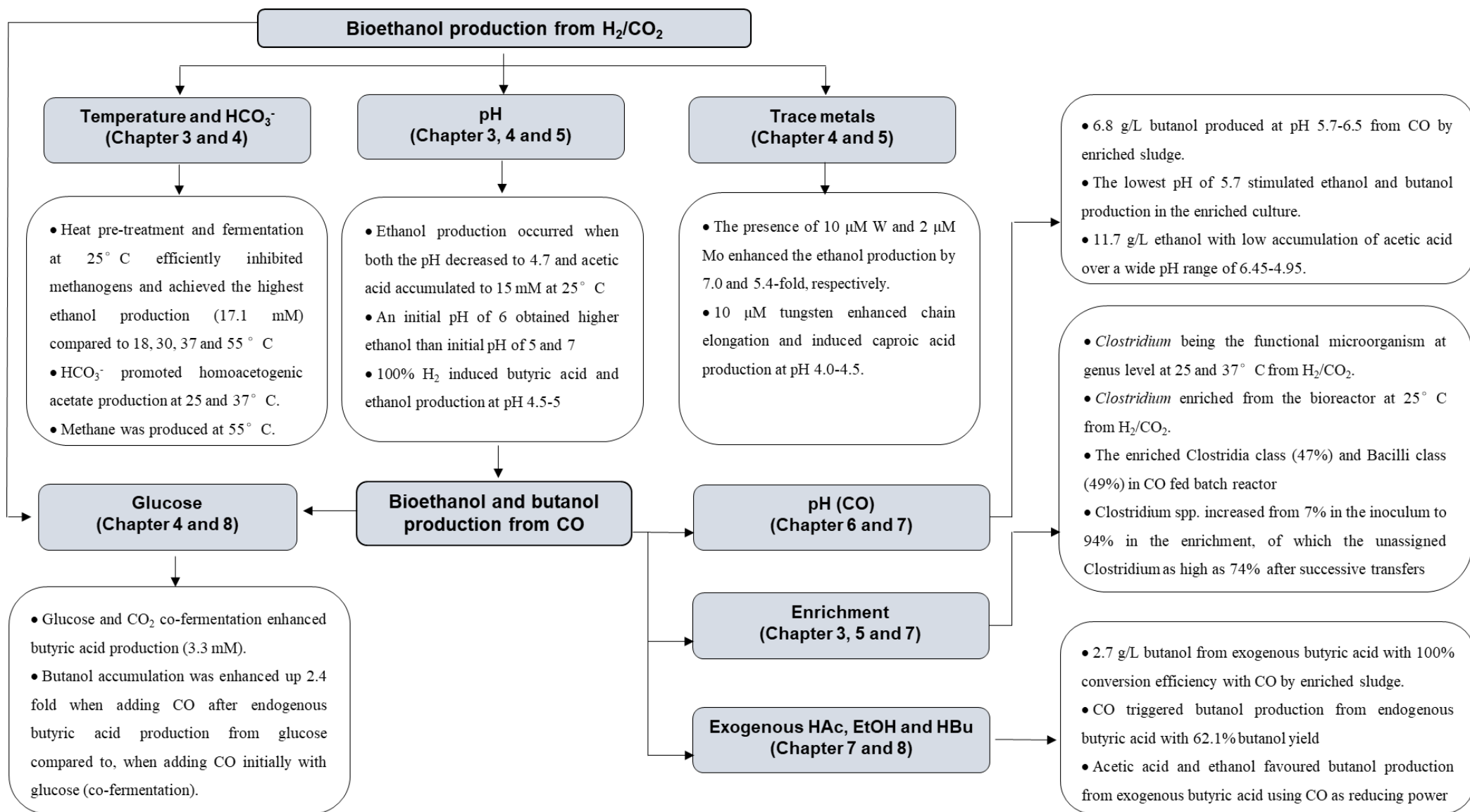


Fig. 9.3 Summary of the major findings of this PhD research

9.1.1 Ethanol production from H₂/CO₂ by mixed cultures

In **chapter 3 and 4**, granular sludge from an industrial wastewater treatment plant was tested as inoculum for ethanol production from H₂/CO₂ via non-phototrophic fermentation at various environmental conditions. **Chapter 3** obtained the highest ethanol concentration (17.11 mM) at 25°C and was 5-fold higher than at 37°C (3.36 mM). This was attributed to the fact that the undissociated acid (non-ionized acetic acid) accumulation rate constant (0.145 h⁻¹) was 1.39 fold higher than at 25°C (0.104 h⁻¹). Ethanol production was linked to acetic acid production with the highest ethanol to acetic acid ratio of 0.514 at 25°C. The addition of bicarbonate inhibited ethanol production both at 25°C and 37°C. Methane was mainly produced at 55°C, while neither acetic acid nor ethanol were formed.

Based on the enhanced ethanol production at submesophilic condition in **chapter 3**, **chapter 4** further demonstrated the highest acetic acid and ethanol production was obtained at 25°C compared to 18 and 30°C with a final concentration of 29.7 and 8.8 mM, respectively. The presence of bicarbonate enhanced acetic acid production 3.0 ~ 4.1-fold, while inhibiting ethanol production and the inhibition of bicarbonate on ethanol production was also observed at 25 and 37°C in **chapter 3**. Chapter 4 showed 0.3 g/L glucose addition induced butyric acid production (3.7 mM), while 5.7 mM ethanol was produced at the end of the incubation at pH 4 in the presence of glucose. Concerning the trace metals, **chapter 4** revealed that 10 μM W addition enhanced ethanol production up to 3.8 and 7.0-fold compared to, respectively, 2 μM W addition and the control. 2 μM Mo addition enhanced ethanol production up to 8.1-fold and 5.4-fold compared to, respectively, 10 μM Mo and the control, which demonstrated ethanol production from H₂/CO₂ conversion using granular sludge as the inoculum can be optimized by selecting the operational temperature and by trace metal addition.

The pH was found to act as an important factor influencing ethanol production from H₂/CO₂ and ethanol and butanol production from CO: a low pH 4.5-5 has been demonstrated to stimulate solventogenesis in **chapters 3, 4 and 5**. **Chapter 3** concluded that ethanol production occurred when both the pH decreased to 4.7 and acetic acid accumulated to 15 mM at 25°C. **Chapter 4** demonstrated an initial pH of 6 obtained higher ethanol concentrations than an initial pH of 5 and 7. **Chapter 5** showed 100% H₂ induced butyric acid and ethanol production at pH 4.5-5.

9.1.2 Enhancement and selective butanol production from CO by anaerobic sludge

Chapters 6, 7 and 8 conducted solventogenic carbon monoxide (CO) fermentation using the same anaerobic sludge and the initial gas pressure of 1.8 bar as in **chapters 3, 4 and 5**. **Chapter 6** operated a CO gas fed batch reactor (FB1) and obtained an anaerobic mixed culture that produced unusual high concentrations of 6.8 g/L butanol at pH 5.7-6.4 (**Fig. 9.2**). At a later pH-controlled CO fed batch reactor (FB2) in **chapter 6**, acetic acid and butyric acid were produced at pH 6.2 and ethanol and butanol were stimulated when the pH decreased to 5.7 (**Fig. 9.2**). **Chapter 7** obtained the highest ethanol concentration of 11.8 g/L with minor accumulation of acetic acid from CO over a wide pH range of 6.45 to 4.95 by the enriched *Clostridium* bacteria (**Fig. 9.2**).

9.1.3 Enrichment of solventogenic acetogens from CO

The enriched sludge obtained in FB1 was diverse in *Clostridia* and *Bacilli* classes, with the relative abundance of unassigned *Clostridium* amounting to 27%, containing known solventogens, e.g. *C. ljungdhalii*, *C. ragsdalei* and *C. coskatii* (**chapter 6**). **Chapter 7** enriched CO metabolizing *Clostridium* spp. from the enriched sludge taken from the FB1 in **chapter 6**. **Chapter 7** enriched as high as 94% relative abundance of *Clostridium* spp. (from 7% in the inoculum) after six successive biomass transfers. The enriched *Clostridium* spp. were able to convert exogenous butyric acid (3.2 g/L) into butanol with nearly 100% conversion efficiency using CO as reducing power, which illustrated the strategy, i.e. exogenous butyric acid supply, for enhanced butanol production in **chapter 8**. The enriched *Clostridium* population also converted glucose to formic, acetic, propionic, and butyric acids in batch tests with daily pH adjustment to pH 6.0. Unassigned *Clostridium* species showed a very high relative abundance, reaching 73% of the *Clostridium* genus in the enriched sludge (6th transfer). The genes at *Clostridium* genus level showed only 7 special genes existed in the 6th transfer compared to the common genes shared among the transfers. Similarly, during the H₂/CO₂ bioconversion in **chapters 3, 4 and 5**, *Clostridium* sp. were the prevalent species at both 25 and 37°C at the end of the incubation, which possibly contributed to the ethanol production.

9.1.4 Enhancement strategies for butanol production by exogenous butyric acid

The enriched sludge with high *Clostridium* spp. showed a high butanol production potential in **chapter 7**. Therefore, **chapter 8** investigated different exogenous butyric acid concentrations on butanol production using the enrichment as inoculum. **Chapter 8** obtained the highest butanol concentration of 3.4 g/L with 14 g/L exogenous butyric acid, which is the

highest butanol concentration fermented from CO/syngas reported in the literature so far. Exogenous acetate and ethanol did not efficiently stimulate butyric acid accumulation although butanol was observed to increase and reached 1.9 g/L at the end of the incubation. However, the presence of acetic acid and ethanol favoured butanol production from exogenous butyric acid by the enriched sludge and enhanced the butanol production to 2.6 g/L. CO addition triggered butanol production from the endogenous butyric acid (from glucose) with a conversion efficiency as high as 58.6% and a 62.1% butanol yield in Glucose+N₂. However, butanol production was not efficiently produced by glucose and CO co-fermentation (Glucose+CO), although a similar amount of endogenous butyric acid was produced compared to Glucose+N₂. The *Clostridium* genus occupied as high as 82% from the initial inoculum, while the *Clostridia* and *Bacilli* class were both enriched and dominated in the Glucose +N₂ and Glucose +CO incubations. This study demonstrated the possible strategy for enhancing butanol production via exogenous butyric acid supply, or endogenously from sugar fermentation such as from wastewaters containing low sugar concentrations.

9.2 Future perspectives

Solventogenic syngas fermentation has been paid increased attention only since the last decade compared to the traditional sugar fermentation with hundred's years of research history. Hence, it is an emerging sustainable biotechnology for biofuel production. The fundamental understanding of the fermentation process for enhanced solvent production still has many undiscovered aspects, such as i) microbial resource management linked with efficient biocatalysis for enhanced ethanol and butanol production, in both pure and mixed cultures and ii) reactor design, mass transfer, production of longer chain solvents and other valuable chemicals production as well as solvent separation. These can be applied in the biorefinery concept and apply it to secondary feedstocks, e.g., gasification of agriculture waste and the organic fraction of municipal solid waste.

9.2.1 Microbial resource management

Baleeiro et al. (2019) raised 'syngas-aided' fermentation, which combines syngas and microorganisms together for valuable chemicals including butanol production. Despite the limited widely studied strains, the application of syngas fermentation in pilot plants has been set up such as the fermentation process developed by Lanza Tech for ethanol production from steel mill gas by a patented *Clostridium* strain (Yu et al., 2015), however, mixed cultures have not raised much attention. This study enriched *Clostridium spp.* that can produce high ethanol

concentrations with low acetic acid accumulation at a wide pH range of 4.95-6.45, which illustrated the merits of resistance to environmental conditions of mixed cultures compared to pure strains. The enrichment of syngas fermentation solventogenic acetogens, especially on CO, as demonstrated in chapter 7, showed advantage with less contamination problems such as methanogens compared to H₂/CO₂ due to the high CO toxicity.

9.2.2 Reactor design

9.2.2.1 Continuous stirred tank reactors (CSTR)

The continuous stirred tank reactor (CSTR) has been widely studied for syngas biotransformation to solvents at lab scale (Arslan et al., 2019; Mohammadi et al. 2012; Riggs and Heindel 2006). The stir agitation accelerates large bubbles breaking into small ones hence improving the gas-liquid mass transfer rate. The shift of high pH of 6 and low pH 4.8 in the CSTR has been shown an efficient way to enhance ethanol production without acid accumulation (Abubackar et al. 2015). However, this approach is not economically feasible for scale production because high agitation rates consume high amounts of energy (Shen et al. 2014a, 2014b).

9.2.2.2 Bubble column

A bubble column reactor without agitation but combined with a microbubble diffusion could highly enhance the mass transfer rate (Datar et al. 2004). The gas is injected and distributed through the bottom by gas sparging thus good mixing can be achieved while avoiding high shear rates that might inhibit or damage microbial cells. A bubble column reactor can be used as second stage solvent fermentation with high cell concentrations reached in the first stage CSTR (Richter et al., 2013).

9.2.2.3 Biotrickling filter

A biotrickling filter or trickle bed reactor equipped with a packed bed and the liquid media flowing down while the gas could move either downward or upward (Cassarini et al., 2017). The packed bed acts as the solid catalyst for gas-liquid interactions and the packing material (He et al., 2018). The power consumption of trickle bed reactors is lower than that of CSTR and some studies also found that trickle bed reactors showed a higher efficiency than bubble columns and CSTR (Cowger et al. 1992).

9.2.2.4 Novel bioreactor designs

The fact that the low water solubility of CO limits the mass transfer rate between the gas and liquid phase and thus low achievable cell density in fermentation media. To avoid this, membrane systems (Jin et al., 2008), attached growth bioreactors (Shen et al., 2014a, 2014b)

and microbubble spargers in suspended-growth bioreactors (Muroyama et al., 2013) allowed more efficient transfer rates.

9.2.3 Mass transfer

Except the process factors investigated in this study, such as temperature, pH, trace metals and C/H ratio in H₂/CO₂ conversion, some other equivalent important factors such as syngas composition, gas pressure, addition of materials that influence the mass transfer rate can further improve the solventogenic yield from CO. Mass transfer is one of the major differences between syngas fermentation and traditional sugar fermentation. Next to the difference in metabolic pathway, the gaseous substrate, especially the low solubility of CO and H₂, alter the alcohol production process design.

9.2.3.1 Added materials

To overcome the low solubility and enhance mass transfer rate, additional materials such as biochar and nanoparticles have been studied very recently (Sun et al., 2018; Yao et al., 2018).

Biochar produced from biomass pyrolysis gasification with high carbon percentage and porous structure, metals and functional groups has been widely used in soil improvement and as adsorbent (Sun et al., 2018a, 2018b). Syngas production during gasification, simultaneously produced biochar but the property of biochar varies in alkalinity, pH buffer capacity, cation exchange capacity and electrical conductivity (Yao et al., 2018). Due to the different biochar properties, its effect on solventogenesis showed varied results and the nutrients and pH buffering function of biochar reduced acid stress. Enhanced ethanol production was obtained in a medium with poultry litter biochar due to its rich mineral and metal content, while inhibited ethanol production was observed with switchgrass biochar addition to *C. ragsdalei* (Sun et al., 2018a). However, *C. carboxidivorans* entered the solventogenic phase in switchgrass biochar treatment earlier than other biochar treatments, resulting in the accumulation of more ethanol and butanol (Sun et al., 2018b).

With methyl-functionalized silica nanoparticles, ethanol production from 0.115 g/L enhanced to 0.306 g/L by *C. ljungdahlii* using CO, CO₂ and H₂ (v/v/v, 20/20/5) because of the enhanced mass transfer rate by addition of nanoparticles (Kim et al. 2014). They also found that the magnetic nanoparticles (SiO₂-CH₃) increased the dissolved concentrations of CO, CO₂ and H₂ by 224%, 78%, and 143%, respectively and ethanol production from 0.156 g/L increased to 0.354 g/L by *C. ljungdahlii* using CO, CO₂ and H₂ (v/v/v, 20/20/5) as the substrate (Kim et al., 2016).

9.2.3.2 Electron shuttles

Exogenous electron shuttles such as neutral red, methylene blue, methyl viologen and benzyl viologen were used to shift fermentative metabolism towards alcohol production (Steinbusch et al., 2010). Even though the exact mechanism whereby electron shuttles regulate the fermentative pathway is not fully understood but adding them to bacterial cultures is an attractive strategy for shifting the direction of electron flow from generating organic acids to solvents and hydrogen. Yarlagadda et al. (2012) investigated the effect of electron shuttles on the end products using glucose as carbon source by *Clostridium sp.* BC1 and found that methyl viologen enhanced ethanol- and butanol-production by 28- and 12- fold, respectively, due to a shift in the direction of electron flow towards enhanced production of ethanol and butanol by reducing hydrogen production.

9.2.4 Longer chain solvents and other valuable chemicals from CO/CO₂

The enhanced butanol production by endogenous butyric acid from glucose and CO in **chapter 8** implied exogenous acids using CO as the gaseous substrate by mixotrophy and mixed cultures can become a strategy for enhanced longer carbon chain alcohol production. Besides, ATP generation during syngas fermentation is rather limited compared to sugar fermentation, which further limited longer carbon chain alcohol production. Several trials have explored butanol and hexanol production by co-cultures in the literature. In this study, chapter 8 observed an unknown small amount of hexanol from endogenous butyric acid and CO (Fig. 8.5). However, more investigations on the conversion mechanisms should be done, such as how the interspecies electron transfer occurred.

9.2.4.1 Mixotrophy

Autotrophic growth faces the challenges of ATP limitation although via acetogenesis, during which ATP is recovered, the ATP recovery limitation still existed (Maru et al., 2018). ATP limitation induced slow cell growth and low cell densities and not enough energy generation for producing large quantities of metabolites with more than 2 carbons (Fast et al. 2015). One promising way to overcome the ATP limitation can involve another ATP generating process such as glycolysis from sugar fermentation, i.e. mixotrophy. Mixotrophy comprises organic and inorganic (CO, CO₂ and H₂) substrate fermentation by autotrophic acetogens. Meanwhile, the mixotrophy can also be reached by co-cultures of heterotrophic and autotrophic acetogens, such as *C. acetobutylicum* and *C. ljungdahlii* for longer carbon chain alcohol production (Diender et al. 2016).

Mixotrophy enhanced carbon utilization since the released CO₂ during the heterotrophic fermentation can be involved in syngas fermentation by autotrophic acetogens. Simultaneously, cells growth was enhanced due to the excess ATP generation. More importantly, longer carbon chain alcohols (>4) production was achieved via reduction of endogenous long chain fatty acids from heterotrophic fermentation (chapter 8).

The potential application of mixotrophy is to use carbohydrate-rich wastewater and syngas co-fermentation (chapter 8). However, this field has not yet been reported for alcohol production, although it has been used for biohydrogen (Liu et al., 2020a) and volatile fatty acids (Liu et al., 2020b). On the other hand, from toxicity view, longer alcohols showed higher toxicity for cells and could cause the low alcohol production, for example, the IC₅₀ of butanol for *Clostridium carboxidivorans* growth was 14.50 g/L after 48 h and ethanol very close to 35 g/L (Fernández et al. 2016). However, the reported maximum ethanol and butanol concentration are much lower than the toxicity values reported in the literature so far.

9.2.4.2 Exogenous electron acceptors and acids

Solventogenesis required minimum acetic acid production, supplementation of acetate during acidogenesis (Chapter 3). Early solventogenesis was reported to result in a significant increase in acetone–butanol–ethanol production (Gao et al. 2016). Ethanol production was enhanced with exogenous ¹³C-labeled acetate by *C. autoethanogenum* using 100% CO as gaseous substrate and simultaneously *aor* gene CAETHG_0102, *codh* gene CAETHG_3005, *adh* genes CAETHG_1841 and CAETHG_1813 were found to be highly up-regulated at higher acetate levels. Exogenous acetate thus played an important role in solventogenesis (Xu et al., 2020).

Due to the two-stage pathway of syngas fermentation, some studies directly added acids such as acetic acid, expecting higher ethanol production (Perez et al. 2013). Besides, electron acceptors like nitrate have been shown to enhance carbon dioxide fixation by *C. ljungdahlii* (Emerson et al. 2019). 15 mM nitrate supplemented H₂ + CO₂ enhanced the yield of the production of heterologous chemicals such as acetic acid and ethanol by boosting ATP production of *C. ljungdahlii* (Emerson et al., 2019). However, nitrate and nitrite can have a negative effect on both growth and alcohol formation of *Clostridium carboxidivorans* under continuous gas supply (CO/CO₂, 80/20) (Rückel et al., 2021).

9.2.5 Scale-up of syngas fermentation

Two aspects should be considered during syngas fermentation application. For instance, some trace components such as NH₃, H₂S, and NO_x need to be paid attention in steel off gas

and gasification processes. NH_3 and H_2S have been recently reported to have a positive effect on both growth and alcohol formation continuous gas supply (CO/CO_2 , 80/20) (Rückel et al., 2021). Another problem is the increase of the salinity resulting from adjustment of pH by adding HCl or NaOH. Fernández-Naveira et al. (2019) reported the salinity with 9 g/L sodium chloride (NaCl) had a negative effect on bacterial growth and CO consumption while and negative effect on cell growth was observed at concentrations above 15 g/L. The scale-up syngas fermentation process in bioreactors combined with a solvent separation system has been developed (Fig. 9.4). To avoid ethanol accumulation and negative effects on cell growth, a separation section can be added in the fermentation bioreactor, such as by a combination of distillation or vapor permeation membranes (Datta et al. 2009). The driving force of membrane distillation is the partial pressure difference between each side of the membrane pores, whereas the selectivity varies according to the properties of the type of polymer used, the membrane characteristics, and the operation conditions (Hatti-Kaul 2010). The driving force for pervaporation is a low vapor pressure on the permeate side of the membrane generated by cooling and condensing the permeate vapor (Hatti-Kaul 2010). The selectivity of separation depends on the affinity of some specific components of a mixture to the membrane material (Baker 2004).

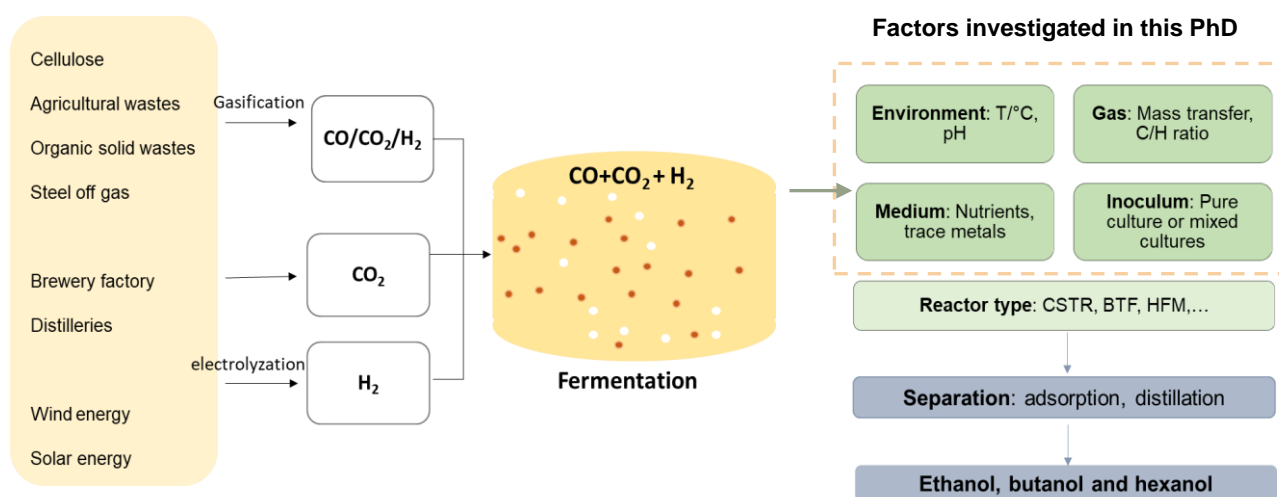


Fig. 9.4 Integrated syngas and CO_2/H_2 bioconversion for ethanol, butanol and hexanol production. CSTR: continuous stirred tank reactor; BTF: Bio-trickling filter; HFM: hollow fiber membrane.

9.3 Conclusions

H_2/CO_2 fermentation for ethanol and CO fermentation to butanol has been comprehensively investigated using anaerobic sludge from wastewater treatment plants. This

PhD dissertation demonstrated the submesophilic temperature, initial pH of 6 and trace metals W and Mo enhanced ethanol production from H₂/CO₂. CO conversion to high and selective butanol production was reached in a CO fed batch reactor by the enriched CO converting sludge. The enriched CO converting acetogens with large *Clostridium* bacterial population showed a high potential for enhanced ethanol and butanol production at a wide pH range (4.95-6.45) using CO as the sole carbon and energy source. Exogenous and endogenous butyric acid enhanced ethanol production using CO as reducing power by the enriched *Clostridium* bacteria. The knowledge gained in this PhD dissertation showed a potential way for enhanced ethanol and butanol production by mixed cultures compared to some widely studied pure *Clostridium* strains. This PhD thesis demonstrated the potential application of solventogenic syngas conversion by mixed cultures for production of ethanol and butanol.

9.4 References

Abrini, J. , Naveau, H. and Nyns, E. J. 1994. *Clostridium autoethanogenum*, sp. nov. an anaerobic bacterium that produces ethanol from carbon monoxide. Archives of Microbiology, 161 (4): 345-351.

Abubackar, H.N., Veiga, M.C. and Kennes, C. 2015. Carbon monoxide fermentation to ethanol by *Clostridium autoethanogenum* in a bioreactor with no accumulation of acetic acid. Bioresource Technology 186: 122-127.

Arslan, K., Bayar, B., Abubackar, H. N., Veiga, M. C. and Kennes, C. 2019. Solventogenesis in *Clostridium acetivum* producing high concentrations of ethanol from syngas. Bioresource Technology 292: 121941.

Baker, R., W. 2004. Overview of membrane science and technology. Membrane Technology and Applications 3: 1-14.

Baleeiro, F. C., Kleinstuber, S., Neumann, A. and Sträuber, H., 2019. Syngas-aided anaerobic fermentation for medium-chain carboxylate and alcohol production: the case for microbial communities. Applied Microbiology and Biotechnology, 103 (6): 8689-8709.

Cassarini, C., Rene, E. R., Bhattarai, S., Esposito, G. and Lens, P. N. L. 2017. Anaerobic oxidation of methane coupled to thiosulfate reduction in a biotrickling filter. Bioresource Technology, S0960852417302730.

Chakraborty, S., Rene, E. R., Lens, P. N. L., Veiga, M. C. and Kennes, C. 2019. Enrichment of a solventogenic anaerobic sludge converting carbon monoxide and syngas into acids and alcohols. Bioresource Technology, 272: 130-136.

Cowger, J. P., Klasson K. T., Ackerson M. D., Clausen, E., and Caddy, J. L. 1992. Mass-transfer and kinetic aspects in continuous bioreactors using *Rhodospirillum rubrum*. *Applied Biochemistry and Biotechnology* 34 (1): 613–24.

Datar, R. P., Shenkman R. M, Cateni, B. G, Huhnke, R. L, Lewis, R. S. 2004. Fermentation of biomass-generated producer gas to ethanol. *Biotechnology and Bioengineering* 86 (5): 587–94.

Datta, R., Rahul B. and Hans E. G. 2009. Ethanol recovery process and apparatus for biological conversion of syngas components to liquid products. U.S. Patent Application 12/036,859.

Devarapalli, M. and Atiyeh, H. K. 2015. A review of conversion processes for bioethanol production with a focus on syngas fermentation. *Biofuel Research Journal*, 2 (3): 268-280.

Diender, M., Stams, A. J. and Sousa, D. Z., 2016. Production of medium-chain fatty acids and higher alcohols by a synthetic co-culture grown on carbon monoxide or syngas. *Biotechnology for Biofuels*, 9 (1): 82.

Emerson, D. F., Woolston, B. M., Liu, N., Donnelly, M., Currie, D. H. and Stephanopoulos, G., 2019. Enhancing hydrogen-dependent growth of and carbon dioxide fixation by *Clostridium ljungdahlii* through nitrate supplementation. *Biotechnology and bioengineering* 116 (2): 294-306.

Fast, A. G., Schmidt, E. D., Jones, S. W. and Tracy, B. P., 2015. Acetogenic mixotrophy: novel options for yield improvement in biofuels and biochemicals production. *Current Opinion in Biotechnology*, 33: 60-72.

Fernández-Naveira, Á., Abubackar, H. N., Veiga, M. C. and Kennes, C., 2016. Carbon monoxide bioconversion to butanol-ethanol by *Clostridium carboxidivorans*: kinetics and toxicity of solvents. *Applied Microbiology and Biotechnology* 100 (9): 4231-4240.

Fernández-Naveira, Á., Veiga, M. C. and Kennes, C., 2017. H-B-E (hexanol-butanol-ethanol) fermentation for the production of higher alcohols from syngas/waste gas. *Journal of Chemical Technology & Biotechnology*, 92 (4): 712-731.

Fernández-Naveira, Á., Veiga, M. C. and Kennes, C. 2019. Effect of salinity on C1-gas fermentation by *Clostridium carboxidivorans* producing acids and alcohols. *ABM Express*, 9: 110.

Gao, M., Tashiro, Y., Wang, Q., Sakai, K. and Sonomoto, K., 2016. High acetone–butanol–ethanol production in pH-stat co-feeding of acetate and glucose. *Journal of Bioscience and Bioengineering*, 122 (2): 176-182.

Hatti-Kaul, R. 2010. Downstream processing in industrial biotechnology. *Industrial Biotechnology: Sustainable Growth and Economic Success*, 279-321.

He, P., Han, W., Shao, L., Lü, F., 2018. One-step production of C₆-C₈ carboxylates by mixed culture solely grown on CO. *Biotechnology for Biofuels* 11, 4.

Jin, Y., Guo, L., Veiga, M. C. and Kennes, C. 2009. Optimization of the treatment of carbon monoxide-polluted air in biofilters. *Chemosphere* 74 (2): 332–337.

Kim, Y. K. and Lee, H., 2016. Use of magnetic nanoparticles to enhance bioethanol production in syngas fermentation. *Bioresource Technology*, 204: 139-144.

Kim, Y. K., Park, S. E., Lee, H. and Yun, J. Y., 2014. Enhancement of bioethanol production in syngas fermentation with *Clostridium ljungdahlii* using nanoparticles. *Bioresource Technology*, 159: 446-450.

Liu, C., Shi, Y., Liu, H., Ma, M., Liu, G., Zhang, R. and Wang, W., 2020a. Insight of co-fermentation of carbon monoxide with carbohydrate-rich wastewater for enhanced hydrogen production: homoacetogenic inhibition and the role of pH. *Journal of Cleaner Production* 267: 122027.

Liu, C., Wang, W., Sompong, O., Yang, Z., Zhang, S., Liu, G. and Luo, G., 2020b. Microbial insights of enhanced anaerobic conversion of syngas into volatile fatty acids by co-fermentation with carbohydrate-rich synthetic wastewater. *Biotechnology for Biofuels* 13 (1): 53.

Maru, B. T., Munasinghe, P. C., Gilary, H., Jones, S. W. and Tracy, B. P., 2018. Fixation of CO₂ and CO on a diverse range of carbohydrates using anaerobic, non-photosynthetic mixotrophy. *FEMS Microbiology Letters*, 365 (8): fny039.

Mohammadi, M., Younesi, H., Najafpour, G. and Mohamed, A. R. 2012. Sustainable ethanol fermentation from synthesis gas by *Clostridium ljungdahlii* in a continuous stirred tank bioreactor. *Journal of Chemical Technology & Biotechnology* 87 (6): 837–843.

Muroyama, K., Imai, K., Oka, Y. and Hayashi, J. 2013. Mass transfer properties in a bubble column associated with micro-bubble dispersions. *Chemical Engineering Science* 100: 464–473.

Perez, J. M., Richter, H., Loftus, S. E. and Angenent, L. T., 2013. Biocatalytic reduction of short-chain carboxylic acids into their corresponding alcohols with syngas fermentation. *Biotechnology and Bioengineering*, 110 (4): 1066-1077.

Phillips, J. R., Klasson, K. T., Clausen, E. C. and Gaddy, J. L. 1993. Biological production of ethanol from coal synthesis gas. *Applied Biochemistry and Biotechnology*, 39 (1): 559-571.

Richter, H., Martin, M. and Angenent, L. 2013. A two-stage continuous fermentation system for conversion of syngas into ethanol. *Energies* 6 (8): 3987–4000.

Riggs, S. S. and Heindel, T. J. 2006. Measuring carbon monoxide gas-liquid mass transfer in a stirred tank reactor for syngas fermentation. *Biotechnology Progress* 22 (3): 903–6.

Rückel, A., Hannemann, J., Maierhofer, C., Fuchs, A. and Weuster-Botz, D., 2021. Studies on syngas fermentation with *Clostridium carboxidivorans* in stirred-tank reactors with defined gas impurities. *Frontiers in Microbiology* 12: 655390.

Shen, Y., Brown R. and Wen Z. 2014a. Enhancing mass transfer and ethanol production in syngas fermentation of *Clostridium carboxidivorans* P7 through a monolithic biofilm reactor. *Applied Energy* 136: 68–76.

Shen, Y., Brown, R., and Wen, Z. 2014b. Syngas fermentation of *Clostridium carboxidivoran* P7 in a hollow fiber membrane biofilm reactor: evaluating the mass transfer coefficient and ethanol production performance. *Biochemical Engineering Journal* 85: 21-29.

Steinbusch, K. J. J. , Hamelers, H. V. M. , Schaap, J. D. , Kampman, C. and Buisman, C. J. N. 2010. Bioelectrochemical ethanol production through mediated acetate reduction by mixed cultures. *Environmental Science & Technology*, 44 (1): 513-517.

Sun, X., Atiyeh, H. K., Huhnke, R. L. and Tanner, R. S. 2019. Syngas fermentation process development for production of biofuels and chemicals: a review. *Bioresource Technology Reports*, 7, 100279.

Sun, X. , Atiyeh, H. K. , Kumar, A. and Zhang, H. 2018a. Enhanced ethanol production by *Clostridium ragsdalei* from syngas by incorporating biochar in the fermentation medium. *Bioresource Technology* 247: 291–301.

Sun, X., Atiyeh, H. K., Ajay, K., Zhang, H. and Tanner, R. S. 2018b. Biochar enhanced ethanol and butanol production by *Clostridium carboxidivorans* from syngas. *Bioresource Technology* 265: 128–138.

Xu, H., Liang, C., Chen, X., Xu, J., Yu, Q., Zhang, Y. and Yuan, Z., 2020. Impact of exogenous acetate on ethanol formation and gene transcription for key enzymes in *Clostridium autoethanogenum* grown on CO. *Biochemical Engineering Journal*, 155: 107470.

Yao, Z., You, S., Ge, T. and Wang, C. H., 2018. Biomass gasification for syngas and biochar co-production: Energy application and economic evaluation. *Applied Energy*, 209: 43-55.

Yarlagadda, V. N., Gupta, A., Dodge, C. J. and Francis, A. J. 2012. Effect of exogenous electron shuttles on growth and fermentative metabolism in *Clostridium sp.* BC1. *Bioresource Technology*, 108: 295-299.

Yu, J., Liu, J., Jiang, W., Yang, Y. and Sheng, Y., 2015. Current status and prospects of industrial bio-production of n-butanol in China. *Biotechnology Advances*, 33 (7): 1493-1501.

Author information

Biography



Yaxue He was born in 13th January 1993 in Xinxiang (Henan Province, China). Yaxue finished her bachelor (BSc) in 2014 in Environmental Engineering at the Zhongyuan University of Technology (China) and obtained her MSc degree in Environmental Engineering at Tongji University (China) in March 2015.

She started as a PhD research fellow at National University of Ireland, Galway (Ireland) from September 2018, then moved to University of La Coruna, Spain for her PhD mobility from February 2020 - January 2021. She investigated the syngas, H₂/CO₂ and CO bioconversion to ethanol and butanol production. During her PhD study, Yaxue supervised Flora Marciano (Department of Civil and Mechanical Engineering, University of Cassino and Southern Lazio, Italy) for Flora's Master internship and helped Flora with her experimental design and master thesis.

Publications

He Y., Lens, P. N. L., Veiga, M. C. and Kennes, C. 2022. Effect of endogenous and exogenous butyric acid on butanol production from CO by enriched *Clostridia*. *Frontiers in Bioengineering and Biotechnology*. Accepted.

He Y., Lens, P. N. L., Veiga, M. C. and Kennes, C. 2022. Selective butanol production from carbon monoxide by an enriched anaerobic culture. *Science of the Total Environment*, 806, 150579.

He Y., Lens, P. N. L., Veiga, M. C. and Kennes, C. 2021. Enhanced ethanol production from carbon monoxide by enriched *Clostridium* bacteria. *Frontiers in Microbiology* 12, 754713.

He, Y., Cassarini, C., Marciano, F. and Lens, P. N. L. 2021. Bioethanol production from H₂/CO₂ by solventogenesis using anaerobic granular sludge: effect of process parameters. *Frontiers in Microbiology* 12, 647370.

He, Y., Cassarini, C., Marciano, F. and Lens, P. N. L. 2020. Homoacetogenesis and solventogenesis from H₂/CO₂ by granular sludge at 25, 37 and 55°C. *Chemosphere*, 128649.

He, Y. 2019. Popular science article: Can greenhouse gases and carbon monoxide be turned into biofuels? Link: <https://www.rte.ie/brainstorm/2019/1111/1090077-can-greenhouse-gases-and-carbon-monoxide-be-turned-into-biofuels/>, RTE, Ireland.

He, Yaxue¹, Yufeng Gong¹, Yiming Su, Yalei Zhang, and Xuefei Zhou. 2019. Bioremediation of Cr (VI) contaminated groundwater by *Geobacter sulfurreducens*: environmental factors and electron transfer flow studies. *Chemosphere*, 221: 793-801. (co-first author)

Gong, Yufeng, Charles J. Werth, **Yaxue He**, Yiming Su, Yalei Zhang, and Xuefei Zhou. Intracellular versus extracellular accumulation of Hexavalent chromium reduction products by *Geobacter sulfurreducens* PCA. *Environmental Pollution*, 240 (2018): 485-492.

Conferences

Yaxue He. 2019. Homoacetogenesis and solventogenesis from H₂/CO₂ by granular sludge at 25, 37 and 55° C. 8th International Conference Biotechniques for Air Pollution Control & Bioenergy, Galway, Ireland.

Yaxue He. 2019. Syngas bioconversion to ethanol and butanol by anaerobic granular sludge. Mid-term review: Science foundation of Ireland Research Professorship- Innovative Energy Technologies for Biofuels, Bioenergy and a Sustainable Irish Bioeconomy (15/RP/2763), Galway, Ireland.

Yaxue He. 2019. Will waste be our future? ----From waste gas to biofuel. Public talk, Potershed, Galway, Ireland.

Courses and modules

	Modules	ECTS	Statue	Remark
Registered in 2019				
GS508	Formulating a Research Project Proposal	5	Completed (Supervisor)	Pass
GS530	Graduate Research Information Skills	5	Completed	Pass
GS5104	Intensive Writing Workshop	5	Completed	Pass
Registered in 2021				
GS515	Research Paper Publication	5	Completed (Supervisor)	Pass
GS511	Research Placement 1	5	Completed (Supervisor)	Pass
GS536	Communication & Outreach	5	Completed (Supervisor)	Pass